IERS TECHNICAL NOTE 16

Results from the SEARCH'92 Campaign

J.O. Dickey and M. Feissel (eds).

September 1994

Central Bureau of IERS-Observatoire de Paris
61, avenue de l'Observatoire
F-75014 PARIS France

ERRATUM

1992 IERS ANNUAL REPORT

p. II-14, line 1 (title)		
p. II-79, 80, 84, 86, Note 1	read	...SSC(IERS) 93 C **03**
p. V-7, last table, lines 1, 3, 5		

1993 IERS ANNUAL REPORT

p. V-4. ACCESS TO THE IERS/CB DATA FILES: *EARTH ROTATION*

The names of the EOP files have changed.

Filename	**Contents**
bulletinb.NN:	Earth orientation parameters (x,y,UT,dψ,dε)
bulletinc.NN:	Announcement of the leap seconds in UTC.
bulletind.NN:	Announcement of the value of DUT1 to be transmitted with time signals.
	NN is the number of the issue.
eopc01.dat:	Normal values of EOP at 0.05 year intervals.
eopc02.YY:	Normal values of EOP at 5-day intervals.
eopc03.YY:	Normal values of UT at 1-day intervals.
eopc04.YY:	Smoothed values of EOP at 1-day intervals.
	YY is the year-1900.
*.guide:	Every file ".guide" contains information on file * .

Editors: J.O.Dickey and M. Feissel

IERS Technical Notes

This series of publications gives technical information related to the IERS activities, e.g. reference frames, excitation of the Earth rotation, computational or analysis aspects, models, etc. It also contains the description and results of the analyses performed by the IERS Analysis Centres for the Annual Report global analysis.

Back issues still available

No 3 : D.D. McCarthy (ed). IERS Standards (1989)

No 4 : C. Boucher and Z. Altamimi. Evaluation of the realizations of the Terrestrial Reference System done by the BIH and IERS (1984-1988).

No 6 : C. Boucher and Z. Altamimi. ITRF89 and other realizations of the IERS Terrestrial Reference System for 1989.

No 7 : E.F. Arias, M. Feissel and J.-F. Lestrade. The IERS extragalactic Celestial Reference Frame and its tie with HIPPARCOS.

No 10: C. Boucher and Z. Altamimi. The IERS GPS Terrestrial Reference Frame.

No 12: C. Boucher and Z. Altamimi. ITRF91 and other realizations of the IERS Terrestrial Reference System for 1991.

No 13: D.D. McCarthy (ed.). IERS Standards (1992).

No 14: P. Charlot (ed.) Earth orientation, reference frames and atmospheric excitation functions submitted for the 1992 IERS Annual Report.*[Superseded by T.N. 17]*

No 15: C. Boucher, Z. Altamimi and L. Duhem. ITRF92 and its associated velocity field

No 16: J.O. Dickey and M. Feissel (eds.). Results from the SEARCH'92 Campaign.

Future issues

No 17: P. Charlot (ed.). Earth orientation, reference frames and atmospheric excitation functions submitted for the 1993 IERS Annual Report.

No 18: C. Boucher, Z. Altamimi and L. Duhem. ITRF93 and its associated velocity field

CONTENTS

* Indicates papers that have been reprinted from Proceedings of the 1993 International GPS Service for Geodynamics (IGS) Workshop, Druckerei der Universitat Bern, G. Beutler and E. Brockman, Eds., with the permission of the authors and the editors.

CONTENTS

PART III (cont)

Geodetic and Atmospheric Measurements

PART IV

Intercomparison and Interpretation of Results

* Indicates papers that have been reprinted from Proceedings of the 1993 International GPS Service for Geodynamics (IGS) Workshop, Druckerei der Universitat Bern, G. Beutler and E. Brockman, Eds., with the permission of the authors and the editors.

Part I

Introduction and Theoretical Considerations

SEARCH'92 CAMPAIGN: AN OVERVIEW

J. O. DICKEY[1], T. A. CLARK[2], T. M. EUBANKS[3], M. FEISSEL[4], W. G. MELBOURNE[1], J. R. RAY[5], D. A. SALSTEIN[6], B. E. SCHUTZ[7] AND C. VEILLET[8]
[1] *Jet Propulsion Laboratory, California Institute of Technology*
[2] *NASA/Goddard Space Flight Center*
[3] *U.S. Naval Observatory*
[4] *Central Bureau, International Earth Rotation Service*
[5] *Laboratory for Geoscience, National Oceanic and Atmospheric Administration*
[6] *Atmospheric and Environmental Research, Inc.*
[7] *University of Texas, Austin*
[8] *OCA/CERGA*

ABSTRACT. High time resolution measurements of Earth rotation and atmospheric angular momentum and torque and their interpretation can provide unique insights into a variety of processes including dynamic coupling between solid Earth and atmosphere, the effects of oceanic tides on the Earth's rotational dynamics, excitation of the polar wobble, and fluid-core resonance effects; hence, an extensive campaign, SEARCH'92, has been held through the coordination of the International Earth Rotation Service (IERS) to obtain these measurements utilizing all space geodetic techniques and to collect the best available complementary geophysical, atmospheric and oceanographic data. This paper discusses its motivation and planning; recent analysis results are highlighted.

1. Introduction

High time resolution measurements of Earth rotation and atmospheric angular momentum (AAM) and torque and their interpretation will improve our understanding of the properties and origin of short-period fluctuations of the Earth's orientation, and will provide new and unique insights into a variety of geophysical processes. These processes include coupling and angular momentum exchange between the solid Earth and atmosphere, the interaction of dynamical ocean tides with the Earth's rotational dynamics and the effects of fluid-core resonances. Hence, a measurement and analysis program has been proposed as a major research area for the 1990s, both by the workshop held at Erice in 1988 on the "Interdisciplinary Role of Space Geodesy" and by the NASA Workshop on Geodynamics and Geology held in July 1989 to plan NASA Solid Earth Science Programs for the coming decade. The importance of the determination of rapid Earth rotation variations and its implication for geodynamics was recognized by the International Union of Geodesy and Geophysics (IUGG) in Vienna (August 1991) through a union resolution. As a result, a major campaign, SEARCH'92 (Study of Earth-Atmosphere Rapid CHanges), for high time resolution (sub-daily) measurements of Earth rotation by all of the space geodetic techniques, was coordinated by the International Earth Rotation Service (IERS) and was held in conjunction with the IGS Campaign (June 21–September 22, 1992). A special intensive period (Epoch'92) extended from July 25 through August 8, 1992.

This paper highlights motivation, planning, and results from SEARCH'92. The second section discusses the rationale and scientific benefits for these measurements, while the third section reviews international cooperation. Section 4 highlights recent advances in analysis and interpretation, while the final section presents a summary.

Recently, Dickey (1993) reviewed atmospheric excitation of the Earth's rotation and provides a detailed account of recent developments. The reader is referred to several more general accounts of the excitation of Earth orientation changes; references to early work can be found in the classical monograph on the subject by Munk and McDonald (1960) and to more recent work in various monographs and other publications (Cazenave, A., 1986; Dickey and Eubanks, 1986; Eubanks, 1993; Hide, 1977, 1984, 1986, 1989; Hide and Dickey, 1991; Lambeck, 1988; Moritz and Mueller, 1987; Wahr, 1988).

2. Motivation and Scientific Benefits

The scientific benefits to be obtained from these campaigns include improved understanding of the properties and origin of short-period fluctuations in the Earth's orientation, improvements to the tidal models at sub-monthly periods, and improved ability to predict changes in the Earth's rotation up to a month in advance. A major goal is to observe and understand the interactions of the atmosphere and ocean with the rotational dynamics of the Earth, and their contributions to the excitation of Earth rotation variations over time scales of hours to months (see Fig. 1). At these frequencies, a number of geophysical processes are thought to be capable of affecting the Earth's rotation, including atmospheric wind and pressure changes, oceanic current and sea level changes, oceanic and solid Earth tidal motions, and seismic motions. High-frequency measurements, together with complementary analyses of geophysical data, can be expected to lead to delineation of short-period tidal, atmospheric, oceanic, and seismic effects on length-of-day (LOD) and polar motion. These in turn will improve our understanding of broad-band wobble excitation processes, fluid-core resonance characteristics, and mechanisms of oceanic/atmospheric dynamic coupling to the solid Earth.

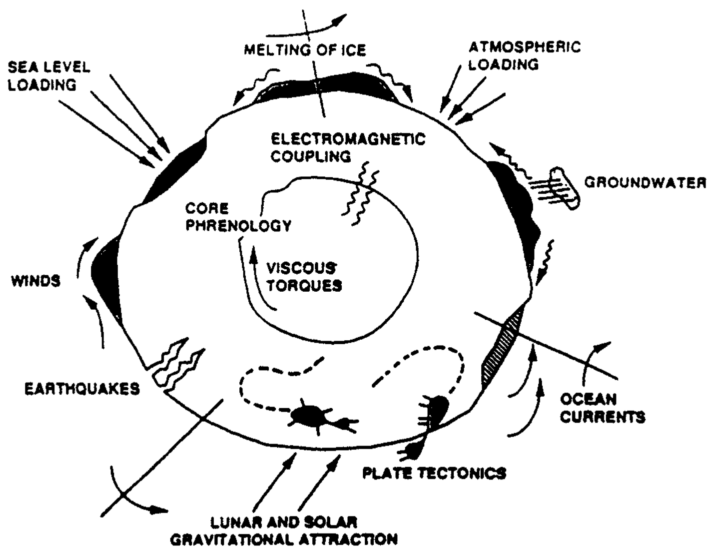

Figure 1. Schematic illustration of the forces that perturb Earth rotation. After Lambeck, 1980.

In particular, the Earth's angular momentum budget (both axial and non-axial) can be examined at high frequencies. The elucidation of the relation between LOD and AAM at high frequencies is central to our understanding of the Earth's angular momentum budget and is currently an area of active research (see for example, Rosen *et al.*, 1990; Herring and Dong, 1991 and 1994; Dickey *et al.*, 1992). Fig. 2 illustrates the striking similarities between these two series. Significant coherence is found between the LOD and AAM at periods down to 8 days, with lack of coherence at shorter periods caused by the declining signal-to-measurement noise ratios of both data types (Dickey *et al.*, 1992). Higher accuracy and more frequent data are needed to resolve the exchange of angular momentum between the Earth and the atmosphere at shorter periods. Although no significant lags or leads at the few day level have been established (indicating little or no non-tidal oceanic contribution), the oceans, via barotropic waves, could contribute on short time scales (a few days or less) to the Earth's angular momentum budget (Ponte, 1990). Hence, a comparison of AAM and LOD at these high frequencies could uncover the ocean's role and further elucidate our understanding of the dynamic interaction between the solid Earth and the atmosphere, allowing the role of the atmosphere and oceans in Earth orientation variations at high frequencies to be quantified. The appropriateness of the inverted barometer approximation for the ocean's response to atmospheric pressure forcing at high frequencies could be investigated, and the respective roles of the mountain and wind stress torque in transferring angular momentum between the solid Earth and atmosphere examined.

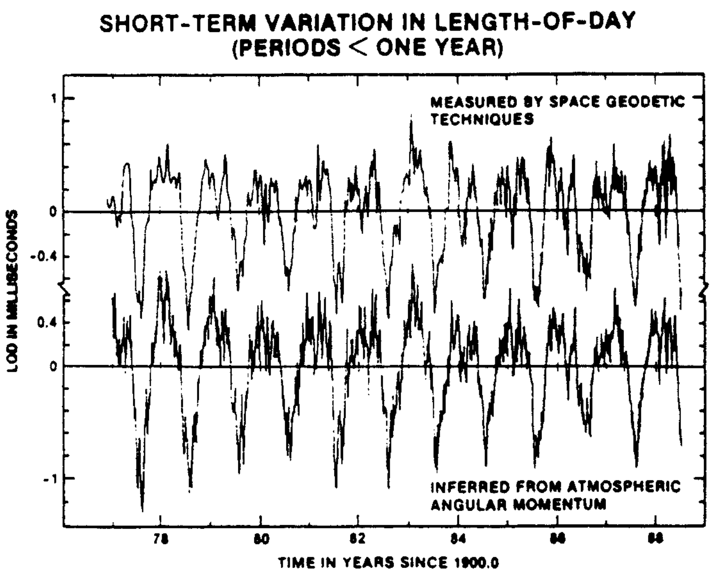

Figure 2. Time series of the sum of the seasonal and intraseasonal LOD components, with the upper curve measured by space geodetic techniques and the lower curve inferred from routine daily determinations of changes in the axial component of the atmospheric angular momentum made by the U. S. National Meteorological Center. Periods greater than one year in both series have been filtered out (after Dickey, 1993).

3. Measurement Campaigns

Thus far, three major campaigns have been coordinated, allowing high temporal resolution measurements of Earth rotation over extended time periods. The NASA Crustal Dynamics Project VLBI (Very Long Baseline Interferometry) Group at Goddard Space Flight Center conducted the first Extended Research and Development Experiment (ERDE) in October, 1989, designed to obtain high time resolution measurements of the Earth's orientation by the VLBI technique and to test improvements in the VLBI measurement system (Clark *et al.*, 1990); these special sessions resulted in nearly continuous sub-hourly measurements over the 17-day period and served as a prototype for future efforts.

The GIG'91 Measurement Campaign (GPS IERS and Geodynamical Experiment), coordinated by the International Earth Rotation Service, was held between January 22 and February 13, 1991 with one of its prime objectives being the evaluation of the ability of GPS to recover Earth rotation parameters. The analysis of these data provided high quality daily measurements of polar motion (Herring *et al.*, 1991; Lindqwister *et al.*, 1992) as well as sub-daily measurements of Earth rotation variations (Lichten *et al.*, 1992).

The SEARCH campaign involved all space geodetic techniques with the best available complementary geophysical, atmospheric and oceanographic data being collected. Coordination was effected by the International Earth Rotation Service (IERS). A joint International Association of Geodesy/International Astronomical Union (IAG/IAU) Special Study Group, Rapid Earth Orientation Variations, has been formed to (1) interface with the IERS in the determination of rapid variations in Earth rotation by the space geodetic techniques; (2) advocate for the best possible auxiliary data from geophysical, atmospheric and oceanographic sources; (3) encourage improvements in measurement techniques (including geodetic, atmospheric, oceanographic and geophysical); and (4) encourage cooperative multidisciplinary studies.

During the SEARCH and EPOCH'92 campaigns, geodetic Earth rotation and polar motion measurements were made from the GPS, VLBI, SLR and LLR techniques; complementary geophysical data sets were also archived. LLR results were sparse and do not support robust subdaily Earth rotation determination. Some results are also described in the IERS Technical Note 14 (IERS, 1993).

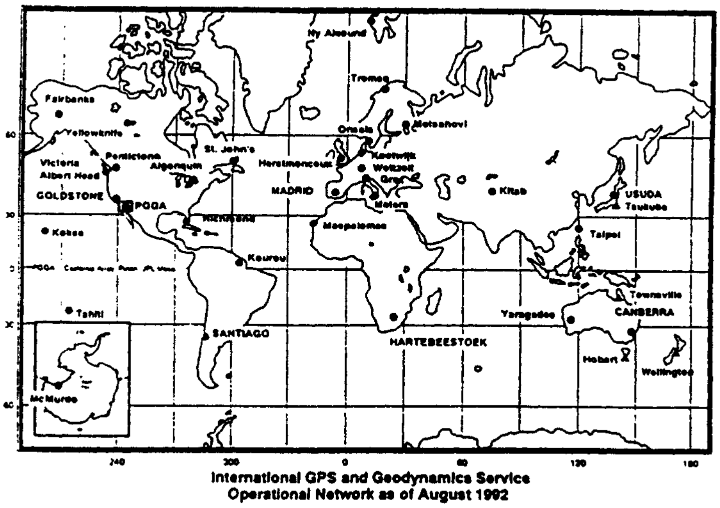

Fig. 3a. GPS Observing Network

3. 1. GLOBAL POSITIONING SYSTEM (GPS)

Recognizing the increasing use of the Global Positioning System (GPS) for geodesy and geophysics and that this system will play a major role in global and regional studies of the Earth, the IUGG in Vienna (August, 1991) recommended through a union resolution that the development of an International GPS Geodynamic Service (IGS) be explored. At its May 1, 1992 meeting the Directing Board of IERS officially adopted GPS as a contributing technique for the terrestrial reference frame and Earth rotation determination. As a test of the IGS concept, the IGS Oversight Committee organized a campaign for the period June 21–September 22, 1992 with a special intensive period (EPOCH'92) extending from July 25 through August 8, 1992. GPS results were received throughout the entire three month campaign (Beulter and Brockman, 1993).

The observing GPS network is displayed in Fig. 3a; it consists of an operational core network of about 30 receivers with up to an additional 80 GPS stations participating during the EPOCH'92 period. Standard GPS ephemerides and polar motion were generated by 7 analysis centers within 2 weeks of receipt of data (Beutler and Brockman, 1993).

3.2. SATELLITE LASER RANGING

An international network of approximately 30 stations supported routine laser ranging to LAGEOS and ETALON (see Fig. 3b). During the SEARCH campaign, estimates of polar motion and Universal Time at 3-day intervals were produced operationally, and in subsequent processing at 1-day intervals. A separate analysis spanning the period 1987-1993 determined tidally coherent diurnal and semidiurnal variations in polar motion and UT1 which were validated during the campaign.

3.3 VLBI

The VLBI measurement program consists both of routine operations (e.g., IRIS-A, NAVNET) as well as intensive observing efforts planned for Epoch'92; the global VLBI Network for SEARCH is given in Fig. 3c. Collectively, IRIS-A and NAVNET operationally provided 3-component Earth rotation (UT1) and polar motion measurements on a twice-a-week basis with 24-hour observing programs; daily intensive UT1 measurements were made utilizing the Westford and Wettzell stations. At other times, there was essentially continuous coverage on two simultaneous VLBI networks during the period July 27-August 10, which are useful in error analysis. During this time, coverage was provided by the NASA-sponsored Extended R&D sessions, the scheduled IRIS A and the augmented USNO NAVNET/NAVEX programs (see Eubanks, Ma and Gipson; and Ray *et al.*, this volume for a fuller discussion).

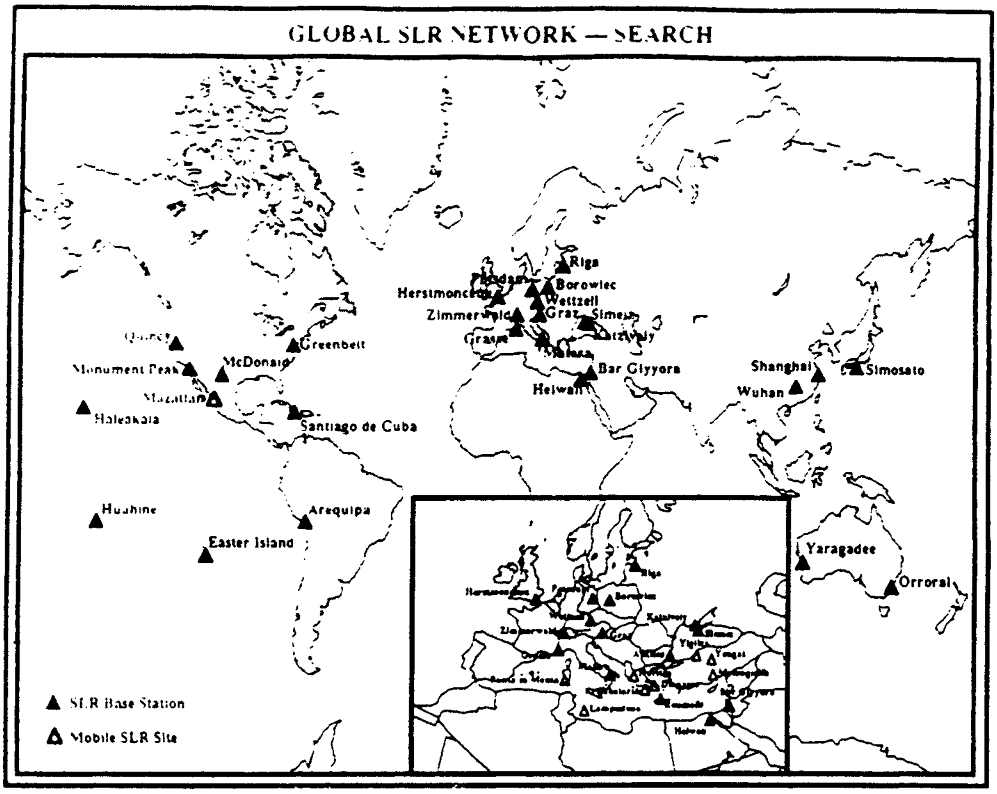

Fig. 3b. SLR Observing Network

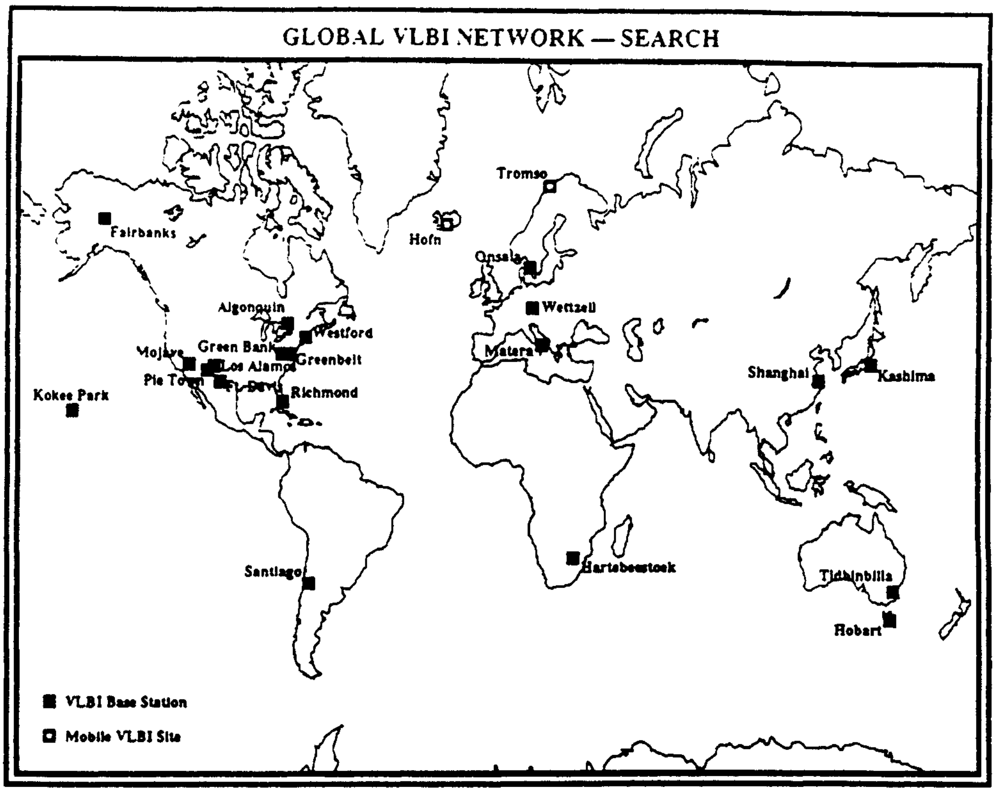

Fig. 3c. VLBI Observing Network

3.4. COMPLEMENTARY GEOPHYSICAL DATA

The primary complementary geophysical data sets collected for SEARCH'92 are series of atmospheric angular momentum functions, in the axial direction related to changes in the length of day and in the equatorial directions related to polar motion, as well as torques at the lower boundary of the atmosphere. There are four meteorological data centers contributing standard AAM products to the IERS Sub-Bureau for Atmospheric Angular Momentum: the European Centre for Medium-Range Weather Forecasts (ECMWF), Japan Meteorological Agency (JMA), National Meteorological Center (NMC) of the United States, and United Kingdom Meteorological Office (UKMO). Data from all centers are available in near real time. Before SEARCH'92, AAM data had been typically archived twice daily, but in response to the requirements of this special campaign, computation and collection of AAM data were initiated at a higher frequency using 6-hourly NMC, ECMWF, and JMA analyses. All data types related to AAM, including ancillary parameters, are outlined in Table 1, and were obtained from the wind, surface pressure and temperature analyses of these centers. Some sets of AAM values include oceanic information indirectly by a modification of the atmospheric mass terms accounting in part for an oceanic inverted barometer response to surface loading. Calculations of Earth-atmosphere torques are now under way at the NMC and will be available to the geodetic community for this campaign. These torques involved the dynamic transfer of momentum between Earth and atmosphere by means of both pressure differences across mountains and friction stresses at the Earth's surface (see Salstein and Rosen, 1994). See Salstein and Kahn (this volume and 1991) or Salstein *et al.* (1993) for further details.

TABLE 1. Atmosphere Data Sets Archived at IERS Sub-Bureau for Atmospheric Angular Momentum (after Salstein and Kann, this volume)

Analysis Parameters	Specification
AAM Equatorial χ_1, χ_2	Hemispheric values for wind,
AAM Axial χ_3	pressure & pressure + inverted barometer (ib)
Zonal Mean Zonal Winds [u]	5°latitude intervals,
Zonal Mean Temperatures [T]	12 mandatory pressure levels
Mean Surface Pressure	Global average
Surface Pressure Coefficients	Triangular truncation to wave 4; zonals only to wave 20
Forecast Parameters	**Specification**
AAM Equatorial χ_1, χ_2	Global forecast values at 12-h
AAM Axial χ_3	intervals to 10 days for wind, pressure, pressure + ib

4. Highlights of Analysis Results

4.1. INTERCOMPARISON

Intercomparison of results are shown in Figs. 4-10. Polar motion results are displayed in Figs. 4, 5, and 6 for VLBI, GPS and SLR, respectively; an analytical model has been used to remove variations over ~ 100 days. One can note similar structure throughout all series, for example, relative maxima in the y-component at ~ 1992.52 and 1992.67 and in the x-component at ~ 1992.57 and 1992.67. Results for UT1 from VLBI, GPS and SLR are shown in Fig. 7; again, one can see quasi-periodic fluctuations in all series with relative maxima at 1992.53, 1992.59, 1992.64 and 1992.69. The celestial pole offset from VLBI analysis is displayed in Fig. 8. Measurements from the intensive period are shown in Figs. 9 (polar motion) and 10 (UT1) with further discussion in the following two sections.

The improved determination of UT1 and its use in determing LOD is currently an area of intense activity. Gambis *et al.* (this volume) discusses the scenario of utilizing the GPS and SLR determinations for short-period UT1 fluctuations, and combining them with VLBI which has long-term stability.

4.2. UNIVERSAL TIME (UT1) RESULTS FROM EPOCH'92

During the full campaign, results were obtained from all techniques (see Figs. 4-10); measurements during an intensive two-week period centered around August 1, 1992, designated as EPOCH'92, were particularly robust with almost continuous VLBI measurements (see Fig. 9-11 and Section II of this volume). Periods of simultaneous observations permit an assessment of data quality by two VLBI networks.

The UT1 series shown in Fig. 11 were estimated from each network every 3 hours after the application of a diurnal and semidiurnal *a priori* tide model [Herring, this volume]; uncertainties varied from 10 to 40 μs and were network dependent. The different VLBI series were then combined from all networks using a mild Gaussian filter to form a continuous series. The GPS series shown was obtained at 30-minute intervals employing a multi-day orbit arc strategy and data from a network of 25 stations using a GPS constellation of 17 satellites (see Freedman *et al.*, this volume and 1994 for details). The data gap in the middle of the time series is due to the use of anti-spoofing (AS) signal encryption; the data before and after this gap were treated as separate arc orbits. For the sake of comparison with VLBI, a light Gaussian smoothing was applied.

A strong diurnal and semidiurnal signature is clearly seen in both data types. Diurnal and semi-diurnal rotational variations were postulated by Yoder *et al.* (1981), who proposed that such signatures should arise from the interactions of the ocean tides with the solid Earth. Estimates of these variations were made by Baader *et al.* (1983) for the M_2 tide and were refined by Brosche *et al.* [1989 and 1991] for the major diurnal and semi-diurnal tides. Seiler [1991] and Wünsch and Seiler [1992] revised the Brosche *et al.* [1989] tidal model using a new numerical ocean model; these calculations were later improved by Gross [1993] through the use of a more realistic rotational model [also see Brosche and Wünsch, 1994]. Herring and Dong [1991, 1994], Sovers *et al.* [1994], and Watkins and Eanes [1994 and this volume] used the approach of empirically fitting the major tidal components to sub-daily Earth rotation observations. Dickman [1993] developed the "broad-band" Liouville equation approach and determined the effects of the dynamic ocean tides on Earth rotation. Comparisons with the independent techniques of VLBI and GPS confirm the reality of a strong diurnal and semi-diurnal signature [~0.1 msec (5 cm) in amplitude — see Fig. 11]. Also evident is a systematic shift of the GPS with respect to the VLBI

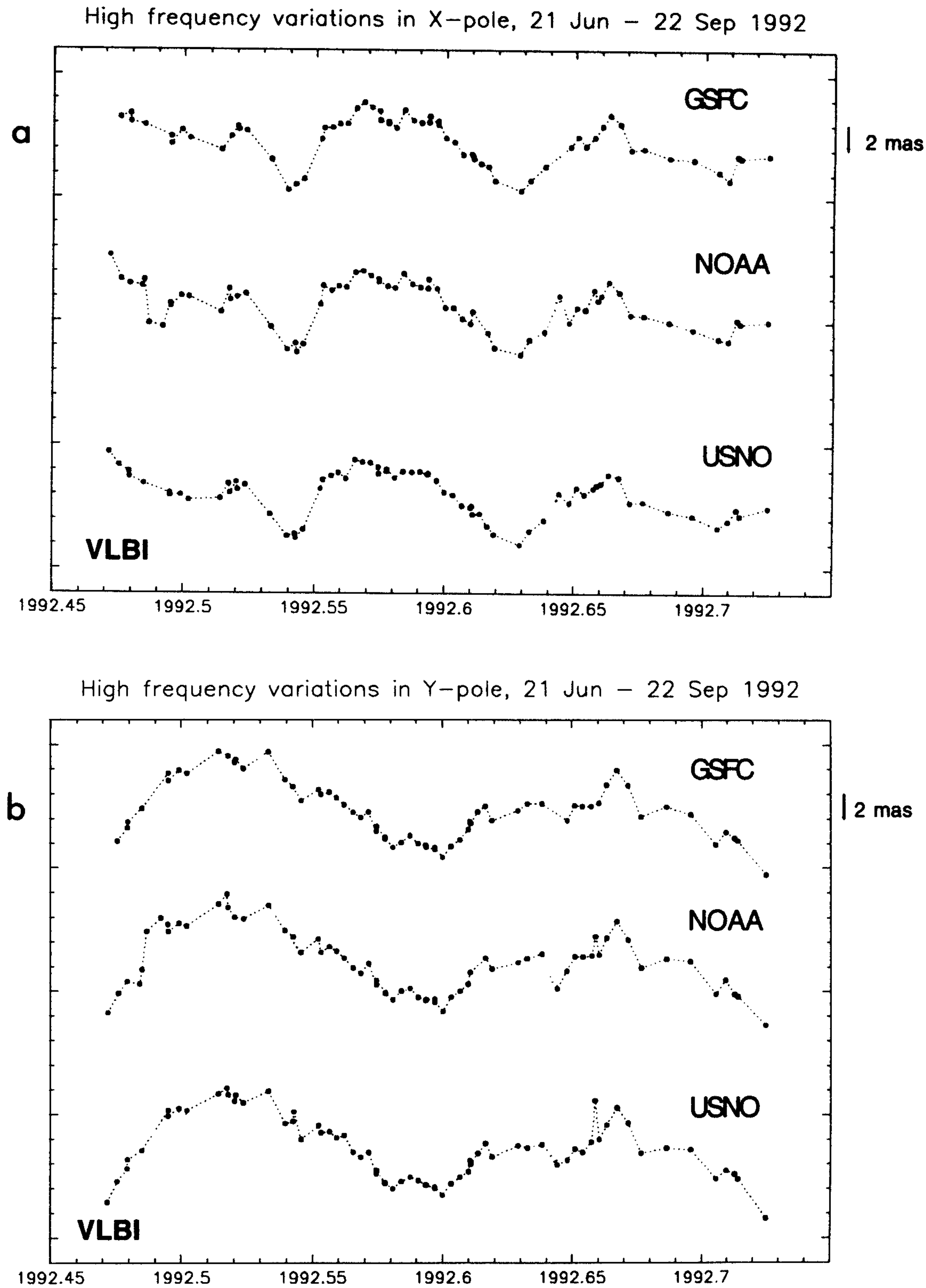

Figure 4. High frequency variations in the coordinates of the pole, 21 Jun - 22 Sep 1992, measured by **VLBI**.

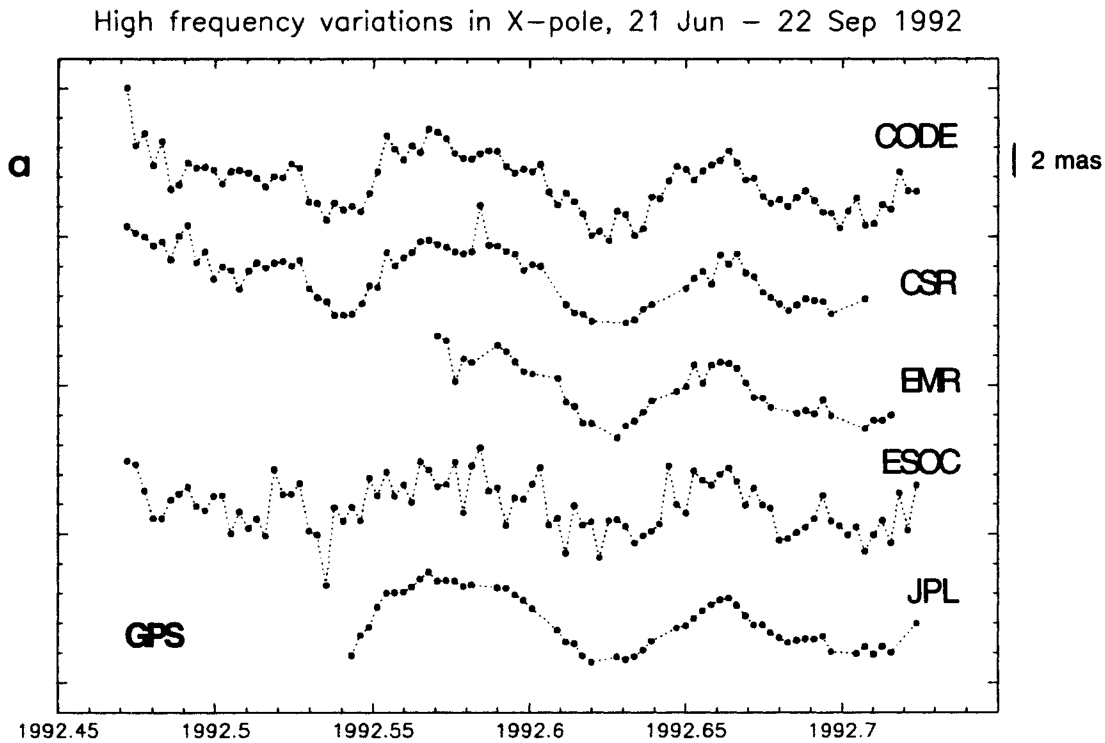

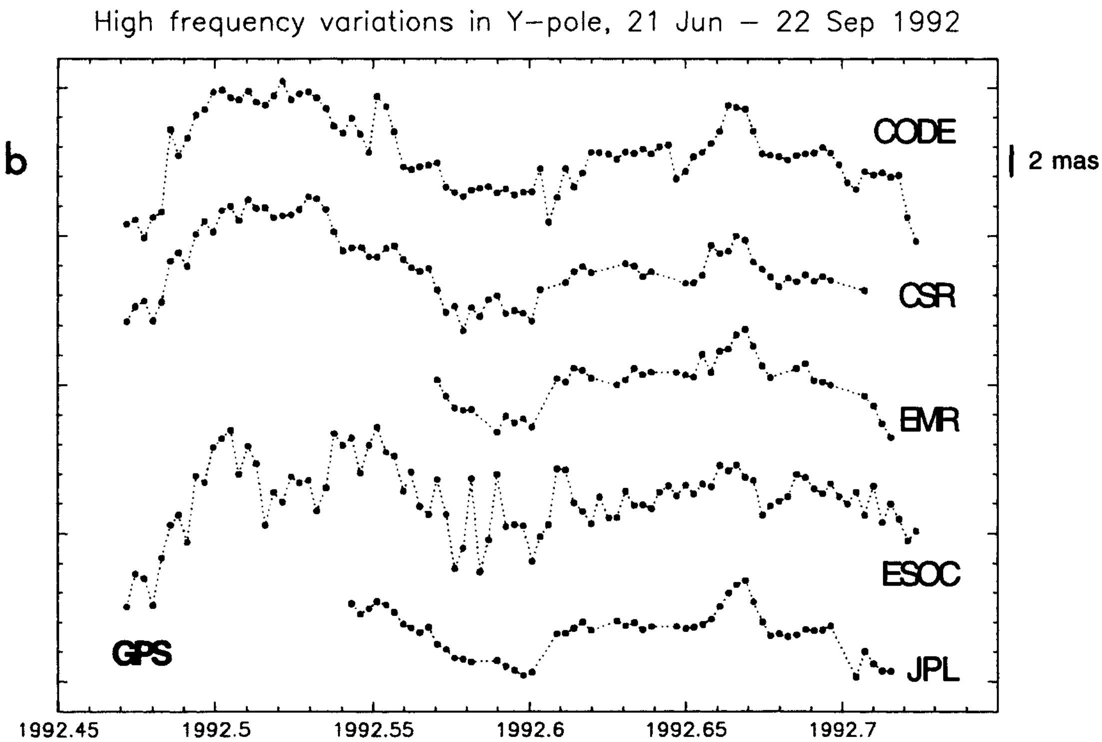

Figure 5. High frequency variations in the coordinates of the pole, 21 Jun - 22 Sep 1992, measured by GPS.

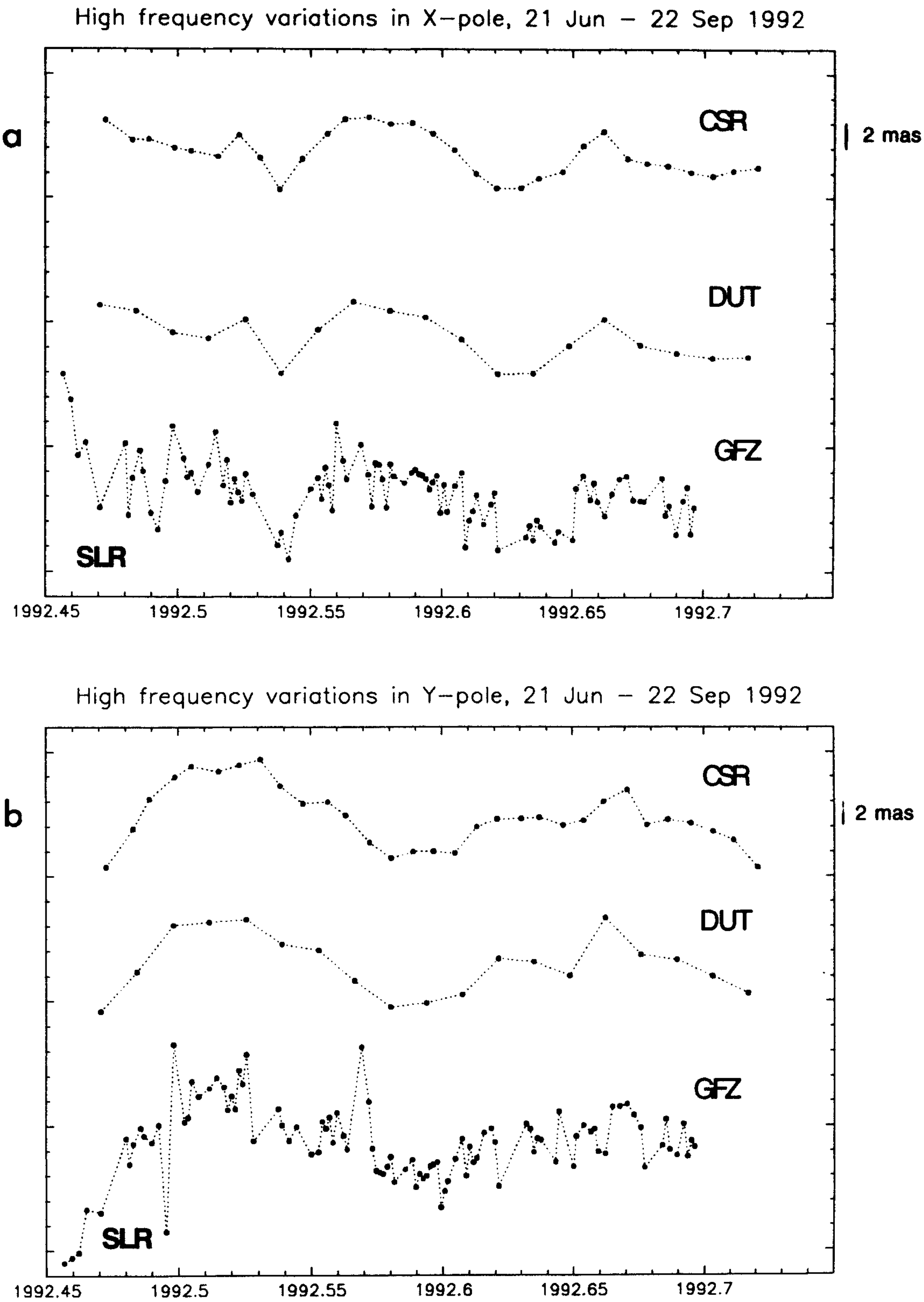

Figure 6. **High frequency variations in the coordinates of the pole, 21 Jun - 22 Sep 1992, measured by SLR.**

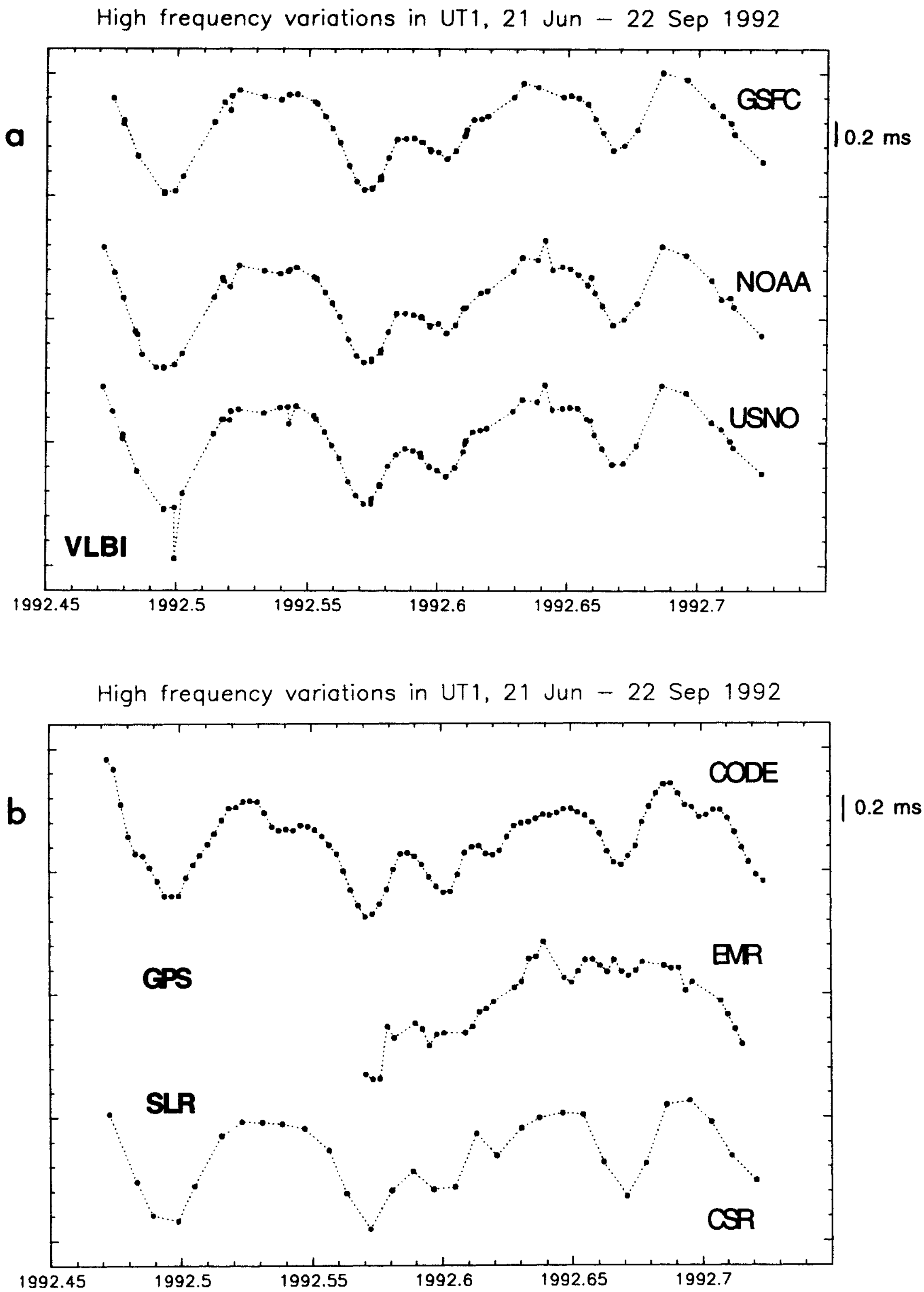

Figure 7. High frequency variations in universal time, 21 Jun - 22 Sep 1992, measured by **VLBI, GPS** and **SLR**.

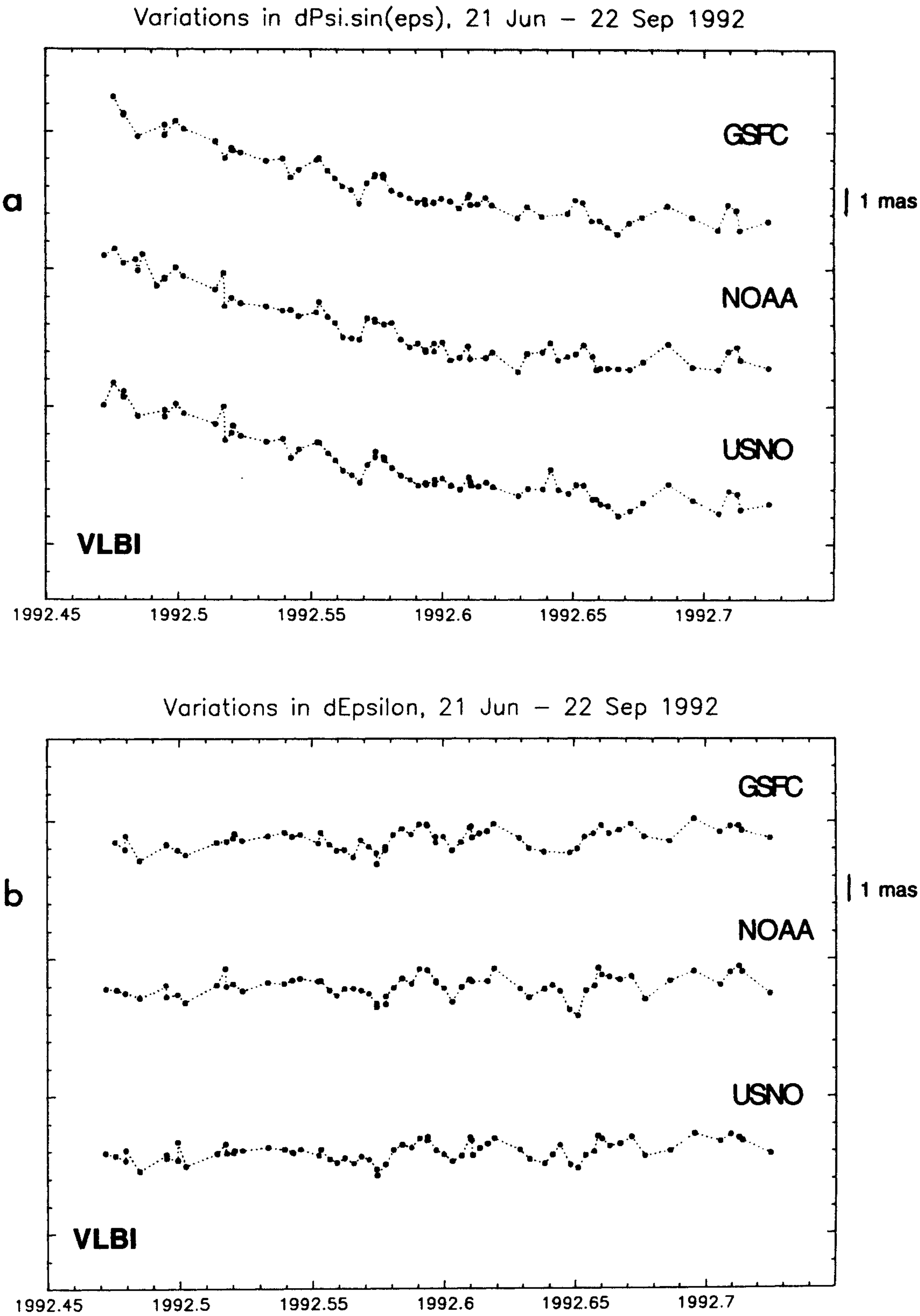

Figure 8. High frequency variations in the celestial pole offsets, 21 Jun - 22 Sep 1992, measured by **VLBI**.

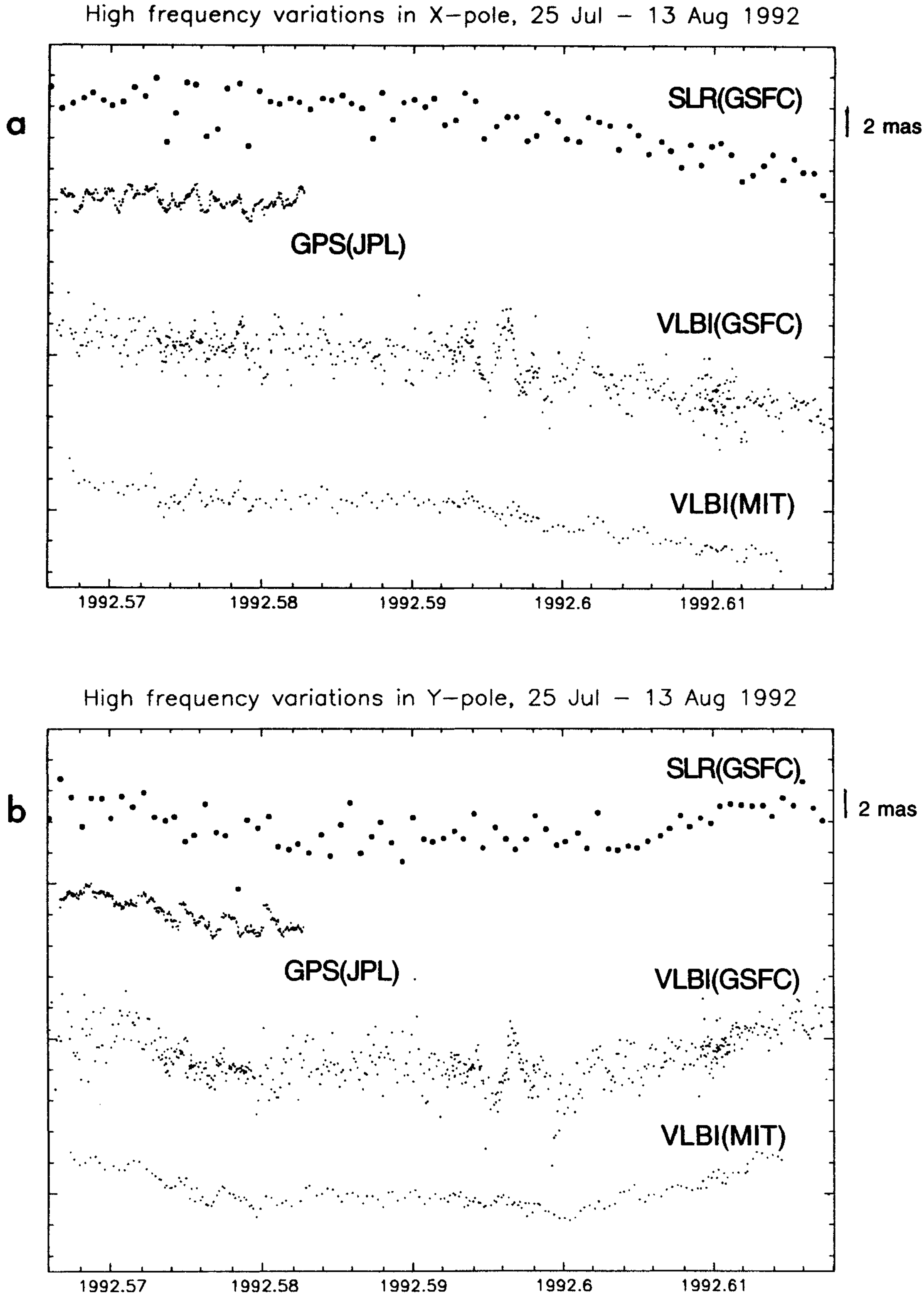

Figure 9. Rapid and sub-daily variations in the coordinates of the pole, 25 Jul - 13 Aug 1992, measured by **VLBI, GPS** and **SLR**.

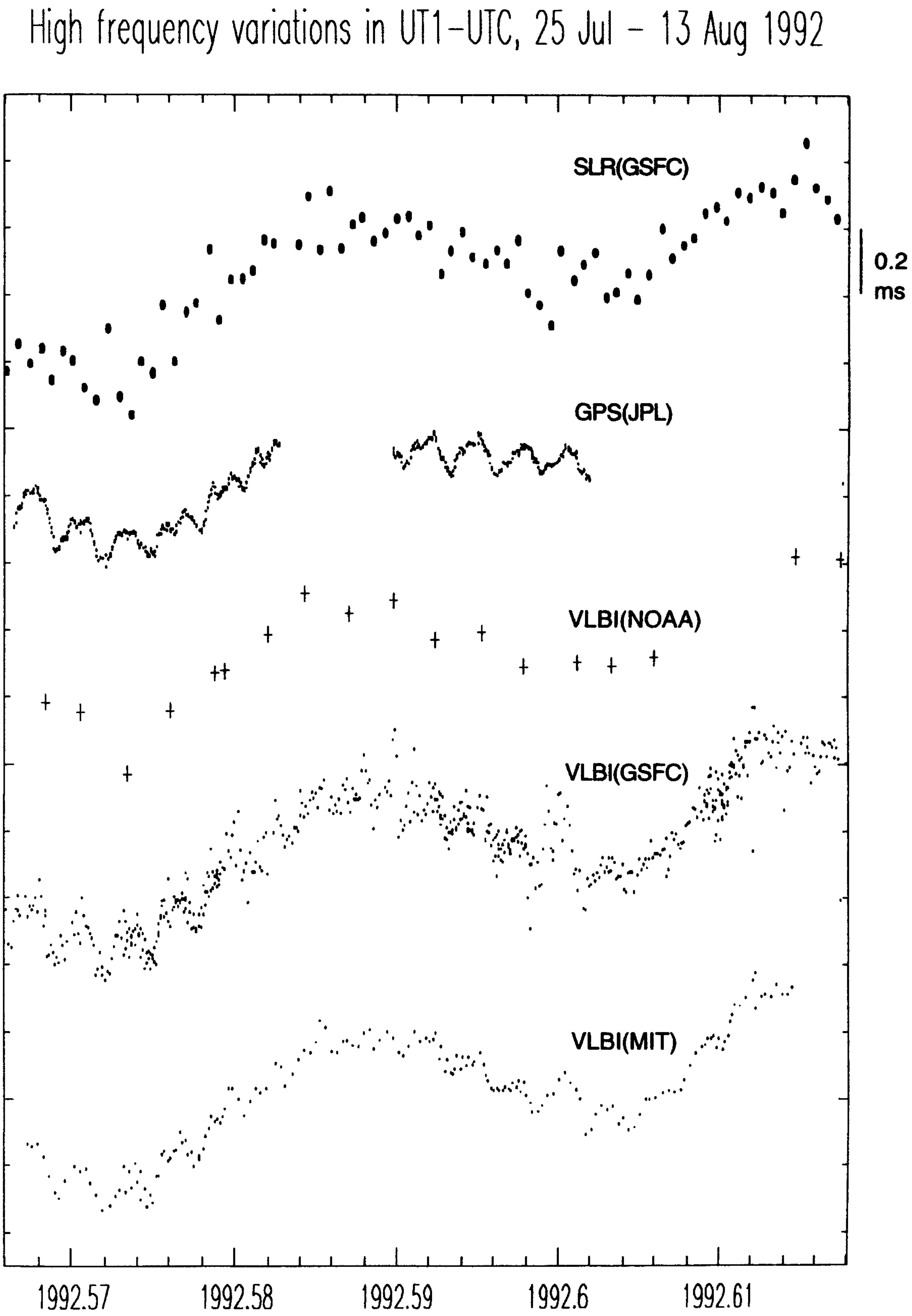

Figure 10. Rapid and sub-daily variations in universal time,
25 Jul - 13 Aug 1992, measured by **VLBI, GPS** and **SLR**.

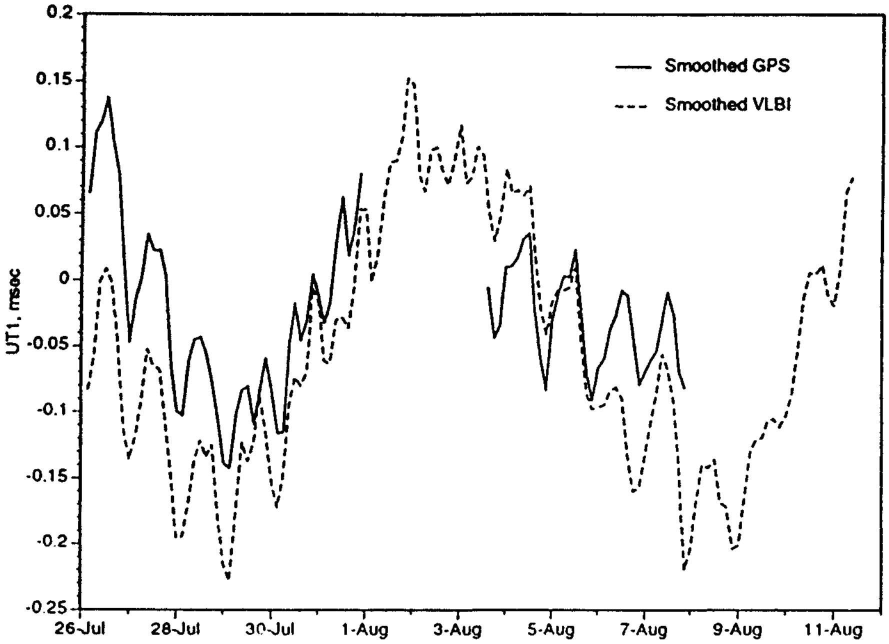

Fig. 11. UT1 from GPS and VLBI evaluated every 3 hours (after Freedman *et al.*, this volume).

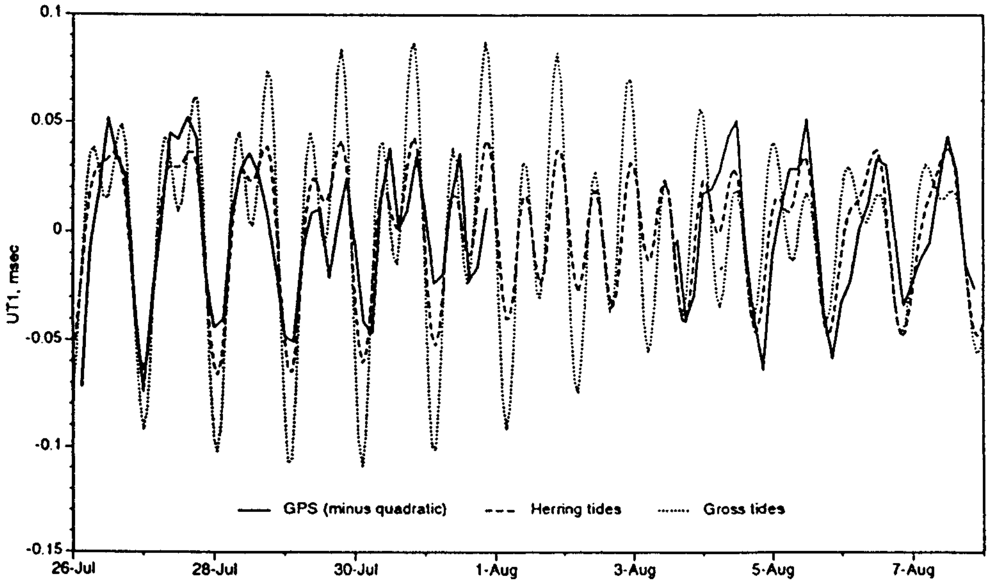

Fig. 12. GPS UT1 compared to two models of tidally induced UT1 variations (after Freedman *et al.*, this volume).

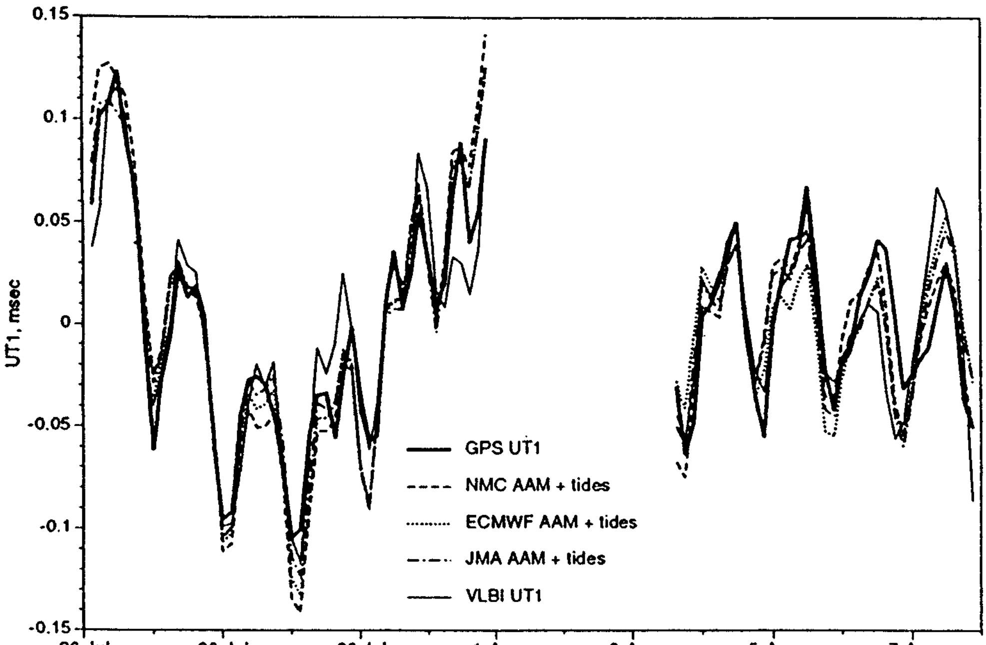

Fig. 13. Comparison of integrated AAM with geodetic UT1 variations (after Freedman *et al.*, this volume).

series, which is most likely due to orbit errors. After removing a quadratic from the GPS series to remove multiday variations (Fig. 12), comparisons can be made directly with results predicted by oceanic tidal models. Two models are examined—a theoretical model computed by Gross (1993), based on an oceanic angular momentum model of Seiler (1991) and an empirical model of Herring and Dong, based on 8 years of VLBI data (1994). As would be expected, better agreement is evident with the empirical model; the RMS scatter decreases from 32 μs to 18 μs (see Fig. 12). Differencing with respect to the Gross tides actually increases the scatter from 32 to 35 μs. Most of the discrepancies arise from the semidiurnal band, where the theoretical model predicts a much larger amplitude. Predicted diurnal variations from the Dickman (1993) model show significant correlation with the observational results, but are too small in amplitude.

Further, one can consider the atmospheric influence by integrating AAM and adding it to the UT1 specified by the empirical tidal model of Herring and Dong (1994). Linear trends were removed from each series for each of the two periods. Most of the geodetic signal can be described by the sum of AAM variation and tidally induced UT1, with tides acting at periods of one day and less and AAM dominating variations at periods greater than a day. The differences between GPS and VLBI are at least as large as those between the AAM series themselves and the AAM and geodetic series (see Fig. 13). Therefore, no atmospheric center or geodetic technique can be considered as the best series. There is no residual signal that exceeds the formal errors. The subdaily variability of the AAM is quite small and at this point cannot be separated from the oceanic effects; however, limits can be expressed. Improved theoretical tide models are needed to unravel the oceanic and atmospheric signals with geodetic measurements providing strong constraints.

4.3. POLAR MOTION

In contrast to the axial component, the equatorial momentum budget is not closed at any frequency. For example, a study by Kuehne and Wilson [1991] investigated the effect of water storage in combination with air mass redistribution on the observed excitation of polar motion near the annual and Chandler frequencies for the period 1900-1985. They concluded that there is a discrepancy in accounting for more than half the variance of polar motion across a broad range of frequencies, suggesting a source of polar motion excitation due to air and water motion which has either not been correctly estimated or is not yet identified. On shorter time scales, Eubanks *et al.* [1988], comparing observed χ-functions derived from geodetic observations with theoretical χ-functions derived from atmospheric data, demonstrated the existence of rapid polar motions with peak-to-peak variations of approximately 2 to 20 mas, fluctuating on time scales between two weeks and several months. These variations are only partly accounted for by atmospheric surface pressure changes and, like the Chandler and annual terms, require an additional source of excitation. The "missing" excitation may be explained by errors in the data sets used (in either the polar motion series or the AAM series), by oceanic angular momentum, or possibly by groundwater redistribution.

Daily polar motion values determined from observations acquired during the GIG'91 measurement campaign permit an unprecedented high time resolution investigation of the effect of the atmosphere on rapid polar motion variations (Gross and Lindqwister, 1992). The wind and pressure terms are found to be of comparable importance in exciting the observed polar motions during this period with somewhat better agreement seen with the application of the inverted barometer approximation. Correlations as high as 0.88 were obtained between the observed polar motion and the AAM-induced series, with AAM variations explaining as much as 74% of the

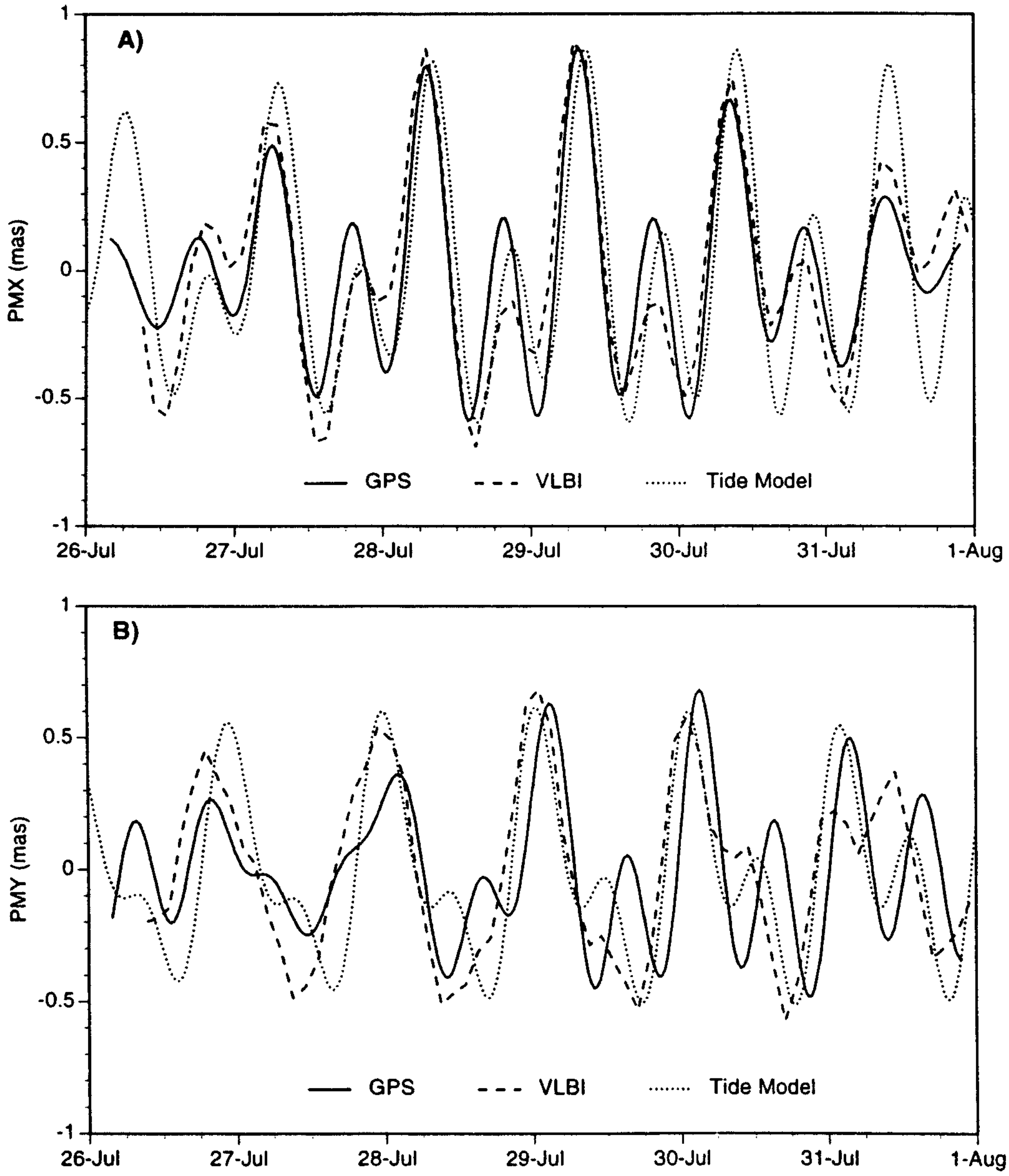

Fig. 14. (a) Polar motion X component for the semidiurnal and prograde diurnal bands for GPS, VLBI, and Herring tide model time series, (b) sames as (a) for the polar motion Y component (after Ibanez-Meier, this volume).

variance of the observed polar motion. Several studies (for example, Kosek, this volume and Hefty, this volume) have also linked the atmosphere to short period (> 1 day) polar motion changes during the SEARCH'92 campaign.

Subhourly polar motion observations (every 30 minutes) were obtained from the GPS tracking network for a six-day period during the EPOCH'92 campaign and were compared to estimates derived from VLBI (see Ibanez-Meier *et al.*, this volume). Like subdaily UT1, subdaily polar motion variations are dominated by a strong diurnal and semi-diurnal signature. Since the retrograde diurnal motion of the pole is degenerate with long period nutations, comparisons are restricted to the semidiurnal (both prograde and retrograde) and diurnal prograde bands. Time domain comparison between these two techniques yields less than 0.3 mas rms differences, which is consistent with their uncertainties (see Fig. 14). Further, comparisons with tidal models confirm the dominance of oceanic tides on these time scales.

5. Concluding Remarks

High time resolution measurement of Earth rotation is an area of intense activity, involving international and interdisciplinary cooperation. The international campaign, SEARCH'92, was successful in obtaining high time resolution (sub-daily and in some cases sub-hourly) measurements of Earth orientation by several space geodetic techniques and in collecting the best available complementary geophysical, oceanographic and atmospheric data. This paper featured the motivation for these measurements, reviewed the progress and planning of SEARCH'92; analysis results were highlighted. The dominance of the atmosphere is seen on time scales of greater than a day to several years with oceanic tides providing the main excitation at diurnal and semidiurnal periods; geodetic measurements provide strong constraints on existing tidal models. Improved theoretical tide models are needed to unravel the oceanic and atmospheric signals. The creation of a new generation of ocean models is now underway through the analysis of TOPEX/Posiedon data. The initial results from SEARCH'92 are indeed encouraging; further analysis of these studies will provide new and unique insights into the properties and origin of short period fluctuations in the Earth's orientation and into solid Earth-atmosphere interactions.

Acknowledgments

The authors gratefully acknowledge the active role played by many of the Special Study Group 5.143 Members (Rapid Earth Orientation Variations): P. Brosche, A. Brzezinski, B. Chao, S. Dickman, R. Gross, T. Herring, R. Hide, B. Kolaczek, R. Langley, S. Manabe, D. McCarthy, J. Miller, Z. Ming, I. Naito, P. Paquet, D. Robertson, R. Rosen, N. Sidorenkov, C. Wilson and K. Yokoyama. The authors also thank R. Neilan for supplying Fig. 3a, C. Noll for supplying Figs. 3b and c, and S. L. Marcus for comments that improved this manuscript. The work of two of the authors presents the results of one phase of research carried out at the Jet Propulsion Laboratory, California Institute of Technology sponsored by the National Aeronautics and Space Administration.

References

Baader, H. -R., P. Brosche, and W. Hovel, Ocean Tides and Periodic Variations of the Earth's Rotation, *J. Geophys.*, 52, 140-142 (1983).

Beutler, G., and E. Brockman, eds, Proceedings of the 1993 International GPS Service for Geodynamics (IGS) Workshop, Druckerei der Universitat Bern (1993).

Brosche, P., U. Seiler, J. Sündermann, and J. Wünsch, Periodic Changes in Earth's Rotation due to Oceanic Tides, *Astron. Astrophys.*, 220, 318-320 (1989).

Brosche, P., J. Wünsch, J. Campbell, and H. Schuh, Oceanic Tide Effects in Universal Time Detected by VLBI, *Astron. Astrophys.*, 245, 676-682 (1991).

Brosche, P., and J. Wünsch, On the "Rotational Angular Momentum" of the Oceans and the Corresponding Polar Motion, *Astron. Nachr.*, 315, 181–188 (1994).

Cazenave, A. (ed.), *Earth Rotation: Solved and Unsolved Problems, NATO Advanced Institute Series C: Mathematical and Physical Sciences Vol. 187*, ed. A. Cazenave, D. Reidel, Boston (1986).

Clark, T. A., J. W. Ryan, and K. D. Baver, ERDE: High Resolution Observations of Earth Orientation Parameters by Very Long Baseline Interferometry, *EOS, Trans. Amer. Geophys. Union*, 71, 1271 (1990).

Dickey, J. O., and T. M. Eubanks, The Application of Space Geodesy to Earth Orientation Studies, Space Geodesy and Geodynamics, eds., A. J. Anderson and A. Cazenave, Academic Press, New York, 221-269 (1986).

Dickey, J. O., Atmospheric Excitation of the Earth's Rotation: Progress and Prospects via Space Geodesy, in Contributions of Space Geodesy to Geodynamics, Earth Dyanimcs, edited by D. E. Smith and D. L. Turcotte, *Am. Geophys. Un.*, Washington, D.C., 55-70 (1993).

Dickey, J. O., S. L. Marcus, J. A. Steppe, and R. Hide, The Earth's Angular Momentum Budget on Seasonal Time Scales, *Science*, 255, 321-324 (1992).

Dickman, S. R., Dynamic Ocean Tide Effects on Earth's Rotation, *Geophys. J. Int.*, **112**, 448-470 (1993).

Eubanks, T. M., J. A. Steppe, J. O. Dickey, R. D. Rosen, D. A. Salstein, Causes of Rapid Motions of the Earth's Pole, *Nature*, 334, 115-119 (1988).

Eubanks, T. M., Variations in the Orientation of the Earth, in Contributions of Space Geodesy to Geodynamics: Earth Dynamics, edited by D. E. Smith and D. L. Turcotte, *Am. Geophys. Un.*, Washington, D.C. , 1-54 (1993).

Gross, R. S., and U. J. Lindqwister, Atmospheric Excitation of Polar Motion during the GIG'91 Measurement Campaign, *Geophys. Res. Lett.*, 19, 849-852 (1992).

Gross, R. S., The Effect of Ocean Tides on the Earth's Rotation as Predicted by the Results of an Ocean Tide Model, *Geophys. Res. Lett.*, 20, 293-296 (1993).

Herring, T. A., and D. Dong, Current and Future Accuracy of Earth Orientation Measurements, *Proceedings of the AGU Chapman Conference on Geodetic VLBI: Monitoring Global Change*, ed. W. Carter (NOAA Technical Report NOS 137 NGS 49), 306-324 (1991).

Herring, T. A., D. Dong, and R. W. King, Sub-milliarcsecond Determination of Pole Position using Global Positioning System Data, *Geophys. Res. Lett.*, 18, 1893-1896 (1991).

Herring, T. A., and D. Dong, Measurement of Diurnal and Semidiurnal Rotation Vartions and Tidal Parameters of the Earth, *J. Geophys. Res.*, in press (1994).

Hide, R., Towards a Theory of Irregular Variations in the Length of the Day and Core-Mantle Coupling, *Phil. Trans. Roy. Soc.*, A284, 547-554 (1977).

Hide, R., Rotation of the Atmospheres of the Earth and Planets, *Phil. Trans. R. Soc. Lond.* A313, 107-121 (1984).

Hide, R., Presidential Address: The Earth's Differential Rotation, *Quart. J. Roy. Astron. Soc.*, 278, 3-14 (1986).

Hide, R. Fluctuations in the Earth's Rotation and the Topography of the Core-Mantle Interface, *Phil. Trans. Roy. Soc.*, A328, 351-363 (1989).

Hide, R., and J. O. Dickey, Earth's Variable Rotation, *Science*, 253, 629 (1991).

IERS Technical Note 14: Earth Orientation, Reference Frames and Atmospheric Excitation Functions, submitted for the *1992 IERS Annual Report*, edited by P. Charlot, Observatoire de Paris, Paris, 1993.

Kuehne, J. and C. R. Wilson, Terrestrial Water Storage and Polar Motion, *J. Geophys. Res.*, 96, 4337-4345 (1991).

Lambeck, K., *Geophysical Geodesy, The Slow Deformation of the Earth*, Clarendon Press, Oxford (1988).

Lambeck, K., Changes in Length of Day and Atmospheric Circulation, *Nature*, 286, 104 (1980).

Lichten, S. M., S. L. Marcus, and J. O. Dickey, Sub-Daily Resolution of Earth Rotation Variations with Global Positioning System Measurements, *Geophys. Res. Lett.*, 19, 536-540 (1992).

Lindqwister, U. J., A. P. Freedman, and G. Blewitt, Daily Estimates of the Earth's Pole Position with the Global Positioning System, *Geophys. Res. Lett.*, 19, 845-848 (1992).

Moritz, H., and I. I. Mueller, *Earth Rotation: Theory and Observation*, The Ungar Publishing Co., New York (1987).

Munk, W. H., and G. J. F. MacDonald, *The Rotation of the Earth*, Cambridge University Press, 1960.

Ponte, R. M., Barotropic Motions and the Exchange of Angular Momentum Between the Oceans and Solid Earth, *J. Geophys. Res.*, 95, 11, 369-11, 374 (1990).

Rosen, R. D., D. A. Salstein, T. M. Wood, Discrepancies in the Earth-Atmosphere Angular Momentum Budget, *J. Geophys. Res.*, 95, 265-279 (1990).

Rosen, R. D., The Axial Momentum Balance of Earth and Its Fluid Envelope, *Surveys Geophys.*, 14, 1-29 (1993).

Salstein, D. A., D. M. Kann, A. J. Miller, and R. D. Rosen, The Sub-Bureau for Atmospheric Angular Momentum of the International Earth Rotation Service: A Meteorological Data Center with Geodetic Applications, *Bull. Amer. Meteor. Soc.*, **74**, 67-80 (1993).

Salstein, D. A. and D. M. Kann, in Developments at the Sub-Bureau for Atmospheric Angular Momentum of the IERS, *Proceedings of the AGU Chapman Conference on Geodetic VLBI: Monitoring Global Change*, ed. W. Carter, NOAA Technical Report NOS 137 NGS49, Wasington, D. C., 228-237 (1991).

Salstein, D. A. and R. D. Rosen, Topographic Forcing of the Atmosphere and a Rapid Change in the Length-of-Day, *Science*, 264, 407-409 (1994).

Seiler, U., Periodic Changes of the Angular Momentum Budget Due to the Tides of the World Ocean, *J. Geophys. Res.*, 96, 10287-10300 (1991).

Sovers, O. J., C. S. Jacobs, and R. S Gross, Measuring Rapid Ocean Tidal Earth Orientation Variations with VLBI, *J. Geophys. Res.*, 98, 19,959-19,971 (1993).

Wahr, J. M., The Earth's Rotation, *Ann. Rev. Earth Planet Sci.*, 16, 231-249 (1988).

Watkins, M. M., R. J. Eanes, Diurnal and Semidiurnal Variations in Earth Orientation Determined from LAGEOS Laser Ranging, *J. Geophys. Res.*, in press (1994).

Wünsch, J, and U. Seiler, Theoretical Amplitudes and Phases of the Periodic Polar Motion Terms Caused by Ocean Tides, *Astron. Astrophys.*, 266, 581–587 (1992).

Yoder, C. F., M. W. Parke, and J. G. Williams, Tidal Variations of the Earth's Rotation, *J. Geophys. Res.*, 86, B2, 881-891 (1981).

Prof. Dr. Peter Brosche
Sternwarte der Universität Bonn, Germany

The angular momentum content of the oceans

While energy has microscopic sources and sinks, the angular momentum is a mechanical quantity which is *macroscopically* conserved. Therefore it is especially suited for the description and understanding of large mechanical systems like the Earth with its 3 main constituents: solid Earth, atmosphere and oceans. Table 1 shows the order of magnitude of the 3 contributions to the average rotation of the present Earth.

Note that the total angular momentum of the Earth-Moon-system is $34.0 \cdot 10^{33}$ kg m^2 s^{-1} (i.e., about 80% represented by the lunar orbit).

The contributions are practically proportional to the mass fractions since the angular velocity is the same for all three parts. Only the larger mean distance from the axis enhances the role of the two last shares (about twice as much for a homogeneous spherical surface than for the actual mass distribution of the whole Earth). The dominant role of the solid Earth ensures the high degree of constancy (or regularity) of Earth' rotation; therefore it served as *the* time standard for most of the human history.

Table 1
Average values

	Mass [kg]	Moment of inertia [kg m^2]	Angular momentum [kg m^2 s^{-1}]
Whole Earth ≈ solid Earth	6.0×10^{24}	8.1×10^{37}	5.9×10^{33}
Oceans	1.4×10^{21}	3.9×10^{34}	2.8×10^{30}
Atmosphere	5.1×10^{18}	1.4×10^{32}	1.0×10^{28}

The main causes of variability, detected by ever refined clocks and angular measurements, are connected with the two outer nonsolid parts despite of their small mass fractions. Moreover, the relative role of oceans and atmosphere is reversed from Table 1 to Table 2 exhibiting the variations.

The key for this lies in the occurence of much greater *relative motions* in the atmosphere as compared with the oceans.

All but the values of the last line in Table 2 mean amplitudes of periodical changes.

In passing by we should mention that the comparison of

Table 2
Variations

	Torque [kg m^2 s^{-2}]	Angular momentum [kg m^2 s^{-1}]	Corresponding change in Universal Time of the solid Earth [ms]
Atmosphere seasonal	5×10^{18}	2.4×10^{25}	21
Oceans			
seasonal	3×10^{17}	1.5×10^{24}	1
tidal (M 2)	3.4×10^{21}	2.4×10^{25}	0.03
Secular retardation of the whole Earth by tidal friction	5×10^{16} (constant)	1.5×10^{24} (loss per year)	3 (change for 1 year)

Reprinted from Wiss. Z. Techn. Univers. Dresden 42 (1993) H. 6

rotational effects by 'size' is a matter of the level of time derivatives: (1) rotation angle (Universal Time), (2) angular velocity (length of day, angular momentum), (3) angular acceleration (torque).

Especially in case of periodic torques of period P and amplitude L_0 it is clear that the amplitudes of level (1), (2) are proportional to L_0P^2 and L_0P respectively. This means that any ordering by the *magnitude* of the effects depends on that level as well.

The changes associated to the oceans could be sorted in a variety of manners:

First by the causes (extraterrestrial or not), second by the time scales (from 1/2 day to infinity) and third by the magnitude of an affected (observed) parameter.

Let us follow the first path. *Exchanges of angular momentum between atmosphere, oceans and solid Earth* are an almost *internal* affair of the Earth. The total angular momentum, i.e. the sum over the 3 constituents is then conserved. This, however, is the only alleviation within an otherwise very complex situation. We are dealing with a so far underexposed branch of weather and climate. From Table 2 we see that the seasonal oceanic effects are of the order of 10% of the atmospheric ones – and this size at present enters the area of measurability! Therefore and for the principal reason of understanding the angular momentum balance in weather and climate problems, now it is indispensable to attack the problem of the distribution and transfer of the oceanic share. Our present state of the art is based on very elaborated numerical hydrodynamical models of the oceans currently used at the Max-Planck-Institut für Meteorologie in Hamburg (eleven depth levels, 3°.5 × 3°.5 mesh size of surface discretization). Our and other models show clearly that the exchange of angular momentum between oceans and solid Earth takes place mainly by the so-called side pressure of the oceans acting on their continental boundaries. This is the analogy to the 'mountain torque' between atmosphere and solid Earth. With regard to the exchange between oceans and atmosphere, a purely theoretical approach is not possible, since, as we all know, our present science is not able to predict the behaviour of the atmosphere for more than a few days. Therefore these models use *empirical wind data* as input.

The surface wind stresses are responsible for the transfer between oceans and atmosphere. We have got results for the average saisonal variation of the winds [1]. At present we try to obtain the effects of the actual wind fields of the last 10 years, since those are the ones for which Earth' rotation is measured with high-precision VLBI. In order to achieve this goal it is not sufficient to run the model for the same years. The oceans have a very long 'memory' of their previous states. Theoretically one should start with a 'state' which implies also all necessary time derivatives as well. In practice, one tries to get the same by integrating over a long time interval with *average* saisonal variations before applying the actual winds. This last part is then used for the comparison with Earth rotation data.

The closure condition for the total angular momentum is especially easy and separable for the axial component. The sum of the angular momenta of the solid Earth J_s and the atmosphere J_A today is observed accurate enough to reveal its non-constancy (see e.g. [2]). Despite of relatively large errors of this partial sum, we would expect some signal in it and that should be mirror-like to the oceanic angular momentum J_0 – so that the total sum is constant. Until now we have found correlation coefficients around

$$r(-J_0, J_S + J_A) \approx +0.30 \pm 0.09$$

thus only slightly significant [3], see Fig. 1.

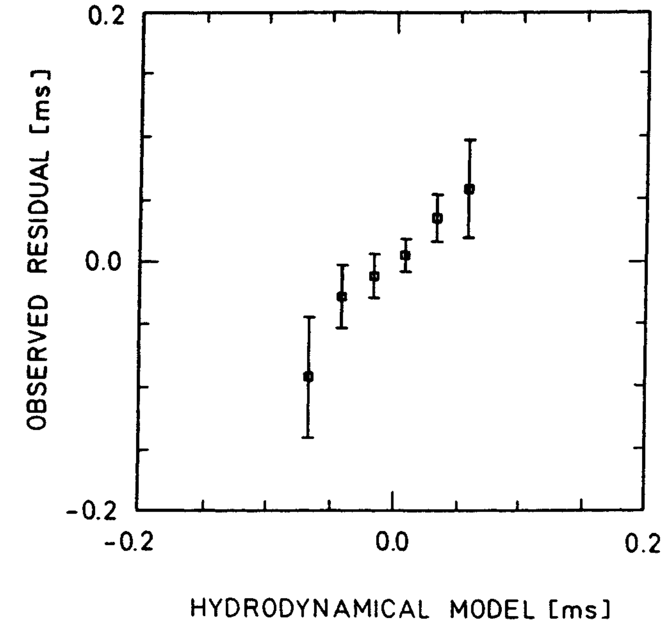

Fig. 1. After subtraction of the mean seasonal variation for the epoch 1981 – 1989, the residual theoretical values of $-J_0$ are compared with the residual observed ($J_S + J_A$), both expressed as differences in the length of day and averaged in intervals of $-J_0$.

Since the signature of very important climate events (such as El Nino) has been claimed to be visible in Earth rotation data, it is appealing to look for it in the J_0-results. However, today we cannot say whether the visible peaks in J_0 are only attributable to such an event or to other causes as well.

Let us now turn to a second kind of variations, *the periodic effects of lunar and solar tides*. Although of extraterrestrial origin (and thereby augmenting the number of participating constituents) their treatment is easier for the following reason. Moon and Sun produce forced oscillations in the oceans with the following properties:

(a) The exchange of angular momentum with the disturbing bodies is small; hence the Earth may be seen as a closed system even in this case.
(b) Unlike the surface wind stresses of the foregoing case, the tidal forces are body forces and affect the whole ocean at once. The changes at the surface are small and an exchange with the atmosphere for this reason may be neglected; the exchange with the solid Earth is the only remaining. Practically we are dealing with a two-component system and we expect associated mirror-like changes in oceans and solid Earth.
(c) The periods of the main partial tides are different from other influences so that a separate determination is possible. Especially the solar day (S_1) is not a frequency of our 10 most important tides.
(d) Solid Earth tides do not interfere because the solid Earth is rather symmetric.

The combination of this advantages has allowed us to confirm the existence of these oceanic effects at a 4σ-level despite of their smallness (0.1 ms in *UT* or a few cm in the position of an equatorial point in space). Fig. 2 compares theory and observations.

Finally, let me briefly mention the secular transfer of angular momentum from the whole Earth into the lunar orbit, better known as *tidal friction*. The physical process is the same as in the foregoing case. Here we are looking at it, however, in the long run. Then the Earth alone is not a closed system

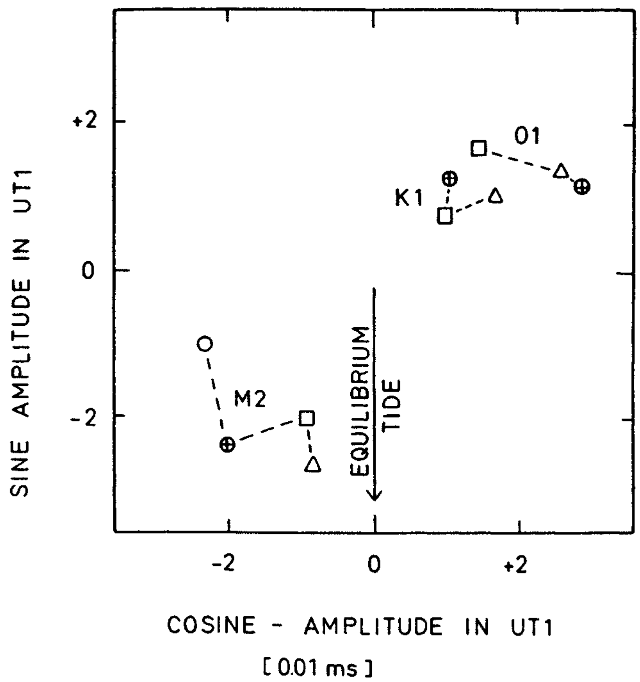

Fig. 2. Periodical effects in UT1 due to oceanic tides: VLBI observations (□ Bonn group [4], Δ HERRING & DONG [5]) versus hydrodynamical models (⊕ 1° mesh size [9] and, for comparison, ○ an elder one with 4° mesh size only for M_2 [7])

anymore. Small amounts of angular momentum transferred per tidal period *accumulate* within millenia of human history into *UT* changes of hours and change the length of day itself by hours if we go back, e.g. to the Devonian epoch of our Earth' history. It is clear then that these changes must have influenced the Earth' evolution in many ways: the length of day is a primary meteorological parameter, its variation causes concomitant changes in the figure of the Earth and these metamorphoses must have left its signatures in the crust. Ultimately, when going further backwards in time the earliest state of the Earth-Moon-system should be arrived.

For this problem, the oceans have been recognized as the main mediators of the transfer of angular momentum, while the phase lag angle of the solid Earth tides is not large enough for a significant share. The present transfer is shown by historical observations of solar eclipses and lunar laser ranging (LLR). Despite of its smallness, it is quite satisfyingly explained by accurate tidal models (see last line in Table 2).

The large remaining problem is the time dependence of the transfer torque. It is sure that schematic formulae cannot be applied for two reasons: (a) the geometry of the oceans changes through continental drift, (b) the oceans have a very rich eigenvalue spectrum and react very sensitively to such changes and to changes in length of day and tidal periods [8].

The observational evidence from paleontology and, most recent, sedimentology is very appealing. Some tide models for ancient oceans illustrate the potentialities of this kind of research – but its infancy as well [9].

References

[1] *P. Brosche; J. Wünsch; A. Frische; J. Sündermann; E. Maier-Reimer; U. Mikolajewicz*: The Seasonal Variations of the Angular Momentum of the Oceans. Naturwissenschaften **77** (1990) 185

[2] *R. D. Rosen; D. A. Salstein,; T. M. Wood*: Discrepancies in the Earth-Atmosphere Angular Momentum Budget. J. Geophys. Res. **95** (1990) B1, 265

[3] Unpublished work with J. Segschneider and J. Wünsch

[4] *J. Wünsch; J. Bußhoff*: Improved observations of periodic UT1 variations caused by ocean tides. Astron. Astrophys. **266** (1992) 588. For details, see also foregoing paper: *P. Brosche; J. Wünsch; J. Campbell; H. Schuh*: Ocean Tide Effects in Universal Time detected by VLBI. Astron. Astrophys. **245** (1991) 676

[5] Private communication. Differs only slightly from previous published work: *T. A. Herring; D. Dong*: 1991, In: *Carter, W. E.* (convenor) Proc. AGU Chapman Conference on Geodetic VLBI: Monitoring Global Change. NOAA Tech. Report NOS 137 NGS 49, p. 306

[6] *P. Brosche; U. Seiler; J. Sündermann; J. Wünsch*: Periodic Changes in Earth's Rotation due to Oceanic Tides. Astron. Astrophys. **220** (1989) 318

[7] *P. Brosche*: Oceanic tides and the Rotation of the Earth. In: Sun and Planetary System (Eds. *W. Fricke and G. Teleki*), Dortrecht 1982, p. 179. *H. R. Baader; P. Brosche; W. Hövel*: Ocean Tides and Periodic Variations of the Earth's Rotation. Zeitschrift für Geophysik **52** (1983) 140

[8] *P. Brosche; W. Hövel*: Variations of the Tidal Torque in a 'Short' Time Scale. Naturwissenchaften **69** (1982) 241

[9] Most of the pertaining problems are adressed in the proceedings of three workshops in Bielefeld:
P. Brosche; J. Sündermann (eds.): Tidal Friction and the Earth's Rotation (Tagung am Zentrum für interdisziplinäre Forschung der Universität Bielefeld vom 26. bis 28. September 1977). Springer-Verlag Berlin – Heidelberg – New York 1978 ISBN 3-540-09046-0 and ISBN 0-387-09046-0.
Tidal Friction and the Earth's Rotation II (Tagung am Zentrum für interdisziplinäre Forschung der Universität Bielefeld vom 28. September bis 2. Oktober 1981). Springer-Verlag Berlin – Heidelberg – New York 1982. ISBN 3-540-12011-4 and ISBN 0-387-12011-4
Earth's Rotation from Eons to Days (Tagung am Zentrum für interdisziplinäre Forschung der Universität Bielefeld vom 26. bis 30. September 1988) Springer-Verlag Berlin – Heidelberg – New York 1990. ISBN 3-540-52409-6

Part II

IERS Reports

INTERNATIONAL EARTH ROTATION SERVICE (IERS)
SERVICE INTERNATIONAL DE LA ROTATION TERRESTRE

BUREAU CENTRAL DE L'IERS
OBSERVATOIRE DE PARIS
61, Av. de l'Observatoire 75014 PARIS (France)
Tél. (33) 1-40 51 22 26 Télex : 270776 OBS
Internet : iers @ iap.fr
Span : IAPOBS::IERS
FAX : (33) 1 - 40 51 22 32

9 November 1992

SEARCH'92/IGS'92 CAMPAIGN

COMPARISONS OF GPS, SLR, AND VLBI EARTH ORIENTATION DETERMINATIONS

(Final report)

Starting with IERS Bulletin B58, issued early December 1992 and covering October 1992, the GPS Earth Orientation Parameters will be introduced in the computation of the Central Bureau of IERS. Section 6 of Bulletin B will include statistics on the VLBI, LLR, GPS and SLR solutions received. The present Earth Orientation Bulletin is the last one issued in support to the IGS'92 campain.

GPS: TERRESTRIAL FRAME ORIENTATION FIXING

Various strategies are tested by the GPS Processing Centres for maintaining the terrestrial frame orientation. The choices concern the nominal orientation (ITRF90 or ITRF91), the site motion model used to transfer the coordinates at the reference epoch, the number of fiducial stations that are fixed, and the source from which the fixed coordinates are taken. We summarize in Table 1 our understanding of the terrestrial frame definitions according to the Centres and to the time periods.

Table 1
GPS SOLUTIONS: TERRESTRIAL FRAME ORIENTATION

Series (IERS label)	MJD from to	GPS weeks	Nominal refrnce	Source	
EOP(CODE) 92 P 04	48792-48923	650-668	ITRF91	IERS	(IGSMail 33)
EOP(CSR) 92 P 01	48794-48870	650-660		CSR+GSFC	(IGSMail 62)
EOP(EMR) 92 P 01	48838-48904	655-665	ITRF91	IERS	(IGSMAIL 90)
EOP(EMR) 92 P 02	48901-48911	655-666	ITRF91	IERS	(IGSMAIL 90)
EOP(ESOC) 92 P 01	48794-48912	650-666	ITRF91	IERS	(IGSMail 90)
EOP(GFZ) 92 P 01	48794-48821	650-653	ITRF90	SIO	(01/91-05/92)
EOP(GFZ) 92 P 02	48822-48918	654-667	ITRF90	SIO	(IGSMail 56)
EOP(JPL) 92 P 01	48794-48821	650-653	ITRF90	JPL	(GIG'91+VLBI vel.)
EOP(JPL) 92 P 02	48820-48918	654-667	ITRF91	IERS	(IGSMail 90)
EOP(SIO) 92 P 03	48780-48918	648-667	ITRF90	SIO	(51 IGS'92 days)

VLBI, LLR, SLR, GPS EOP DETERMINATIONS: AGREEMENT WITH THE IERS SYSTEM

In this section, the VLBI, LLR, SLR, and GPS observations available over the time period of the IGS'92 Campaign and its continuation (MJD 48779-48923) are compared to the IERS series EOP(IERS) 90 C 04, which is a combination of the series of Table 2.

Table 2
IERS OPERATIONAL SERIES OF EOP

Techn.	Series	Time span	Time interv.	EOP determined
VLBI	EOP(NOAA) 92 R 01	24 h	3/4 d	x, y, UT1, dPsi, dEps
VLBI	EOP(NOAA) 92 R 02	1 h	1/2 d	UT1
VLBI	EOP(USNO) 92 R 03	24 h	7 d	x, y, UT1, dPsi, dEps
LLR	EOP(UTXMO) 92 M 02	1 h	0.1/30d	UT1
SLR	EOP(CSR) 91 L 01	72 h	3 d	x, y, "UT1"
SLR	EOP(DUT) 91 L 02	120 h	5 d	x, y, "UT1"

The GPS series are those listed in Table 1. They give the x,y coordinates of the pole, except CODE, which gives a series of UT1 that is tied at the beginning of the complete series to an a priori value,and the new EMR series, whith UT1 tied to an a priori value at the beginning of each week. The "UT1" determinations obtained by the SLR Analysis Centre at DUT is left free, whereas in the CSR SLR solution, it is tied to a VLBI solution for periods longer than about 60 days.

The GPS results are obtained from one-day observations of 16 to 18 satellites in a network of 11 to 29 stations: 14-19 for CODE, 14-20 for CSR, 17-18 for EMR, 11-18 for ESOC, 22-27 for JPL, and 17-29 for SIO.

Most of the centres treat independently the successive daily arcs, the exceptions being CODE (three-day overlapping arcs) and GFZ (two-day overlapping arcs). The centres estimate the EOP at 12h UT.

Table 3 gives the differences of the VLBI, SLR,and GPS series with EOP(IERS) 90 C 04 under the form of a constant bias, corrected for the predicted value of the systematic difference. In the case of the GPS results, which are referred directly to ITRF, the predicted bias and its uncertainty are derived from Table I-3, p.II-13 of the 1991 IERS Annual Report. It reflects the slight misalignment of the IERS EOP relative to the IERS terrestrial frame. In the case of the SLR and VLBI results, the expected values are derived from analyses of previous years results.

Table 3
SYSTEMATIC DIFFERENCES OF EOP RESULTS WITH IERS

Techn	Series	x (0.001")	y(0.001")	UT1(0.0001s)	Nmes
VLBI	EOP(NOAA) 92 R 01	-0.15 ± 0.08	-0.03 ± 0.09	0.00 ± 0.06	39
VLBI	EOP(NOAA) 92 R 02			0.11 ± 0.05	90
VLBI	EOP(USNO) 92 R 03	-0.43 ± 0.06	-0.12 ± 0.08	0.03 ± 0.06	27
LLR	EOP(UTXMO) 92 M 02			-0.91 ± 0.29	17
SLR	EOP(CSR) 91 L 01	0.09 ± 0.07	0.17 ± 0.05	0.10 ± 0.09	48
SLR	EOP(DUT) 91 L 02	0.98 ± 0.18	-0.84 ± 0.21		29
GPS	EOP(CODE) 92 P 04	-0.31 ± 0.36	-0.07 ± 0.45		122
GPS	EOP(CSR) 92 P 01	-0.18 ± 0.37	2.46 ± 0.48		69
GPS	EOP(EMR) 92 P 01	-0.44 ± 0.45	1.08 ± 0.46		44
GPS	EOP(EMR) 92 P 02	0.71 ± 0.39	-0.22 ± 0.46		8
GPS	EOP(ESOC) 92 P 01	1.01 ± 0.38	0.01 ± 0.48		112
GPS	EOP(GFZ) 92 P 01	-2.68 ± 0.43	-3.29 ± 0.56		27
GPS	EOP(GFZ) 92 P 02	+1.68 ± 0.36	1.92 ± 0.45		
68					
GPS	EOP(JPL) 92 P 01	-0.19 ± 0.38	1.51 ± 0.50		28
GPS	EOP(JPL) 92 P 02	0.09 ± 0.35	0.14 ± 0.45		79
				LOD: 0.16 ± 0.15	43
GPS	EOP(SIO) 92 P 03	0.35 ± 0.35	1.68 ± 0.44		137

GPS: FORMAL AND ESTIMATED UNCERTAINTIES

The correlation of high frequency variations in the GPS polar motion results was estimated on the basis of the residuals of each series of daily values relative to its own smoothing (frequency cutoff: 1 cycle/10 days). The common time intervals between two series cover 17 to 109 days. No significant correlation was found.

Using the days which are common to pairs of series without change of reference system, we estimate the true uncertainty of the daily EOP values by the Allan variance (or pair variance) based on the 15 series of differences two by two (see the 1991 IERS Annual Report, p.II-52). Table 4 shows the uncertainties thus estimated for every GPS series, together with the corresponding rms formal uncertainty provided by the Processing Centre.

Table 4
ESTIMATED AND FORMAL UNCERTAINTY OF DAILY GPS POLAR MOTION VALUES

Techn	Series	x (0.001")		y(0.001")		Nmes
		estim.	formal	estim.	formal	
GPS	EOP(CODE) 92 P 04	0.50	0.13	0.58	0.13	66
GPS	EOP(CSR) 92 P 01	0.59	0.20	0.69	0.20	75
GPS	EOP(EMR) 92 P 01	0.69	0.55	0.49	0.37	66
GPS	EOP(EMR) 92 P 02	0.48	0.23	0.39	0.20	8
GPS	EOP(ESOC) 92 P 01	1.02	0.39	1.14	0.42	82
GPS	EOP(GFZ) 92 P 01	1.11	0.86	1.11	0.89	26
GPS	EOP(GFZ) 92 P 02	0.75	0.47	0.40	0.52	66
GPS	EOP(JPL) 92 P 01	0.37	0.25	0.47	0.30	26
GPS	EOP(JPL) 92 P 02	0.10	0.21	0.42	0.23	66
GPS	EOP(SIO) 92 P 03	0.38	0.33	0.22	0.30	82

VLBI, LLR, SLR, GPS EOP DETERMINATIONS: DAY-TO-DAY AGREEMENT WITH IERS

The series of EOP obtained by VLBI, LLR, SLR and GPS already considered in Table 3 are considered now under the form of the weighted rms residual to EOP(IERS) 90 C 04, after the biases of Table 2 are taken out. The statistics are listed in Table 5.

Table 5
WEIGHTED RMS DIFFERENCES OF EOP RESULTS WITH EOP(IERS) 90 C 04
The biases of Table 3 are taken out.

Techn Nmes	Series	x (0.001")	y(0.001")	UT1(0.0001s)	
VLBI	EOP(NOAA) 92 R 01	0.47	0.58	0.36	39
VLBI	EOP(NOAA) 92 R 02			0.48	90
VLBI	EOP(USNO) 92 R 03	0.30	0.42	0.29	27
LLR	EOP(UTXMO) 92 M 02			1.18	17
SLR	EOP(CSR) 91 L 01	0.47	0.37	0.62 (1)	48
SLR	EOP(DUT) 91 L 02	0.90	1.08	3.41 (2)	29
GPS	EOP(CODE) 92 P 04	0.83	0.89	0.89 (3)	132
GPS	EOP(CSR) 92 P 01	0.90	1.57	2.73	69
GPS	EOP(EMR) 92 P 01	1.45	0.80		44
GPS	EOP(EMR) 92 P 02	0.49	0.39		8
GPS	EOP(ESOC) 92 P 01	1.29	1.73		112
GPS	EOP(GFZ) 92 P 01	1.35	1.83		27
GPS	EOP(GFZ) 92 P 01	1.04	0.72		76
GPS	EOP(JPL) 92 P 01	0.72	1.31		28
GPS	EOP(JPL) 92 P 02	0.42	0.48		78
				LOD : 0.99	43
GPS	EOP(SIO) 92 P 03	0.67	0.62		137

Notes : 1 - CSR - Referred to VLBI in the long term (p > 60 d).
2 - DUT - With a drift of +0.027 ms/d and a quadratic term taken out.
3 - CODE - With a drift of +0.045 ms/d, a quadratic term and a 92d periodic term taken out.

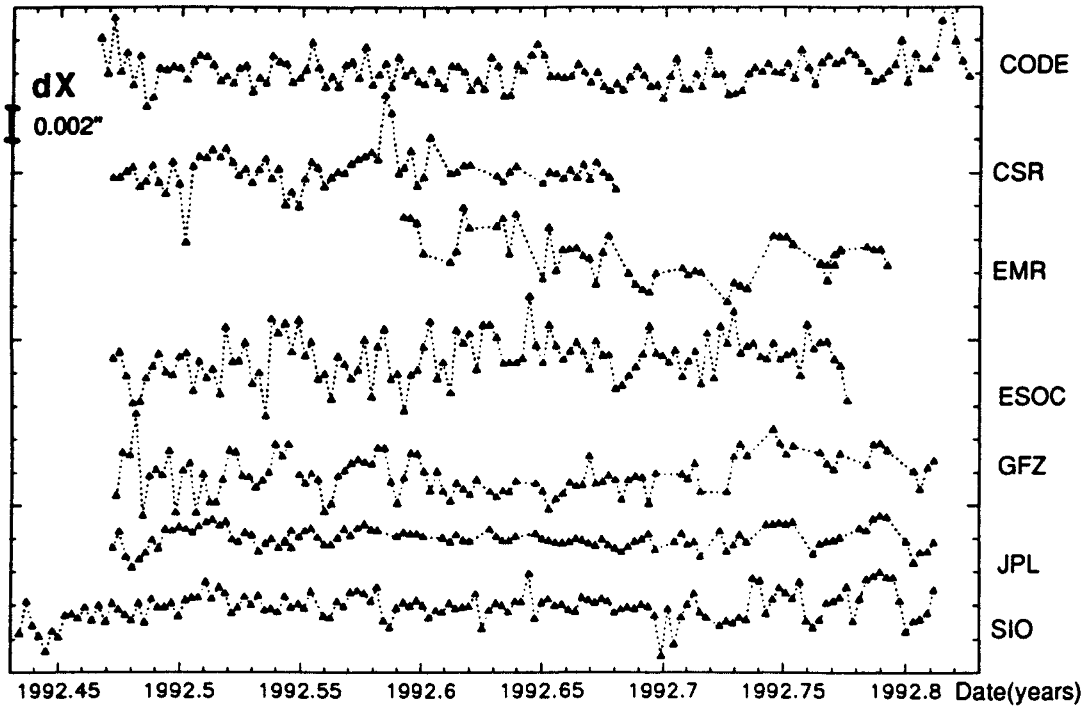

Fig. 1 Differences of the GPS series of the x coordinate of the pole with EOP(IERS) 90 C 04

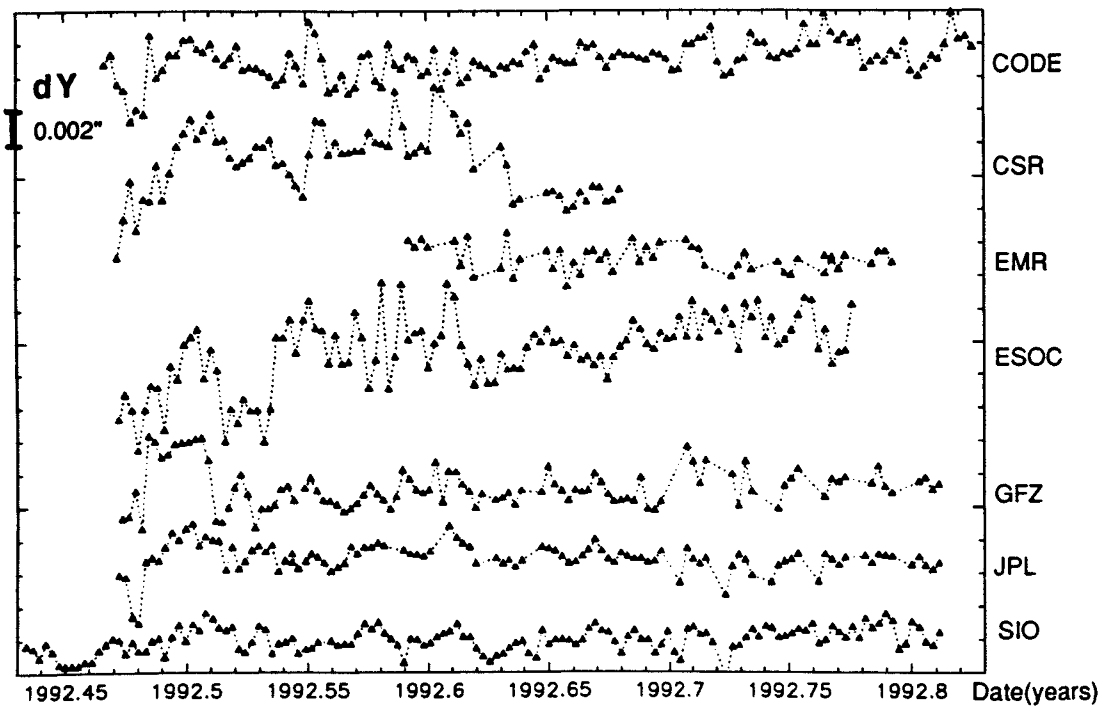

Fig. 2 Differences of the GPS series of the y coordinate of the pole with EOP(IERS) 90 C 04

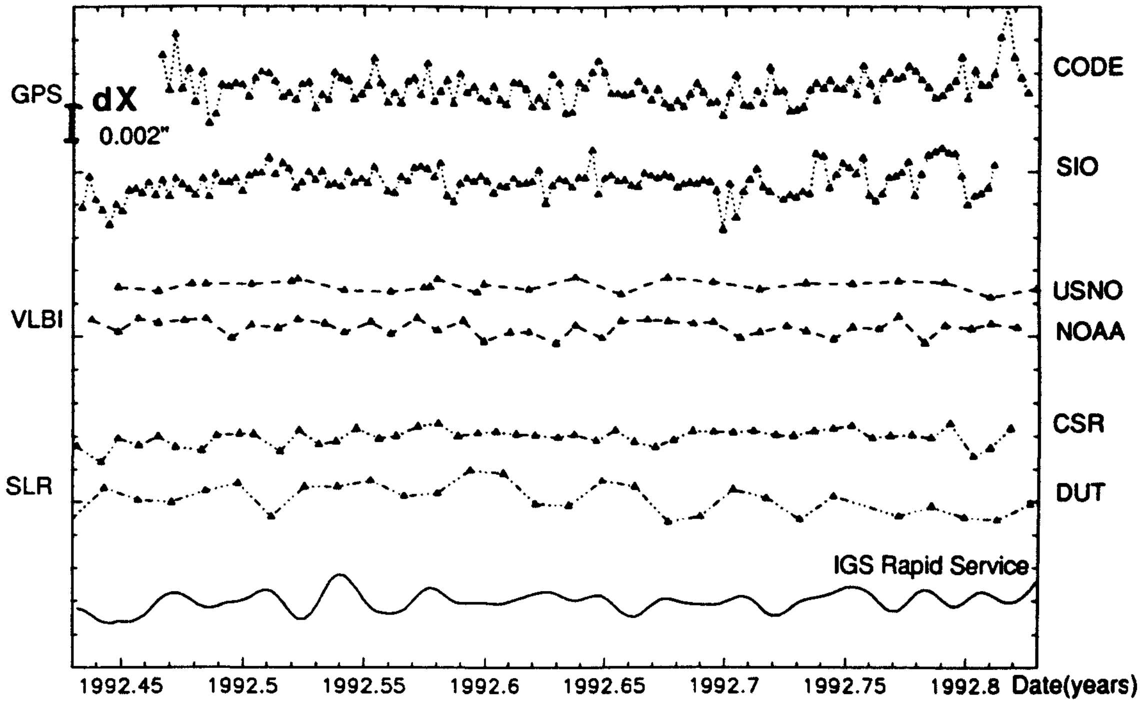

Fig. 3 Differences of GPS, SLR, VLBI, and Rapid Service series of the x coordinate of the pole with EOP(IERS) 90 C 04

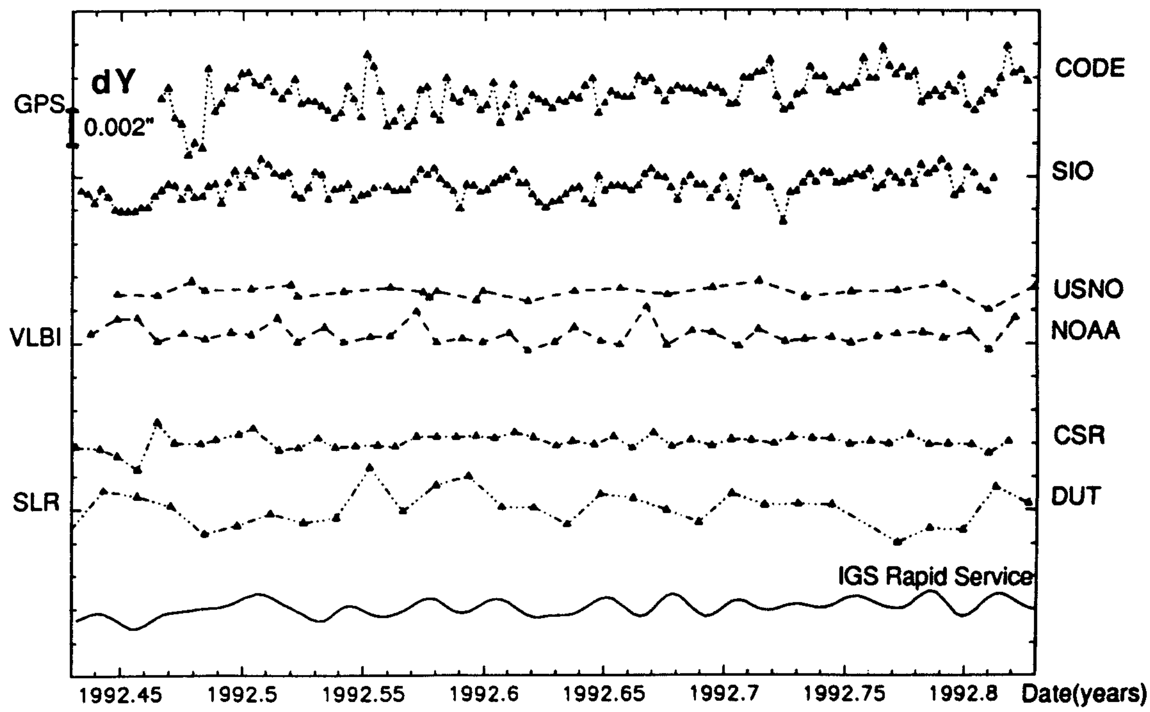

Fig. 4 Differences of GPS, SLR, VLBI, and Rapid Service series of the y coordinate of the pole with EOP(IERS) 90 C 04

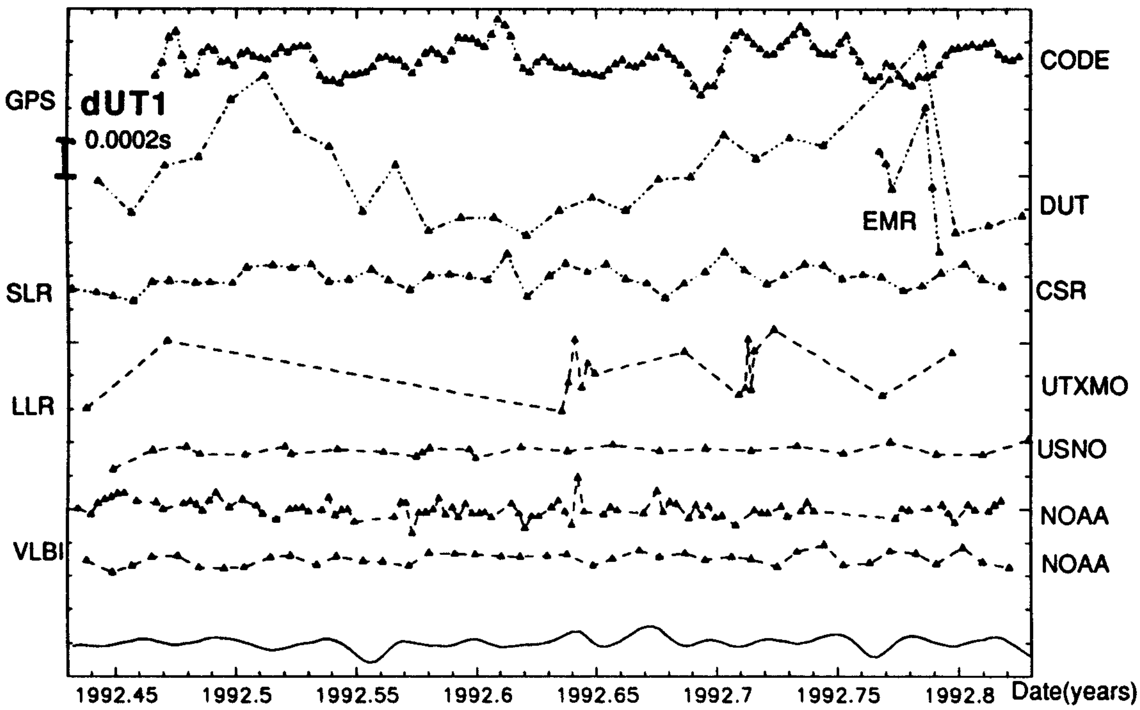

Fig. 5 Differences of GPS, SLR, VLBI, and Rapid Service series of Universal time with EOP(IERS) 90 C 04

Notes : 1 - CSR - Referred to VLBI in the long term (p > 60 d).
2 - DUT - With a drift of +0.027 ms/d and a quadratic term taken out.
3 - CODE - With a drift of +0.045 ms/d, a quadratic term and a 92d periodic term taken out.

THE USE OF GPS EARTH ORIENTATION DATA BY THE INTERNATIONAL EARTH ROTATION SERVICE SUB-BUREAU FOR RAPID SERVICE AND PREDICTIONS

Dennis D. McCarthy
U. S. Naval Observatory
Washington, DC 20392 USA

The International GPS Service provides polar motion data which have become an important contribution to the operation of the International Earth Rotation Service (IERS) Sub-bureau for Rapid Service and Predictions. Comparison with other techniques shows that these data provide estimates of the position of the rotational pole with an accuracy of approximately ± 0.5 milliseconds of arc. This accuracy along with the fact that the daily data are available soon after observation could make this source of data a valuable addition to the contributors to the IERS.

INTRODUCTION

Analyses of the orbits of the satellites of the Global Positioning System (GPS) by participants in the International GPS Service (IGS) (Mueller and Beutler, 1992) have provided daily observations of high-accuracy polar motion described by the pole coordinates, x along the Greenwich meridian, and y along the meridian of ninety degrees west. These data are used routinely by the IERS Sub-bureau for Rapid Service and Prediction in its normal operations. The GPS data have also been analyzed by some centers to produce estimates of UT1-UTC. Because of unresolved apparent systematic error in these data, however, they are not being used operationally by the Sub-bureau. Also, a longer series of GPS Earth orientation information is required to assess the value of the data in maintaining a reference system over a long period of time. The purpose of this paper is to provide an assessment of these observations and show how this information is used currently.

The National Earth Orientation Service (NEOS) serves as the IERS Sub-bureau for Rapid Service and Predictions. It is comprised of the U. S. Naval Observatory and the National Ocean Services of the National Oceanic and Atmospheric Administration of the United States. Each week NEOS publishes, in IERS Bulletin A, information for approximately 350 users regarding the orientation of the Earth with respect to a celestial reference frame. These data are near real-time estimates of the orientation of the Earth as well as their predictions. This information is obtained from contributors who provide data obtained from very long baseline radio interferometry, laser ranging to satellites and the Moon, and now, from the analyses of GPS orbits.

SOURCES OF DATA

Daily estimates of pole positions have been provided by contributors to the IGS. These contributors include the Department of Energy, Mines, and Resources (EMR), the European Space Agency (ESOC), the GeoForschungsZentrum (GFZ), Jet Propulsion Laboratory (JPL), Scripps Institute of Oceanography, the University of Berne, and the University of Texas Center for Space Research. Estimates of UT1-UTC are contributed by EMR and the University of Berne.

ANALYSIS OF GPS DATA

The time series contributed by each of the institutions mentioned above were analyzed by comparing them with the National Earth Orientation Service (NEOS) combination series produced for the International Earth Rotation Service (IERS) Bulletin A. The data used to produce this series are derived from Very Long Baseline Interferometry (VLBI), Satellite Laser Ranging (SLR) and Lunar Laser Ranging (LLR). Figures 1 and 2 show plots of recent differences in polar motion after the removal of biases. Table 1 shows the statistical analysis of the polar motion data.

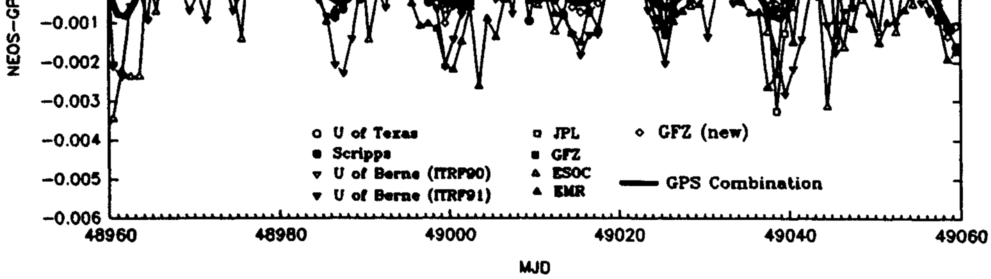

Figure 1. GPS data in x.

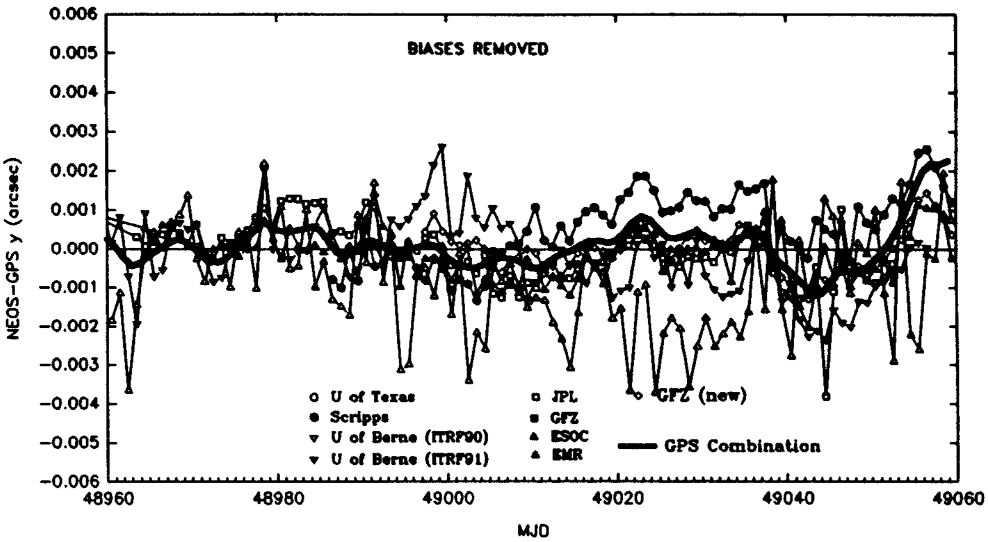

Figure 2. GPS data in y.

Table 1. Comparison of GPS data with NEOS. Units are milliseconds of arc.

Contributor	Data Span (MJD)	Points	Mean (NEOS-GPS) x	Mean (NEOS-GPS) y	Standard Deviation x	Standard Deviation y
U. of Texas	48794.5-48880.5	76	-1.89	-3.11	0.82	0.63
Scripps	48780.5-49052.5	236	-1.56	-0.81	0.65	0.67
U. of Berne (ITRF90)	48792.5-48799.5	8	-0.89	1.21	1.52	1.88
U. of Berne (ITRF91)	48800.5-49056.5	257	-0.51	-0.19	0.95	0.89
JPL'	48794.5-49045.5	220	-0.79	0.01	0.82	0.74
GFZ	48795.0-48925.5	107	-2.33	-1.99	1.13	1.12
ESOC	48794.5-49052.5	259	-1.17	-0.89	1.42	1.85
EMR	48838.5-49059.5	176	-1.06	0.32	1.07	0.74
GFZ (New Series)	48997.0-49059.5	63	1.89	-1.48	0.57	0.58

USE OF GPS DATA IN IERS BULLETIN A

The NEOS now makes use of GPS data contributed to the IERS in its combination series. This is done by smoothing the contributed data separately using algorithms similar to that used in the procedure to combine the VLBI, SLR and LLR data now (McCarthy and

Luzum, 1991). The smoothed fit is shown in Figures 1 and 2 as a thick solid line. Statistical weights are assigned to each of the contributors based on their past agreement with the NEOS combination series. Figures 3 and 4 show the agreement between the smoothed GPS estimates and those derived using data from other techniques for recent times.

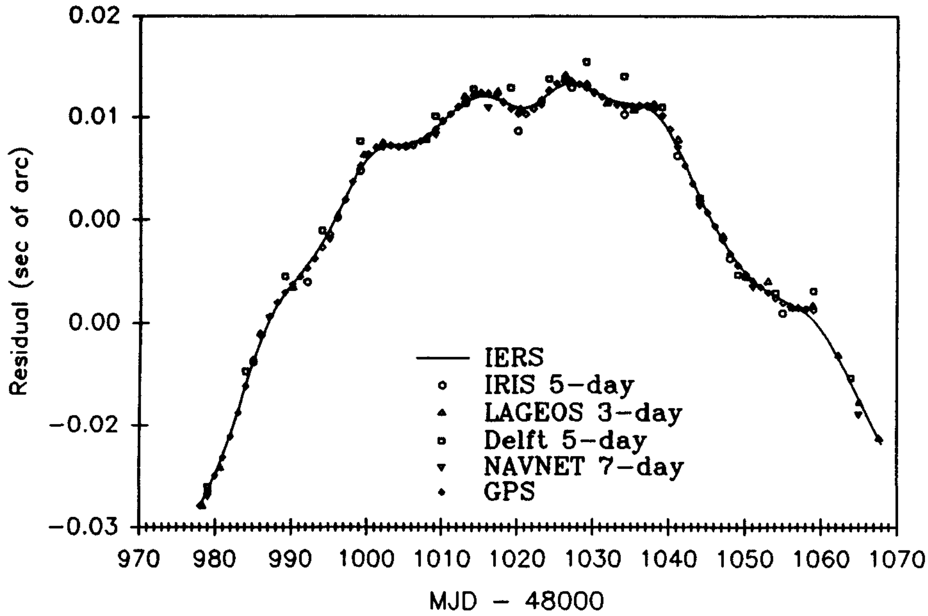

Figure 3. x minus a linear fit.

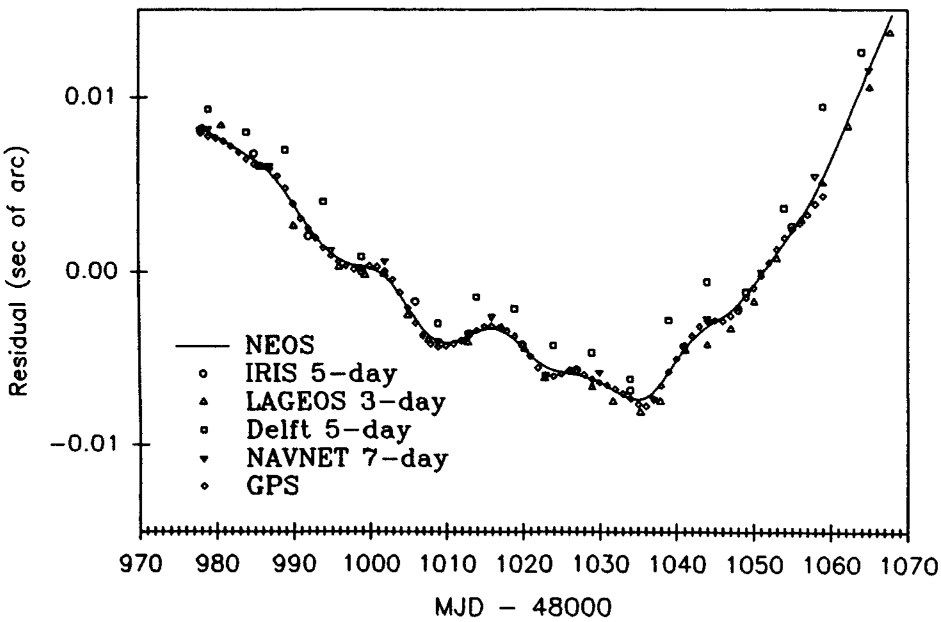

Figure 4. y minus a linear fit.

ACCURACY

Comparison with the other techniques shows that the combined GPS series has an accuracy of ±0.55 msec of arc in x and ±0.48 msec of arc in y. Figures 1 and 2 show that serious systematic differences between the contributors remain which must be resolved to obtain further improvement.

CONTRIBUTION TO RAPID SERVICE AND PREDICTIONS

The contribution to the rapid service estimates of polar motion and prediction are shown graphically in Figure 5. The term "contribution" is estimated by taking into account the frequency with which the data are reported, the adopted *a priori* accuracy of each contributor, and the time delay between the epoch of the last available data point and the date of the weekly publication. It is a measure of the overall weight of the data in the weekly solution.

The contribution of the GPS data to the long-term maintenance of the reference frame remains unclear. A longer series of data is required to assess the value of the information in preserving a reference system over an extended period.

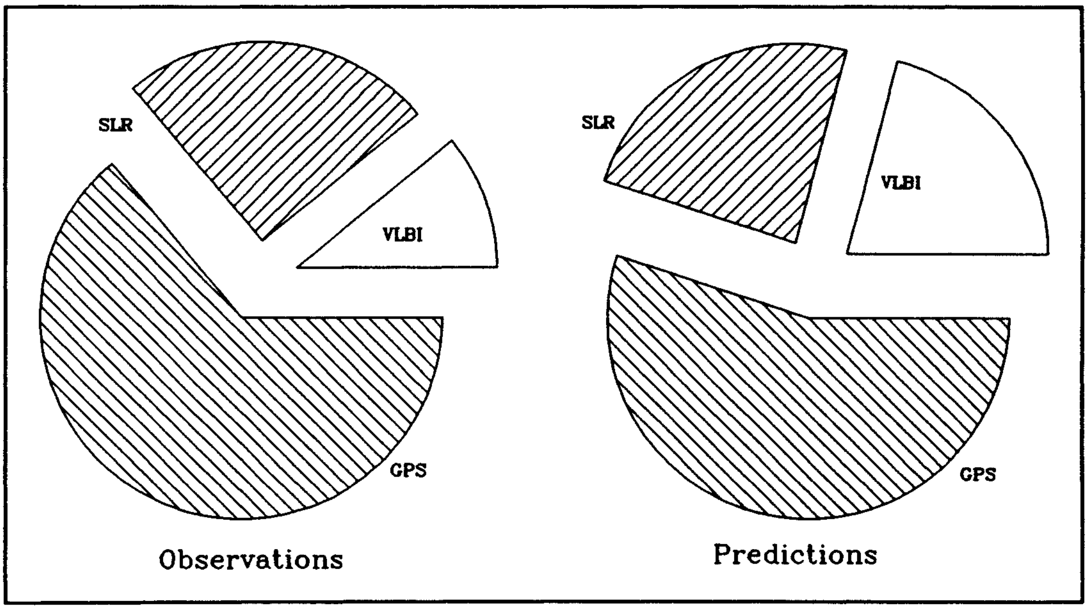

Figure 5. Contribution to rapid service and prediction.

REFERENCES

McCarthy, D. D. and Luzum, B. J. (1991). Combination of precise observations of the orientation of the Earth, *Bulletin Géodésique*, **65**, 22-27.

Mueller, I. I., and Beutler, G. (1992). The International GPS Service for Geodynamics - Development and Current Structure, *Proceedings of the Sixth International Geodetic Symposium on Satellite Positioning*.

ACTIVITIES OF THE SUB-BUREAU FOR ATMOSPHERIC ANGULAR MOMENTUM IN SUPPORT OF SEARCH'92

David A. Salstein
Atmospheric and Environmental Research, Inc.
840 Memorial Drive, Cambridge, MA 02139, USA

Deirdre M. Kann
Climate Analysis Center, National Meteorological Center
Washington, DC 20233, USA

ABSTRACT. This article describes the role that the Sub-bureau for Atmospheric Angular Momentum (SBAAM) of the International Earth Rotation Service (IERS) played during the special SEARCH'92 (Study of Earth-Atmosphere Rapid Changes) campaign. During this period, atmospheric angular momentum values and related parameters from all four participating meteorological centers were received and archived by the SBAAM. Also, values of components of the torques linking the atmosphere and its underlying surface were received from one of the centers. These data sets are most useful for studying the high-frequency dynamic interactions which were the focus of the SEARCH'92 campaign.

1. Introduction

During portions of the SEARCH'92 campaign, held during the three-month period 21 June-22 September 1992, the Sub-bureau for Atmospheric Angular Momentum received very high frequency atmospheric angular momentum data, at 6-hourly resolution, from three meteorological centers, the U.S. National Meteorological Center (NMC), the Japan Meteorological Agency (JMA), and the European Centre for Medium Range Weather Forecasts (ECMWF). Data from the fourth participating center, the United Kingdom Meteorological Office, was received at 12-hourly resolution. The atmospheric angular momentum parameters, which are related to Earth rotation, were made available to a network of international scientists, as well as to the IERS. In addition, personnel at the U.S. NMC have been producing values of the components of torques between the atmosphere and solid Earth, which are derived from the weather forecasting and analysis models.

2. SBAAM Parameters

Effective atmospheric angular momentum (EAAM) functions were developed by Barnes *et al.* (1983), who related atmospheric motions and mass distribution to Earth rotation and polar motion, and their use in an operational setting has been discussed by Salstein et al. (1993). The first two functions, χ_1 and χ_2, are the equatorial components and are associated with the excitation of polar motion. The axial component, χ_3, is involved with changes in the length of day. The functions can be further partitioned into contributions by wind and pressure. The calculation of wind contributions involves the computation of integrals over the depth of the atmosphere, which varies in the global models. Therefore, wind contributions to 100 hPa, as well as to the top of the model, were specified so that values from the various centers could more accurately be compared. Changes in the mass distribution, and hence the moment of inertia, of the atmosphere, are closely related to its two-dimensional surface pressure field. The pressure-related components from the centers can be compared without regard to the vertical construction of the model. A key issue is the extent to which an equilibrium response of the ocean modifies the changes in the pressure distribution felt by the solid Earth. At certain time scales, this inverted barometer (IB) response acts to reduce the equivalent angular momentum fluctuations of the atmosphere. Because the IB exists to at least a certain extent, calculations with a global IB correction are performed in parallel to the regular pressure terms. These excitation parameters are given at very high resolution for much of the SEARCH'92 period.

Other meteorological parameters are included in the Sub-Bureau files. Zonal mean zonal wind, from which the χ_3 term can be calculated, and zonal mean temperatures, whose gradients are related to overall zonal winds, are SBAAM analysis fields. Routine specification of the mass distribution of the atmosphere, expressed in low-order spherical harmonic expansions, is important in the study of various problems in geodynamics and geodesy, including the effects of mass redistribution on satellite orbits. These coefficients are also SBAAM fields.

The analysis file at high resolution is calculated either six-hourly (00, 06, 12, and 18 UTC) or twelve hourly (00 hr and 12 hr UTC), as specified, and consists of the following set of parameters:

1) hemisphere values of χ_1, χ_2, and χ_3, for wind to top of model, wind to 100 hPa, and pressure, and pressure + inverted barometer (6 hourly)

2) zonal mean zonal winds (m/s) at 5 degree latitude interals at 12 mandatory pressure levels (1000, 850, 700, 500, 400, 300, 250, 200, 150, 100, 70 and 50 hPa) (12 hourly)

3) zonal mean temperatures (K) at the same grid as the zonal mean zonal winds (12 hourly)

4) mean surface pressure (hPa) over the globe (6 hourly) ; and

5) low-order coefficients of surface pressure, including spherical harmonics in full triangular truncation to degree 4 and zonal harmonics to degree 20 (6 hourly).

In addition, forecasts of the EAAM functions are part of the normal SBAAM products. These are made at 12-hour lead times out to 10 days or to the limit of the model if less than 10 days. The 12-hour interval was selected so that models with different start times could be validated at the same time. The EAAM functions χ_1, χ_2, and χ_3, are globally integrated for wind to top of model, for wind to 100 hPa, for pressure, and for pressure + inverted barometer.

3. Results for the SEARCH'92 Period

Figs. 1a-1c show the excitation quantities for the three-month SEARCH'92 period from NMC, ECMWF, and JMA, the centers which have provided very high resolution analysis data. Some points to note are as follows. The winds terms are to the top level of the center, noted in the figures, and so vary from the different centers. Values are given at the highest temporal resolution possible.

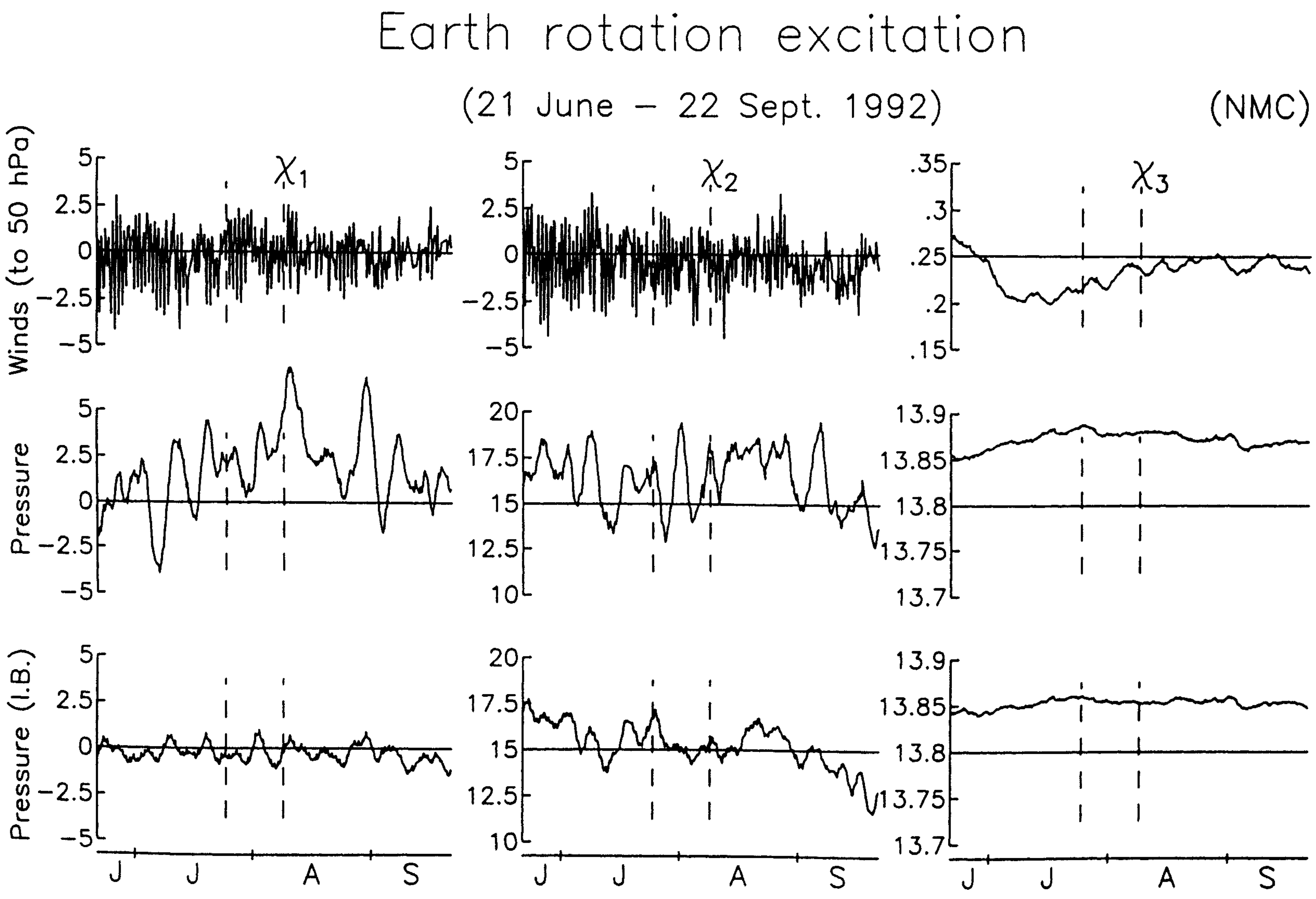

Figure 1a. Values of the global effective atmospheric angular momentum functions χ_1, χ_2, and χ_3 for wind, pressure, and pressure (inverted barometer) from the NMC analysis system for the whole period of SEARCH'92 (21 June-22 September 1992), given four times per day, as available. Units are non-dimensional multiplied by 10^{-7}. Vertical dashed lines denote the intensive period of the campaign.

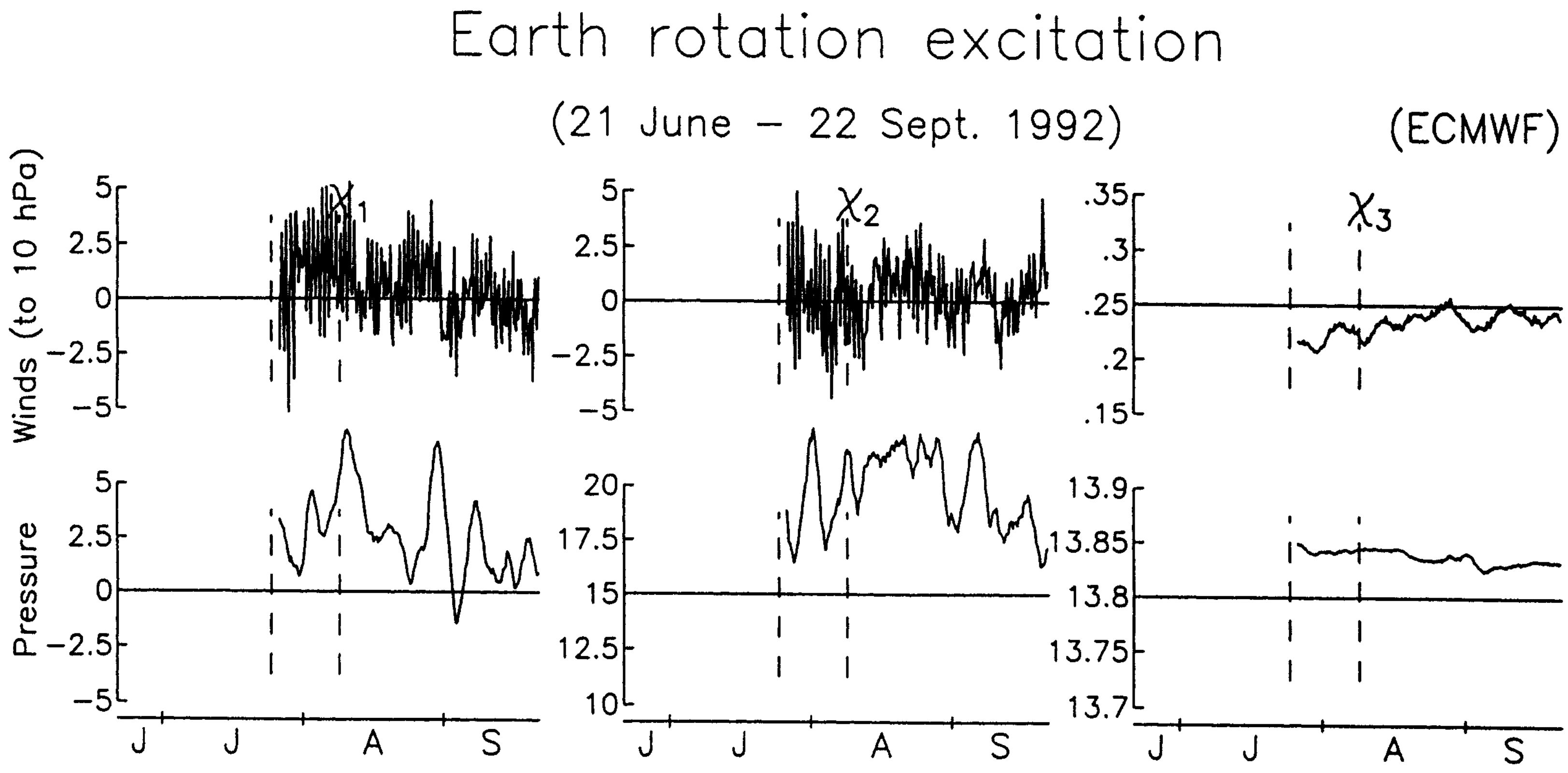

Figure 1b. Same as Figure 1a, but for the ECMWF system.

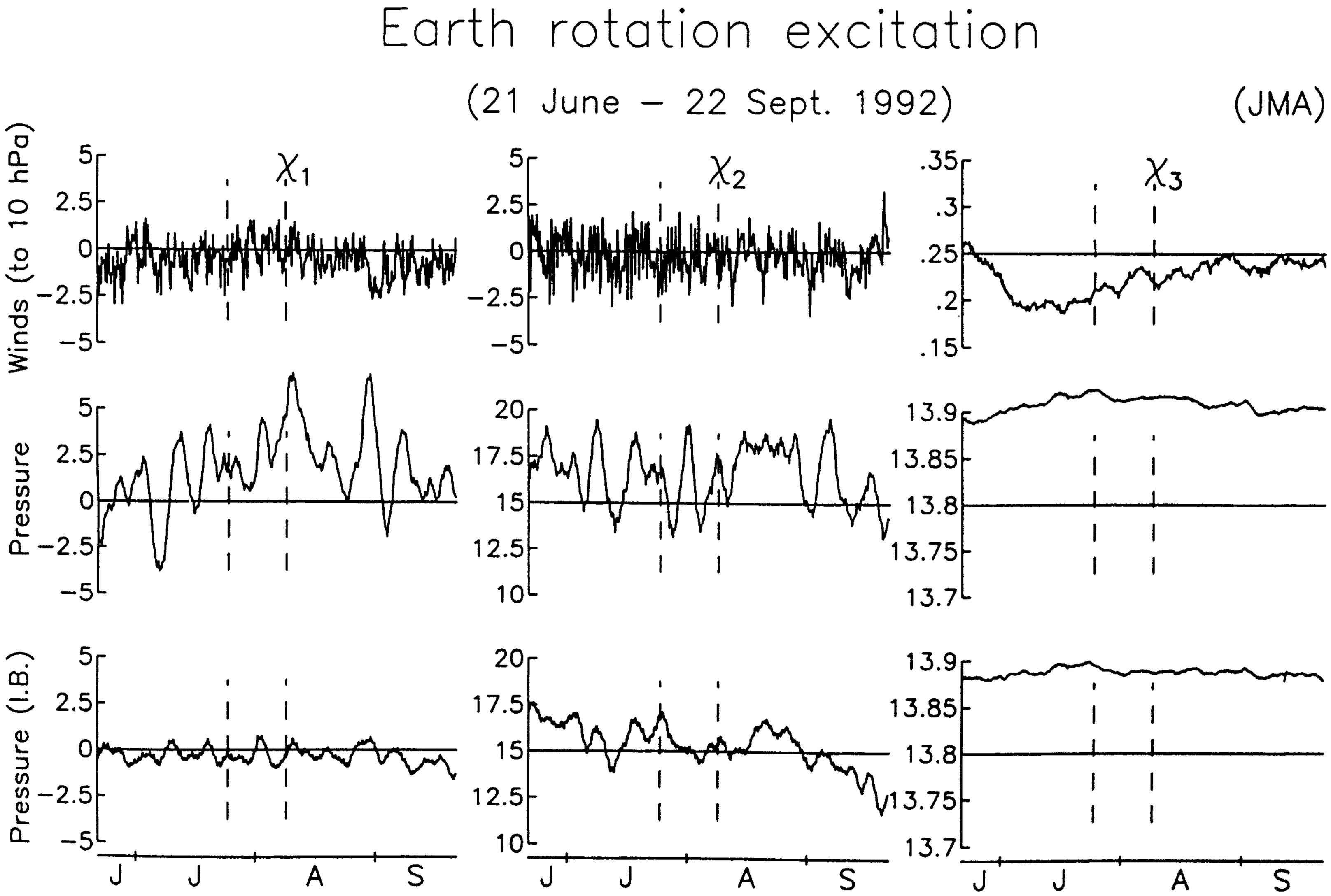

Figure 1c. Same as Figure 1a, but for the JMA system.

In order to best observe the diurnal variations, data from the two week intensive period, 25 July-8 August are given in Fig. 2 for the three centers. The sub-diurnal variability present in the χ_1 and χ_2-wind terms are likely due to the tidal response of the atmosphere to thermal forcing; such types of variations have been discussed by Hsu and Hoskins (1989). Six-hourly data are necessary to resolve these parameters, and so the SEARCH'92 period was the first in which we examined such fluctuations in both these equatorial wind parameters. The amplitude of the tidal response appears greater in the ECMWF fields than in the NMC fields, probably due to the higher level over which the former center calculated its wind values. Values for 06 and 18 UTC from the JMA, in particular, provided a weaker amplitude of this tidal signature during these synoptic times than the other centers. These hours are ones when fewer meteorological observations are taken.

The different mean values of the pressure-related excitation terms are likely due to the differences in topography of the three models. Each of the models uses its own representation of the surface topography, which relates to the overall surface pressure, and mass, of the atmosphere, and hence the pressure-based excitation (χ-p) terms.

Values of the low-order coefficients of a spherical harmonic representation of the surface pressure, truncated to degree 4, based on the NMC system, are given in Figure 3a and b for the intensive period of SEARCH'92. The two portions of the figure contain the real and imaginary coefficients, respectively.

4. Earth-Atmosphere Torques during the SEARCH'92 Period

The atmosphere exchanges its momentum with the underlying surface by means of two separate processes involving forces applied at the atmosphere's underlying boundary whose moment arm is the distance from the Earth's surface to its axis. These two torques arise from (i) a normal pressure gradient force against the Earth's topography, usually called a mountain torque, and (ii) a tangential stress against the underlying surface, either ocean or solid land, which is termed a friction torque. Global values of these two torques have been computed from the U.S. National Meteorological Center's analysis-forecast system every 6 hours for the SEARCH'92 period and kindly supplied by G.H. White. The procedure used to calculate these values is described by White (1991).

In Fig. 4 the global values of the 6-hourly mountain and friction torques, as well as their diurnal average is given. Also shown is the sum of the two terms on a daily averaged basis and changes in the axial angular momentum of the atmosphere. This daily agreement is good, but not perfect; whereas momentum is derived from a combination of observations and values forecast by the meteorological prediction model in data sparse areas, the torque terms are related also to physical parameterizations and other approximations in the forecast portion of the NMC model. On a 6-hourly basis, however, the two terms agree less, raising the difficulty of defining the momentum variation at these extremely short time scales. One item to note is that friction torque tends to be less variable that mountain torque, over these short periods.

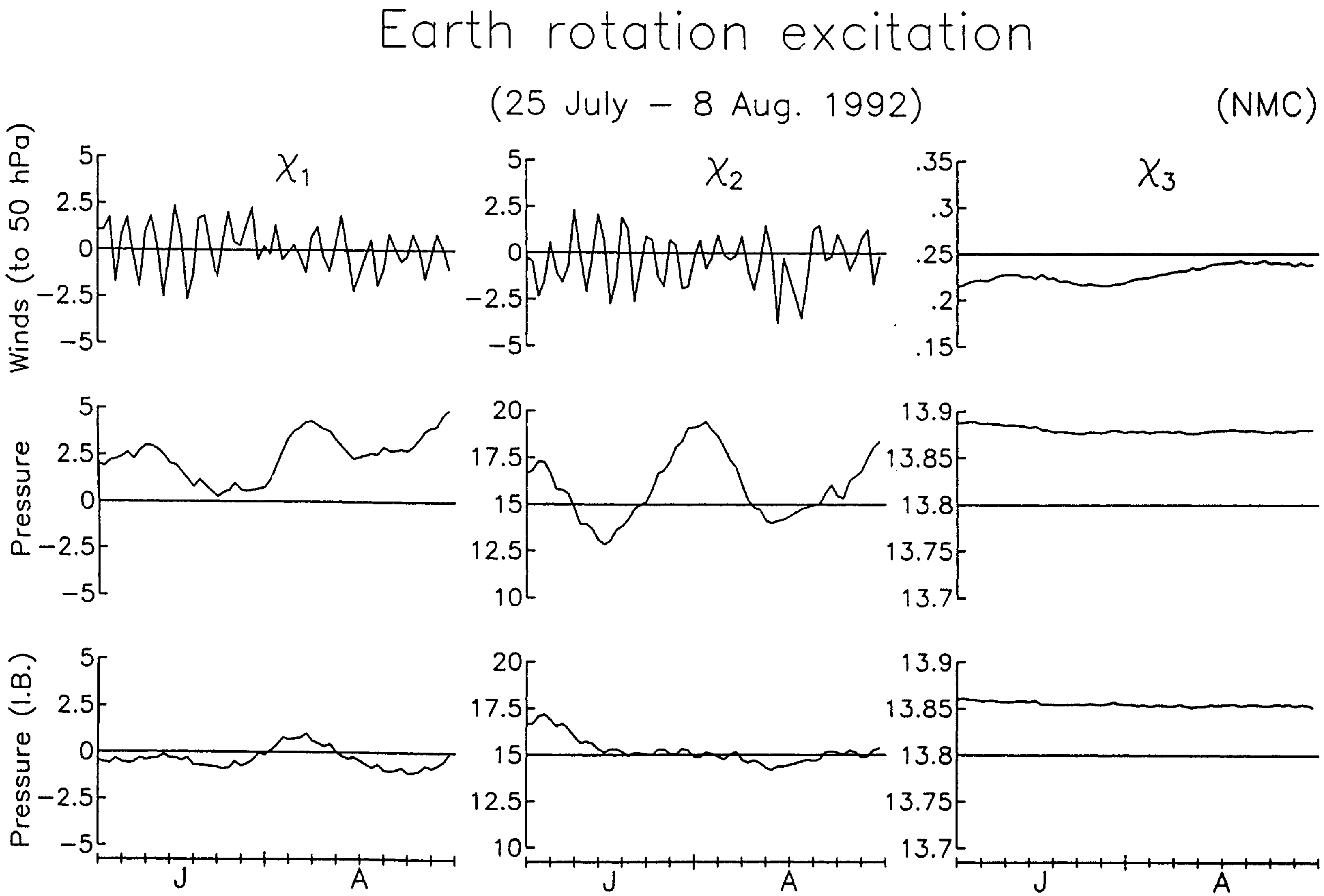

Figure 2a. Same as Figure 1a, but for the intensive period of SEARCH'92 (25 July-8 August 1992).

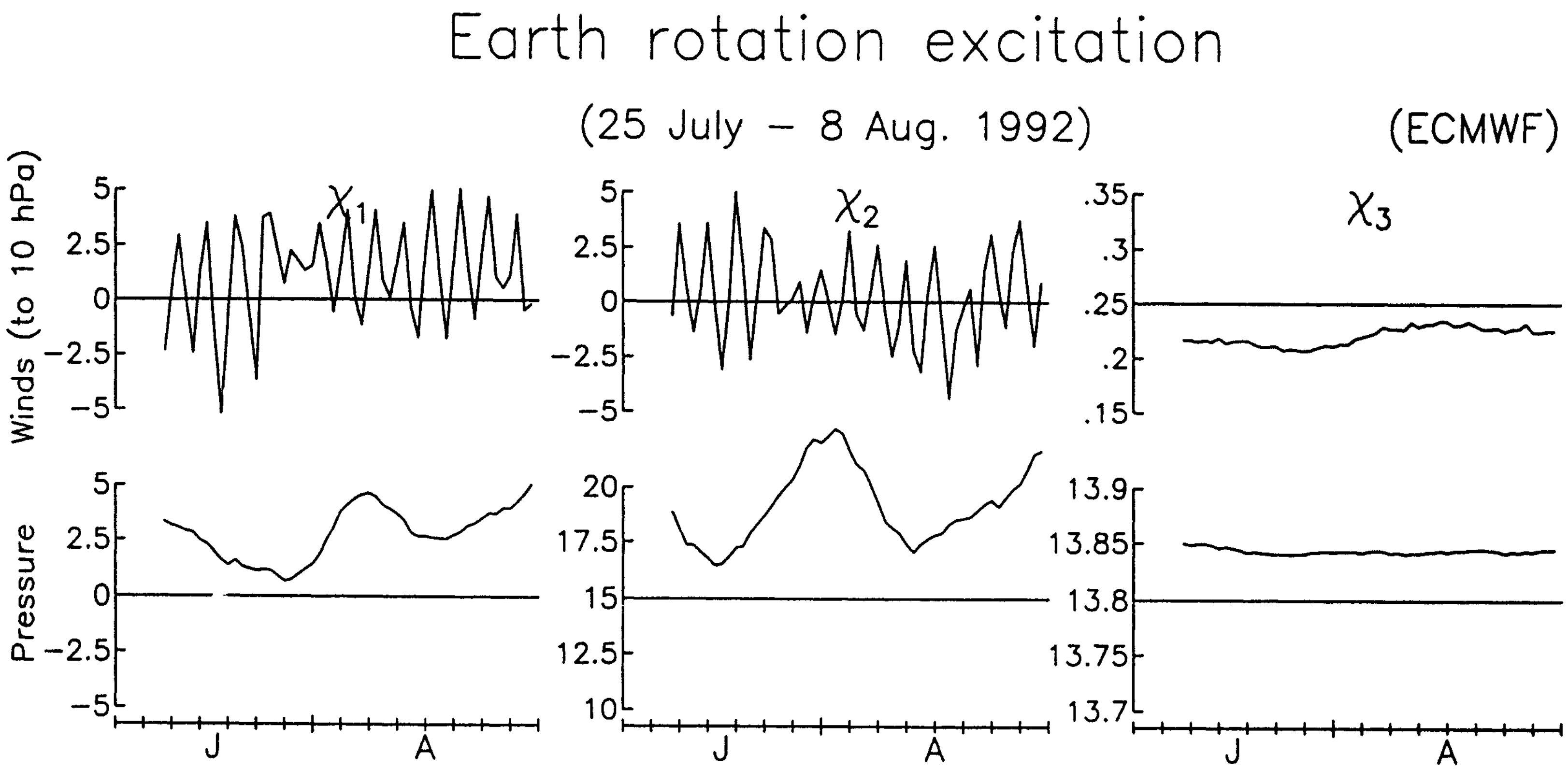

Figure 2b. Same as Figure 2a, but for the ECMWF system.

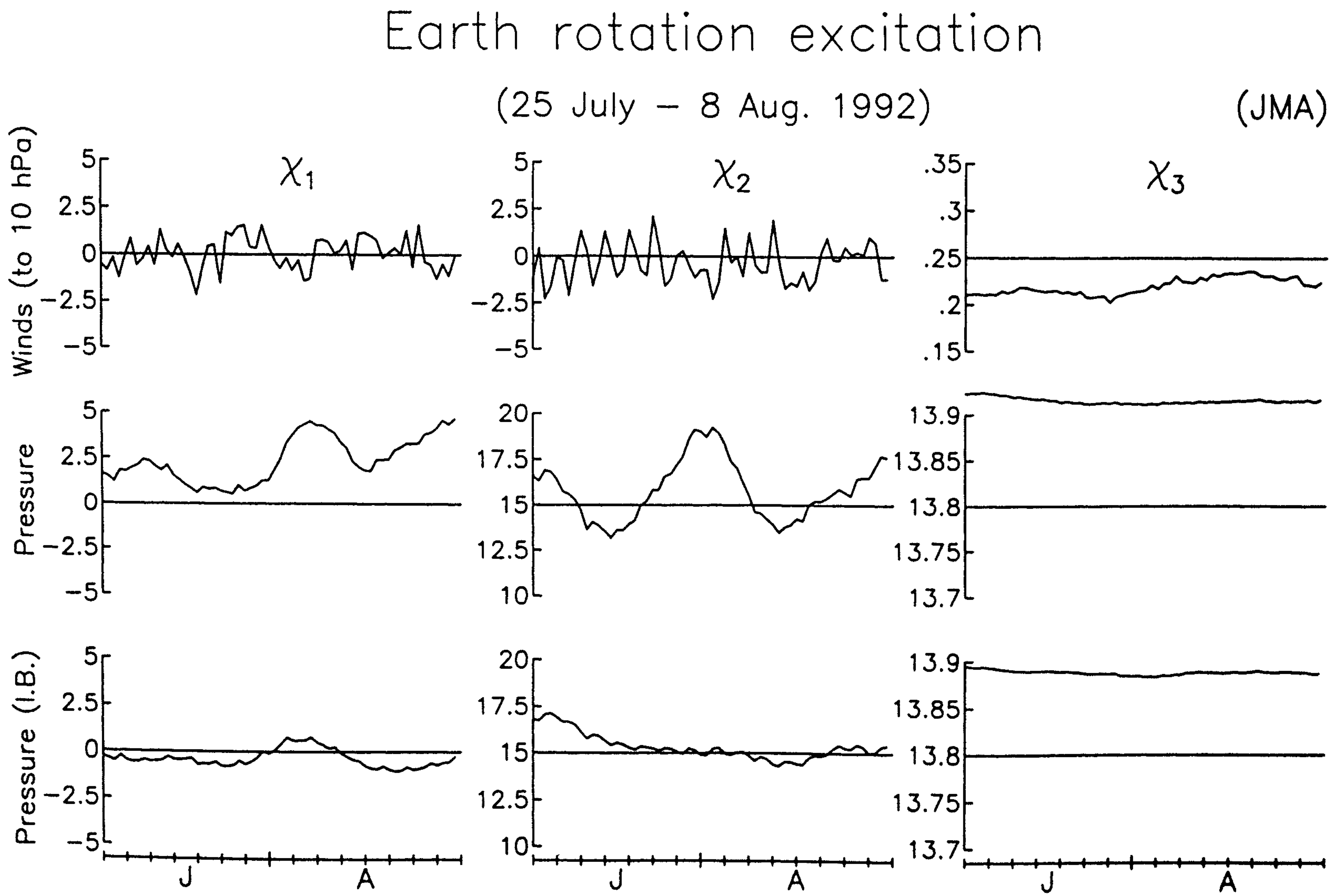

Figure 2c. Same as Figure 2a, but for the JMA system.

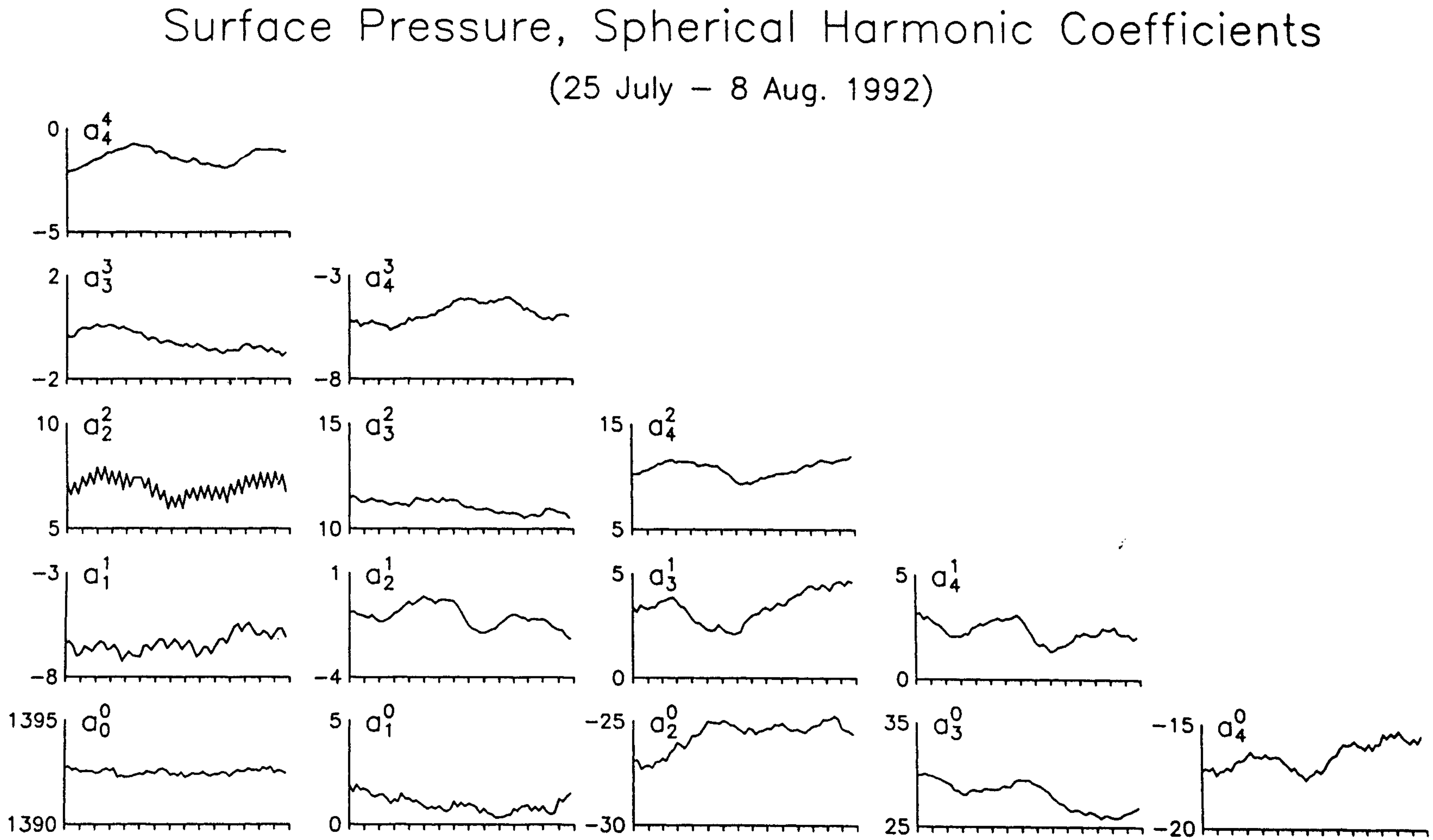

Figure 3a. Values of real coefficients of a triangular truncation (to degree 4) of a spherical harmonic expansion of the 6-hourly NMC surface pressure field. Units are hPa. The value of a_0^0, when divided by $2^{1/2}$, yields the global mean pressure.

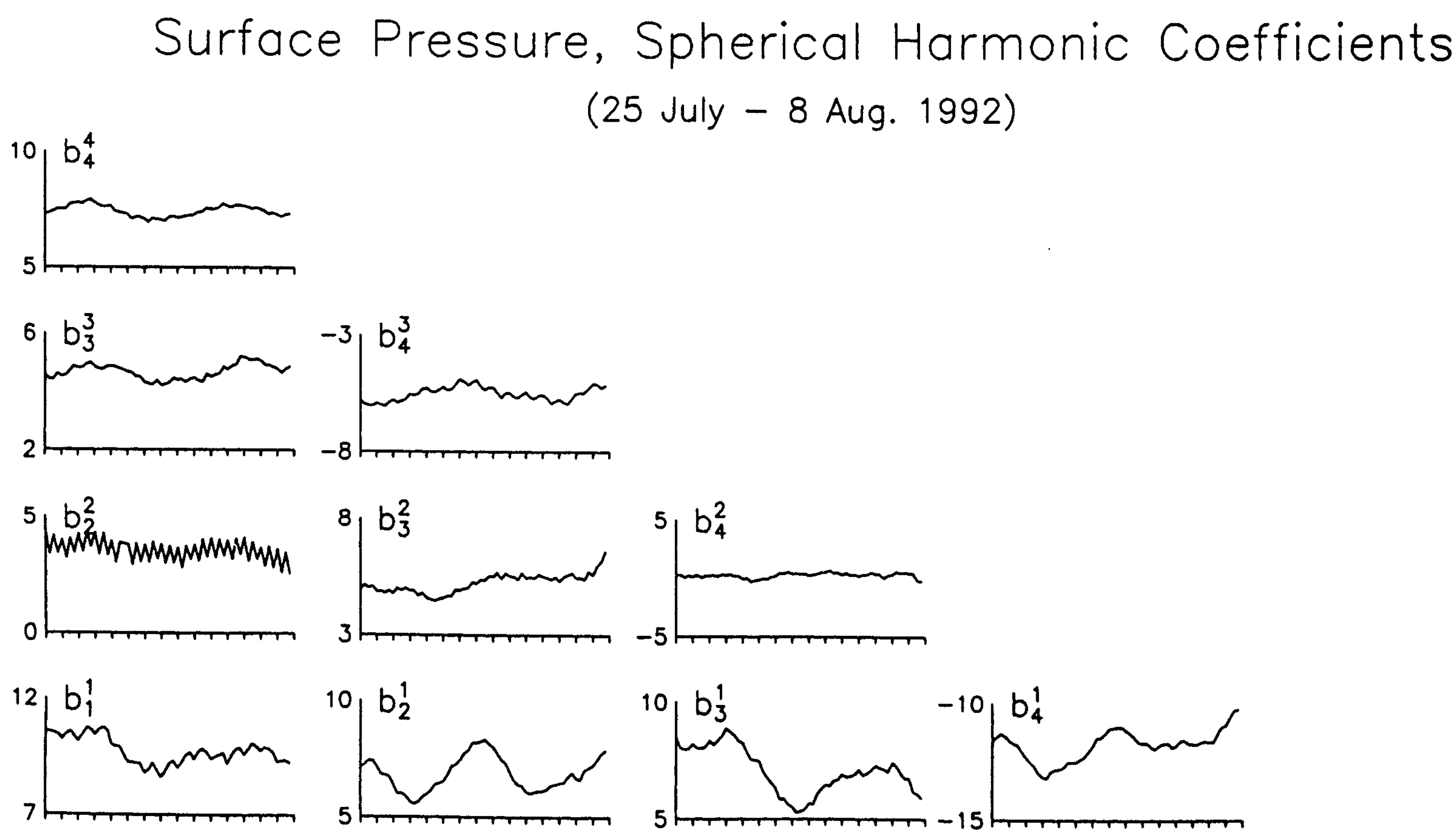

Figure 3b. Same as Figure 3a, but for imaginary coefficients. The zonal terms are equivalent to zero and are not given.

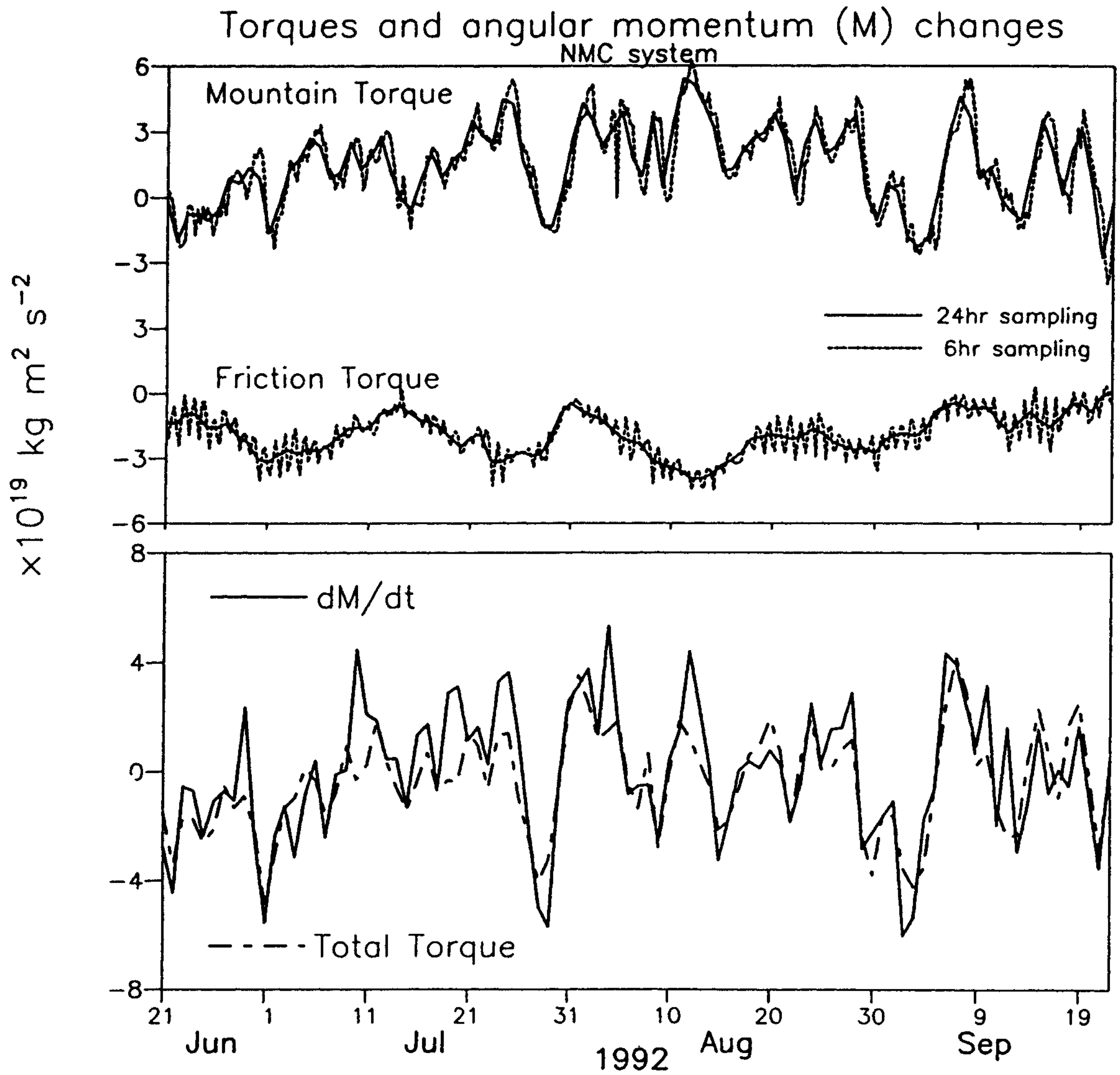

Figure 4a. (Top). Values of both mountain torque and friction torque, given every 6 hours, for the NMC analysis-forecast system. (Courtesy G.H. White of NMC). The daily means are given by the dashed lines. (Below) A comparison of the sum of the daily mean mountain and friction torque with the time derivative of axial angular momentum, proportional to the sum of the χ_3 wind and χ_3 pressure terms.

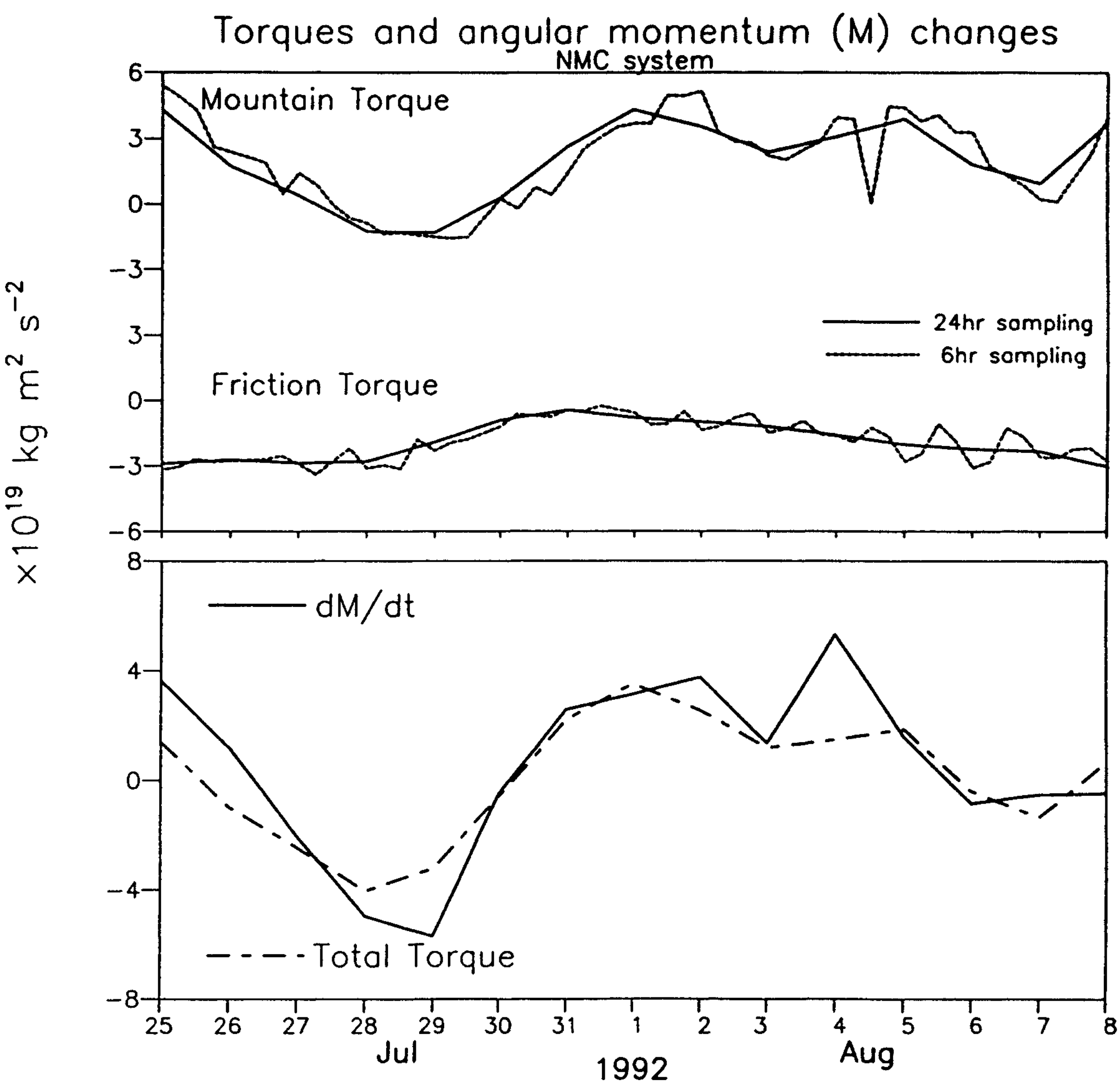

Figure 4b. Same as Figure 4a, but restricted to the intensive period of SEARCH'92.

5. Relevant Bilbliography

A discussion of the support for SEARCH'92 by the SBAAM was presented by Salstein et al. (1992) [Abstract in Appendix A] highlighting the intensive period. Further analysis of the local mechanisms responsible for rapid changes in atmospheric angular momentum, and hence in length of day, was presented by Salstein and Rosen (1993 and 1994). [Abstracts in Appendices B and C]. The particularly important regions for the intensive period were isolated to the low latitude southern hemisphere, where weather systems moving across the spine of the high Andes mountains of South America played a special role in accelerating the atmosphere during one phase (31 July-5 August) of a 1-2 week wave during this period.

6. References

Barnes, R.T.H., R. Hide, A.A. White, and C.A. Wilson (1983) 'Atmospheric angular momentum fluctuations, length-of-day changes and polar motion', *Proc. Roy. Soc. Lond. A*, 387, 31-73.

Hsu, H.-H. and B.J. Hoskins (1989) 'Tidal fluctuations as seen in ECMWF data', *Q. J. R. Meteorol. Soc.*, 115, 247-264.

Salstein, D.A., R.D. Rosen, D.M. Kann, G.H. White, and A.J. Miller (1992) 'Activities of the IERS Sub-bureau for Atmospheric Angular Momentum in support of SEARCH'92', (abstract) *Eos. Trans. AGU,* 73 (43), Fall Meeting Suppl., 134.

Salstein, D.A., D.M. Kann, A.J. Miller, and R.D. Rosen (1993) 'The Sub-bureau for Atmospheric Angular Momentum of the International Earth Rotation Service: A meteorological data center with geodetic applications', *Bull. Amer. Meteorol. Soc.*, 74, 67-80.

Salstein, D.A. and R.D. Rosen (1993) 'Momentum variability and dynamic Earth-atmosphere interactions during SEARCH'92' (abstract) *Eos. Trans. AGU*, 74 (16), Spring Meeting Suppl., 103.

Salstein, D.A., and R.D. Rosen (1994) 'Topographic forcing of the atmosphere and a rapid change in the length of day', *Science*, 264, 407-409.

White, G. (1991) 'Mountain and surface stress torques in NMC analyses', Proceedings of the AGU Chapman Conference on Geodetic VLBI: Monitoring Global Change, U.S. Department of Commerce/NOAA/NOS, NOAA Technical Report NOS 137 NGS 49, Washington, DC, 262-269.

Appendix A

Abstract from the Fall Meeting of the American Geophysical Union, 1992

Activities of the IERS Sub-bureau for Atmospheric Angular Momentum in support of SEARCH'92

D. A. Salstein and R. D. Rosen
Atmospheric and Environmental Research, Inc.
840 Memorial Drive, Cambridge, MA 02139; 617-547-6207

D. M. Kann
Research and Data Systems, Corp.
Greenbelt, MD 20770

G. H. White and A. J. Miller
National Meteorological Center
Washington, DC 20233

During summer 1992, excitation functions for Earth orientation were received at the SBAAM from our four participating meteorological centers, the U.S. National Meteorological Center, the United Kingdom Meteorological Office, the Japan Meteorological Agency, and the European Centre for Medium-Range Weather Forecasts. These functions, which measure the role of the atmosphere in changing the length of day and polar motion, are based on global integrals of winds and surface pressures and are now being reported at either a 6- or 12-hourly frequency, depending on the center. The higher frequency data now available reveal a strong diurnal signal in the polar motion-related wind term, in particular. The ability to capture this signature, which has been attributed to atmospheric tides, suggests that useful information is provided by the meteorological analyses at all four synoptic hours, despite the smaller number of observations available at some of these hours.

The interfacial torques that are responsible for the transfer of axial angular momentum across the atmosphere's lower boundary have begun to be computed from the operational analysis-forecast system at NMC. These values, computed on a 6-hourly basis, consist of the so-called friction and mountain torques, which are caused, respectively, by tangential stress forces over land or ocean, and normal pressure gradient forces against topography. Although the stress torque is the less variable of the two over a season, it appears to contain a relatively large diurnal signal. As a check on the accuracy of the calculations, the sum of the two torques is found to closely match the independently computed time deriviative of global atmospheric angular momentum for this system.

Appendix B

Abstract from the Spring Meeting of the American Geophysical Union, 1993

Momentum variability and dynamic Earth-atmosphere interactions during SEARCH'92

D. A. Salstein and R. D. Rosen
Atmospheric and Environmental Research, Inc.
840 Memorial Drive, Cambridge, MA 02139; 617-547-6207

A special campaign to study Earth's rapid rotational variations and related atmospheric momentum variability was held in June-September 1992. As part of this effort, high temporal resolution angular momentum data from a number of meteorological data centers, especially during a two-week intensive period, were collected. The global axial component of atmospheric angular momentum during part of the SEARCH'92 period was observed to undergo oscillations on about a 10-day time scale, superimposed on a longer seasonal signal. Analysis in zonal belts indicates the importance of low and middle sourthern latitudes in contributing to the variance in these global signals. Further examination based on models and analyses of the U.S. National Meteorological Center reveals the relative importance of the two agents of dynamic momentum transfer, the frictional stress torque and the pressure-gradient mountain torque. In particular, the South American Andes region appears to have had special significance in producing a rapid transfer of momentum from Earth to atmosphere during the intensive period.

Appendix C

Abstract of Paper in *Science*: Vol. 264, pages 407-409, 1994

Topographic forcing of the atmosphere and a rapid change
in the length of day

David A. Salstein and Richard D. Rosen
Atmospheric and Environmental Research, Inc.
840 Memorial Drive, Cambridge, MA 02139

ABSTRACT: During June-September 1992, a special campaign was held to measure rapid changes in Earth's rotation rate and to relate these to variations in the atmosphere's angular momentum, due principally to changes in zonal winds. A strong rise in both length of day and atmospheric momentum during a particular six-day subperiod is documented. For the first time, such a high-frequency perturbation is identified with a regional coupling mechanism. Mountain torques within the southern tropics appear to account for most of the rapid momentum transfer between the solid Earth and atmosphere, with those across the South American sector dominating.

Part III

Geodetic and Atmospheric Measurements

SEARCH'92 CAMPAIGN: NOAA EARTH ORIENTATION RESULTS USING VLBI OBSERVATIONS

J.R. Ray, M.D. Abell, W.E. Carter, W.H. Dillinger, M.L. Morrison, and D.S. Robertson
Geosciences Laboratory
NOAA/NOS/OES13, SSMC 4
1305 East-West Highway
Silver Spring, MD 20910 USA

ABSTRACT. Earth orientation results are reported for the SEARCH'92 campaign period (21 June - 22 September 1992) based on VLBI observational data analyzed by NOAA.

1. Analysis Procedures

The very long baseline interferometry (VLBI) data sets and the analysis procedures, methods, and models used by the U.S. National Oceanic and Atmospheric Administration (NOAA) have been described by Carter *et al.* (1993). The only significant difference in the analysis results presented here is the inclusion of more observational data, primarily collected during 1993. For the current solution, a total of 849,480 bandwidth-synthesis group delay observations from 1336 one-day observing sessions was included, 21.8% more than in our previous report. In general, the latest *IERS Standards* (McCarthy, 1992) are enforced and our reference frames are aligned with the IERS celestial (ICRF-91) and terrestrial (ITRF-91) frames.

Data from 14 new VLBI sites were used, including: six of the 25-m VLBA antennas, the newly erected 14.2-m antenna at Fortaleza (Brazil), the new 20-m Kokee antenna on Kauai (Hawaii, USA), a new 10-m dish at Mizusawa (Japan), and the 9-m antenna at the O'Higgins Base (Antarctica). Geocentric coordinates for all the VLBI reference points (at epoch 1988.0) are given in the file SSC (NOAA) 93R03. The associated three-dimensional velocities for these sites are given in SSV (NOAA) 93R03. Of the 69 sites, 31 have insufficient data spans (less than about 2 years) to permit meaningful velocity estimates. For those sites (denoted by velocity uncertainty values of zero), the NNR-NUVEL-1 global plate motion model (Argus and Gordon, 1991) has been used to project station coordinates to the 1988.0 reference epoch.

The number of radio source positions in our current solution, RSC (NOAA) 93R03, has increased by 45 to 152. However, most of the new sources are only sparsely observed.

Our Earth orientation parameter (EOP) time series are presented in two files. Results from the 24-hour observing sessions are given in EOP (NOAA) 93R07. File EOP (NOAA) 93R08 contains an independent series of quasi-daily UT1 values from the 1-hour single-baseline IRIS 'Intensive' observing sessions.

2. Tidal Variations in Earth Rotation

The NOAA analysis procedures to account for tidal variations in the rotation of the Earth have already been described by Carter *et al.* (1993). However, because of the significance of sub-daily tidal effects, their relevance to the SEARCH'92 campaign objectives, and the fact that this frequency regime is not dealt with in the *IERS Standards*, our methodology is repeated here.

In the least-squares modelling of the VLBI delay observables, five Earth orientation offset parameters are adjusted for each 24-hour observing session: x and y coordinates of the pole position, UT1, and celestial pole offsets in longitude and obliquity. (For the 1-hour Intensive sessions, only UT1 is adjusted.) Consequently, it is important that the time-variation of the *a priori* EOP values, apart from a possible offset error, reflect as closely as possible the actual variations of the Earth's rotation. Most significant in this respect are tidal variations with periods of about one day or less. The procedure we have developed to form *a priori* EOP values at any VLBI observation epoch is: 1) tabulated EOP values are taken from a previous NOAA solution for the set of all IRIS-A, NAVNET, and NEOS-A observing sessions (with spacings of 3.5, 5, or 7 days depending on epoch); 2) known tidal contributions based on models described below are removed from the tabular values; 3) a cubic spline interpolation is performed on the tidally corrected EOP values from the five nearest tabular epochs; 4) the model tidal contributions are restored. The models used to account for the tidal contributions are: 1) 'UT1S' tidal terms, which include periods between 5.64 days and 18.6 years with corrections due to oceanic tides for the largest terms (see *IERS Standards*, McCarthy, 1992); 2) diurnal and semi-diurnal variations of x, y, and UT1 derived by Herring (1992) based on analysis of 8.5 years of VLBI data. To minimize the effects of residual unmodelled Earth orientation variations, the EOP adjustments are made at the weighted mid-point epoch of each observing session. Non-periodic sub-daily EOP variations will be at least partially averaged out in our analysis. The EOP results reported here are 'total' values, in the sense of including the effects of diurnal and semi-diurnal variations, rather than being strongly smoothed over the 24-hour observing periods or otherwise modified after the least-squares adjustment.

Our *a priori* modelling of the time-variation of the nutation offsets follows analogously the procedure described above for x, y, and UT1. However, the ZMOA-1990.2 nutation model of Herring (1991) is used instead of a tidal model. The reported nutation offsets are with respect to the IAU 1980 model.

3. Discussion of Results

The NOAA EOP results for the SEARCH'92 period (21 June through 22 September 1992) are displayed in Figures 1-3 relative to the IERS combination series EOP (IERS) 90C04. Corrections for diurnal and semi-diurnal variations in x, y, and UT1 have been applied using the model of Herring (1992). Results from a few regional networks, with poor sensitivity to EOP variations, have not been included in Figures 1-3. The weighted rms differences, after removing mean offsets, are: 399.4 μas for x, 496.2 μas for y, 31.4 μs for UT from the 24-hour sessions only, 32.7 μs for UT from all sessions including the 1-hour 'Intensives', 594.0 μas for nutation offset in longitude ψ, and 248.6 μas for nutation offset in obliquity

ϵ. Included in these statistics are results from 62 24-hour VLBI sessions plus an additional 68 1-hour sessions to measure UT1.

The NOAA-IERS residuals are not entirely random but appear to be most systematic for UT1. Figure 1 shows periods of a week or longer with apparently systematic variations of up to about 100 μs. Considering that the results are determined from a variety of independent observing networks and that the largest VLBI technique-dependent systematic errors (such as atmospheric propagation effects) are expected to be primarily site-dependent, we conclude that the systematic residuals are caused either by: 1) deficiencies in the NOAA analysis methods or 2) excessive smoothing of UT1 variations in the IERS combination series EOP (IERS) 90C04. Comparisons of our results with independent analyses of the same VLBI data sets should determine whether the first possibility is significant.

In addition, there are occasional VLBI results that appear to be true outliers. The most obvious example is the UT1 determination from the Intensive session on 22 August 1992 (see lower plot in Figure 1). In this particular case, only one of the usual two low-declination radio sources produced useful data. Apparently, the nearly 50% increase in the formal error for that session, compared to neighboring Intensive sessions, does not fully account for the systematic UT1 error introduced by this data loss.

4. References

Argus, D.F. and Gordon, R.G. (1991) 'No-net rotation model of current plate velocities incorporating plate motion model NUVEL-1', *Geophys. Res. Lett.*, **18**, 2039-2042.

Carter, W.E., Abell, M.D., Dillinger, W.H., Morrison, M.L., Ray, J.R., and Robertson, D.S. (1993) 'NOAA Earth orientation time series and reference frames from VLBI observations: 1. Description of analysis procedures', in P. Charlot (ed.), *IERS Tech. Note 14*, IERS, Observatoire de Paris, pp. R-47 - R-52.

Herring, T.A. (1991) 'The ZMOA-1990 nutation series', in J.A. Hughes, C.A. Smith, and G.H. Kaplan (eds.), *Proc. IAU Coll. 127 -- Reference Systems*, U.S. Naval Observatory, Washington, pp. 157-166.

Herring, T.A. (1992) 'Diurnal and semi-diurnal variations in Earth rotation', in M. Feissel (ed.), *Adv. Space Res.*, *13*, Pergamon, pp. 11281-11290.

McCarthy, D.D. (1992) 'IERS Standards 1992', *IERS Tech. Note 13*, IERS, Observatoire de Paris, 150 pp.

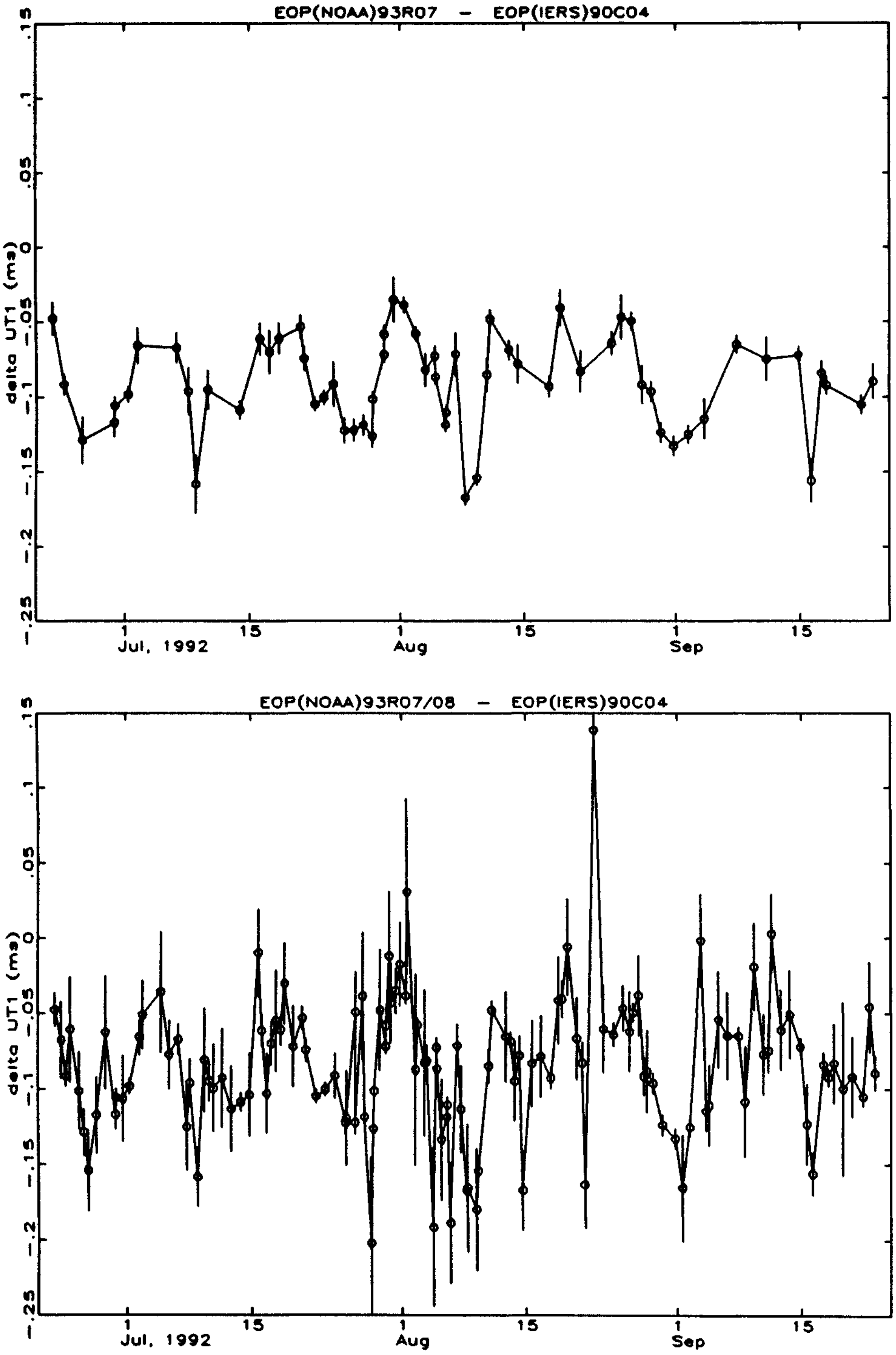

Figure 1. NOAA UT1 results for the SEARCH'92 period relative to the IERS combination series EOP (IERS) 90C04. Results for only the 24-hour sessions are shown in the top plot; 1-hour sessions are included in the bottom plot. Corrections for diurnal and semi-diurnal variations (Herring, 1992) have been applied.

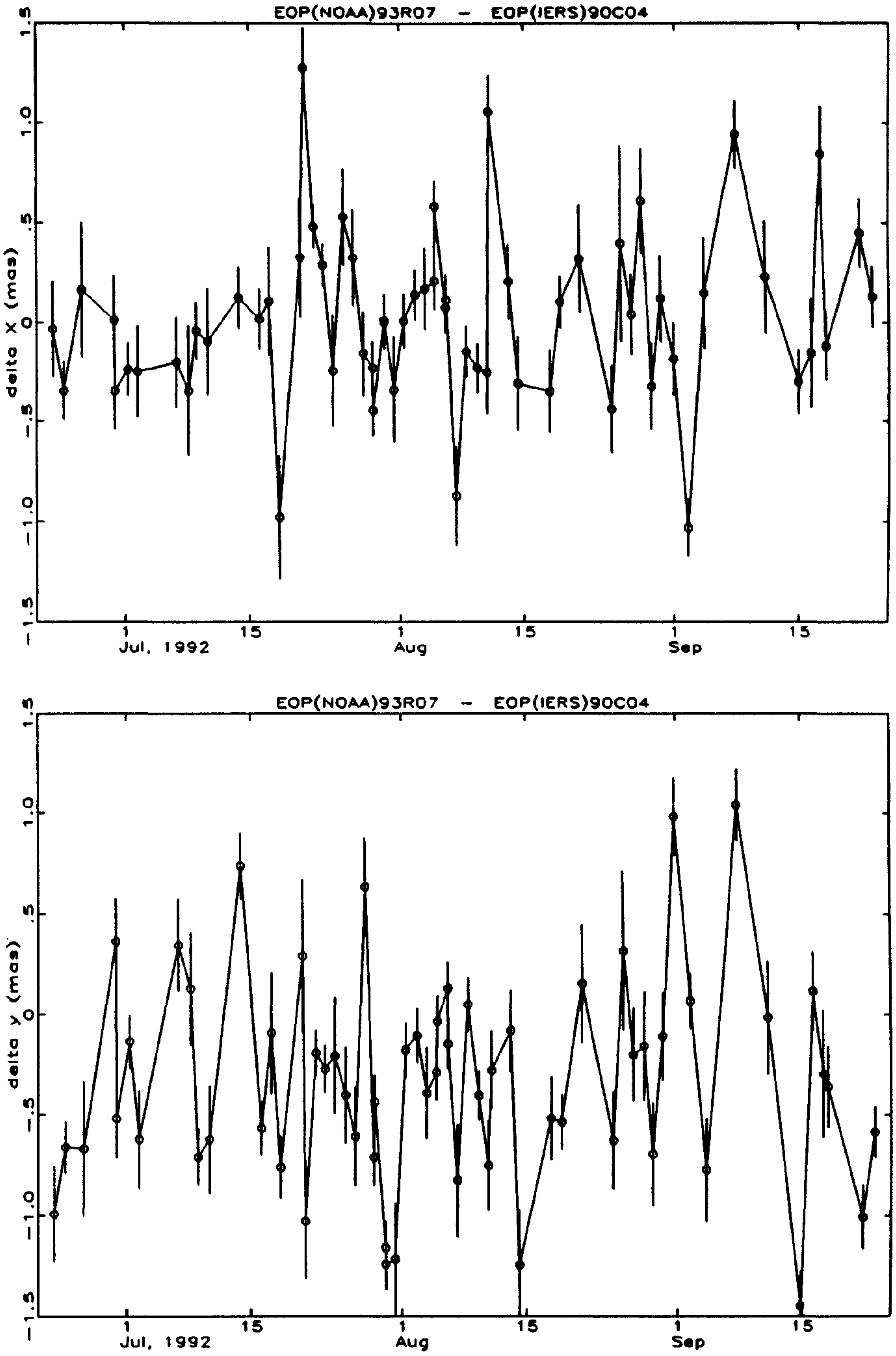

Figure 2. NOAA results for pole coordinates x (top) and y (bottom) shown relative to the IERS combination series EOP (IERS) 90C04. Corrections for diurnal and semi-diurnal variations (Herring, 1992) have been applied.

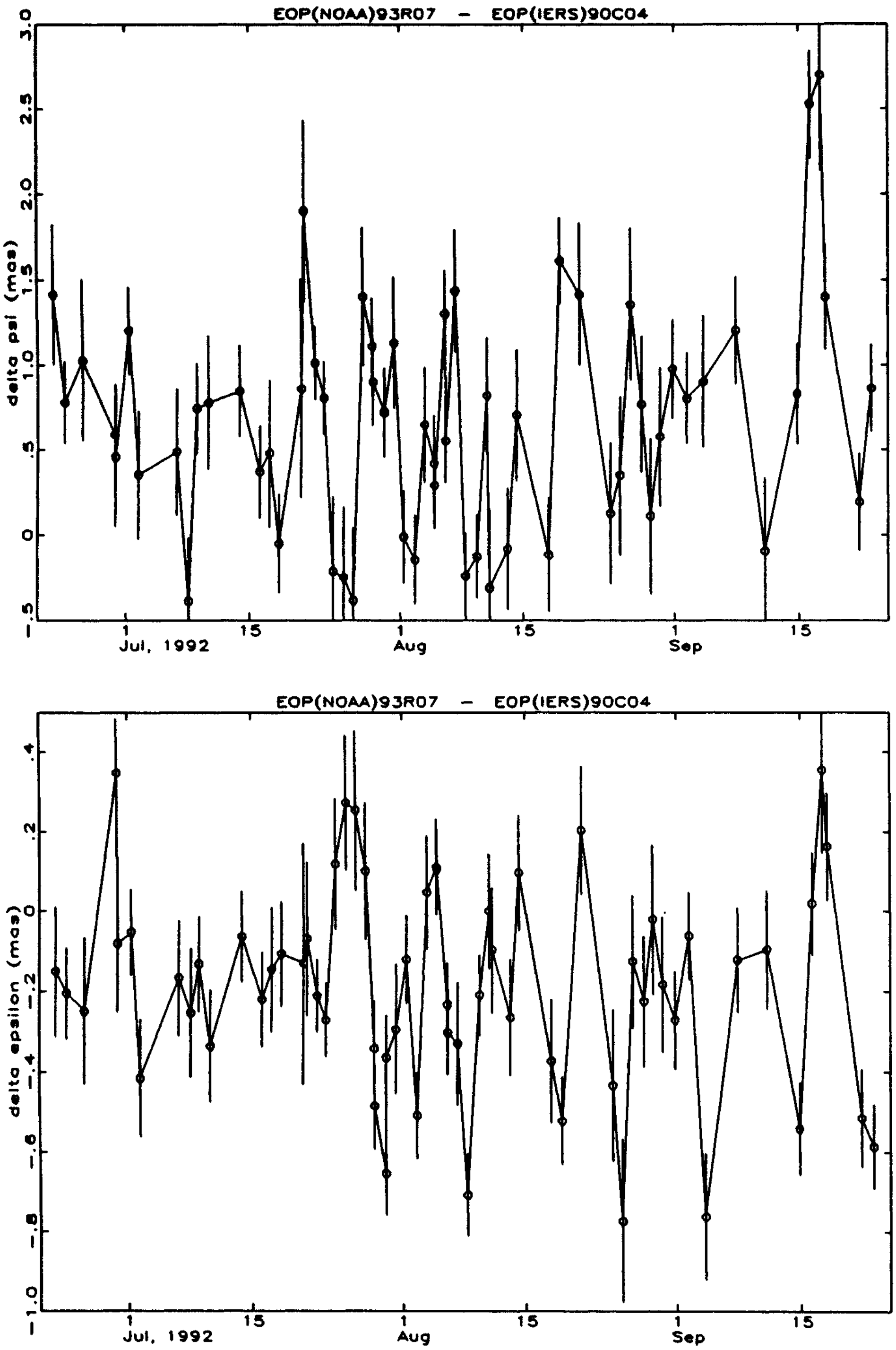

Figure 3. NOAA nutation offset results relative to the IERS combination series EOP (IERS) 90C04.

SUMMARY SHEET FOR THE DESCRIPTION OF THE TERRESTRIAL SYSTEM ATTACHED TO A SET OF STATION COORDINATES

1 - Technique: Bandwidth-synthesis Mark III VLBI

2 - Analysis Center: NOAA VLBI Analysis Center, N/OES13
SSMC 4
1305 East-West Highway
Silver Spring, MD, USA 20910

3 - Solution ID: solution rundate = 05 January 1994
IERS filenames: SSC (NOAA) 93R03, SSV (NOAA) 93R03, RSC (NOAA) 93R03, EOP (NOAA) 93R07 and 93R08

4 - Software Used: COREL and FRNGE for the Mark III data correlation; DE200 ephemerides, CALC-7.6, and SOLVE-3 for data analysis

5 - Relativity Scale: Radio source coordinates are in solar system barycentric system; Terrestrial site coordinates are geocentric (ignoring the local gravitational potential of the Earth)

6 - Permanent Tidal Correction on Station: No correction is applied to remove the zero-frequency displacement introduced by the solid Earth tide model.

7 - Tectonic Plate Model: NNR-NUVEL-1 is used to specify the large-scale motion of the entire terrestrial reference frame in both translational and rotational senses for nine VLBI sites (see Carter *et al.*, 1993); the same model is also used to propagate the relative positions of sites with data spans too brief to permit reliable determinations of VLBI velocities.

8 - Velocity of Light: 299792458. m/s

9 - Geogravitiational Constant: not applicable

10 - Reference Epochs: Station coordinates -- 1988 January 01
Source coordinates -- J2000.0
EOP fixed epoch -- 1991 August 12 19:49:50 UT

11 - Adjusted Parameters: XYZ geocentric station coordinates and linear station velocities adjusted globally for all sites at their mean observation epochs;
radio source coordinates adjusted globally for all sources;
pole x and y coordinates, UT1, nutation longitude and obliquity offsets adjusted for each 24-hour observing session;
UT1 is the only EOP adjusted for 1-hour Intensive sessions;
clock polynomial coefficients adjusted for all but one station in each observing session;
atmosphere offset parameters for each hour interval for each station

for each 24-hour observing session (no atmosphere parameters are included in the analysis of the 1-hour Intensive sessions)

12 - Definition of the Origin: The coordinate origin of the terrestrial reference frame is specified by setting the vector sum of the adjusted coordinates for 16 VLBI sites equal to the corresponding vector sum for ITRF-91 (see Carter *et al.*, 1993);
the right ascension origin of the celestial reference frame is specified by setting the sum of the adjusted right ascensions for 36 radio sources equal to the corresponding sum for ICRF-91

13 - Definition of the Orientation: The relative orientation of the terrestrial and celestial reference frames is specified by fixing the EOP values to those interpolated from the EOP (IERS) 90 C 04 series (corrected for the offsets and drift rates reported by the IERS to give consistency with the ITRF-91 and ICRF-91 frames) for the reference epoch 1991 August 12 19:49:50; the interpolation method is described in the text.

14 - Constraint for Time Evolution: The secular translational velocity and rotational velocity of the terrestrial reference frame are specified through constraints; see item 7 above and text.

Format Notes:

SSC & SSV files -- Instead of the DOMES information in fields 2-4, the CDP monument number is given. X, Y, and Z values and their formal errors are reported to the 0.1 mm level so that the decimal points are shifted by one column from the specified format. Instead of reporting the time span of observations for each site in field 10, the number of observations is given.

RSC file -- Fields 11 (correlation coefficient), 12 (epoch of coordinates), 14 (time span of source observations), and 15 (number of sessions for each source) are filled with 0 values.

EARTH ORIENTATION FROM VLBI DURING SEARCH'92

C. MA
Goddard Space Flight Center
Geodynamics Branch
Greenbelt, Maryland 20771
USA

J. M. GIPSON
NVI, Inc./Goddard Space Flight Center
Geodynamics Branch
Greenbelt, Maryland 20771
USA

ABSTRACT. 66 VLBI sessions suitable for measuring Earth orientation parameters were conducted during SEARCH'92 including normally scheduled programs and a special continuous period with simultaneous networks between July 27 and August 10, inclusive. 53491 group delay observations from 24 stations spanned 1372 hours with 240 hours of overlapping networks. Both one-day and hourly Earth orientation values have been estimated. The best 1σ formal errors of the one-day values are 90 μas in pole and 4 μs for UT1, and the best corresponding errors of the hourly values are 140 μas and 8 μs.

1. INTRODUCTION

Since its inception in 1980, geodetic VLBI measurements to monitor Earth orientation parameters (EOP) have provided the stable reference series for geophysical and geodynamical research. The connection of VLBI to the essentially inertial celestial reference frame of extragalactic radio sources provides the key link for the long term measurement of UT1, while the precision of VLBI permits estimates of EOP at intervals much less a day. During SEARCH'92 a particular effort was made to collect as much useful VLBI data as feasible for the purposes of comparison and investigation of subdiurnal harmonic and nonharmonic signals. The cooperation of the coordinating organizations and participating observatories was essential to achieve this goal.

2. OBSERVING PROGRAMS

During the SEARCH'92 period the groups engaged in VLBI geodesy conducted an unusually extensive set of observations. These included the routine twice-weekly EOP measurements using the IRIS-A and NAVNET networks coordinated by NOAA (National Oceanic and Atmospheric Administration) and USNO (U. S. Naval Observatory), respectively, and the monthly EOP sessions using the IRIS-S(outh), IRIS-P(acific), and SHS (Southern Hemisphere Survey) networks coordinated by the Institute for Applied Geodesy (Germany), National Astronomical Observatory (Japan), and NOAA, respectively. The Space Geodesy Program (SGP) of the National Aeronautics and Space Administration had its regular monthly R&D sessions to test advances in geodetic VLBI technique as well as several sessions to improve the terrestrial reference frame. In addition, mobile VLBI measurements were made in Germany, Norway and Iceland with networks including stations in North America. In support of SEARCH'92 special sessions using the SGP R&D and the USNO NAVEX (NAVy EXtended) networks were scheduled to fill the gaps between the normal IRIS-A and NAVNET days in the period from July 27 to August 10. The SGP network used the stations KAUAI (Hawaii), GILCREEK (Alaska), LA-VLBA (New Mexico), FD-VLBA (Texas), WESTFORD (Massachusetts), and WETTZELL (Germany), while the NAVEX networks included MATERA (Italy), HARTRAO (South Africa), KASHIMA (Japan), NRAO85 3 (West Virginia), and SANTIA12 (Chile). The 66 dates, session types, and stations are shown in Table 1. Each session was ~24 hours or more. Eleven other sessions during SEARCH'92 used networks unsuitable for measuring EOP and were not included in the work below. Most of the SGP R&D and USNO NAVEX time between July 27 and August 10 overlapped. With six other days of simultaneous networks, the total overlapping time during SEARCH'92 was 240 hours. In all 1372 hours (61%) of the total SEARCH'92 interval was covered by VLBI observations.

The observing schedules for each SGP and NAVEX session were prepared using an automatic schedule algorithm developed at the Geodetic Institute of the University of Bonn and enhanced at Goddard. The software permits both covariance optimization and rule-based selection. The schedules were optimized for measuring EOP and atmosphere parameters while having a wide distribution of observing geometry at each station. The SGP observations were distributed quite unevenly over the sources with ~5 sources having the preponderance of the observations. The NAVEX schedules used a larger set of sources with more even distribution. While the same radio source catalog was used each day, the exact sequence of sources and the distribution of observing elevations and azimuths were different.

Since one aspect of the SGP R&D program is the study of troposphere modeling as an undesirable, nongeodetic signal, very low elevation observations were scheduled at certain stations. However, because the current troposphere models are insufficiently accurate at the lowest elevations, not all the data were included in the analysis. With a 7 degree cutoff, 14975 SGP observations and 2283 NAVEX observations were analyzed during the July 27 - August 10 period along with 3187 IRIS-A and 1294 NAVNET observations.

3. DATA ANALYSIS

The EOP values included in the present work were taken from a much larger complete solution including 1098090 observations between August 1979 - August 1993. The adjusted global parameters included positions and velocities of 117 sites and positions of 224 sources. The arc parameters included pole position, UT1, UT1 rate, offsets in obliquity and longitude, and piecewise-linear, continuous clocks and atmospheres. The geophysical, astronomical, and theoretical VLBI models generally followed the IERS standards. In addition, a model for the

TABLE 1. Stations and type for each session

			ADDFG	HHHKK	LMMMN	ORSSW	WHKT
			LSSDI	AAOAA	AAEOR	NIAEE	EOAR
			GSS-L	RYBSU	-TDJA	SCNSS	TFRO
			O14VC	TSAHA	VEIAO	AHTHT	TNLM
			P55LR	RTRII	LRCV8	LMIAF	Z BS
			A BE	AATM	BAIE5	AOANO	E UO
			R AE	OC2A	A N1	6N12R	L RN
			K K	K6	A23	0D25D	L GO
1	$92JUN22XI	IRIS-A	*----	-----	---*-	-*--*	*---
2	$92JUN23XH	IRIS-South	-----	*----	---*-	-*--*	*---
3	$92JUN23XO	USNO NAVEX	*---*	----*	-*--*	-----	----
4	$92JUN25XO	USNO NAVNET	----*	----*	----*	-*---	----
5	$92JUN29X	SGP Polar	-*--*	-*-*-	--*--	*----	----
6	$92JUN29XI	IRIS-A	*----	-----	---*-	-*--*	*---
7	$92JUN30X	SGP Research	---**	----*	*----	----*	*---
8	$92JUL02XO	USNO NAVNET	----*	----*	----*	-*---	----
9	$92JUL06XI	IRIS-A	-----	-----	---*-	*---*	*-*-
10	$92JUL07XQ	SGP Quake	---**	----*	---*-	-----	----
11	$92JUL08XH	IRIS-South	-----	*----	-----	-**-*	*---
12	$92JUL08XO	USNO NAVEX	*---*	----*	-*--*	-----	----
13	$92JUL09XO	USNO NAVNET	----*	----*	----*	-*---	----
14	$92JUL13XI	IRIS-A	----*	-----	---*-	-*--*	*---
15	$92JUL15X	SGP Pacific	--*-*	---**	-----	--**-	----
16	$92JUL16XO	USNO NAVNET	----*	----*	----*	-*---	----
17	$92JUL17XP	IRIS-Pacific	----*	--***	-----	-----	----
18	$92JUL20XI	IRIS-A	----*	-----	-----	*---*	**--
19	$92JUL20XS	NGS S. Survy	-----	*-*--	-----	--*--	----
20	$92JUL21X	SGP Global	----*	*-***	-----	--***	*---
21	$92JUL22X	SGP Global	----*	*-***	-----	--***	*---
22	$92JUL23XO	USNO NAVNET	----*	----*	----*	-*---	----
23	$92JUL25X*	Europe Mobil	----*	-----	-----	*---*	*---
24	$92JUL26X*	Europe Mobil	----*	-----	-----	*---*	**--
25	$92JUL27XI	IRIS-A	----*	-----	-----	*---*	**--
26	$92JUL28X	SGP Research	---**	----*	*----	----*	*---
27	$92JUL28XO	USNO NAVEX	-----	*--*-	-*--*	--*--	----
28	$92JUL29X	SGP Research	---**	----*	*----	----*	*---
29	$92JUL29XO	USNO NAVEX	*----	*--*-	-*--*	--*--	----
30	$92JUL30XO	USNO NAVNET	----*	----*	---*-	-*---	----
31	$92JUL31X	SGP Research	---**	----*	*----	----*	*---
32	$92AUG02X	SGP Research	----*	----*	*----	----*	*---
33	$92AUG03XI	IRIS-A	*----	-----	---*-	-*--*	*---
34	$92AUG04X	SGP Research	---**	----*	*----	----*	*---
35	$92AUG04XO	USNO NAVEX	-----	*--*-	-*--*	--*--	----
36	$92AUG05X	SGP Research	---**	----*	*----	----*	*---
37	$92AUG05XO	USNO NAVEX	*----	*--*-	-*--*	--*--	----
38	$92AUG06XO	USNO NAVNET	----*	----*	---**	-*---	----
39	$92AUG07X	SGP Research	---**	----*	*----	----*	*---
40	$92AUG09X	SGP Research	---**	----*	*----	----*	*---
41	$92AUG10XI	IRIS-A	*----	-----	---*-	-*--*	*---
42	$92AUG10XO	USNO NAVEX	----*	---**	-*--*	-----	----
43	$92AUG10XS	NGS S. Survy	-----	*-*--	-----	--*--	----
44	$92AUG11X	SGP T. Asia	--*--	*-**-	-----	---*-	*---
45	$92AUG12X*	Europe Mobil	----*	-----	-----	*---*	*---
46	$92AUG13XO	USNO NAVNET	----*	----*	----*	-*---	----
47	$92AUG17XI	IRIS-A	----*	-----	-----	*---*	*---
48	$92AUG18XH	IRIS-South	-----	*----	-----	-**-*	*---
49	$92AUG20XO	USNO NAVNET	----*	----*	----*	-*---	----
50	$92AUG24XI	IRIS-A	----*	-----	---*-	----*	*---
51	$92AUG25X*	Europe Mobil	-----	-----	-----	*---*	*--*
52	$92AUG26X*	Europe Mobil	----*	-----	-----	*---*	*--*
53	$92AUG27XO	USNO NAVNET	----*	----*	----*	-----	----
54	$92AUG28X*	Europe Mobil	----*	-----	-----	*---*	*--*
55	$92AUG29X*	Europe Mobil	----*	-----	-----	*---*	*--*
56	$92AUG31XI	IRIS-A	----*	-----	---*-	----*	*---
57	$92SEP01X	SGP Research	---*-	----*	*----	----*	*---
58	$92SEP03XO	USNO NAVNET	----*	----*	----*	-----	----
59	$92SEP07XI	IRIS-A	----*	-----	-----	*---*	*---
60	$92SEP10XO	USNO NAVNET	----*	----*	----*	-----	----
61	$92SEP14XI	IRIS-A	----*	-----	-----	----*	*---
62	$92SEP15XP	IRIS-Pacific	----*	--**-	-----	-----	----
63	$92SEP16XS	NGS S. Survy	-----	*-*--	-----	--*--	----
64	$92SEP17XO	USNO NAVNET	*---*	-----	----*	-----	*---
65	$92SEP21XI	IRIS-A	*---*	-----	-----	----*	*---
66	$92SEP22XO	USNO NAVEX	----*	---*-	-*--*	-----	----

diurnal and semidiurnal effects of ocean tides on UT1 and pole position was applied. The coefficients of this model (Gipson et al., 1993) were estimated directly from VLBI data in an earlier solution using the tidal frequencies and are given in Table 2. The effect of atmospheric pressure loading was calibrated using local pressures and coefficients derived from VLBI data and from global weather models (MacMillan and Gipson, 1994).

TABLE 2. Diurnal and semidiurnal EOP coefficients

Ten components for UT1

Tidal vector						cos (microseconds)	sin (microseconds)	Tidal Component
0	0	0	0	0	-1	7.486602	16.707637	K1
0	0	2	-2	2	-1	-3.500205	-5.392255	P1
0	0	2	0	2	-1	-15.575852	-16.762598	O1
1	0	2	0	2	-1	-3.394904	-3.902930	Q1
0	1	0	0	0	-1	.593333	1.932245	S1
1	0	0	0	0	-1	1.003345	1.299982	M1
0	0	0	0	0	-2	.261715	3.896805	K2
0	0	2	-2	2	-2	-1.182862	8.706599	S2
0	0	2	0	2	-2	-8.517385	12.338927	M2
1	0	2	0	2	-2	-4.378455	1.168543	N2

Twelve components for X and Y pole

Tidal vector						cos (microarcseconds)	sin (microarcseconds)	
0	0	0	0	0	1	125.285183	-38.476327	K1 p
0	0	-2	2	-2	1	-54.470359	26.152833	P1 p
0	0	-2	0	-2	1	-136.319298	63.668538	O1 p
-1	0	-2	0	-2	1	-33.990240	18.096315	Q1 p
0	0	0	0	0	-2	-15.899321	15.676795	K2 r
0	0	2	-2	2	-2	-76.296961	105.813157	S2 r
0	0	2	0	2	-2	15.018756	285.140733	M2 r
1	0	2	0	2	-2	-24.572257	58.610024	N2 r
0	0	0	0	0	2	22.589310	-5.801947	K2 p
0	0	-2	2	-2	2	-7.259654	-11.309321	S2 p
0	0	-2	0	-2	2	30.337902	-72.186765	M2 p
-1	0	-2	0	-2	2	-11.643736	-30.168262	N2 p

The orientation of the terrestrial reference frame (TRF) is essentially arbitrary and is derived from the EOP values adopted for the reference day, Feb. 12, 1993, and from the celestial angles of the standard precession/nutation models for the same reference day. The right ascension origin of the celestial reference frame is defined by the value assigned to the radio source 0420-012. The origin of the TRF is set by minimizing the adjustment of nine widely distributed, well observed stations with respect to their a priori values, which are within a few cm of ITRF92. The remaining degeneracies are removed by requiring no net rotation or vertical translation of eight stations (WESTFORD, GILCREEK, ONSALA60 (Sweden), WETTZELL, KAUAI, DSS45 (Australia) and HOBART26 (Tasmania)) with respect to the NUVEL-1 NNR plate model (Argus and Gordon, 1991). These stations are chosen to be minimally affected by plate boundary deformations, local movements, and as yet unexplained anomalies. It should be noted that any differences between the real relative motion of the reference stations and that predicted by the NUVEL-1 NNR model will cause all the stations to have fictitious apparent motions in the TRF.

The entire set of one-day EOP values and UT1 rates was estimated iteratively to improve the short-term accuracy, which affects the fit of each session. For each VLBI session, an offset from the a priori model was estimated for each component of polar motion. In addition, an offset and a rate were estimated for UT1. The total EOP at the middle of each session and the UT1 rate served as input to a simple Kalman filter, which estimated the EOP values at daily intervals. This new one-day-interval series served as the new a priori model for EOP. The a priori EOP values between tabular points at each observation epoch were obtained by linear interpolation. The one-day nutation offsets from the last iteration were spline fit to obtain daily nutation estimates for use in estimating the subdiurnal EOP values.

The solution to estimate subdiurnal EOP parameters modeled X-pole, Y-pole and UT1 as piecewise-linear, continuous functions with very weak constraints (1000 mas for pole, 100 ms for UT1) to bridge data gaps. The length of each linear segment was one hour. The global parameters and non-nutation arc parameters were the same as the solution for one-day EOP. The one-day-interval nutation series described above was used to remove the nutation errors that would have aliased into diurnal polar motion. Because of the weakness of the constraints, the hourly EOP values are noisy. However, the diurnal and semidiurnal harmonic signals are not significantly attenuated. A harmonic analysis of the hourly values from the complete solution gives components that are consistent with the direct estimate of the coefficients. With a stronger constraint to reduce the (visual) noise level, the simultaneous determination of hourly EOP from different networks shows generally good agreement. See Figure 1.

4. EOP RESULTS

The EOP results are presented in two forms. The one-day estimates are submitted in the standard IERS format as EOP (GSFC) 93 R 06. It should be noted that the values include the diurnal and semidiurnal tidal effects evaluated at the stated epoch as well as terms with longer periods. No smoothing or model removal has been done. The hourly values are submitted in a straightforward format for each session as EOP (GSFC) 93 R 07. Some epochs appear more than once because observing sessions using different networks overlapped in time. Only the formal uncertainties are given.

The formal uncertainties of the results during SEARCH'92 are quite good. The best 1σ one-day errors are 90 μas in pole and 4 μsec in UT1. The best one-hour errors are 140 μas in pole and 8 μs in UT1. The median errors are somewhat worse for the one-day values, 190 μas in pole and 7 μs in UT1, but the median hourly errors are considerably worse, 650 μas for pole and 29 μs for UT1. The hourly EOP results are more affected by data dropouts.

5. OTHER ACTIVITIES

Because of the success of continuous VLBI EOP measurements during SEARCH'92, the Goddard VLBI group in cooperation with USNO and the VLBA (VLBI Array) undertook a similar continuous observing period called CONT94 between January 10-28, 1994. Up to three networks observed simultaneously. The SGP network included KOKEE (Hawaii), GILCREEK, LA-VLBA, FD-VLBA, WESTFORD, WETTZELL, and ONSALA60 and observed for 12 days

Figure 1. R&D (dot) and Navex–G (square) Measurements of EOP

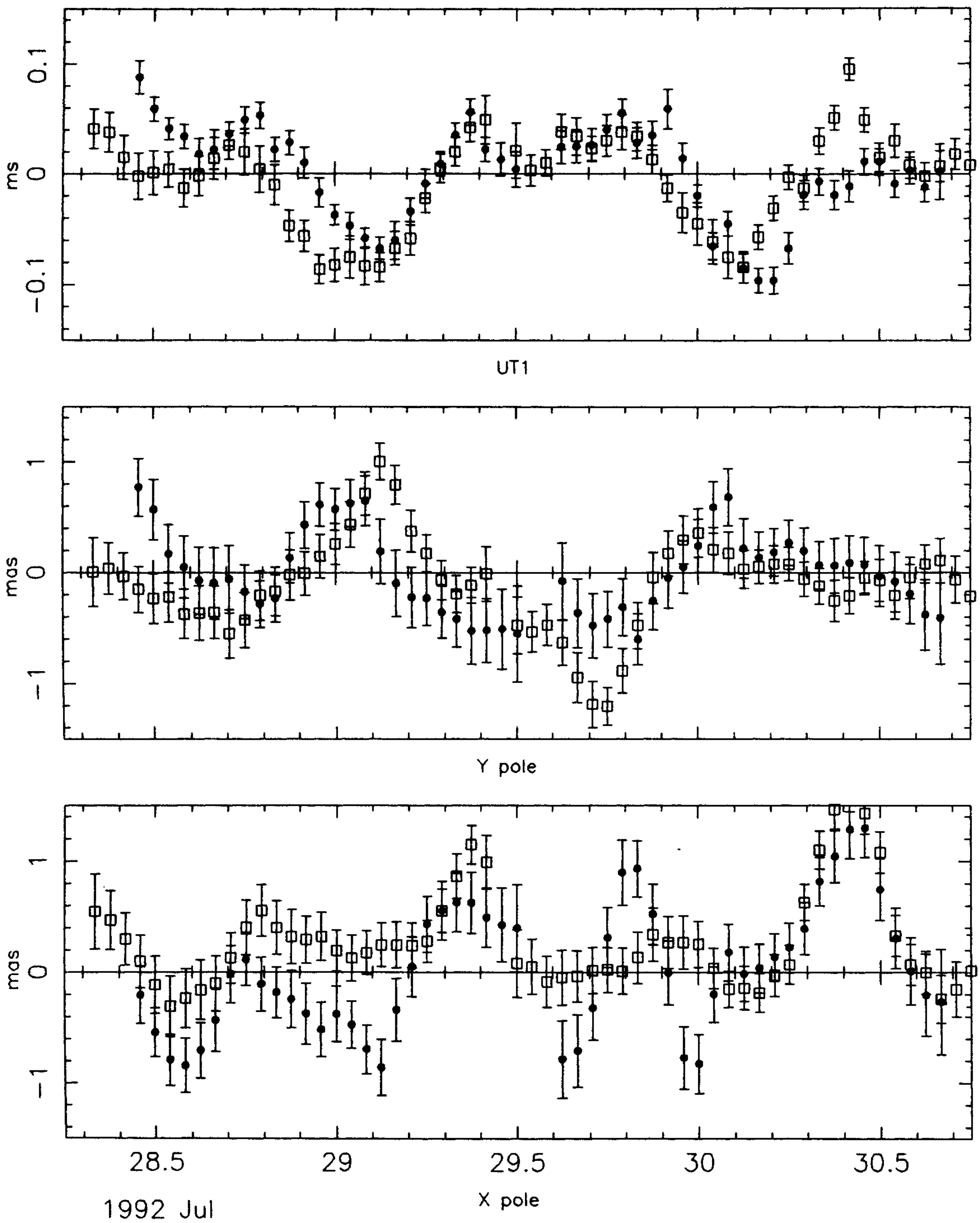

between the routine weekly NEOS-A sessions. With 98% data yield, 42000 observations are expected. The remaining VLBA stations were used as an independent network. Because of extreme weather conditions and some station problems (particularly at Hancock and Kitt Peak), the data only covered 10 days with 40000 observations expected. The USNO NAVEX network observed on nine days with varying networks including NRAO85 3, ALGOPARK (Canada), FORTLEZA (Brazil), MATERA, HARTRAO, KASHIMA, MIZNAO10 (Japan), HOBART26, and KAUAI. The best EOP results should be a factor of two better than the results from SEARCH'92. The raw data will be correlated at the Mark IIIA correlators at the Haystack Observatory and USNO. This set of data will provide a complementary set to SEARCH'92 during the winter when the wet troposphere should be nearly negligible. The data and results should be available to investigators before the end of 1994.

6. REFERENCES

Argus, D.F. and Gordon, R.G. (1991) 'No-Net-Rotation Model of Current Plate Velocities Incorporating Plate Motion Model NUVEL-1', *Geophys. Res. Let.* **18**, 2039.

Gipson, J.M., Chao, B. and Ma, C. (1993) 'Rapid EOP Variations Measured by VLBI', *EOS Spring Suppl.*, 103.

MacMillan, D.S. and Gipson, J.M. (submitted) 'Atmospheric Pressure Loading Parameters from VLBI Observations', *J. Geophys. Res.*

EARTH ROTATION PARAMETERS DERIVED FROM SLR DATA ON LAGEOS-1

B.A.C. AMBROSIUS, D.C. KUYPER, H. LEENMAN, G.J. METS, R. NOOMEN, K.F. WAKKER
Delft University of Technology
Faculty of Aerospace Engineering
Kluyverweg 1
2629 HS Delft
The Netherlands

ABSTRACT. This paper describes the computation of ERP(DUT) 93L05A, the contribution of Delft University of Technology to the SEARCH'92 Campaign. The analysis is based on satellite laser range observations to LAGEOS-1. The resulting 5-daily solutions for x, y and UT1 agree with IERS EOP90C04 at a level of 0.4 and 0.8 marcsec and 0.045 ms, respectively.

1. Introduction

The orbital characteristics of the geodetic satellite LAGEOS-1 (altitude 5900 km, inclination 109 degrees) make it a highly visible target for Satellite Laser Ranging (SLR) observatories around the world. Combined with the fact that the trajectory of the satellite can be modeled with an unparalleled accuracy, LAGEOS-1 is an ideal instrument to study a variety of global geodetic phenomena. Delft University of Technology (DUT) has been involved in the analysis of SLR data on this satellite since 1977. The analysis effort is aimed at crustal deformations and earth rotation in particular. Here, the computation of Earth Rotation Parameters (ERPs) for the SEARCH'92 Campaign (June 21 - September 22, 1992) will be discussed. The emphasis of this paper is on the computation procedure.

2. Technique

The computation of crustal deformations is a primary goal of the analysis of LAGEOS-1 SLR measurements at DUT. Serving this objective, the observations are processed in batches of 13 weeks on average. The deformations are then computed from the differences between the resulting consecutive network solutions.

The computation of the ERPs is performed in three steps. First, solutions for all global parameters (station coordinates and 5-daily ERPs) are computed for each of the quarterly intervals independently. The model that is used for the analysis is summarized in Table 1. It closely follows the IERS Standards (McCarthy, 1992), with a few exceptions: (i) the NASA/GSFC JGM-1 solution for the representation of the gravity field and ocean tides, including constants like GM, a_e and the flattening of the Earth and time-dependent terms, is used instead of the advised GEM-T3 and Schwiderski models; (ii) the effect of atmospheric pressure loading and ocean loading on station positions is not taken into account; and (iii) no plate motion is applied during each 13-week sub-interval. The orbital analysis and parameter estimation is performed using the GEODYN-II/SOLVE-II software package (Eddy et al., 1990; Majer, 1986). To limit the effect of potential dynamic errors in the computation model, each sub-interval is divided into a number of consecutive 1-week data arcs, and the trajectory of LAGEOS-1 is fitted to the observations for each data arc independently, adjusting a state-vector at epoch and a few force-scaling parameters only. It is important to realize that, to avoid the inversion becoming numerically singular, the longitudes of the ascending nodes of each week arc are kept fixed at values derived in a preliminary data analysis, where polar motion is not adjusted but kept fixed at the a priori (IERS 90C04) values. Consequently, it is to be expected that the UT1 solutions presented here will very closely follow the IERS values, and cannot be considered as a very meaningfull analysis result.

In the second step, the series of individual, independent 13-week solutions for the global network of laser stations are converted into a model for the position of each individual station as a function of time. In this way, it is possible to eliminate potential systematic differences between the global network solutions, and bring coherency into the terrestrial reference frame. The model for the station positions includes an initial position at a reference epoch and a simple linear time-dependency for each position component. Although the SEARCH'92 Campaign is limited to 3 months in 1992 only, the analysis was actually performed on LAGEOS-1 observations acquired in the 1983-1992 time frame. The length of this time frame guarantees that very accurate solutions for the tectonic motions for each station can be derived. To eliminate numerical singularities in this step, the motion of a total of 12 globally well-distributed stations was kept fixed at the value given by the NUVEL-1 No Net Rotation model (DeMets et al., 1990). These stations (Yarragadee, Easter Island, Greenbelt, Platteville, Huahine, Mazatlan, Maui, Wettzell, Graz, RGO, Orroral Valley and Kootwijk) are located on the rigid part of 5 of the major tectonic plates, and have a good tracking history.

Finally, the model for station positions as a function of time is then back-substituted and provides the means to bring coherency into the series of ERP solutions. The latter are adjusted without any constraint, whereas the station positions (and the longitudes of the ascending nodes of the weekly satellite state-vectors) are kept fixed at the interpolated values of step 2. Since the normal equations that were already generated for step 1 are being used here, the computation model is the same as the one described in Table 1.

3. Results

The resulting ERP solutions are presented in Table 2. The solution is designated ERP(DUT) 93L05A. It represents an improved version of the ERP(DUT) 93L02 solution, which was submitted to the IERS Central Bureau for inclusion in the 1992 Annual Report. Column 4 provides UT1-UTC values. The standard deviations are 1-σ formal uncertainties. The number in the final column indicates the sub-interval, from which the solutions were taken. For the SEARCH'92 Campaign, only intervals 36 and 37 are relevant.

Statistics of the differences with respect to the a priori values (IERS EOP90C04) are shown in Table 3. After subtraction of the mean difference, the pole position solutions show an agreement of 0.39 and 0.81 marcsec, which is about 3-4 times the formal uncertainty provided along with the solutions here. As for the UT1 values, the agreement is about 0.045 ms, which exceeds the formal uncertainties by a factor of 3-4 also.

4. References

DeMets, C., R.G. Gordon, D.F. Argus and S. Stein, Current plate motions, *Geophys. J. Int.*, **101**, 425-478, 1990.

Eddy, W.F., J.J. McCarthy, D.E. Pavlis, J.A. Marshall, S.B. Luthke, L.S. Tsaoussi, G. Leung and D.A. Williams, GEODYN-II system operations manual Vol. 1-5, contractor report, ST System Corp., Lanham MD, USA, 1990.

Majer, V., SOLVE program mathematical description, NASA contractor report, Business and Technological Systems, Inc., Seabrook MD, USA, Dec., 1986.
McCarthy, D.D., (ed.), IERS Standards (1992), *IERS Technical Note 13*, Observatoire de Paris, France, July, 1992.

Table 1: Models and constants applied in the analysis.

Dynamic model:	
Gravity field	NASA/GSFC JGM-1 model, truncated at 20x20
GM	398600.4415 km^3/s^2
c	299792.458 km/s
a_e	6378.1363 km
1/f	298.2564
Solid earth tides	Wahr model
Ocean tides	NASA/GSFC JGM-1 model
Solar radiation	CR fixed at 1.13; occultation by Earth and Moon; umbra and penumbra
Along-track acceleration	constant value; adjusted
Radial acceleration	sine and cosine 1cpr term; adjusted
Third body attraction	Sun, Moon, Venus, Mars, Jupiter, Saturn; positions from JPL DE200/LE200 ephemeris
Pole tide (dynamic part)	applied
Reference frame:	
Station coordinates	adjusted (step 1); SSC(DUT) 93L05 (step 3)
Earth rotation	adjusted at 5-day intervals; IERS EOP90C04 a priori values
CIS	mean equator and equinox of J2000.0
Precession	IAU 1976 (Lieske model)
Nutation	IAU 1980 (Wahr model)
Plate motion	not applied
Tidal uplift	h_2 = 0.609; l_2 = 0.0852
Pole tide (geometric part)	applied
Atmospheric, ocean loading	not applied
Measurement model:	
Observations	release A normal points, computed at Bendix (June); quick-look normal points (July-September)
Data weighting	overall model accuracy plus system characteristics
Tropospheric refraction	Marini-Murray model

Table 2: The solution ERP(DUT) 93L05A. Only parameters for the interval June 21 - September 22, 1992, are selected here.

date (mjd)	x (marcsec)	y (marcsec)	UT1-UTC (s)	σ(x) (marcsec)	σ(y) (marcsec)	σ(UT1-UTC) (s)	interval
48794	-152.90	356.19	-0.54265923	0.48	0.44	0.00003646	36
48799	-146.66	367.30	-0.55079802	0.29	0.23	0.00002428	36
48804	-141.85	380.24	-0.55816557	0.33	0.26	0.00002062	36
48809	-135.73	390.83	0.43571062	0.28	0.22	0.00001770	36
48814	-127.29	402.32	0.42957544	0.23	0.19	0.00001554	36
48819	-124.15	412.26	0.42320903	0.19	0.19	0.00001493	36
48824	-112.47	424.05	0.41646921	0.18	0.18	0.00001461	36
48829	-101.18	433.90	0.40893665	0.17	0.20	0.00001693	36
48834	-91.95	443.70	0.40174805	0.16	0.19	0.00001461	36
48839	-81.60	455.29	0.39408749	0.15	0.17	0.00001306	36
48844	-71.63	466.30	0.38579321	0.16	0.17	0.00001594	36
48849	-61.92	478.40	0.37731885	0.22	0.21	0.00001678	36
48854	-48.83	486.10	0.36840449	0.15	0.15	0.00001287	36
48859	-33.21	491.68	0.35904445	0.19	0.17	0.00001446	36
48864	-17.61	501.74	0.34899572	0.34	0.27	0.00002395	36
48869	-6.38	503.10	0.33930739	0.27	0.21	0.00001772	37
48874	5.92	506.21	0.33025067	0.16	0.14	0.00001375	37
48879	17.88	507.84	0.32037788	0.19	0.15	0.00001389	37
48884	29.54	509.15	0.31051683	0.14	0.13	0.00001094	37

Table 3: Statistics of the differences between ERP(DUT) 93L05A and IERS EOP90C04. The numbers in the column "rms difference" are obtained before and after subtraction of the mean value, respectively.

quantity	number of solutions	rms difference
x	19	0.52/0.39 marcsec
y	19	1.70/0.81 marcsec
UT1-UTC	19	0.064/0.045 ms

HIGH RESOLUTION EOP FROM LAGEOS SLR DATA ANALYSIS AT GSFC

E. C. PAVLIS
Laboratory for Terrestrial Physics
NASA/Goddard SFC
Space Geodesy Branch, Code 926
Greenbelt, MD 20771-0001
USA

ABSTRACT. A six-hour resolution Earth Orientation Parameter (EOP) series was the product of a complete re-analysis of the 1992 observational data set of Satellite Laser Ranging (SLR) to LAGEOS. This new analysis is a first step towards the complete reduction of the entire tracking data set since LAGEOS' launch (1976). Several improvements in the modeling of the observations have been incorporated. In addition to the EOP series a set of station positions was recovered along with the Fourier coefficients describing the tidally coherent motions of the center of mass implied by this network of stations.

1. Introduction

The improvement of mathematical and physical modeling of the processes involved in the analysis of precise laser ranging data to artificial satellites necessitates the revision of those analyses at a few years' intervals. GSFC revises their modeling at yearly or bi-yearly intervals. Currently we are in the process of analyzing the entire set of data with several new modeling options recently incorporated in our software package (Geodyn/Solve II). While doing so, we have used the tracking data obtained over 1992 as a test data set to verify those new models. The series obtained from this analysis has been included here as a contribution of the SLR group to the characterization of the Earth's variable orientation during the SEARCH '92 campaign.

2. Orbit and Measurement Models

The numerical values of adopted constants and the majority of orbit (force) and measurement models utilized are described in Table 1. In comparison to our previous submission to IERS (in IERS Tech. Note No 14, [Charlot,1993]), it is worth pointing out the major changes in our analysis strategy. We adopted a six-hour averaging interval for the estimation of polar motion and length-of-day variations. Weak *a priori* constraints were applied to prohibit the singularities on intervals void of data. We estimated site-network implied center-of-mass variations at tidal frequencies: semi-daily, daily, and long period. In addition to center of mass motions at tidal frequencies, we have implemented the capability of modeling and estimating Fourier coefficients describing similar effects in polar motion and Earth rotation. These however were not applied in the present solution. Though we still use the IAU 1980 nutation series, we have adopted the IERS-disseminated (VLBI-derived) $\delta\Delta\psi$, $\delta\Delta\varepsilon$ correction series to complement our model.

As far as the force model is concerned, more frequent (every five days) adjustment of a constant along-track acceleration and two once-per-revolution accelerations in the along-track and cross-track directions were deemed appropriate. These are still necessary until we develop a definitive model of the atmosphere-driven perturbations to reduce the impact on LAGEOS' trajectory, [Klosko et al., 1993]. This is one of the major topics to be addressed in the new analysis (SL9). A departure from the IERS recommendations (IERS Standards, Tech. Note No 13, [McCarthy, 1992]), is the use of the latest gravitational model, JGM-2 and an expanded set of tides' coefficients including the 18.6 yr tide. Our evaluation of the new solution over a variety of orbital configurations indicates that JGM-2 is significantly superior to our older solution GEM-T3, [Nerem, 1993].

3. Results

We will refer to the results presented herein as our solution SL9.0. This is our internal number that indicates a preliminary solution within the frame of the final major re-analysis SL9. The solution comprises 12 monthly arcs. The overall rms of fit to the data is 29.3 mm.

3.1 CONTENT

The results obtained from this solution include a set of station positions at epoch 1988.0 with unadjusted velocities constrained to the *a priori* values, the EOP series at six hour intervals (polar motion and length-of-day variations), a set of Fourier coefficients describing the motion of the center of mass (at tidal frequencies) with respect to the origin implied by the (adjusted) tracking site positions, and a number of nuisance parameters required to fit the data to the orbit (e.g. initial state-vector and acceleration parameters per arc). There is no smoothing of any kind applied to the EOP series. In addition to these direct products, we also computed the excitation functions for the resulting EOP series so that they can be later compared to the effective atmospheric angular momentum equivalents.

3.2 EOP COMPARISONS

The resulting EOP series are compared to the *a priori* series, IERS 90 C 04, and to the Kalman filtered combination series SPACE '92 [Gross, 1993a]. The residual differences with respect to these series are displayed in figures 1, 2, 3, and 4. Tables 2 and 3 summarize the statistics of the differences between our results and the aforementioned series.

There is a total of 1460 reporting epochs, 1459 for LODR, of which only 133 had to be constrained for lack or very poor data distribution. Considering that there is at least one occasion per arc that we need to apply absolute constraints on the value of UT1, we conclude that for this particular year we were able to estimate six hour averaged EOPs with a success rate of 92%. This can be further improved when the data from additional stable targets such as LAGEOS II are combined into a single solution. This is intended to be the case for the final SL9 product. Preliminary results of such a combination were shown by M.H. Torrence at the 1993 Fall AGU, [Smith et al., 1993].

For the proper interpretation of the tabulated statistics, one must consider that the displayed kurtosis values are normalized. That is to say, the nominal value of this statistic for a normal distribution (=3) has been subtracted from the tabulated values. The SL9.0 results agree slightly better in rms with the *a priori* series, but they show a slightly smaller mean difference with respect to SPACE '92. The UT1 series were obtained by a simple integration of the LOD values. Since the only estimable quantity in the orbit determination problem is the variation of UT1, i.e. LOD, we have to apply absolute constraints on UT1 to keep it as close as possible to the values implied by the *a priori* series. It is no surprise then that in terms of UT1, our results agree better in the mean as well as in the rms with the *a priori* series. Interestingly, the skewness and kurtosis values indicate that the shape of the residual distribution is still closer to normal for the comparison with SPACE '92. This in fact is true for all four components of the series.

3.3 EXCITATIONS

The effective atmospheric angular momentum (EAAM) functions χ_1, χ_2, and χ_3 as archived and distributed by the AAM Sub-bureau were kindly provided by David Salstein [private communication, 1992]. The series covered the SEARCH'92 period with values given at six hour intervals. Both, the NMC and the ECMWF series were provided, however, we limit our comparisons to the NMC series using their wind terms to the top of the model (50 mb). For the pressure terms we have compared to both EAAM series, those consistent with the Inverted Barometer (IB) hypothesis as well as the ones that do not invoke it (non-IB). These comparisons are limited to the period over which the EAAM data are available to us: Jun. 21 - Sept. 22, 1992, Day-of-Year (DoY): 173-266.

The polar motion excitation functions obtained from the raw six-hour values are displayed in figure 5. At this resolution and scale they seem random, with no underlying structure. The EAAM functions are given at the same interval but they are actually based on a single set of measurements per day, the other values being "model" values that are reported at six hour intervals during the assimilation process. One therefore would not expect the model to be able to forecast high frequency, very rapid changes. After passing the polar motion excitations and our LODR series through a moving average procedure, we start to see the same structure as that depicted by the EAAM functions. We have used various windows from 12 hours to 1, 2, 5 , 10, and 30 days. As expected, the longer windows produce results that agree with the EAAM series only at long wavelength.

The series we show here for comparison purposes are the 2 and 5-day window results. From the six cases we investigated, these seem to depict best the agreement in structure with the EAAM functions. Figures 6, 7, and 8 display these series. The top figure is the windowed EOP excitation functions and the bottom figure shows the corresponding EAAM functions (both non-IB and IB cases). In the polar motion series, the non-IB case functions seem to agree better than do the IB ones. In the LOD case the excitation function seems to wonder between the two cases, sometimes in better agreement with one and at other times with the other. A slope difference is obvious.

What seems to emerge from this comparison is the need for (even short) intensive atmospheric data gathering campaigns during different periods of the year (covering the four seasons). If we are to understand the rapid changes in the EOP series, we need to be able to compare them with data of equivalent frequency content. The EAAMs are the best candidates for the explanation of those rapid changes [Barnes et al., 1983].

3.4 CENTER OF MASS MOTION

The point about which a satellite orbits is the instantaneous center of mass of the planet. We can view our planet as a three-part system: the atmosphere, the oceans, and the solid earth. If there is no mass redistribution within each of these parts and no relative motions between them, then the center of mass remains at rest with respect to the system. We know however that this is not the case for any of the three parts. Most notably, the fluid parts, the atmosphere and the oceans, undergo continuous mass redistribution due to winds, currents, and external (tidal) forces. The solid part is affected by rather well known tidal forces, as well as other sources of mass redistribution that work on geological time-scales (e.g. convection currents, plate tectonics). We cannot expect of course to see the effects of the latter with such a short data set.

The tidally driven redistribution though, produce coherent changes in the inertia tensor that in turn induce motions of the pole, changes in the spin rate of the planet, and translations of the "ensemble" center of mass from its equilibrium position due to the asymmetric distribution of land and oceans over the surface of the planet. Such changes impose a time dependence on the low degree and order gravitational harmonics which are associated with the inertia tensor [Heiskanen and Moritz, 1967]. The standard solutions for gravity field models do not account yet for these effects. Moreover, they impose an absolute constraint on the origin of the reference frame in which the coefficients are described, namely, to be the center of mass, (i.e. $C_{10}=C_{11}=S_{11}\equiv 0$). The origin of that frame is defined by the estimated positions of the tracking stations, all attached to the solid earth. Those positions, except for the tectonic motions and the standard tidal and loading corrections, they are mean positions over the span of the data. That implies that they also define an origin which coincides with the mean center of mass over that time span. A high resolution and precision EOP series requires that these perturbations be either modeled or estimated.

The rotational perturbations were theoretically predicted as early as 1983 [Baader et al., 1983], and the translational ones in [Brosche and Hövel, 1982]. Recently, several new elaborate theoretical studies have been published addressing both parts [Brosche and Wünsch, 1993], [Gross, 1993b], [Ray et al., 1994]. Additionally, all modern space techniques have observed one or the other (or both), [Herring and Dong, 1993], [Watkins and Eanes, 1993], [Gross and Lindqwister, 1992], [Pavlis and Rowlands, 1993]. In SL9.0 we tested the ability of our analysis procedure to estimate a wide spectrum of tidally coherent motions of the center of mass. We allowed for the annual, the semi-annual, the monthly, the fortnightly, the daily and the semi-daily frequencies to be solved for. With a single year of data, we would not place a lot of confidence on the annual and semi-annual components. The other frequencies though should be close to what we will obtain from the complete data set analysis. The results for this preliminary solution are tabulated in Table 4. The astronomical arguments and the phase convention used is consistent with the IERS Standards.

4. Summary

We produced a high resolution Earth orientation series at six hour intervals covering the entire 1992. The series was based on the analysis of LAGEOS SLR data. The analysis procedure follows closely the one proposed for the re-analysis of the entire LAGEOS data set (1976-present), within the framework of the SL9 solution. The present series indicates a very good agreement with smoothed series based on several techniques, e.g. IERS 90 C 04 and SPACE '92. Comparisons of the derived excitation functions with the EAAM functions indicate that the latter are not of sufficient resolution at the reported six hour interval. The 2 and 5-day smoothed EOP excitations though show very good agreement, indicating that with higher resolution atmospheric data we should be able to explain a significantly larger variance in the EOP excitations. Station positions were also estimated for the tracking sites and at the same time a model for the tidally coherent translations of the center of mass with respect to the origin defined by these positions was also solved for.

5. References

Baader, H.R., P. Brosche, W. Hövel (1983) 'Ocean tides and periodic variations of the Earth's rotation', *J. Geophys.*, *52*, 140-142.

Barnes, R.T.H., R. Hide, A.A. White, and C.A. Wilson (1983) 'Atmospheric angular momentum fluctuations, length-0f-day changes and polar motion', *Proc. Roy. Soc. London, Ser. A*, *387*, 31-73.

Brosche, P. and W. Hövel (1982) 'Tidal friction for times around the presence' in P. Brosche and J. Sündermann (eds.), Tidal Friction and the Earth's Rotation II, Springer, Berlin-Heidelberg-New York, 175.

Brosche, P. and J. Wünsch (1993) 'Variations of the Earth's center of mass due to oceanic tides', *Astron. Nachr.*, 314, 2, 87-90.

Gross, R.S. (1993a) 'A Combination of Earth Orientation Data: SPACE92', an electronic article with the disseminated series, 1-11.

Gross, R.S. (1993b) 'The effect of ocean tides on the Earth's rotation as predicted by the results of an ocean tide model', *Geophys. Res. Letters*, 20, 293-296.

Gross, R.S. and U.J. Lindqwister (1992) 'Atmospheric Excitation of Polar Motion During the GIG'91 Measurement Campaign', *Geophys. Res. Letters*, 19, 849-852.

Heiskanen, W.A. and H. Moritz (1967) 'Physical Geodesy', W.H. Freeman and Company, San Francisco and London.

Herring, T.A. and D. Dong (1993) 'Measurement of Diurnal and Semidiurnal Rotation Variations and Tidal Parameters of the Earth', submitted to *J. Geophys. Res.*.

Klosko, S.M., R.S. Nerem, N.K. Pavlis and R.G. Williamson (1993) 'Long Wavelength Atmospheric Tides from SLR Data', (abs.), *EOS Trans. AGU, 74(43), 1993 Fall Meeting Suppl.*, 196.

McCarthy, D.D. (ed.) (1992) 'IERS Standards (1992)', *IERS Technical Note 13*, Central Bureau of IERS, Observatoire de Paris.

Nerem, R.S. (1993) 'Gravity Model Determination from Satellite Data: Current Status and Future Developments', (abs.), *EOS Trans. AGU, 74(43), 1993 Fall Meeting Suppl.*, 64.

Pavlis, E.C. and D.D. Rowlands (1993) 'Daily Resolution Earth Orientation Series During SEARCH '92', (abs.), *EOS Trans. AGU, 74(43), 1993 Fall Meeting Suppl.*, 189.

Ray, R.D., B.F. Chao, D.J. Steinberg and D.E. Cartwright (1994) 'Diurnal and semidiurnal variations in the earth's rotation rate induced by oceanic tides' in H. Hus (ed.) Proceedings of the 12th International Symposium on Earth Tides, Aug. 4-7, Beijing, China.

Smith, D.E., R. Kolenkiewicz, P.J. Dunn, S.M. Klosko, J.W. Robbins, M.H. Torrence, R.G. Williamson and E.C. Pavlis (1993) 'Earth Orientation Parameters from GSFC Solution SL8.2 GSFC 93 L 01', in P.Charlot (ed.), *IERS Technical Note 14*, Central Bureau of IERS, Observatoire de Paris.

Smith, D.E., R. Kolenkiewicz, M.H. Torrence and P.J. Dunn (1993) 'A Multi-Satellite Global SLR Solution', (abs.), *EOS Trans. AGU, 74(43), 1993 Fall Meeting Suppl.*, 185.

Watkins, M.M. and R.J. Eanes (1993) 'Tidally Coherent Diurnal and Semidiurnal Geocenter Variations Observed with Lageos Laser Ranging', (abs.), *EOS Trans. AGU, 74(16), 1993 Spring Meeting Suppl.*, 103.

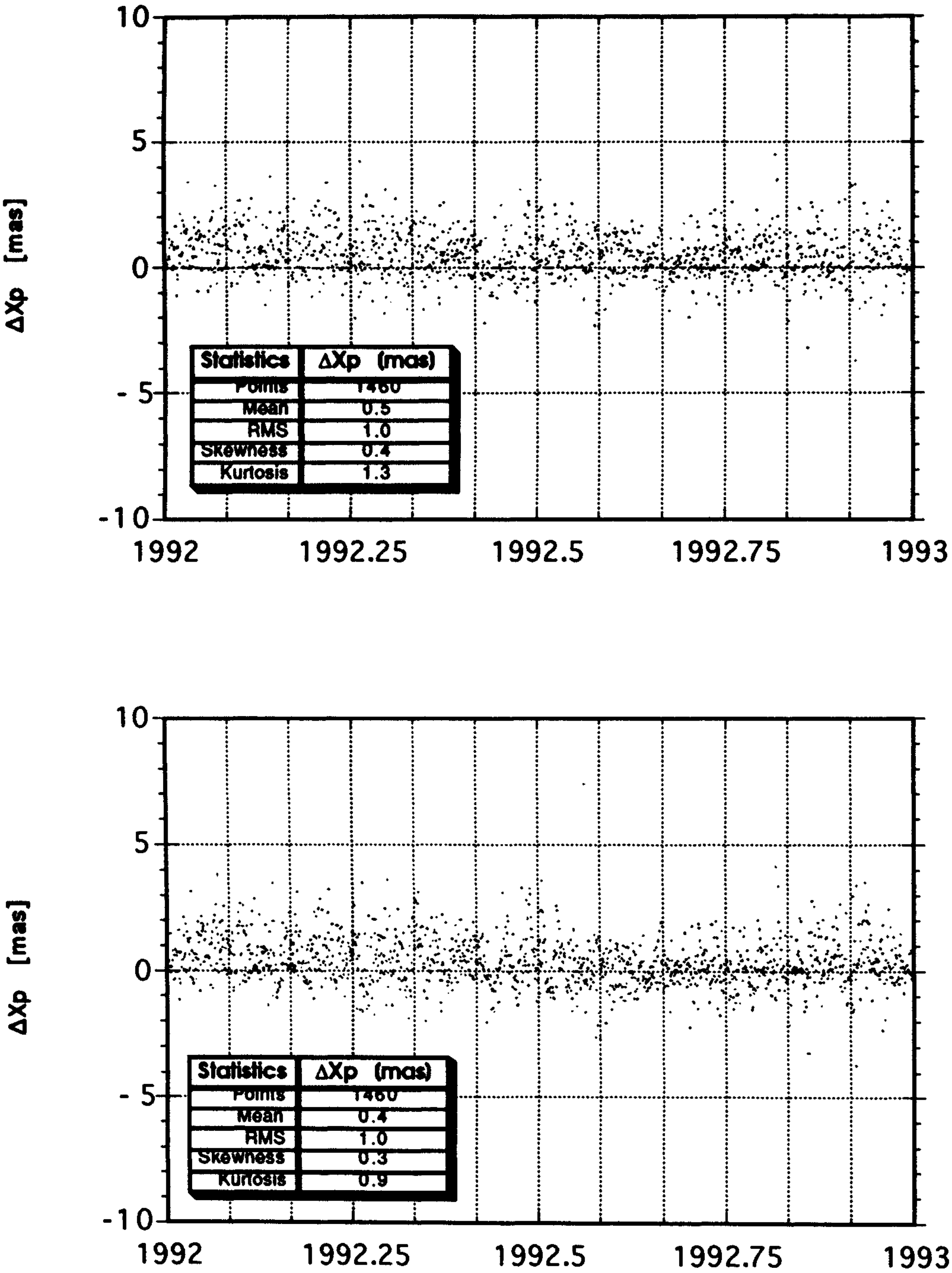

Figure 1. Comparison of the x component of polar motion from SL9.0 to IERS 90 C 04 (top) and SPACE '92 (bottom).

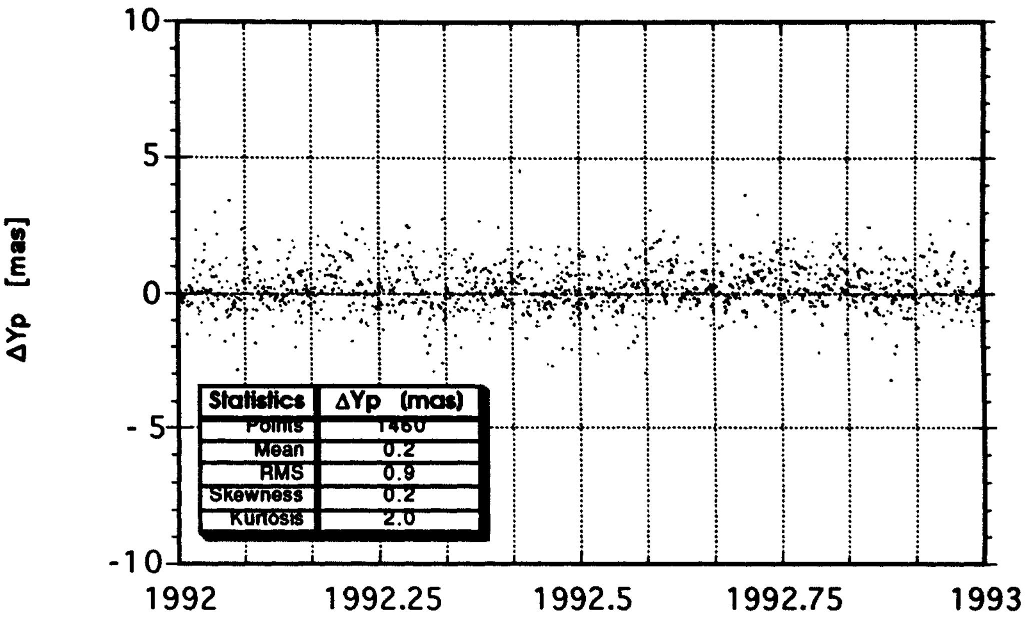

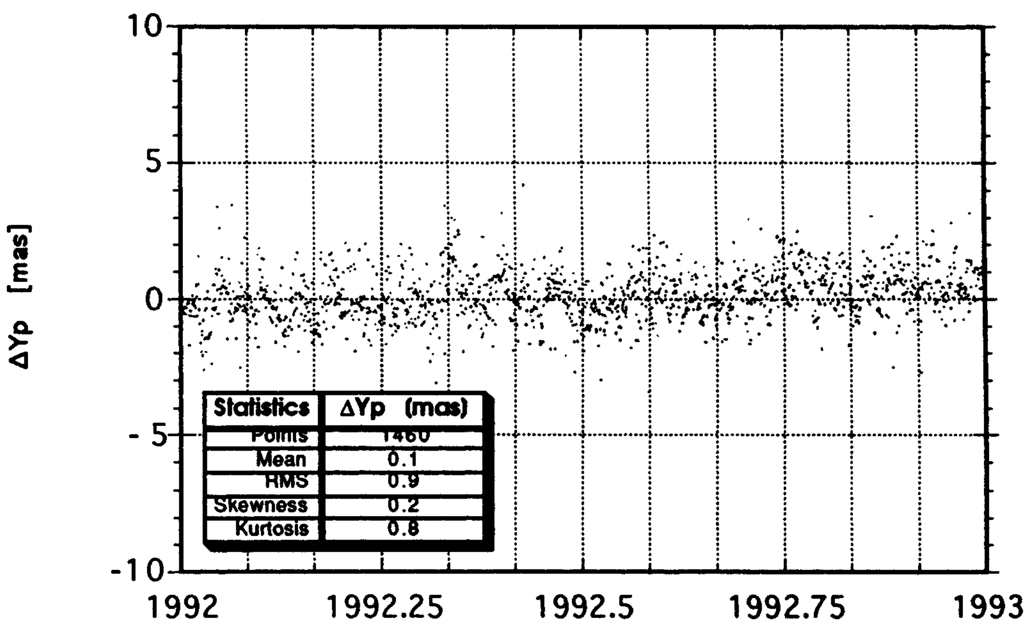

Figure 2. Comparison of the y component of polar motion from SL9.0 to IERS 90 C 04 (top) and SPACE '92 (bottom).

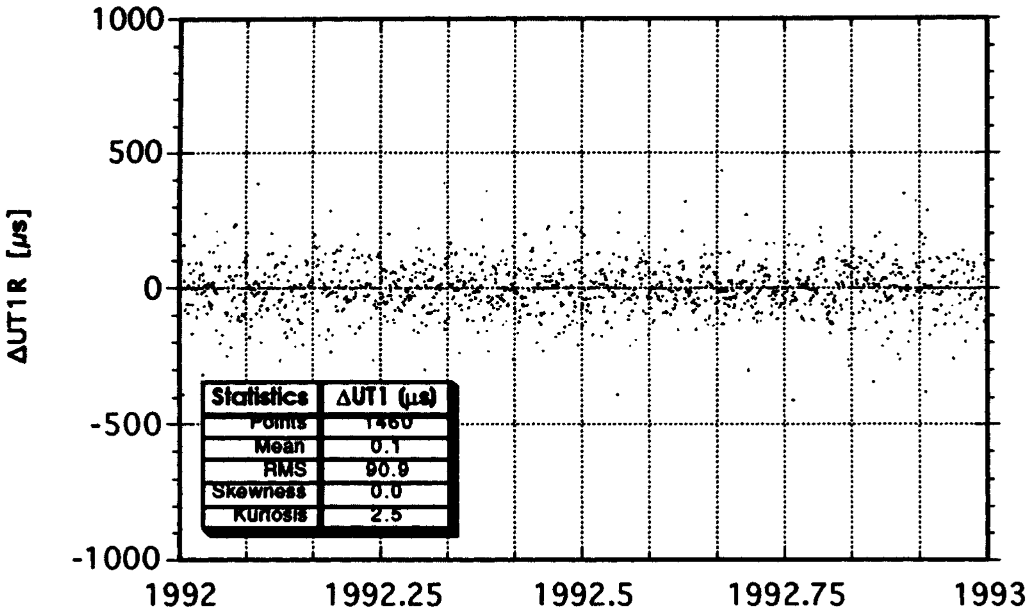

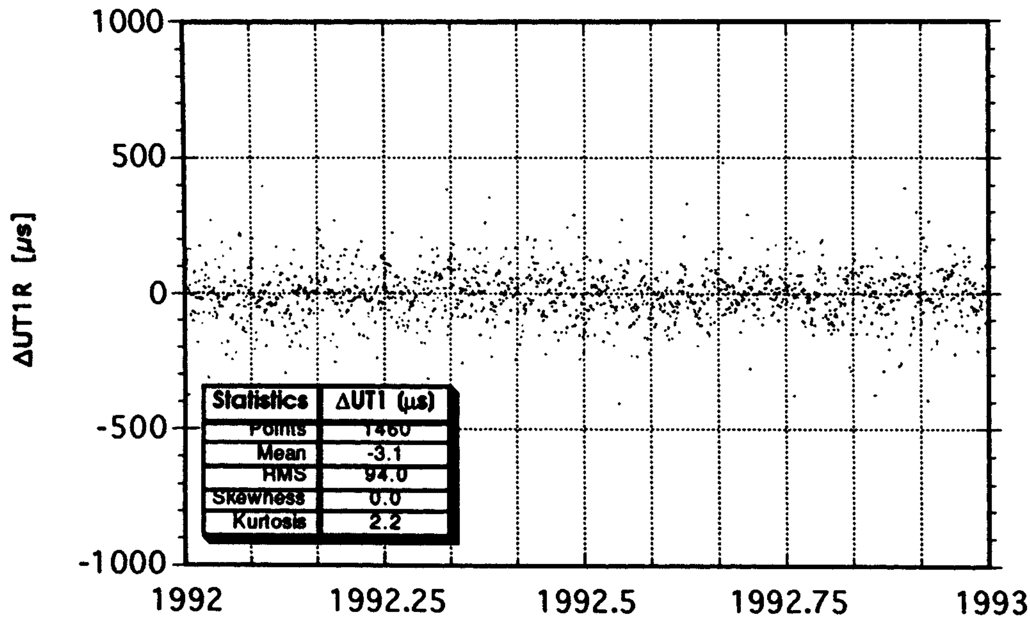

Figure 3. Comparison of inferred UT1R from SL9.0 to IERS 90 C 04 (top) and SPACE '92 (bottom).

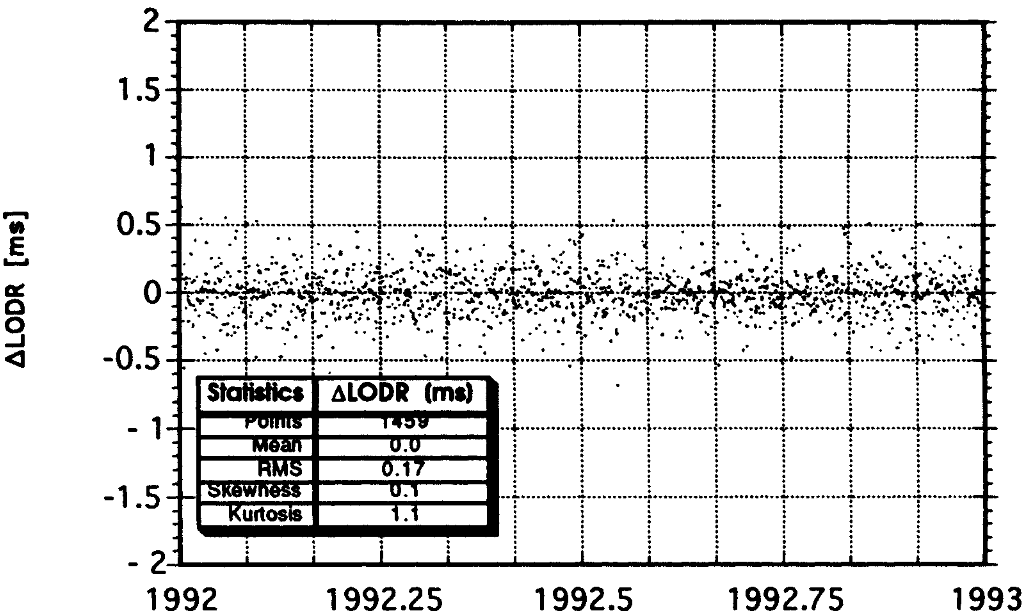

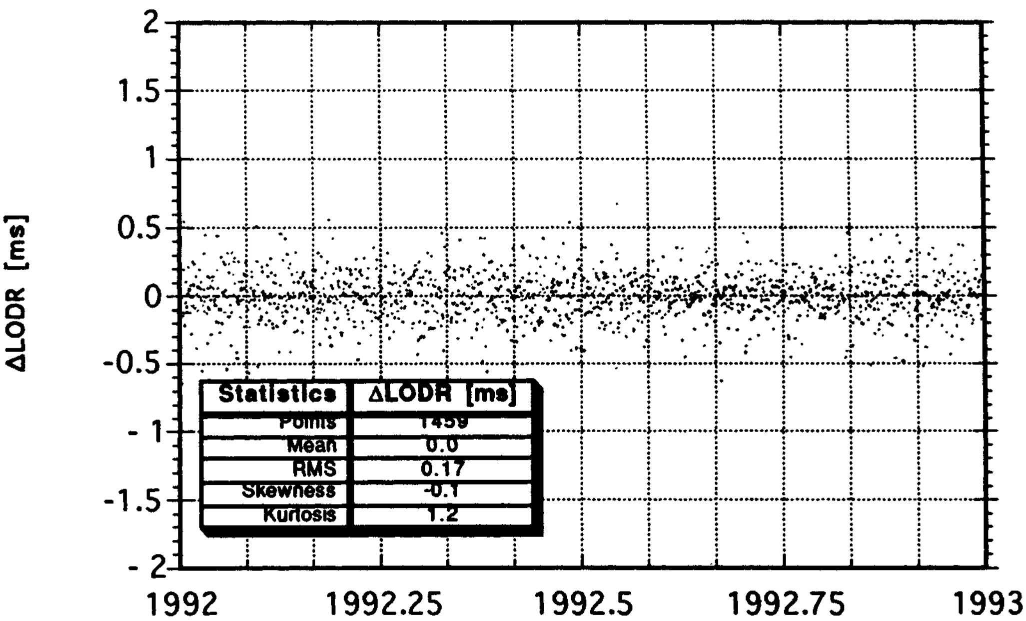

Figure 4. Comparison of Length-of-Day variations from SL9.0 to IERS 90 C 04 (top) and SPACE '92 (bottom).

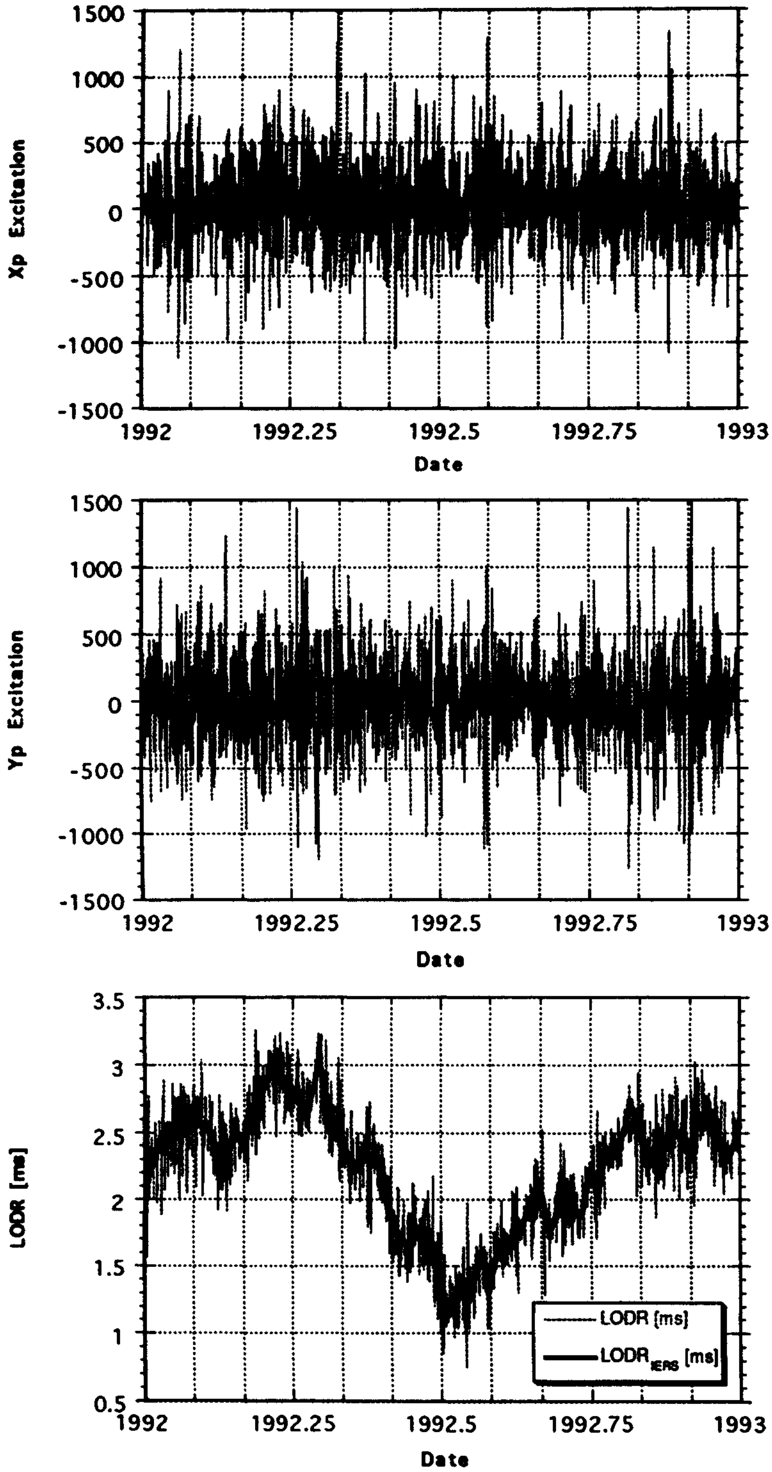

Figure 5. Polar motion and Earth rotation Excitation functions from the raw 6 hr resolution SL9.0 series.

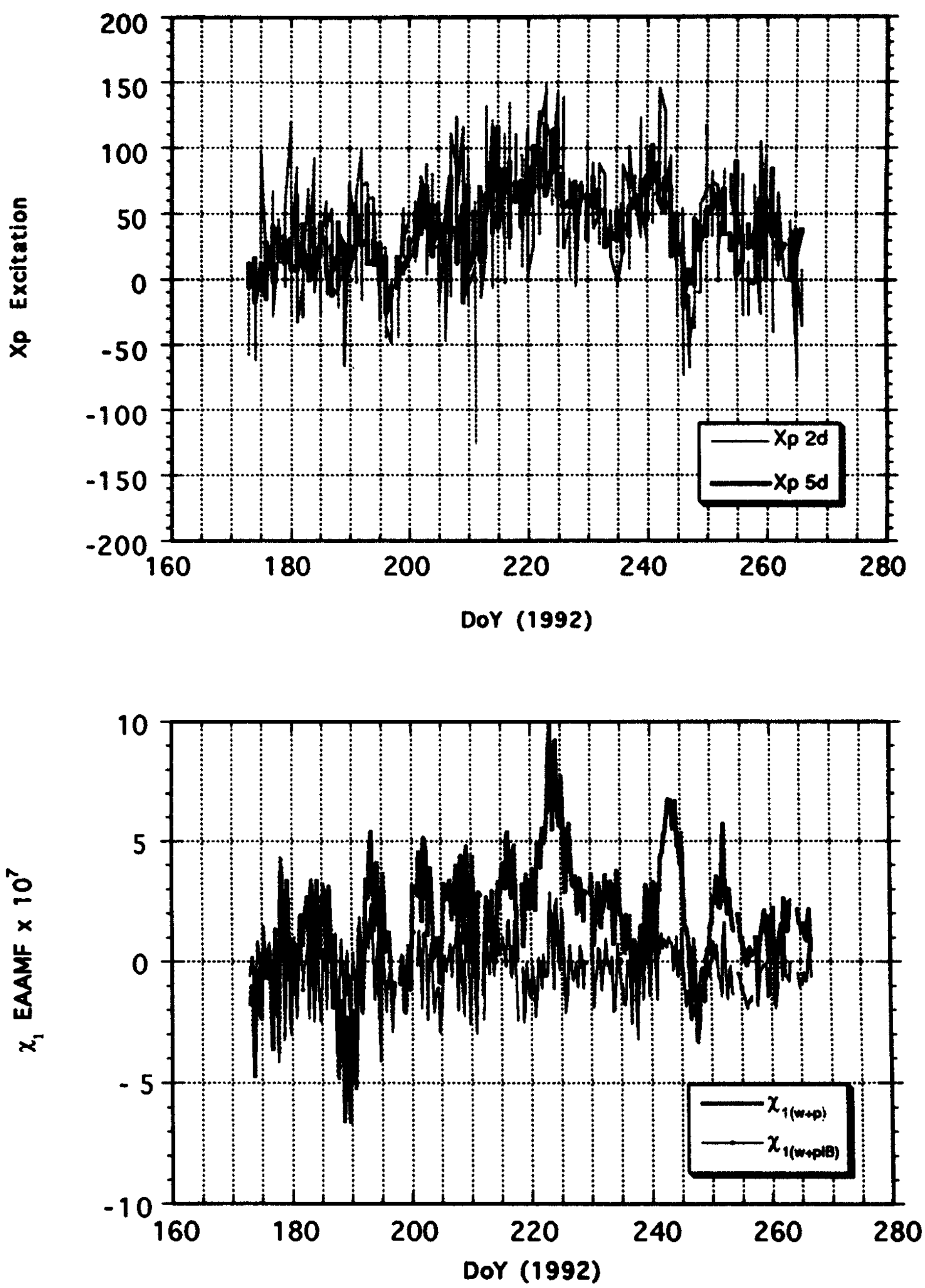

Figure 6. X component of polar motion excitation functions with 2-day and 5-day sliding window smoothing (top) and EAAM function χ_1 from NMC series (bottom) with and without the inverted barometer hypothesis.

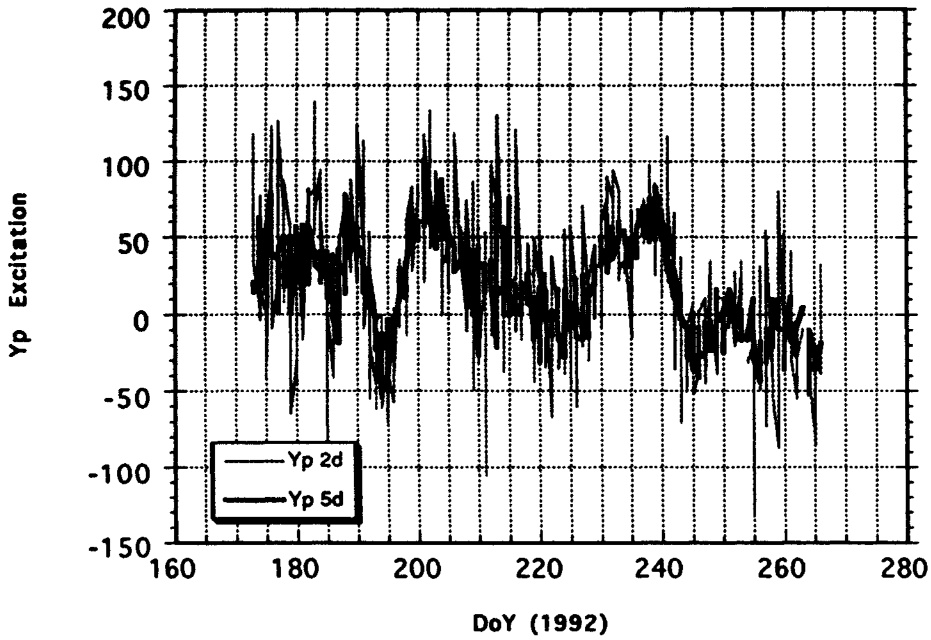

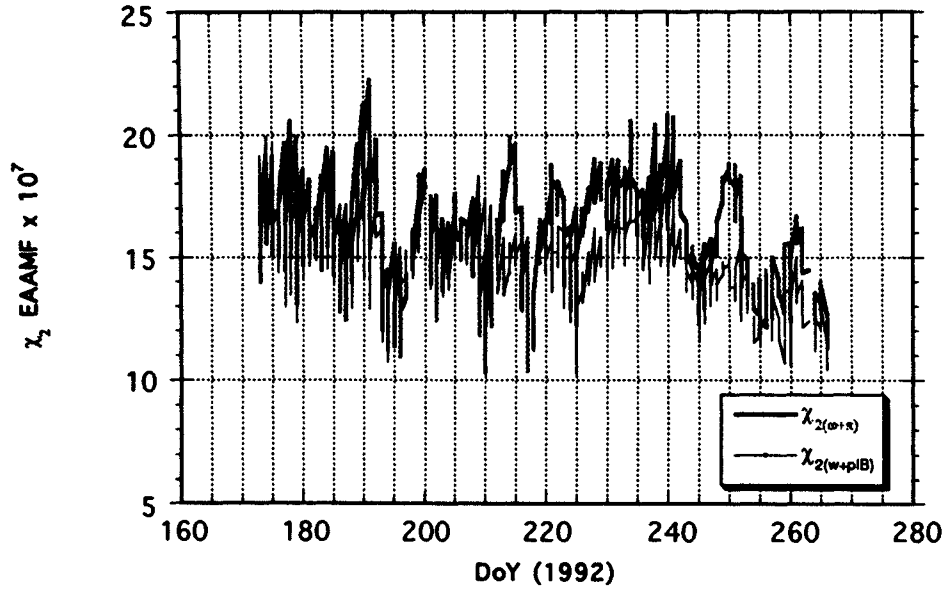

Figure 7. Y component of polar motion excitation functions with 2-day and 5-day sliding window smoothing (top) and EAAM function χ_2 from NMC series (bottom) with and without the inverted barometer hypothesis.

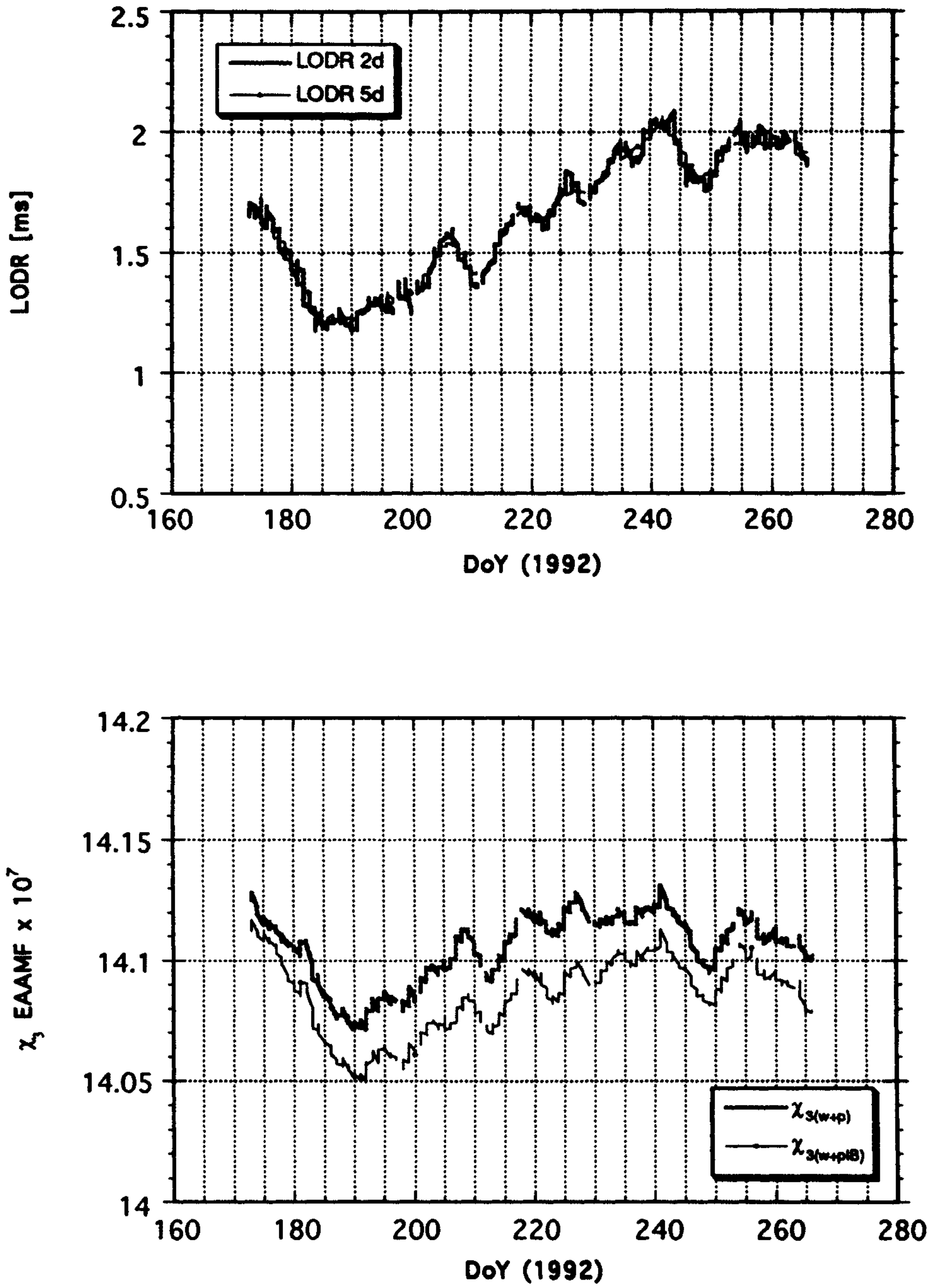

Figure 8. Earth rotation excitation functions with 2-day and 5-day sliding window smoothing (top) and EAAM function χ_3 from NMC series (bottom) with and without the inverted barometer hypothesis.

TABLE 1. Description of the Terrestrial Frame underlying the EOP(GSFC) 93 L 02 series.

1 - Technique		:	SLR to LAGEOS
2 - Analysis Center		:	NASA/GSFC
3 - Solution identifier		:	SL9.0
4 - Software used		:	GEODYN II / SOLVE II
5 - Relativity Scale		:	Local Earth
6 - Station tidal correction		:	Earth tides & ocean loading (Scherneck)
7 - Tectonic plate model		:	GSFC SL8.2
8 - Velocity of light (C)		:	299 792 458 m/s
9 - Geogravitational const. (GM_o)		:	398600.4415 km3/s2
10 - Reference epoch		:	88 01 01
11 - Adjusted parameters	Orbit	:	6 elements/30(35) days along track accel./5 days once per rev. accel./5 days
	Stations	:	Epoch positions adjusted for all sites except lat/lon of 7105 and lat of 7210.
	EOP	:	x,y and UT1 every 6hr (centered at 0300, 0900, 1500, 2100 UTC), one UT1 interval fixed per arc. Intervals without data fixed to *a priori*.
12 - Definition of the origin		:	Geocentric
13 - Definition of the orientation		:	EOP(IERS) 90 C 04
14 - Constraint for time evolution		:	SL8.2 velocity field

TABLE 2. Statistics of the comparison of SL9.0 to the *a priori* series IERS 90 C 04.

Statistics	ΔXp (mas)	ΔYp (mas)	ΔUT1 (μs)	ΔLODR (ms)
Points	1460	1460	1460	1459
Mean	0.47	0.22	0.10	0.00
RMS	1.01	0.86	90.86	0.17
Skewness	0.38	0.20	0.04	0.10
Kurtosis	1.35	1.98	2.49	1.10

TABLE 3. Statistics of the comparison of SL9.0 to the Kalman smoothed SPACE'92 series.

Statistics	ΔXp (mas)	ΔYp (mas)	ΔUT1 (μs)	ΔLODR (ms)
Points	1460	1460	1460	1459
Mean	0.39	0.13	-3.07	0.00
RMS	1.03	0.94	93.99	0.17
Skewness	0.34	0.20	0.028	-0.11
Kurtosis	0.95	0.75	2.24	1.19

TABLE 4. Estimated coefficients of tidally coherent motions of the center of mass.

Doodson's Number	Cos Coeff. [mm]	Sin Coeff. [mm]	Coordinate Component	Tidal Wave Designator
56554	4.5 ± 1.	2.0 ± 1.	X	
	-9.5 1.	-5.0 1.	Y	S_a
	-12.0 3.	14.0 3.	Z	
57555	3.1 ± 1.	-3.5 ± 1.	X	
	0.3 1.	-2.6 1.	Y	S_{sa}
	-10.8 2.	5.2 2.	Z	
65455	2.3 ± 1.	-0.4 ± 1.	X	
	-0.6 1.	0.0 1.	Y	M_m
	-3.2 2.	-5.9 2.	Z	
75555	-1.6 ± 1.	-0.7 ± 1.	X	
	-3.5 1.	1.6 1.	Y	M_f
	-12.3 1.	- 2.4 1.	Z	
135655	-0.4 ± 1.	-3.5 ± 1.	X	
	-6.1 1.	-0.8 1.	Y	Q_1
	-1.5 1.	-0.9 1.	Z	
145555	-6.0 ± 1.	-1.0 ± 1.	X	
	-2.2 1.	1.0 1.	Y	O_1
	-2.5 1.	-1.1 1.	Z	
163555	3.8 ± 2.	3.6 ± 2.	X	
	-6.7 2.	-6.4 2.	Y	P_1
	-5.2 1.	1.8 1.	Z	
164555	-2.9 ± 2.	13.6 ± 2.	X	
	14.3 2.	4.7 2.	Y	S_1
	-2.4 1.	8.1 1.	Z	
165555	6.0 ± 2.	1.8 ± 2.	X	
	3.7 2.	-2.3 2.	Y	K_1
	-2.5 1.	-5.1 1.	Z	
245655	-1.9 ± 1.	3.5 ± 1.	X	
	0.8 1.	-1.3 1.	Y	N_2
	1.0 1.	0.1 1.	Z	
255555	0.0 ± 1.	5.3 ± 1.	X	
	1.8 1.	4.1 1.	Y	M_2
	-0.3 1.	-3.6 1.	Z	
273555	0.9 ± 1.	0.9 ± 1.	X	
	-6.5 1.	-5.8 1.	Y	S_2
	-1.2 1.	-0.7 1.	Z	
275555	8.3 ± 1.	-4.9 ± 1.	X	
	-4.1 1.	-9.1 1.	Y	K_2
	-1.0 1.	0.0 1.	Z	

HIGH RESOLUTION EARTH ROTATION PARAMETERS AS COMPUTED FROM SLR AND GPS DATA

REIGBER, CH.; MONTAG, H.; GENDT, G.; DICK, G.;
GeoForschungsZentrum
Dept. on Recent Kinematics and Dynamics of the Earth
Telegrafenberg, D-14473 Potsdam, Germany

ABSTRACT. Earth rotation parameters with a daily and sub-daily resolution were determined using SLR and GPS data. Although both techniques can deliver highly accurate results the GPS data have clear advantages because of the better data distribution.

1. Introduction

The daily and sub-daily resolution of the Earth Rotation Parameters (ERP's) with an aimed accuracy of 0.1 mas and 0.01 ms, respectively, is currently an area of intensive investigations, particularly also of the SEARCH'92 Campaign. Both the higher time resolution and accuracy will essentially contribute to a further improvement of the understanding of the interaction of outer and inner forces with the Earth's rotational behaviour.

One of the problems of all methods of determining high-frequency ERP's is the decomposition of EOP's and nutation terms. In the case of satellite methods the correlation with orbital elements has an additional influence (Montag et al. (1993)). Therefore, the high resolution of ERP's requires high-accurate measurements and modelling. Furtheron the data should be fairly even distributed around the whole day. This latter condition can be better fulfilled by GPS measurements than by Satellite Laser Ranging (SLR). On the other side using dense distributed SLR data for certain time intervals high-accurate ERP's results can be obtained as an independent reference for comparisons.

2. Model Parameters, Data and Reference Frame

The analyses were performed by means of the GFZ orbital program packages EPOS.P.V1 for SLR and EPOS.P.V2 for GPS data. The model parameters used are according to IERS standards, generally. The exceptions are:

GM	398600.440 km^3s^{-2} (initial, adjusted)
Lageos:	
Cross-section to mass relation	0.000694 m^2/kg
Nominal reflectance coefficient	c_R = 1.12 (adjusted)
Empirical acceleration	c_e (adjusted)
GPS	
Tropospheric correction	Saastamoinen, 1973
Solar radiation pressure	ROCK 4 and 42 including thermal reradiation
Vehicle masses	Fliegel (1992), Feltens (1991)

Lageos data were analysed since 1980. The typical orbital fit for a 5-day arc is ± 4 cm.
In the case of GPS undifferenced ionospheric-free phases were analysed since the IGS '92 campaign. The sampling rate is 6 minutes and the arc length 32 hours. Different parameters were adjusted for different time intervals (Gendt et al (1993 a, b)), namely:

SLR:

c_e, c_R	-	global, every 30 days
Orbital parameters	-	5- or 6-day intervals
ERP's	-	5, 3, 2 days; for selected intervals further 1d, 12h, 6h
Station coordinates	-	quarterly, semiannual or for longer time intervals

GPS:

Orbital parameters	-	32-hour arcs
c_R and y-bias	-	32-hour arcs
ERP's	-	1d, 12h
Tropospheric zenith path delay	-	e. g. 4h
Ambiquities		
Epoch time parameters		

As a result of the analyses two sets of station coordinates were obtained. The laser station coordinate set SSC (GFZ) 93L01 consists of 101 monument positions. The average accuracy is better than ± 2 cm. The comparison after a 7-parameter similarity (Helmert) transformation with the combined ITRF solution is shown in Table 1. Besides the position for 69 monuments also the motion velocities were adjusted (the other sites were fixed to the NUVEL-1 model motions).

The fiducial-free GPS station coordinate set SSC (GFZ) 93G01 shows a similar accuracy (Tab. 1).

TABLE 1. Comparison with combined ITRF-SSC

	rms (cm)	Scale (10^{-8})	Translation of geocenter (x, y. z; in cm)		
SSC (GFZ)93G01 - SSC (ITRF)93C01	1.6	.38	8.3	2.6	- 2.2
SSC(GFZ)93L01 - SSC (ITRF) 91	1.9	.01	- .4	-0.3	2.8

3. Results for the ERP's

3.1. ERP's BASED ON SLR DATA

It was shown that generally a high accuracy for highly resolved ERP's can be obtained too if at least SLR data from 4 relevant passes for each of the pole coordinates are available (Montag (1989)). But it can happen that even one well measured relevant satellite pass delivers high accurate results too. By means of numerical investigations a better criterion was found in the use of correlation between the solved-for ERP's. These correlations depend mainly from the data distribution and the sampling time interval for the solve-for-ERP's. If the correlation is higher than 0.9, certain parameters are deleted in the following way:

correlation > 0.9 between	deleted parameters
x_P, y_P x_P, UT (LOD) y_P, UT (LOD) x_P, UT (LOD) and y_P, UT (LOD)	x_P and y_P x_P y_P x_P, y_P, UT (LOD)

TABLE 2. Percentage of deleted pole coordinates and average correlation between ERP's after deletion

Time resolution		2d	1d	12h	6h
Percentage deleted	x_P y_P	1... 2 5...10	5...10 20	25 40	45-50 55-60
Mean correlation between ERP's		0.25	0.3	0.4...0.5	0.6

TABLE 3. R.m.s. difference between high resolution solution and 3-day solution (constant offset neglected)

Time resolution	R.m.s. differences in pole coordinates in mas Example 1 average data distrib.	Example 2 average data distrib.	dense data distrib.
1 d	0.9	1.4	0.3
12 h	1.4	2.2	0.9
6 h	2.5	3.3	1.6

TABLE 4. R.m.s. difference between 3- resp. 5-day solution and 1-day solution of ERP's (constant offset neglected)

Time resolution of reference	R.m.s. differences in pole coordinates in mas. over 2 years (from 6.90 to 9.92)	over 90 days Example 1	Example 2
3 day	1.2	0.9	1.4
5 day	1.4	1.0	1.8

Using this criterion ERP's were computed with different time resolutions. For sub-daily resolution (12h, 6h) two examples were analysed:

- Example 1: 90 days from Dec. 1990 to March 1991 (incl. GIG'91 Campaign)
- Example 2: 90 days from June 1992 to Sept. 1992 (SEARCH'92 Campaign).

The percentage of pole coordinate results eliminated in this way is shown in Table 2 as a function of the time resolution. This Table further indicates that for the remaining results the average correlation ranges between 0.25 for the 2d solution and 0.6 for a resolution of 6h.

Several results having different time resolutions are displayed in Figure 1 to 3 (as corrections to IERS combined solution) together with the number of station and passes observed per day.

Figure 1 shows a part of the results of the Example 1 as correction to IERS, namely the 1d solutions for x and y, and the 12h solutions for the y component of the pole coordinates. The 3d solution is included as reference. The dependence of the scattering and the number of deleted points on the number of the stations and the observed passes is evident, especially for the 12h results. The effect of Christmas - New Year time (45249 - 257) is also clear visible.

More detailed results are shown for Example 2 (SEARCH'92 Campaign) in Figures 2 and 3. Here one can see the results for both the x- (Fig. 2) and y-component (Fig. 3) with a time resolution of 1d, 12h and 6h together with the 5d and 3d results as references. Comparing with Example 1 the scattering of the Example 2 is apparently higher. This is confirmed numerically in Table 3. It shows the r.m.s. differences (constant offset neclected) between the 3d solution on the one side and the 1d, 12h and 6h solution on the other. For an average data distribution the r.m.s. differences are in all cases significantly higher for the SEARCH'92 campaign. For the 1d resolution pole coordinates this is confirmed also using the 5d solution as a reference (Table 4). Table 4 also displays the r.m.s. differences between the 1d solution and the 3d and 5d solution for a time span of two years. Because the quality and quantity of the observations are nearly the only cause for the amount of these differences one can conclude, that apparently the SLR observing activity was during the GIG'91 campaign better, but during the SEARCH'92 campaign even worse than in average.

Selecting only time intervals with a dense data distribution the results can be much better (Table 3). The r.m.s. differences are about 0.3 mas for the 1 d resolution and still better than 1 mas (0.9) for the 12h resolution.

TABLE 5. R.m.s. difference to the smoothed mean 1-day curve (time period 1993, Jan. - June)

Time resolution	Center	Pole coordinates in mas	
		x-pole	y-pole
1d	JPL	0.71	0.73
1d	SIO	0.36	0.49
1d	EMR	0.53	0.43
1d	GFZ	0.34	0.29
12h	GFZ	0.35	0.36

3.2. ERP's BASED ON GPS

Using the GPS data of the SEARCH Campaign ERP's were determined with a time resolution of 1d (Zhu et al. (1993)). Besides the 1d resolution for 1993 also ERP's with a time resolution of 12h were analysed. A section of these results is presented in Figure 4 together with the corresponding solution of SIO. Apparently the scattering of the GPS results is generally smaller than that of SLR results. Numerically this is confirmed in Table 5. Here the r.m.s. differences to the smoothed 1d curve are shown (not to the 3d or 5d solution as in the case of SLR; this makes the GPS results somewhat more optimistic). It is clearly visible from this table that most of the IGS Analysis Centers have reached a 0.5

Figure 1. Diurnal and semidiurnal SLR polar motion results (Example 1)
3d solution (–) as reference

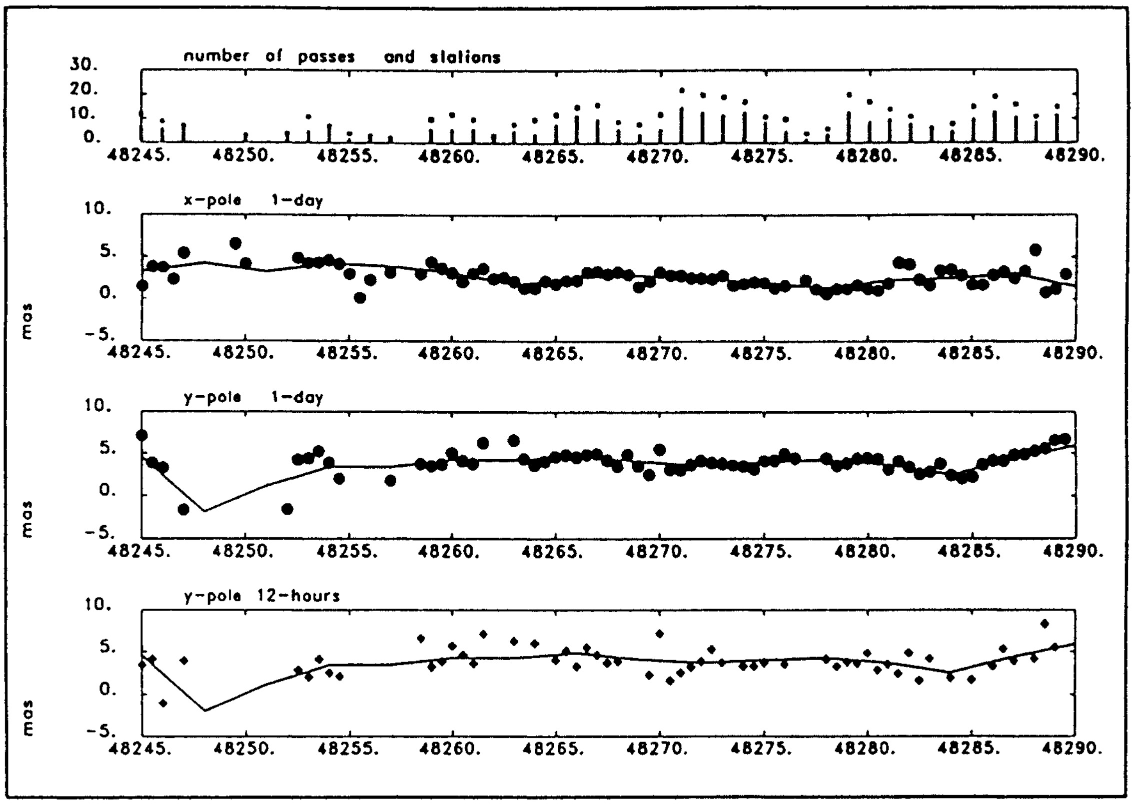

Figure 2. Highly resolved SLR x-pole (Example 2)
5d (—) and 3d (–) solution as reference

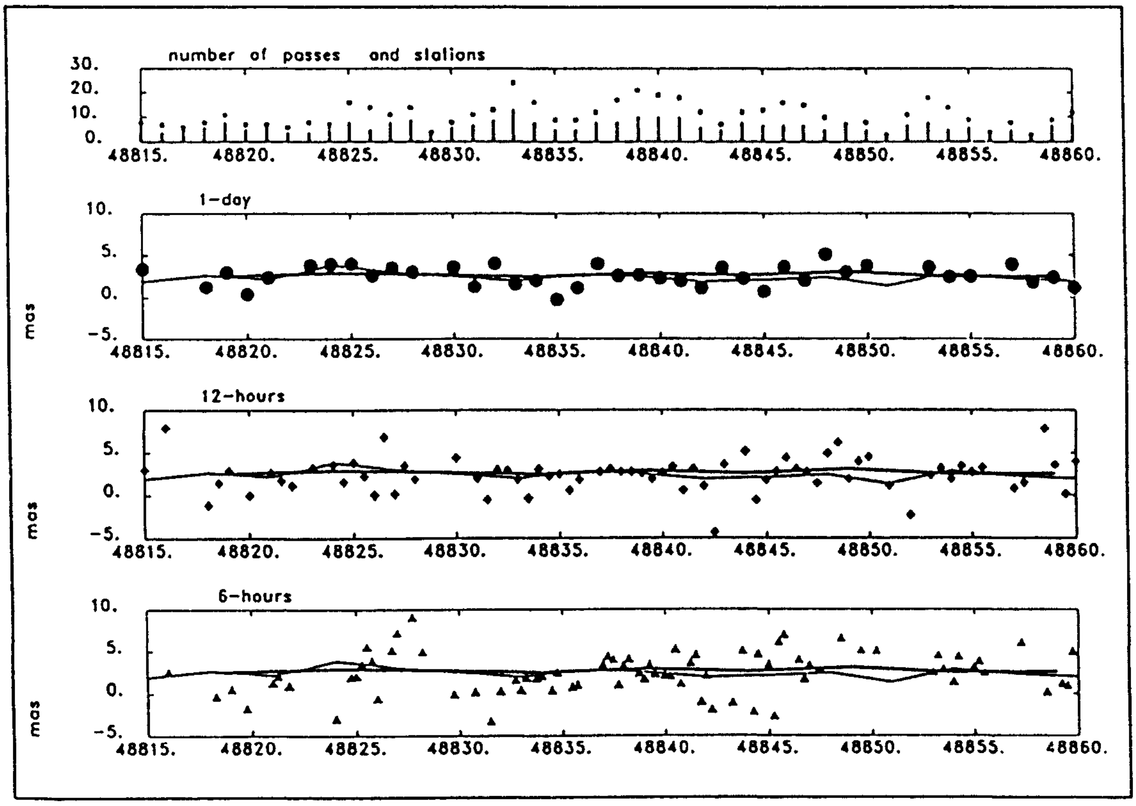

Figure 3. Highly resolved SLR y-pole (Example 2)
5d (⟷) and 3d (–) solution as reference

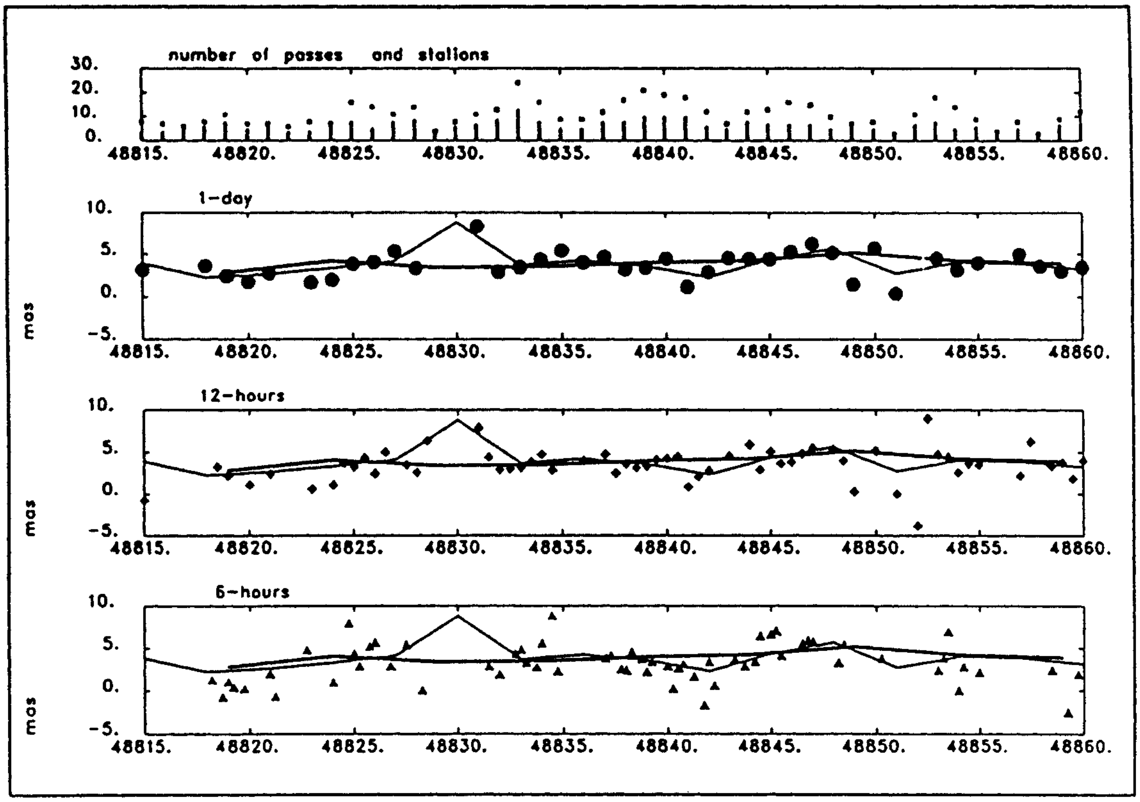

Figure 4. Highly resolved polar motion from GPS
1d GFZ (⟶), 1d SIO (–), 12h GFZ (◆)

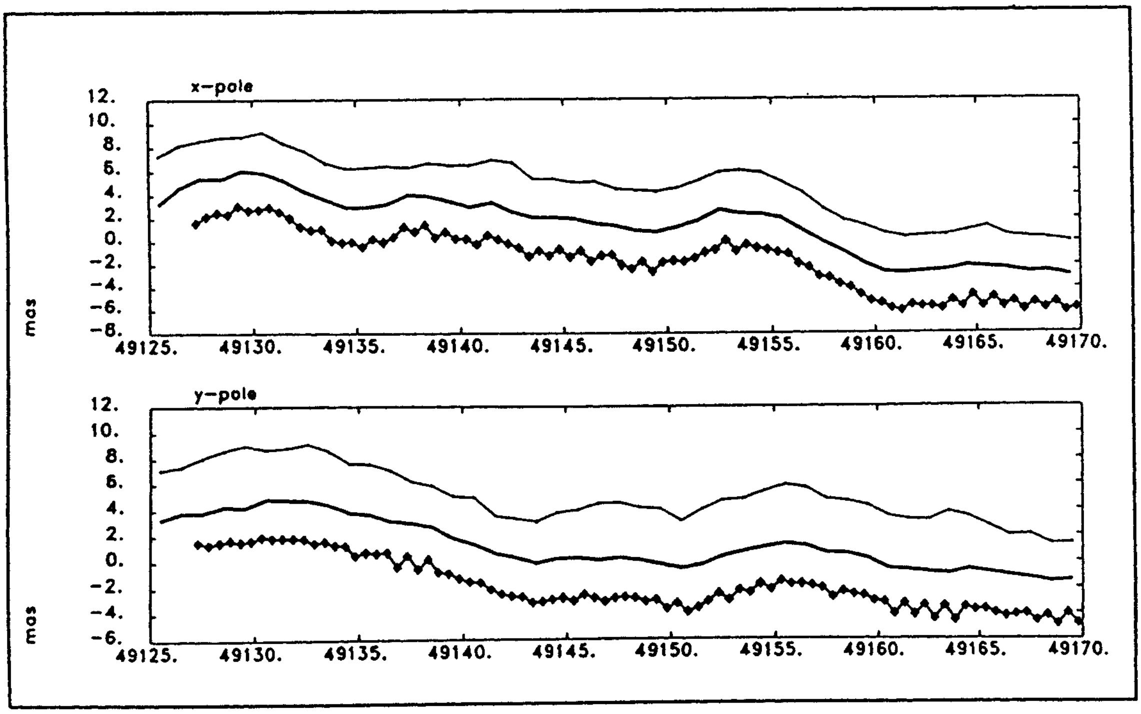

mas precision for their daily products. An increase in the time resolution only slightly increases the uncertainty of the GPS derived ERP's.

4. Conclusions

For highly resolved ERP's, generally, the GPS data have advantages because of the dense data distribution (all weather capability, good coverage and geometry). This holds especially for the sub-daily products where a precision of better than 0.5 mas can be obtained for a 12h resolution.

In certain time intervals with well distributed and accurate SLR data the ERP's results also reach a precision of better than 0.5 mas, but up to a resolution of 1d only. In the sub-daily region the precision is several times worse, generally. Therefore both SLR and GPS can complement each other for the determination of ERP's with a lower time resolution (e. g. from 5d to 1d). Here the SLR results can serve as independent reference series for the investigation of systematic errors (bias, drift). On this basis ERP's with a sub-daily resolution should be derived from GPS data in the future.

References

Feltens, J. (1991) 'Nicht-gravitative Störeinflüsse bei der Modellierung von GPS-Erdumlaufbahnen', Publication of the Deutsche Geodätische Kommission C 371, München.

Fliegel, H. F., Gallini, T. E. and Swift, E. R. (1992) 'Global Positioning System radiation force model for geodetic applications', J. of Geophys. Res. 79, B 1, 559-568.

Gendt, G., Montag, H., Dick, G. (1993a) 'Analysis of crustal deformations based on SLR data', in H. Montag and C. Reigber (eds.) Geodesy and Physics of the Earth, Springer Verlag, IAG Series No 112,pp. 303-307.

Gendt, G., Dick, G., Förste, C., Nischan, T., Sommerfeld, W. (1993b) 'Global and regional network analysis form GPS phase observations', in H. Montag and C. Reigber (eds.) Geodesy and Physics of the Earth, Springer Verlag, IAG Series No 112, pp. 339-343.

Montag, H., Gendt, G., Dick, G., Förste, C., Nischan, T., Sommerfeld, W. (1993) 'High resolution of Earth Rotation Parameters by means of satellite data', in H. Montag and C. Reigber (eds.) Geodesy and Physics of the Earth, Springer Verlag, IAG Series No 112, pp. 404-408.

Montag, H. (1989) 'Some experiences on high resolution ERP determination by means of Lageos data', Veröff. Z.I.f. Physik der Erde Nr. 102, Teil 1, Potsdam.

Saastamainen, J. (1973) 'Contributions to the theory of atmospheric refraction', Bull. Geod., 107, Paris, 13-34.

Shu, S. Y., Reigber, C., Angermann, D., Galas, R., Gendt, G., Sommerfeld, W., Nischan, T. (1993) 'Global geometric parameters determined from multi-months GPS data', in Beutler, G., Brockmann, E. (eds.) Proceedings of the 1993 IGS Workshop, Druckerei Uni Bern, pp. 148-153.

GPS DATA ANALYSIS FOR EARTH ORIENTATION AT THE JET PROPULSION LABORATORY

J. ZUMBERGE, F. WEBB, U. LINDQWISTER, S. LICHTEN, D. JEFFERSON, R. IBANEZ-MEIER, M. HEFLIN, A. FREEDMAN, G. BLEWITT
Jet Propulsion Laboratory,
California Institute of Technology
Pasadena, California 91109

ABSTRACT. Beginning in June 1992 and continuing indefinitely as part of our contribution to FLINN (Fiducial Laboratories for an International Natural Science Network), DOSE (NASA's Dynamics of the Solid Earth Program), and the IGS (International GPS Geodynamics Service), analysts at the Jet Propulsion Laboratory (JPL) have routinely been reducing data from a globally-distributed network of Rogue Global Positioning System (GPS) receivers. Three products are produced and distributed weekly: (i) precise GPS satellite ephemerides, (ii) estimates of daily polar motion and length-of-day, and (iii) a descriptive narrative of the analysis for the week. These are typically made available to the public approximately two weeks following the data recording. In addition, more sophisticated data reduction techniques have been developed for non-routine, research-oriented GPS data analysis. These have been successfully utilized to measure sub-daily Earth orientation fluctuations. Based on comparisons of our earth orientation parameters with independent techniques, we estimate daily pole position accuracies (1σ) of ±0.6 milliarcseconds and length-of-day accuracies of ±0.13 msec. Ongoing work at JPL is aimed at continuing the trend of producing more and higher-quality results at lower cost.

1. Introduction

The first GPS geodynamics experiment for the IERS (GIG '91), a two-week campaign in early 1991, saw the first globally-distributed deployment of precise Global Positioning System receivers, and demonstrated few-parts-per-billion precision [1] in estimates of terrestrial site locations. Largely as a result of the success of GIG '91, the International GPS Geodynamics Service (IGS) began informal operation in June 1992 and formal operation in January 1994. JPL has contributed to the IGS since it began and, in conjunction with its ongoing support of NASA's Dynamics of the Solid Earth (DOSE) program, will continue to contribute. JPL has also contributed in a research capacity to the analysis of the GPS data and resulting scientific products.

Shown in Figure 1 is the distribution of terrestrial GPS P-code receivers as of February 1993. Global coverage is very good, with only a few noticeable "holes". Within the next two years, it is anticipated that these holes will be plugged with new receivers at strategic locations. Figure 2 summarizes the steadily increasing number of stations and satellites beginning in early 1992 and continuing to the present. One can speculate on whether the trend will continue, but currently the data volume, as measured by (# stations × # satellites), doubles in just over a year!

IERS(1994) Technical Note No 16.

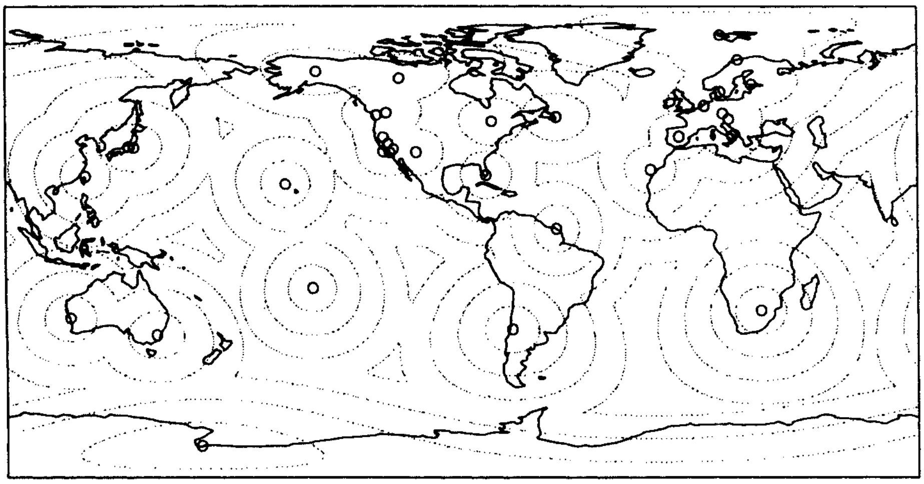

Figure 1. Distribution of terrestrial GPS receivers used in the daily analyses. The dotted lines represent contours of the distance-to-nearest-site function. The contour interval is 1000 km.

Described in this paper are the routine analysis procedures used at JPL, the resulting Earth orientation data products, and their estimated accuracies. Also described are more sophisticated and CPU-intensive analysis procedures being used for the non-routine, research-oriented tasks. We conclude with a brief look at JPL's plans for improving the efficiency and quality of its analyses.

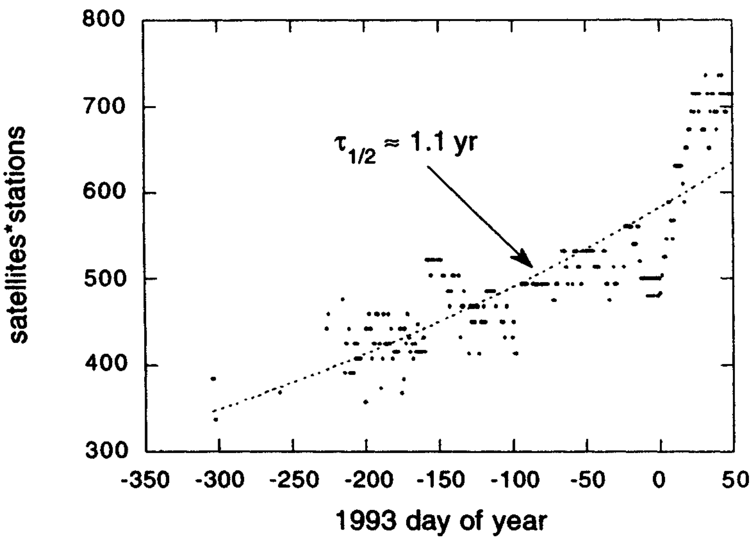

Figure 2. The number of satellites times the number of stations used in daily analyses beginning early 1992. At the current rate, the data volume doubles in a little over 1 year.

2. Procedure and Products

Figure 3 gives a simplified overview of the routine procedure. JPL's GPS Networks Operations (GNO) Group retrieves data from the global network, organizes them by time and site, converts them to the Rinex format, and makes them available for analysts. Once it is determined that sufficient data are available for a given day, a file is created which specifies what data are to be used in that day's analysis, as well as specific sites or GPS satellites from which data should be deleted or deweighted due to known problems.

Based on input from this file, a daily script that runs several programs is launched, requiring a total of approximately 19 hours of cpu time on a 17-Mflop Unix workstation when data from 30 stations and 20 satellites are included. When completed, the daily analysis results in estimates for Earth orientation, GPS satellite ephemerides, and locations of terrestrial sites.

The operational cycle is one week, during which seven daily analyses are completed. Together with the result from Saturday of the previous week and Sunday of the following week, these are used in quality control. Four files are produced and distributed weekly, with naming convention `jpl0www7`, where www is the GPS week and 7 indicates the results are for the entire week. The files are distinguished by their extensions: `.sum` for a narrative summary, `.sp1` or `.sp3` for GPS ephemerides [2,3], and `.erp` for Earth orientation. The orbit product and orbit accuracy comparisons are discussed further in [4].

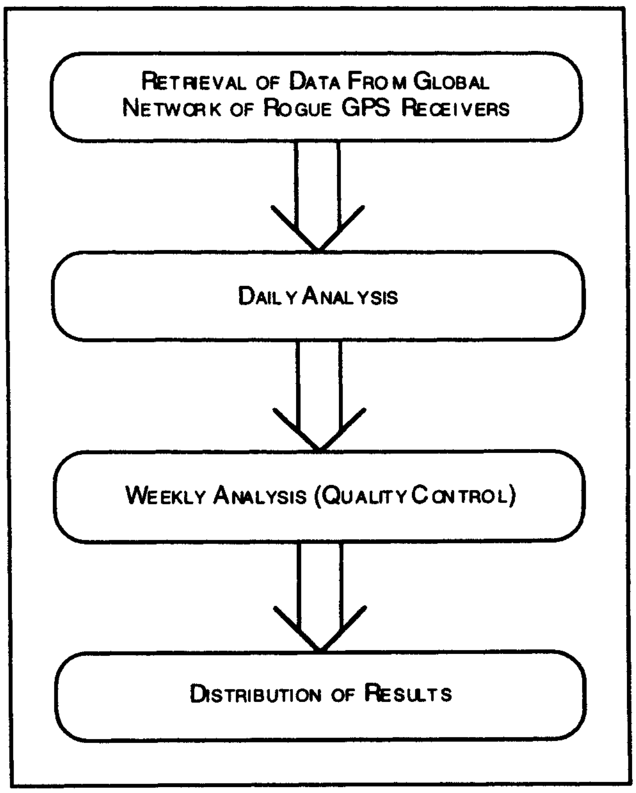

Figure 3. Simplified Flow Chart of FLINN Analysis

The analysis software used is the JPL-developed GIPSY-OASIS II. This software, which incorporates Kalman filtering, and various standard JPL GPS estimation strategies are described in detail in [5,6,7].

In normal operation, each day is processed separately using the 24 hours of the UTC day plus the last 3 hours of the previous day and first 3 hours of the following day. Normal points are formed every 10 minutes. The data types we use are the undifferenced ionosphere-free phase and pseudorange, with assumed noise of 5 mm and 50 cm, respectively.

The GPS satellite motion is modeled as a 9-parameter epoch state vector which includes three-dimensional position, velocity, and solar radiation pressure. Additional parameters allow the solar radiation pressure to vary in a stochastic way about its average value. The noise model for this variation is first-order Gauss-Markov with a 4-hour time constant and 10% standard deviation. Especially during periods when a satellite is in the Earth's shadow, the extra variation allows significantly better modeling of its motion.

The nominal value for the Earth's pole position (x and y) is obtained from the IERS Bulletin B predicts, and its deviation from that nominal is modeled as a linear function of time. The deviation of UT1R – UTC from the nominal (again, IERS Bulletin B predicts) is also assumed to be linear with time, but in this case only the rate is estimated. This rate is the negative of length of day (LODR).

The terrestrial sites include eight which are assumed to be at known locations. These are Algonquin Park, Ontario, Canada; Fairbanks, Alaska, U.S.; Hartebeesthoek, South Africa; Kokee Park, Hawaii, U.S.; Madrid, Spain; Santiago, Chile; Tromso, Norway, and Yaragadee, Australia. The fixed values are updated at the beginning of each month to account for site velocities from ITRF91 (IGS mail message 90) [8]. Location of all other terrestrial sites are solved for every day starting from ITRF91 nominal positions.

GPS carrier phase biases are estimated as real-valued parameters. Clock biases for transmitters and receivers are estimated as white noise processes, except for one reference station clock. The zenith troposphere delay at each receiver site is modeled as a random walk process. The 1980 International Astronomical Union (IAU) nutation model, the Yoder et al. [9] Earth and ocean tide model, and the GEMT3 (more recently, JGM2) gravity field model are assumed.

3. Results

3.1. DAILY EARTH ORIENTATION

Shown in Figure 4 are the Earth orientation results. A discontinuity at days 200-201 (July 18-19, 1992) is a consequence of the change in fiducial strategy which went from three (Fairbanks, Algonquin, and Madrid) fixed sites to the eight described earlier. From July 19 through the end of 1992, excluding some days during which anti-spoofing was in effect, the average difference between JPL's pole position measurements and those from the IERS Bulletin B Final values is about 0.8 mas for x and 1.2 mas for y, with standard deviations of about 0.6 mas for both x and y.

Although GPS measurements are almost completely insensitive to UT1R – UTC, they are sensitive to its time derivative, essentially the Earth's spin rate. With T ≡ 1 day, the quantity

$$\mathrm{LODR} \equiv -\mathrm{T}\frac{d}{dt}(\mathrm{UT1R} - \mathrm{UTC}) \qquad [1]$$

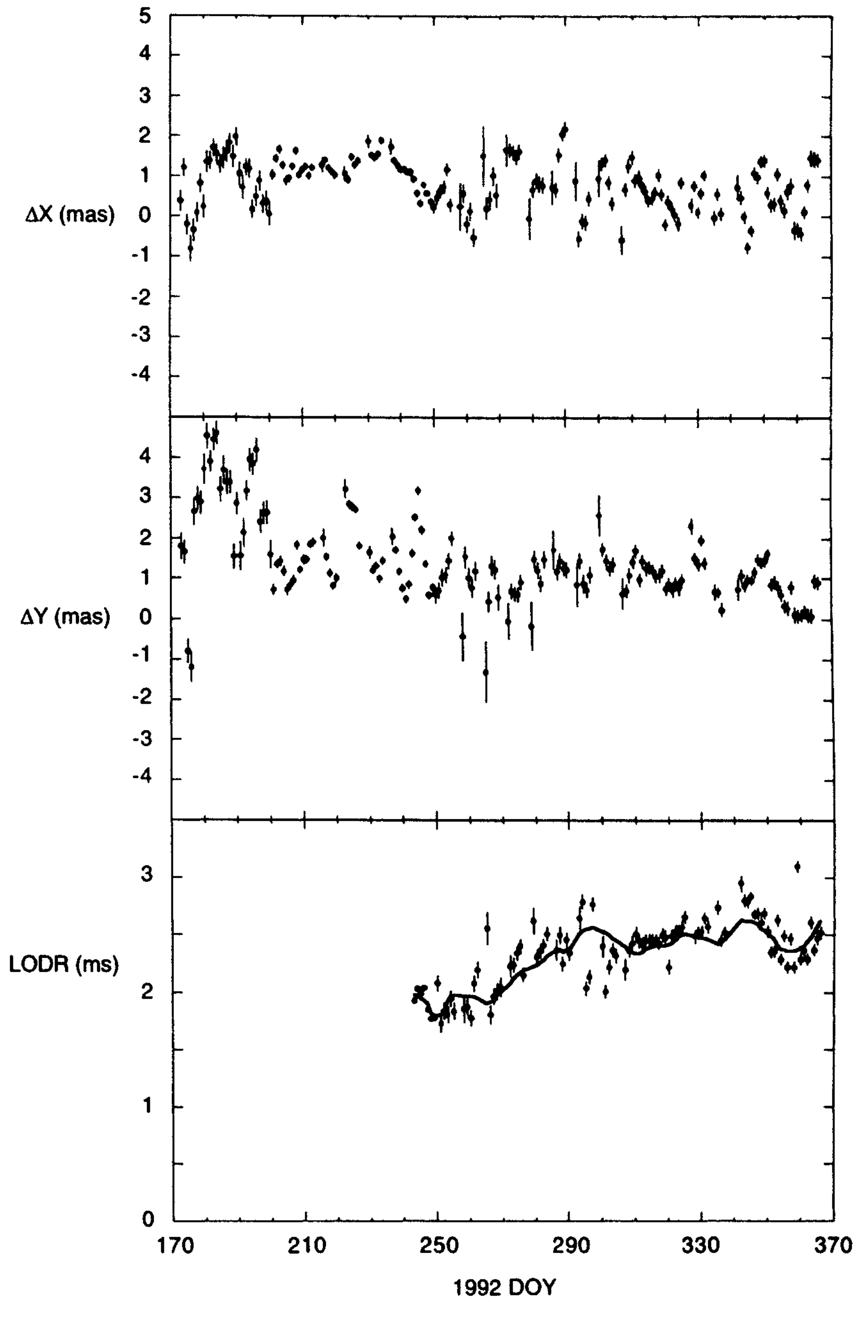

Figure 4. GPS estimates of Earth orientation parameters compared with IERS Bulletin B Final Values. For pole position, the values shown (ΔX and ΔY) are the GPS measurements minus the IERS values, and the error bars reflect the formal uncertainty in the GPS measurements. For LODR, the solid line indicates the negative time derivative of the IERS value of UT1R-UTC, and the points indicate the GPS measurements and formal uncertainties.

is the conventional measure of this spin rate. We began including daily estimates of LODR beginning with GPS week 660 (August 30, 1992). Shown at the bottom of Figure 4 are our daily estimates of LODR and a smooth curve which represents the negative derivative of the IERS Bulletin B Final values of UT1R – UTC. Excluding a few 3σ outliers, the agreement is approximately 0.13 msec (1σ) with a negligible bias.

Because the daily estimates of LODR are for the most part independent, an integration of them to recover UT1R – UTC (given some initial starting value) would exhibit random walk behavior. Thus, some method is required to prevent the walk from wandering too far away. We are currently investigating the forward-running filter

$$\text{UT1R} - \text{UTC}(t + T) = \alpha\,\Lambda + (1 - \alpha)\,[\text{UT1R} - \text{UTC}(t) + \text{LODR}(t + T/2)], \qquad [2]$$

where Λ is a separate estimate of UT1R – UTC(t + T) and α is a free parameter. (We continue to use $T \equiv 1$ day.) The parameter α should be small enough so that the resulting UT1R – UTC series will exhibit a time variation consistent with the daily GPS-measured LODR values, and only just large enough to suppress large random-walk excursions. A reasonable choice for Λ is the most-recent IERS Bulletin B *Final* value of UT1R – UTC (typically 30- to 60-days old), incremented to the present by the daily GPS measurements of LODR. In the near future we intend to include the results of such a procedure in our `.erp` files.

The Epoch '92 campaign, running from July 26 - August 8 1992, was a particularly intensive period of observation for other geodetic techniques. It occurred when our estimation strategy had not matured to its current state. Therefore, these days were reprocessed in early 1993 with the current estimation strategy. The results are on JPL's `bodhi` distribution computer, and are also available on the Crystal Dynamics Data Information System (CDDIS) at Goddard Space Flight Center. The reprocessed data show marked improvement over the original analyses in both orbit quality and Earth orientation accuracy.

3.2. SUB-DAILY EARTH ORIENTATION

The analysis strategy for obtaining estimates of sub-daily Earth orientation fluctuations has much in common with the operational procedure described above. Differences in strategy are discussed here; the Earth orientation results, however, are discussed in detail in Freedman et al. [this volume] and Ibanez-Meier et al. [this volume].

The principle changes made to the daily FLINN strategy deal with the use of multiple day data arcs in place of the 30-hour data arcs of FLINN. To utilize multi-day arcs, the dynamic orbit models for the GPS satellites must be modified. This may involve modifying the solar radiation pressure models or giving up the goal of a single epoch state for each satellite over the entire data arc. In addition, the estimation strategies for both UT1 and polar motion x and y are different from those of the daily analyses. Finally, two minor changes include the use of 6-minute normal point spacing and assumed data noise levels twice as large as those assumed by FLINN.

Variations in UT1 – UTC starting from an initial fixed value were estimated every 30 minutes by using a first-order Gauss-Markov process update with a correlation time of 4 hours and a steady-state process noise 1-σ constraint of 0.06 ms. Polar motion variations were modeled as a white noise process with weak (120 mas) constraints. For both UT1 and polar motion, a variety of estimation intervals were tried, ranging from the normal point interval of 6 minutes up to 3 hours. Figure 5 illustrates the UT1 values that result from various estimation intervals. All curves have been differenced with a reference series [Freedman et al., this volume] and are offset for clarity.

Curves A and B represent two sets of 30-minute estimates (whose differences are explained below), curve C shows UT1 estimated every 6 minutes, and curves D and E show two sets of 3-hour estimates. D and E differ in that an apriori diurnal and semidiurnal tide model was explicitly used in the estimation of time series E, whereas no such model was used in D. The optimal estimation interval, in the sense of yielding the best signal to noise ratio without undue attenuation of the expected diurnal signal, was 30 minutes.

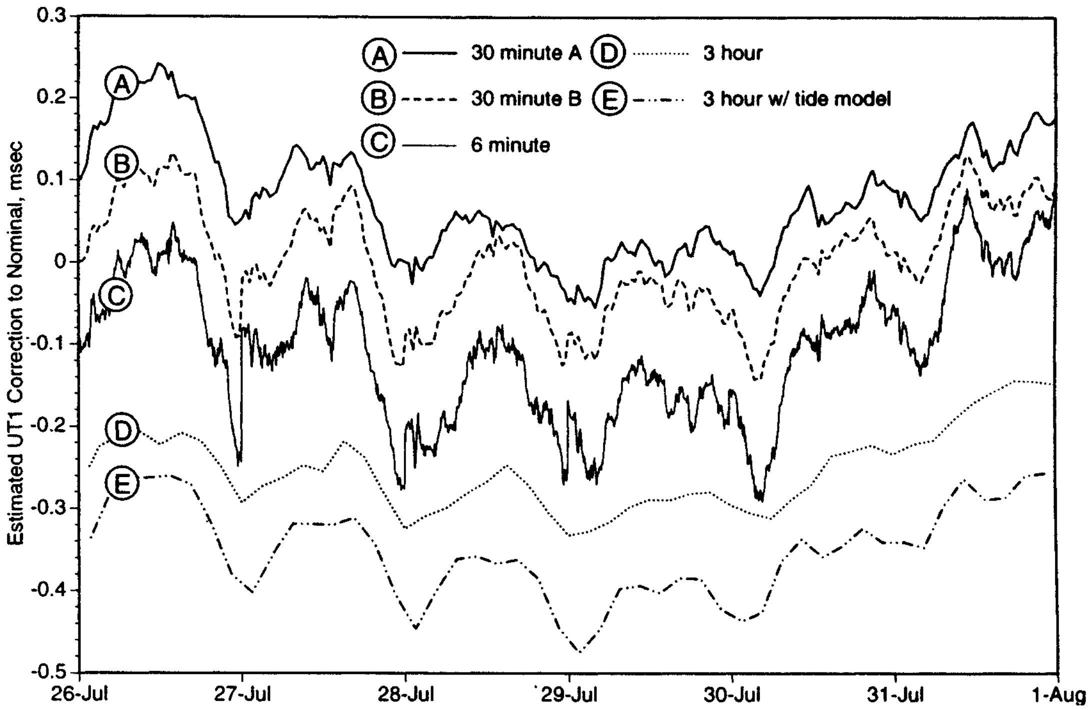

Figure 5. Comparison of sub-daily UT1 time series estimated with various strategies. Time series are offset vertically for ease of comparison. See text for explanation of curves and labels.

Two different estimation strategies for the satellite orbits were employed. In the earlier strategy [5,10], one set of satellite states (positions and velocities) was estimated for each satellite over the course of the multi-day arc. The solar radiation pressure coefficients Gx, Gy, and Gz were estimated as constants with 10 percent colored noise added and updated every hour. The biases for the Gx and Gz parameters were constrained to be 100% correlated. The stochastic portion of the solar radiation model consisted of a first-order Gauss-Markov process with a correlation time of 4 hours. We found that this strategy, although adequate for estimating UT1 – UTC variations, tended to attenuate much of the polar motion signal, presumably absorbing it within the satellite orbit and solar pressure force models. Curve A in Fig. 5 shows the 30-minute UT1 series resulting with this strategy.

A second strategy [11] consisted of re-estimating each satellite state (position, velocity and solar radiation pressure coefficients) every 24 hours. In this case, the solar radiation parameters were modeled as constants over 24 hours. The white noise restarts for each GPS satellite were staggered over a 5-hour interval around noon to maintain continuity in the UT1 series. Figure 5 curve B shows the 30-minute UT1 series obtained with this strategy, and all other curves in Fig. 5

use this latter strategy. Typical postfit rms residuals were close to 6 mm for carrier phase and 35 cm for pseudo-range data.

4. Conclusions and Future Prospects

Since the first half of 1992, JPL has made regular contributions to the IGS, consisting of precise GPS orbits and daily Earth orientation results. We expect to continue these contributions. Accuracies are currently estimated to be a few tens of centimeters for GPS orbits, about half a milliarcsec for pole position, and a bit over 0.1 msec for LODR.

Additional strategies for multi-day arcs, for routine as well as research use, are being tested. These may be utilized routinely as cpu speeds increase, and are sure to be used in future sub-daily Earth orientation research.

Accuracies of all quantities may improve significantly once we start resolving carrier phase bias ambiguities [12], which should begin sometime this calendar year (the current limitation comes from our computing resources). Quality control will be enhanced by daily monitoring of several regional baselines.

A number of weekends during 1992 saw implementation of anti-spoofing (AS). Only recently has the Rogue receiver software been upgraded to handle AS data. Since the upgrade, AS has been processed successfully, although with somewhat degraded accuracies. Analysts at JPL will be investigating modifications of the nominal strategy to better accommodate AS data.

As was shown in Figure 2, the quantity of data has steadily increased, and will probably continue to increase in the near future owing to both more satellites and more receivers. So that the computational burden remains tractable, we may need to process a select number of stations to fix orbits, and then use fixed orbits for the remaining stations.

In addition to the current offerings, new products that may be distributed soon are satellite and station clock solutions. If a demand exists, troposphere estimates and stochastic solar radiation pressure estimates could also be made available.

Finally, additional automation in routine processing may reduce the manpower required to keep up to date with the analyses. The current turnaround time of approximately two weeks could conceivably be reduced to a few days, or even less.

ACKNOWLEDGMENTS. The work described in this paper was carried out by the Jet Propulsion Laboratory, California Institute of Technology, under contract with the National Aeronautics and Space Administration.

5. References

[1] Blewitt, G., M. B. Heflin, F. H. Webb, U. J. Lindqwister, and R. P. Malla, Global coordinates with centimeter accuracy in the International Terrestrial Reference Frame using the Global Positioning System, *Geophys. Res. Lett.*, *19*, pp. 853-856, 1992.

[2] Remondi, B. W., NOAA Technical Report NOS 133 NGS 46, *Extending the National Geodetic Survey Standard GPS Orbits Format*, November, 1989

[3] Remondi, B. W., *NGS Second Generation ASCII and Binary Orbit Formats and Associated Interpolation Studies*, presented at the Twentieth General Assembly of the International Union of Geodesy and Geophysics, Vienna, Austria, August 11-24, 1991.

[4] Zumberge, J. F., D. C. Jefferson, G. Blewitt, M. B. Heflin, F. H. Webb, Jet Propulsion Laboratory IGS Analysis Center Report, 1992, in *Proceedings of the 1993 IGS Workshop*, edited by G. Beutler and E. Brockmann, pp. 154-163, Astronomical Institute, University of Berne, 1993.

[5] Lichten, S. M., Toward GPS Orbit Accuracy of Tens of Centimeters, *Geophys. Res. Lett.*, *17*, 215-218, 1990a.

[6] Lichten, S. M., Estimation and Filtering for High-Precision GPS Positioning Applications, *Man. Geod.*, *15*, 159-176, 1990b.

[7] Blewitt, G., Advances in Global Positioning System Technology for Geodynamics Investigations: 1978-1992, in *Contributions of Space Geodesy to Geodynamics: Technology*, edited by D. E. Smith and D. L. Turcotte, pp. 195-213, Am. Geophys. Un., Washington, D.C., 1993.

[8] Boucher, C., Z. Altamimi, and L. Duhem, ITRF 91 and Its Associated Velocity Field, *IERS Technical Note 12*, Central Bureau of IERS, Observatoire de Paris, October 1992.

[9] Yoder, C. F., J. G. Williams, and M. E. Parke, Tidal Variations of Earth Rotation, *J. Geophys. Res.*, *86*, 881-891, 1981.

[10] Lichten, S. M. , and W. I. Bertiger, Demonstration of Sub-Meter GPS Orbit Determination and 1.5 Parts in 10^8 Three-Dimensional Baseline Accuracy, *Bull. Geod.*, *63*, 167-189, 1989.

[11] Lichten, S. M., S. L. Marcus, and J. O. Dickey, Sub-Daily Resolution of Earth Rotation Variations With Global Positioning System Measurements, *Geophys. Res. Lett.*, *19*, 537-540, 1992.

[12] Blewitt, G., and S. M. Lichten, Carrier phase ambiguity resolution up to 12000 km: Results from the GIG '91 experiment, in *Proc. of the Sixth Int. Symp. on Satellite Positioning*, Ohio State University, Columbus, 1992.

EFFECTIVE ATMOSPHERIC ANGULAR MOMENTUM FUNCTIONS COMPUTED FROM THE JAPAN METEOROLOGICAL AGENCY DATA

T. OZAKI and K. KUMA
Japan Meteorological Agency,
Chiyoda-ku, Tokyo, 100 JAPAN

I. NAITO
National Astronomical Observatory,
Mizusawa, Iwate, 023 JAPAN

ABSTRACT. The Atmospheric Angular Momentum (AAM) functions based on the 6-hourly Japan Meteorological Agency (JMA) data are briefly introduced.

The effective atmospheric angular momentum (EAAM) functions proposed by Barnes, Hide, White and Wilson (1983) have been computed from the Japan Meteorological Agency (JMA) global analysis data since September 28, 1983. In general, the operational numerical weather prediction produces the three data sets called the analysis data, the initialized analysis data and the predicted values. The JMA global analysis data are the analysis data.

For the use of this file, it should be noticed that the results during 1983/12/1 - 1986/6/30 are 24-hourly (daily mean) values computed from the JMA global analysis averaged data at each grid and each level, during 1986/7/1 - 1992/6/20 are 12-hourly (00UTC and 12UTC) values computed without averaging, and from 1992/6/21 are 6-hourly (00UTC, 06UTC, 12UTC, 18UTC) values. The most important fact is that the 6-hourly values from 1992/6/21 are based on a new computational method different in part from an old computational method for the other values. It should be thus noticed that the 12-hourly values during 1992/6/21 - 1992/9/30 based on the old method are also added in the file prior to the 6-hourly values for comparison.

The JMA global analysis data have been made on 1.875-degree (2.5-degree before 1988/3/1) latitude-longitude grid system at sixteen levels (fifteen levels before 1988/3/1) from surface to 10hPa. The data are made from the forecast-analysis cycle by the following analysis and forecast models. The analysis model is based on a multi-variate optimum interpolation method with the initial guess of 6 hour forecast in troposphere, and on a sinusoidal fitting method in stratosphere. It should be noted that the predicted values are not used for the analysis above 100hPa. The forecast model is a global spectral model with a horizontal resolution of triangular truncation at wavenumber 106 (63 before 1989/11/14, and 42 before 1988/3/1), and vertically it has 21 levels (16 levels before 1989/11/14, and 12 levels before 1988/3/1). Full physical processes are incorporated in the model through 1.125-degree Gaussian grid, and a non-linear normal mode initialization is applied. The details for the analysis and forecast models from 1989/11/14 can be found in Numerical WeatherPrediction Division, Japan Meteorological Agency (1990), during 1988/3/1-1989/11/13 in Kitade (1988), and before 1988/3/1 in Kashiwagi (1987) and Kanamitsu, Tada, Kudo, Sato and Isa (1983).

For computing the EAAM functions, the sea level pressure, the height of the each level, and the wind velocity at each level of the global analysis data are used. In addition, mountain height of the same grid system made from the 10-minute (1-degree for the 12-hourly values) latitude-longitude grid data are used for estimating surface pressures on land that are computed from the geopotential height by using a cubic spline interpolation technique applied for the thickness temperatures. Also land-sea index data of the same grid system made from the 1-degree latitude-longitude grid data are used for computing sea level pressures on ocean with the Inverted Barometer (IB) hypothesis. Vertical integration of the wind terms of the EAAM functions is carried out from surface pressure on land (or the sea level pressure on ocean) to 10hPa. However, surface wind data are not used for the 6-hourly values from 1992/6/21.

The integral formula to evaluate the EAAM functions are basically due to the equations (5.1), (5.2), and (5.3) of Barnes et al (1983), but the axial component of the EAAM functions is multiplied by -1 for convenience. No smoothing have been done after evaluation. Details of the evaluation can be found in Naito, Kikuchi and Yokoyama (1987).

The file is given as

Year, Month, Day, MJD,
Chi-1-wind, Chi-1-press without IB, Chi-1-press with IB,
Chi-2-wind, Chi-2-press without IB, Chi-2-press with IB,
Chi-3-wind, Chi-3-press without IB, Chi-3-press with IB

with format (I4, I3, F6.2, F9.2, 9F10.6), where the EAAM functions have been multiplied by 1.0E7.

The variations during SEARCH'92 (6/21-9/22, 1992) are shown in Figure 1.

References:

Barnes, R.T.H, Hide, R., White, A.A. and Wilson, C.A. (1983) Atmospheric angular momentum fluctuations, length-of-day changes and polar motion, Proc. R. Soc. Lond., A387, 31-73.

Kanamitsu, M., Tada, K., Kudo, T., Sato, N. and Isa, S. (1983) Description of the JMA operational spectral model, J. Meteorol. Soc. Japan, 65, 189-220.

Kitade, T. (1988) Numerical weather prediction in the Japan Meteorological Agency, JMA/NPD Technical Report, No.20.

Naito, I., Kikuchi, N. and Yokoyama, K. (1987) Results of estimating the effective atmospheric angular momentum functions based on the JMA global analysis data, Publ. Int. Latit. Obs. Mizusawa, 20, 1-11.

Numerical Weather Prediction Division, Japan Meteorological Agency, (1990) Outline of Operational Numerical Weather Prediction at Japan Meteorological Agency, Appendix to Progress Report on Numerical Weather Prediction.

Figure 1. The variations of the AAM functions based on the 6-hourly JMA data during SEARCH'92 (6/21-9/22, 1992), where units are 10E-7.

X_1(n-IB) : Chi-1-Wind plus Chi-1-Press without IB.
X_1(IB) : Chi-1-Wind plus Chi-1-Press with IB.
X_2(n-IB) : Chi-2-Wind plus Chi-2-Press without IB.
X_2(IB) : Chi-2-Wind plus Chi-2-Press with IB.
X_3(n-IB) : Chi-3-Wind plus Chi-3-Press without IB.
X_3(IB) : Chi-3-Wind plus Chi-3-Press with IB.

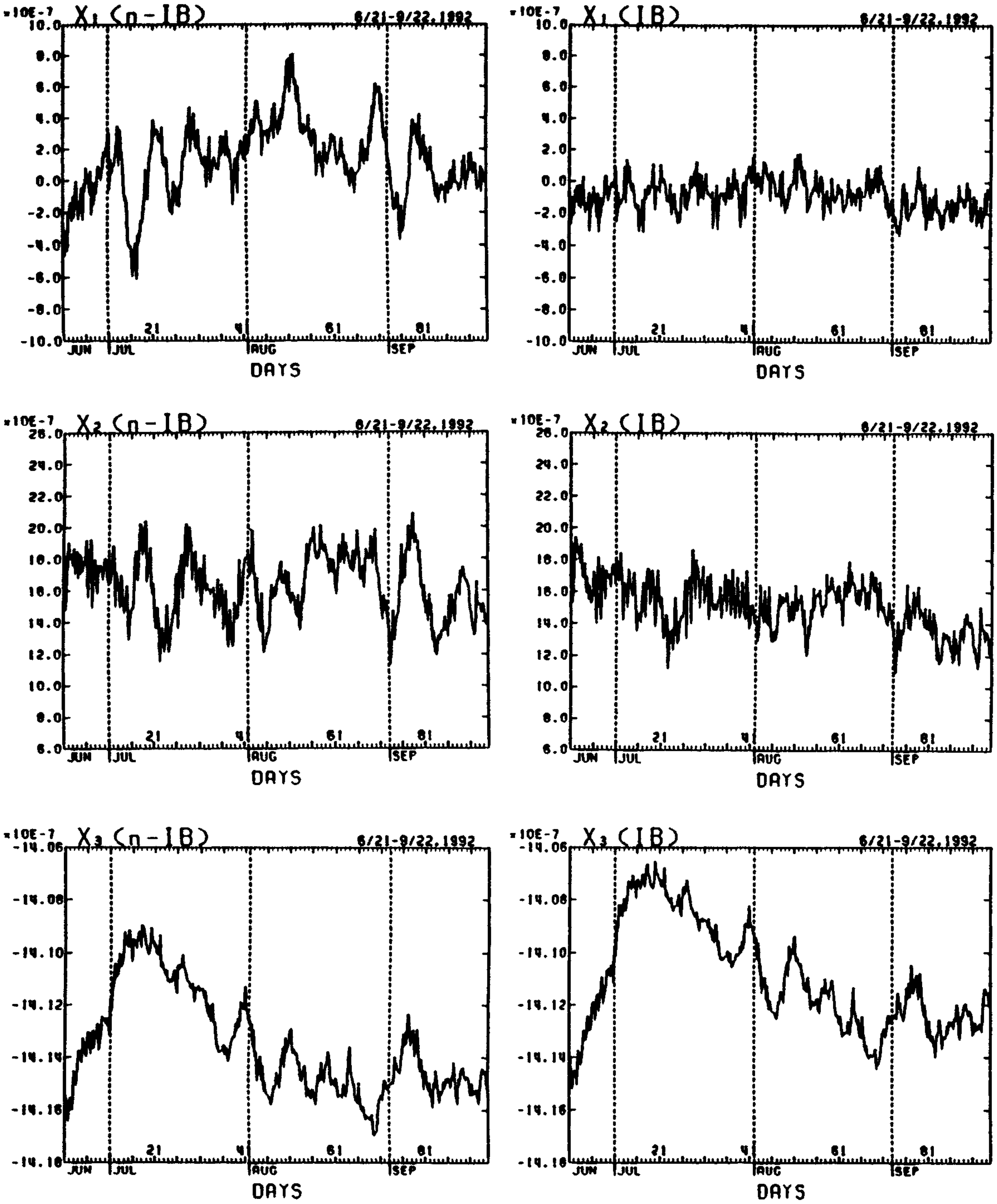
X1 (n-IB)
X1 (IB)
X2 (n-IB)
X2 (IB)
X3 (n-IB)
X3 (IB)
6/21-9/22,1992
*10E-7
JUN
JUL
AUG
SEP
DAYS

Part IV

Intercomparison and Interpretation of Results

Scientific Results from the EPOCH'92 Observations Organized by the USNO

T.M. Eubanks, B.A. Archinal, M.S. Carter, F.J. Josties, K.A. Kingham, J.O. Martin, D.N. Matsakis and D.D. McCarthy

U.S. Naval Observatory, Washington, D.C., 20392

ABSTRACT. In order to assess the reality of any high frequency rotational variations observed during the EPOCH'92 campaign, a series of special Navy-Experimental Global (or NAVEX-G) sessions were coordinated by the USNO to provide periods of observations by two independent Very Long Baseline Interferometry (VLBI) networks during part of EPOCH'92. The NAVEX-G network used the NAVNET Green Bank antenna together with radio telescopes in Chile, Italy, South Africa, Canada and Japan. This truly global network provided orientation accuracy comparable to the lower noise (but smaller) NASA network run simultaneously, and thus a means of assessing the validity of any small high frequency variations in Earth orientation observed during this period. This paper presents a brief description of these NAVEX-G observations and the results obtained from them.

1. INTRODUCTION

The SEARCH-92 campaign organized by the International Earth Rotation Service included a special observing period called EPOCH'92 (July 25-August 8, 1992), intended to study high-frequency variations in Earth rotation. To complement the period of almost continuous VLBI observations organized by the U.S. National Aeronautics and Space Administration (NASA), the U.S. Naval Observatory (USNO), in addition to the on-going weekly NAVNET VLBI sessions, organized a series of four Navy Experimental-Global (NAVEX-G) observing sessions using VLBI antennas in Green Bank, (U.S.A.), Algonquin (Canada), Kashima (Japan), Matera (Italy), Santiago (Chile) and Hartebeesthoek (South Africa). The primary purpose of these NAVEX-G observations was to determine the reality of high frequency variations in the orientation of the Earth, and the level of systematic and random errors in VLBI determinations of these variations, through comparisons between independent simultaneous VLBI sessions of the highest possible quality. The NAVEX-G observations were fully successful in meeting these goals, and high quality data were obtained from each session, with a total of 2247 successful observations being obtained (in addition to the 1293 observations obtained from regular NAVNET sessions during EPOCH'92).

2. RESULTS OF THE NAVEX-G EPOCH'92 OBSERVATIONS

The NAVEX-G measurements sessions were intended to, and did, provide Earth orientation estimation accuracy comparable to the simultaneous NASA Research and Development (R&D) sessions. The NAVEX-G achieved this accuracy through the use of a truly global network with up to 6 stations in 5 continents, the size of the network being specifically intended to compensate for the sensitivity of the R&D observations. Data were obtained on baselines up to 12,419 km long, and the bulk of the data were obtained from baselines of about 1 1/2 Earth radii in length. Good results were obtained from these long baselines, and the actual UT1 and polar motion formal errors from the two networks were roughly equal. Both networks provided roughly a factor of two increase in sensitivity over that obtained by the IRIS-A and NAVNET sessions during the same period.

The existing IERS standards [1] were found to be inadequate to reduce the global scale NAVEX-G sessions due to their neglect of the tidally driven diurnal and semidiurnal variations in UT1 and polar motion. This effect is striking in the NAVEX-G sessions during EPOCH'92. When these data are reduced in the standard fashion, estimating one set of 24 hour averaged values for UT1, polar motion and nutation offsets, the weighted root mean square (rms) post-fit residual scatter of the interferometric delays was

±52.0 picoseconds. When the data are used to estimate hourly piecewise linear variations in UT1 and polar motion, the weighted rms drops to ±43.6 picoseconds (a strongly significant 30% reduction in variance). The data processing for future global NAVEX sessions was modified to do a final editing and weighting of the data using the hourly piecewise linear parametrization of high-frequency Earth orientation changes.

The NAVEX-G data have been used in a number of initial comparisons between simultaneous VLBI sessions ([2], [3]), as well as in comparisons between VLBI and data from the Global Positioning system (see, e.g., [4]), and with other data types such as atmospheric angular momentum data. When the EPOCH'92 R&D and NAVEX-G VLBI data are used to estimate the UT1 and polar motion on an hourly basis, there are 104 hourly values with simultaneous data. The R&D and NAVEX-G data have an rms difference (in all three components of Earth orientation) of about ±0.5 milli arc seconds (mas). Although in polar motion the observed residual scatter is consistent with the root sum square (rss) of the R&D and NAVEX-G formal errors, the UT1 differences are significantly larger than would be expected from the formal errors, evidence of roughly ±0.4 mas of unmodeled errors. In general, the observed hourly fluctuations in UT1 and polar motion agree well, but not perfectly, with independent models of the tidally forced diurnal and semi-diurnal orientation changes, and it is clear that these tidal variations are the dominant source of orientation changes at periods between about two days and one hour. These comparisons bound any non-tidal variations in orientation in this period range during EPOCH'92 to be ≤ about 0.4 mas rms in all three components of orientation

The EPOCH'92 results show that accurate, high quality VLBI Earth orientation results can be obtained from global networks. Global scale VLBI offers a number of advantages, including the maximum sensitivity to Earth orientation changes and the best means of decoupling orientation changes from local and regional motions of the antennas, such as those caused by ocean tidal loading. Global scale VLBI also avoids the "edge effect" found in smaller networks, where certain stations on the edge of the network cannot obtain complete sky coverage due to their distance from the rest of the network. In order to investigate the long term stability and accuracy of orientation results from global networks the USNO organized a series of six global sessions during 1993, with the number of stations used being increased from six to a maximum of ten. These large networks thus have sufficient redundancy to be divided into sub-networks, each providing independent orientation data of good quality. This on-going work thus extends and complements the EPOCH'92 NAVEX-G simultaneous sessions, in order to determine better the sources of systematic error limiting the accuracy of geodetic VLBI. Similar global experiments were organized during the January, 1994, CONT-94 period, to provide another period of simultaneous observations between independent VLBI networks.

ACKNOWLEDGEMENTS. These results represent a truly international effort, and would not have been possible without contributions from (among others) the Agenzia Spaziale Italiana, the Hartebeesthoek Radio Astronomy Observatory, the Communications Research Laboratory in Japan, the Institut fur Angewandte Geodasie in Germany, the National Radio Astronomy Observatory and the NASA/Goddard VLBI group.

REFERENCES

1. McCarthy, D.D., (edt.), IERS Standards (1992), International Earth Rotation Service Technical Note Number 13, Observatoire de Paris, Paris (1992).
2. Eubanks, T.M., B.A. Archinal, M.S. Carter, F.J. Josties, K.A. Kingham, J.O. Martin, D.N. Matsakis and D.D. McCarthy, The Contribution to the EPOCH'92 Measurement Campaign Organized by the U.S. Naval Observatory, EOS Trans. AGU, 73, 135, (1992).
3. Ma, C., T.A. Clark, J.W. Ryan, J.M. Gipson, D.S. MacMillian, C.C. Thomas, N.R. Vandenberg, D. Gordon and A.E. Niell, VLBI EOP Observations during the EPOCH'92 Campaign, EOS Trans. AGU, 74, 105, (1993).
4. Freedman, A.P., R. Ibanez-Meier, J.O. Dickey, S.M. Lichten and T.A. Herring, Sub-Daily Earth Rotation during the Epoch'92 Campaign, pp. 202-211 in the Proceedings of the 1993 IGS Workshop, Beutler and Brockmann, edt., Druckerei der Universitat Bern (1993).

KALMAN FILTER ANALYSIS OF SEARCH 92 VLBI DATA

T. A. HERRING
Massachusetts Institute of Technology,
77 Massachusetts Avenue,
Cambridge, MA 02139
USA

ABSTRACT: An analysis of the very long baseline interferometer data collected during the Epoch 1992 campaign is presented. A standard analysis is discussed in which tidally coherent, diurnal and semidiurnal polar motion and UT1-UTC variations are applied prior to Kalman filtering the VLBI data for stochastic estimates of 3-hourly binned estimated of pole position and UT1-UTC. Variants of this analysis are discussed to show the sensitivity of the results choice of process noise parameters and the apriori application of the tidally coherent models. Here the residuals between a smoothed VLBI polar motion and UT1 apriori series are shown. For pole position, this apriori series is very similar to IERS Bulletin B. For UT1, the use of the VLBI series reduces by half the size of the UT1 residuals compared to IERS Bulletin B.

1. Introduction

We present here the analysis of the SEARCH 92 VLBI data set using two different analysis techniques: (1) estimation of sub-daily variations in polar motion and UT1 using a batched Kalman filter technique; and (2) direct estimation of the cosine and sine components of diurnal (frequency 1-cycle-per-sidereal day) and semidiurnal (2-cycles-per-sidereal day) signals in polar motion and UT1. The experiments analyzed here are listed in Table 1 along with the station participating in each experiment.

2. Data Analysis

The VLBI data were analyzed using the techniques discussed in Herring and Dong [1994]. The coordinates of the radio telescopes were constrained at the values determined from the analysis of VLBI data obtained between 1990 and 1993, and apriori constraint was taken to be the standard deviations obtained from the coordinate solution. The radio source positions were held fixed at the values obtained from 1990-1993 analysis. The MTT hydrostatic and wet functions used in the analysis [Herring, 1992] and the process noise used to stochastically model the wet delay variations was obtained using the algorithm discussed in Herring et al. [1990]. The ZMOA-1990-2 nutation series given in Herring [1991] was used as the apriori nutation series. Daily estimates of correction to this series were made in all analyses. The hydrogen masers were model with Allan standards of 10^{-14} at sampling intervals of 30 minutes as discussed in Herring et al. [1990].

TABLE 1: VLBI experiments analyzed

Start date	Description	Sites (first four characters)					
92/07/26	EUR9-HOFN-4	HOFN	WEST	GILC	WETT	ONSA	
92/07/27	IRISA-751	HOFN	WEST	GILC	WETT	ONSA	
92/07/28	Navex-G3	SANT	NRAO	KASH	HART	MATE	
92/07/28	RD-E-92A	WEST	FD-V	LA-V	GILC	KAUA	WETT
92/07/29	Navex-G4	SANT	ALGO	NRAO	KASH	HART	MATE
92/07/29	RDE-92B	WEST	FD-V	LA-V	GILC	KAUA	WETT
92/07/30	Navnet 187	RICH	MOJA	GILC	KAUA		
92/07/31	RDE-92C	WEST	FD-V	LA-V	GILC	KAUA	WETT
92/08/02	RDE-92D	WEST	LA-V	GILC	KAUA	WETT	
92/08/03	IRISA-752	WEST	ALGO	RICH	MOJA	WETT	
92/08/04	Navex-G5	SANT	NRAO	KASH	HART	MATE	
92/08/04	RDE-92E	WEST	FD-V	LA-V	GILC	KAUA	WETT
92/08/05	Navex-G6	SANT	ALGO	NRAO	KASH	HART	MATE
92/08/05	RDE-92	WEST	FD-V	LA-V	GILC	KAUA	WETT
92/08/06	Navnet-188	NRAO	RICH	MOJA	GILC	KAUA	
92/08/07	RDE-92G	WEST	FD-V	LA-V	GILC	KAUA	WETT
92/08/09	RDE-92H	WEST	FD-V	LA-V	GILC	KAUA	WETT
92/08/10	IRISA-753	WEST	ALGO	RICH	MOJA	WETT	
92/08/10	Navex-25	NRAO	GILC	KAUA	KASH	MATE	
92/08/11	XASIA-2	DSS45	HOBA	KASH	SESH	HART	WETT

The treatment of polar motion and UT1 subdaily variations differed between analyses. In our standard analysis, estimates of pole position and UT1 were make from batches of data approximately of 3 hours duration. The estimated values of the pole position and UT1 for each batch of data are reported at the epoch of the VLBI observation closest to the mid-point time of the batch. Constraints of 0.3 mas and 0.04 mts were placed on the changes between adjacent values of the adjustments to the apriori polar motion and UT1 values. Apriori corrections were made for the tidal coherent variations in pole position and UT1 based on the coefficients given in Herring and Dong [1994]. Residuals to the apriori polar motion and UT1 from this analysis are shown in Figures 1, 2 and 3. As has been shown in numerous pervious studies, the subdaily variations in polar motion and UT1 are dominated by diurnal and semidiurnal variations. Also shown in the Figures 1, 2 and 3 (offset from previous values) are the time variations in the rotation parameters computed from estimates of the cosine and sine terms with periods of exactly 1- and 2-cycles per sidereal day. The estimates of the coefficients used to generate these temporal variations are given in Tables 2 and 3 with the cosine and sine terms defined in Herring and Dong [1994]. For comparison, and offset from the previous values, we show the lower parts of Figures 1, 2 and 3, the temporal variations expected from the tidally coherent model given in Herring and Dong [1994].

To evaluate the sensitivity of our standard stochastic analysis to applying apriori the tidally coherent model to analysis, we repeated the standard analysis with the tidally coherent model removed. The results of this analysis along with the differences between it and the standard analysis are shown in Figures 4, 5 and 6. Visually the types of analysis look very similar although at individual times the differences can be large as 0.9 mas and 0.05 mts. The larger excursions are for points with large uncertainties and most likely result form the filter not being able to track the rapid variations that occur in the diurnal and semidiurnal variations. The root-mean-square (RMS) scatters of the differences between the two analysis are 0.18 mas, 0.14 mas and 0.05 mts for the X and Y pole positions and UT1, respectively. The RMS differences are between 15 and 34% of the standard deviations of the stochastic estimates of the pole position and UT1.

Table 2. Estimates of the cosine and sine components of diurnal and semidiurnal UT1 variations. The time refers to the time of the midpoint of each 24-hour session of VLBI data.

Date	Hr:min	Diurnal				Semidiurnal			
		cos (ms)	± (ms)	sin (ms)	± (ms)	cos (ms)	± (ms)	sin (ms)	± (ms)
7/26	17:58	-0.039	0.013	0.068	0.013	0.004	0.010	0.007	0.008
7/27	20:02	-0.015	0.017	0.021	0.015	0.010	0.012	0.019	0.009
7/28	21:01	-0.053	0.011	0.037	0.007	-0.007	0.007	0.020	0.008
7/28	23:02	-0.032	0.006	0.024	0.004	-0.026	0.004	0.021	0.004
7/30	03:01	-0.048	0.006	0.018	0.006	-0.030	0.005	0.015	0.005
7/30	03:01	-0.040	0.004	-0.008	0.006	-0.032	0.004	-0.003	0.004
7/31	05:59	-0.018	0.032	-0.036	0.038	-0.038	0.024	-0.045	0.022
8/01	09:59	-0.015	0.005	-0.023	0.004	-0.021	0.004	-0.014	0.004
8/02	16:02	0.000	0.004	-0.008	0.005	-0.024	0.005	-0.021	0.004
8/03	20:03	0.037	0.031	0.028	0.017	-0.024	0.015	-0.036	0.015
8/04	21:06	-0.005	0.011	0.033	0.007	0.024	0.007	-0.006	0.009
8/04	23:01	-0.008	0.007	0.041	0.006	0.007	0.006	-0.021	0.005
8/06	03:11	-0.005	0.007	0.033	0.007	0.001	0.006	-0.003	0.007
8/06	03:01	-0.005	0.005	0.043	0.008	-0.009	0.005	0.001	0.005
8/07	06:04	0.005	0.029	0.067	0.030	-0.029	0.020	-0.018	0.018
8/08	10:00	-0.016	0.004	0.036	0.004	0.010	0.004	0.005	0.003
8/09	16:01	-0.004	0.004	0.019	0.004	-0.003	0.004	0.007	0.003
8/10	19:59	-0.035	0.025	0.049	0.014	-0.006	0.012	0.025	0.013
8/11	04:32	-0.020	0.005	-0.003	0.009	-0.016	0.005	0.020	0.007
8/12	03:56	0.036	0.013	-0.054	0.024	-0.007	0.013	0.017	0.014

3. Discussion

In general, the continuity between adjacent VLBI experiments is very good in this analysis although in the figures this agreement can be deceptive because of the large diurnal and semidiurnal signals present in the result. Differences between adjacent days and for the overlapping experiments are less than 0.5 mas for pole position and 0.08 ms for UT1-AT. The largest difference between simultaneous experiments if for the experiments that start on

July 28. While this difference may be related to the coordinates of the stations being in slightly different reference frames, this explanation seem unlikely because the networks used in the simultaneous experiments starting on July 29 are almost identical. (Algonquin Observatory was added to the USNO experiment on July 29, Also the discontinuity from the previous day is for the R&D experiment which used the same network on July 29.). We have investigated the possible effects of azimuthal asymmetry in the atmosphere using the model discussed in Rogers et al. [1993] but estimation of such parameters only slightly reduced (to 0.07 ms) the difference in UT1-AT for the experiments starting July, 28. The gradients estimated at Westford were the largest during this R&D experiment (magnitude corresponding to 80 mm delay at 5° elevation angle) and may indicate that the difference is atmospheric delay related but that the parameterization used in our analysis is not adequate to represent the phenomena.

The other aspect of this data set is the differences between the precision of different VLBI networks to measure high frequency Earth rotation changes. Most of these differences seem related to size and shape of the VLBI networks themselves. The variations in the standard deviations of the diurnal and semidiurnal signals given in Tables 2 and 3 show the amount variation in the current networks. From these tables, there is almost a factor of ten between the smallest and largest deviations of the estimates of these signals.

References

Herring, T. A., J. L. Davis, and I. I. Shapiro, (1990) Geodesy by radio interferometry: The application of Kalman filtering to the analysis of VLBI data, *J. Geophys. Res., 95*, 12561–12581.

Herring, T. A., (1991) The ZMOA-1990 nutation series, in *Proceedings of IAU colloquium No. 127, Reference Systems*, 157–166, US Naval Observatory,, Washington. D.C..

Herring, T. A., Modeling (1992) Atmospheric Delays in the Analysis of Space Geodetic Data, in *Proceeding of Refraction of Transatmospheric Signals in Geodesy*, edited by J. C. D. a. T. A. Th.Spoelstra, pp. 157–164, Netherlands Geodetic Commission, Publications on Geodesy, The Hague, Netherlands.

Herring, T. A., and D. Dong (1994) Measurement of Diurnal and Semidiurnal rotational variations and tidal parameters of the Earth, *J. Geophs. Res.*, in press.

Rogers et al., (1993) Improvements in the accuracy of geodetic VLBI, in Contributions of Space Geodesy to Geodynamics: Technology, eds. D. E. Smith and D. L. Turcotte, AGU Geodynamics Series Vol 25, pp. 47–64.

Table 3. Estimates of the cosine and sine components of diurnal and semidiurnal polar motion variations. The time refers to the time of the midpoint of each 24-hour session of VLBI data.

Date	Hr:min	Retrograde Semidiurnal				Prograde Semidiurnal			
		cos (mas)	± (mas)	sin (mas)	± (mas)	cos (mas)	± (mas)	sin (mas)	± (mas)
7/26	17:58	-0.282	0.201	-0.142	0.215	-0.048	0.213	0.448	0.216
7/27	20:02	0.070	0.249	0.013	0.233	0.521	0.246	0.370	0.253
7/28	21:01	0.270	0.081	-0.076	0.077	0.011	0.085	0.200	0.075
7/28	23:02	0.366	0.088	-0.412	0.091	0.014	0.083	0.036	0.092
7/30	03:01	0.464	0.061	0.108	0.059	0.231	0.064	-0.083	0.055
7/30	03:01	0.435	0.075	-0.241	0.079	0.040	0.077	0.088	0.078
7/31	05:59	0.276	0.332	-0.246	0.276	-0.348	0.271	0.557	0.306
8/01	09:59	0.432	0.069	0.468	0.073	0.086	0.065	-0.080	0.073
8/02	16:02	0.083	0.080	0.478	0.079	-0.108	0.077	0.129	0.081
8/03	20:03	-0.510	0.218	0.261	0.208	-0.202	0.214	0.496	0.223
8/04	21:06	-0.050	0.102	0.116	0.103	-0.026	0.104	-0.012	0.101
8/04	23:01	0.261	0.091	0.411	0.092	0.152	0.089	0.221	0.096
8/06	03:11	-0.040	0.073	0.059	0.067	-0.075	0.071	-0.249	0.065
8/06	03:01	-0.362	0.078	0.253	0.078	-0.080	0.077	0.040	0.082
8/07	06:04	-0.194	0.228	0.101	0.202	-0.001	0.207	0.119	0.216
8/08	10:00	0.083	0.068	-0.067	0.063	0.093	0.062	0.147	0.070
8/09	16:01	0.206	0.075	-0.267	0.070	0.041	0.070	0.002	0.075
8/10	19:59	0.149	0.179	0.049	0.173	-0.130	0.175	0.000	0.195
8/11	04:32	0.163	0.114	0.034	0.120	0.157	0.108	0.092	0.121
8/12	03:56	0.145	0.087	0.154	0.081	0.034	0.084	-0.054	0.080

Date	Hr:min	Prograde diurnal			
		cos (mas)	± (mas)	sin (mas)	± (mas)
7/26	17:58	-0.841	0.290	0.038	0.329
7/27	20:02	-0.037	0.332	-0.229	0.358
7/28	21:01	0.036	0.092	0.316	0.092
7/28	23:02	-0.260	0.103	0.359	0.115
7/30	03:01	0.016	0.060	0.429	0.065
7/30	03:01	0.136	0.106	0.253	0.099
7/31	05:59	0.312	0.406	0.248	0.442
8/01	09:59	0.106	0.085	0.219	0.072
8/02	16:02	-0.145	0.090	0.063	0.092
8/03	20:03	-0.188	0.314	0.410	0.340
8/04	21:06	-0.198	0.132	0.001	0.146
8/04	23:01	-0.168	0.124	-0.392	0.101
8/06	03:11	-0.279	0.074	-0.041	0.075
8/06	03:01	-0.244	0.107	-0.128	0.103
8/07	06:04	-0.691	0.289	0.049	0.313
8/08	10:00	-0.365	0.076	-0.010	0.072
8/09	16:01	-0.133	0.087	-0.026	0.083
8/10	19:59	-0.247	0.267	-0.427	0.297
8/11	04:32	-0.241	0.137	0.173	0.168
8/12	03:56	-0.216	0.130	0.335	0.100

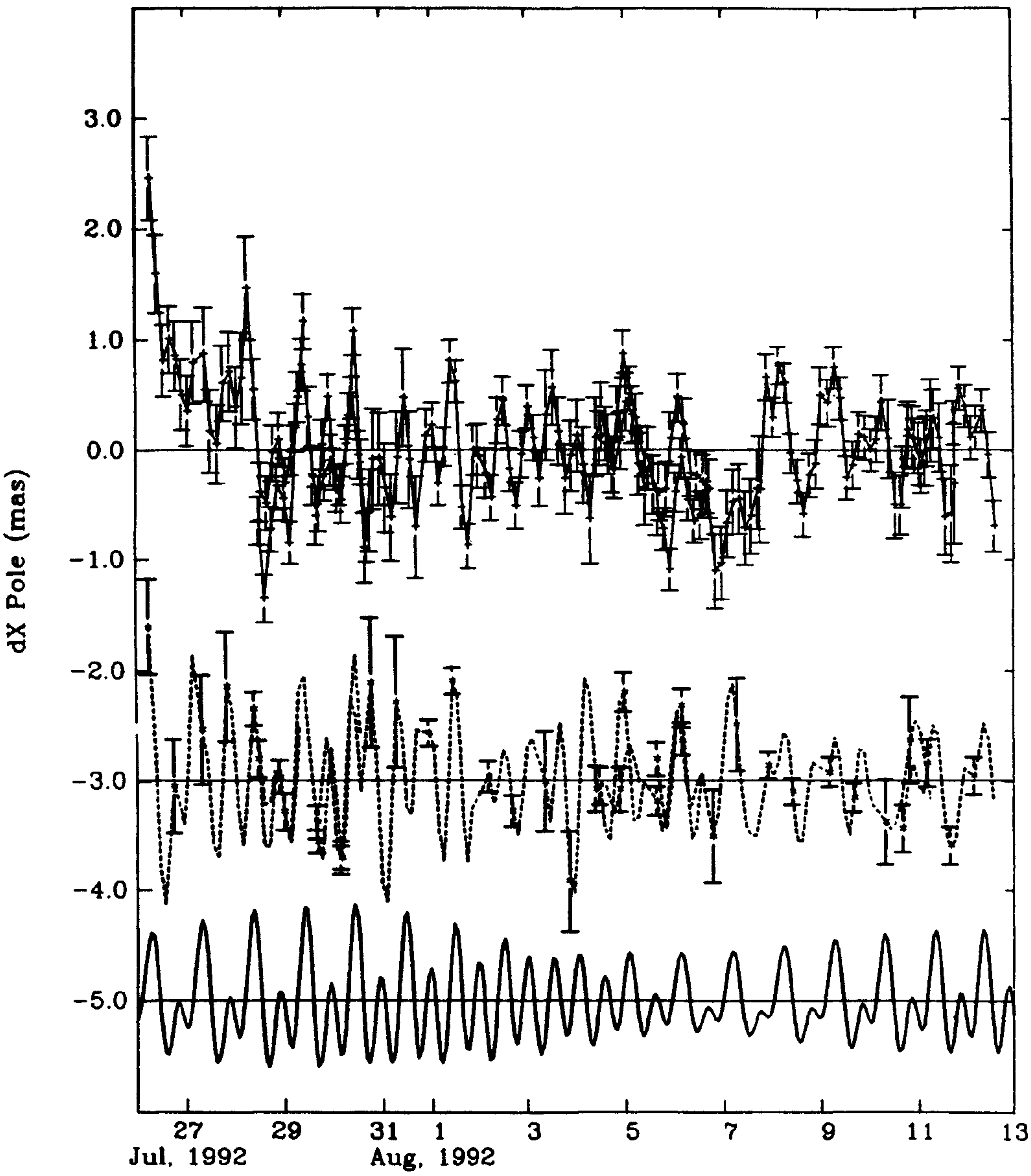

Figure 1. Differences between the stochastic estimates of the X-pole position for the standard analysis discussed in the text (top part of figure). The middle portion of the figure shows with a dashed line the time-domain representation of the diurnal and semidiurnal coefficient estimates (Table 2). Occasional one-standard deviation error bars are shown computed from the standard deviations of the coefficient estimates. The lower part of the figure shows the time domain representation of the tidally coherent signals given in Herring and Dong [1994]

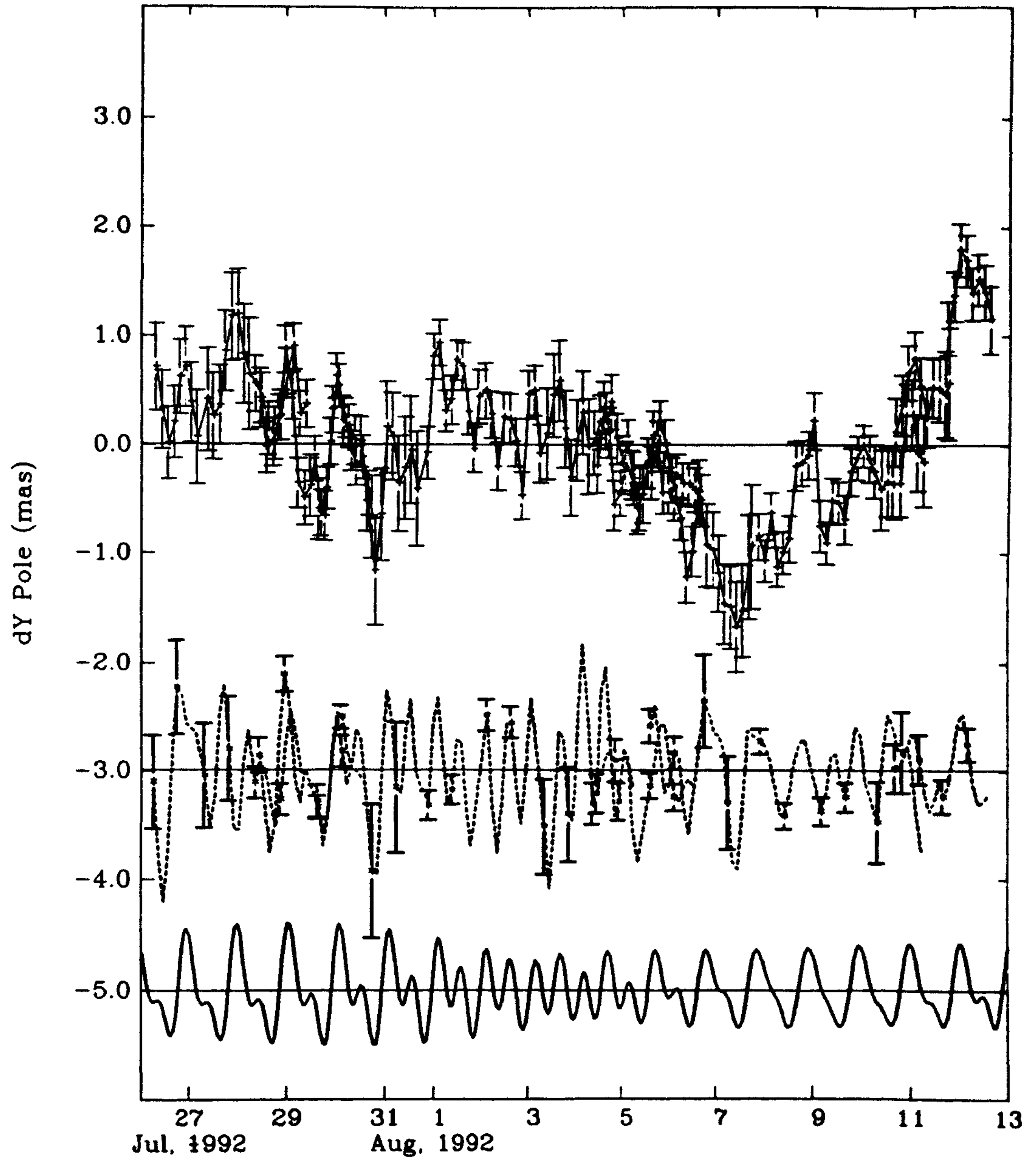

Figure 2. Same as Figure 1 except Y-pole position differences are shown.

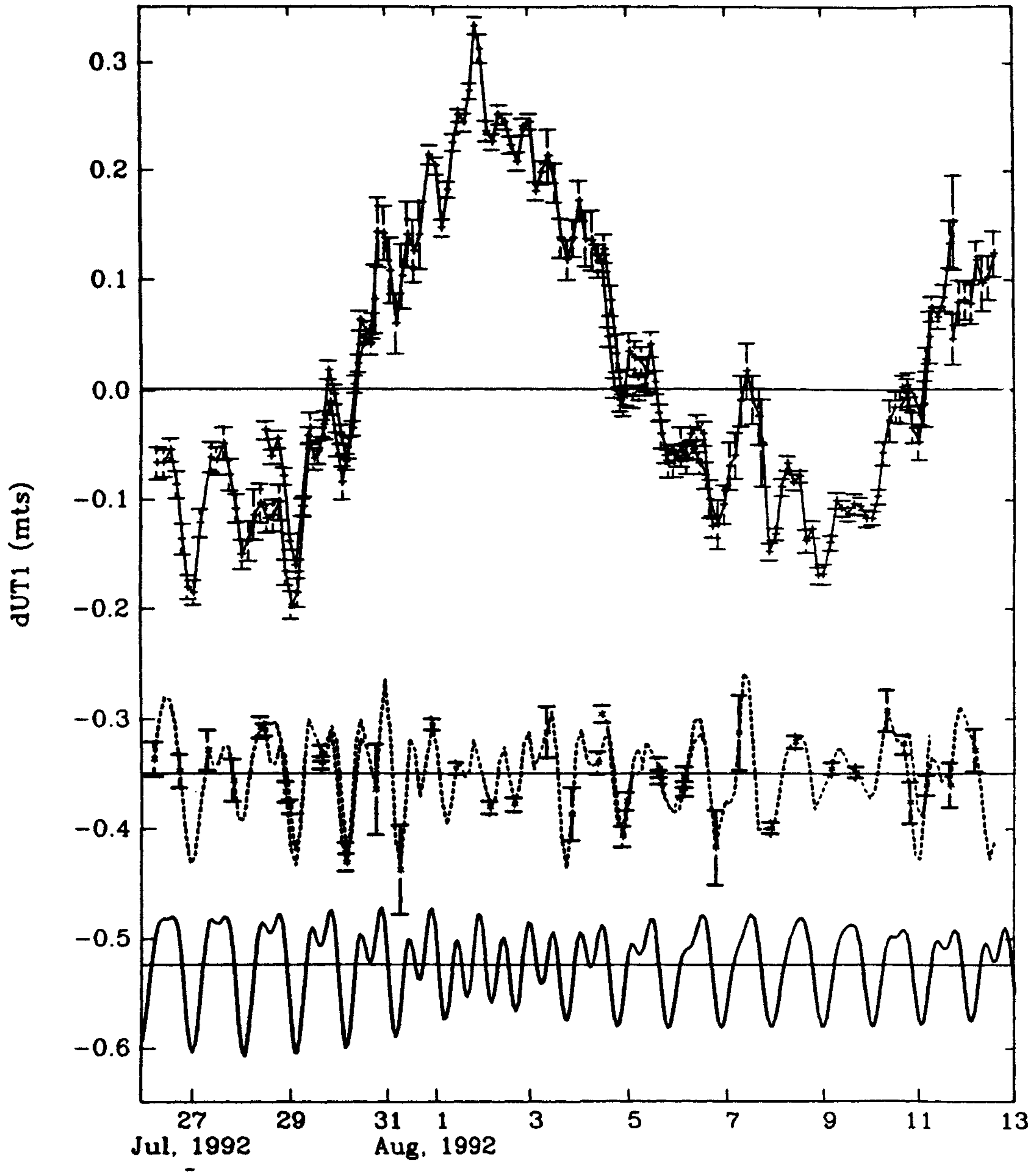

Figure 3. Same as Figure 1 except UT1-AT differences are shown.

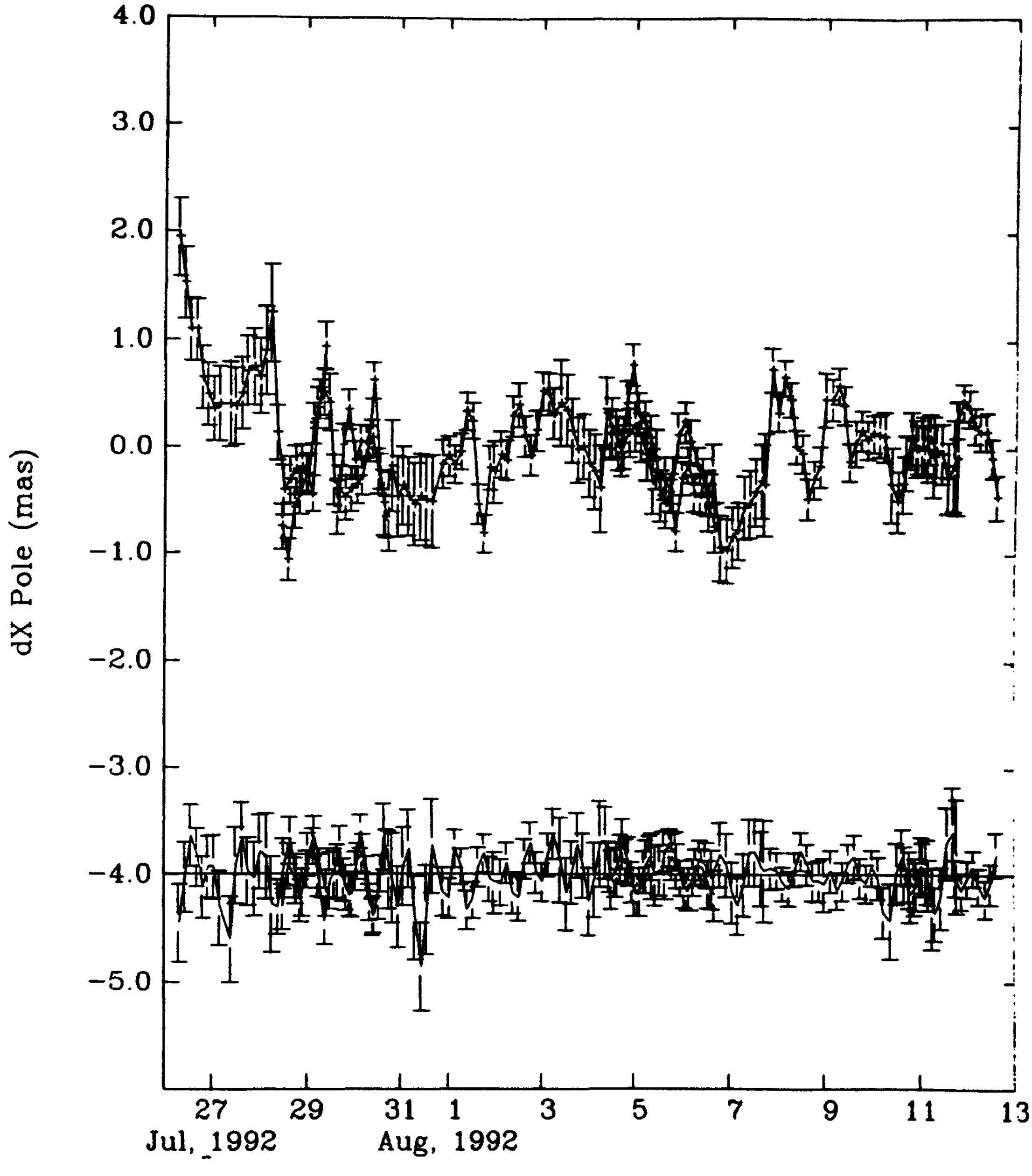

Figure 4. Differences between the stochastic estimates of the X-pole position for the standard analysis discussed in the text except that no diurnal and semidiurnal polar motion and UT1 variations were applied apriori (top portion of figure). The lower portion the differences between the standard analysis and this analysis are shown. Most of the differences can be explained by the stochastics not being able to track the rapid variations in the diurnal and semidiurnal signals when the VLBI data geometry is weak.

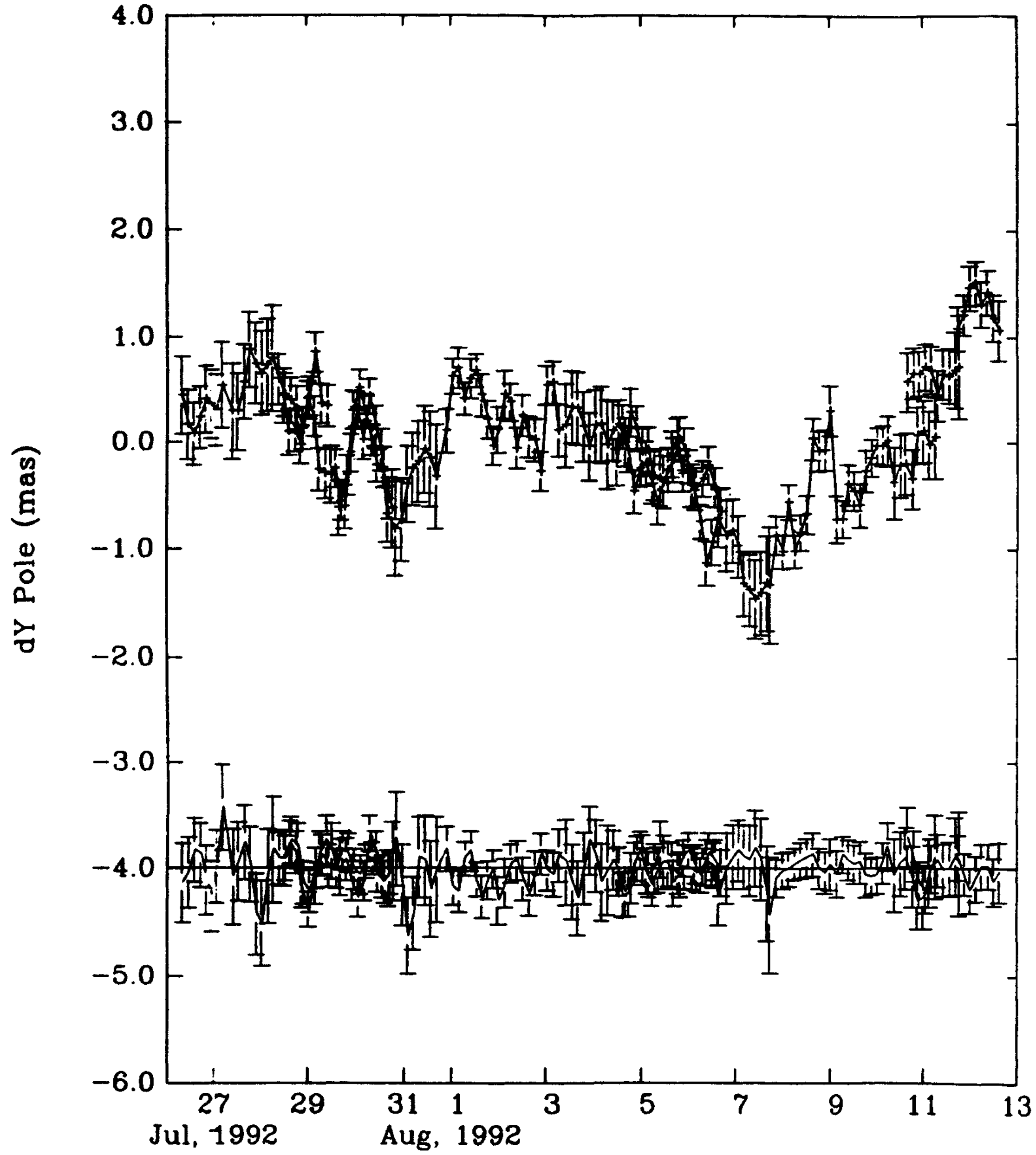

Figure 5. Same as Figure 4 except Y-pole position differences are shown.

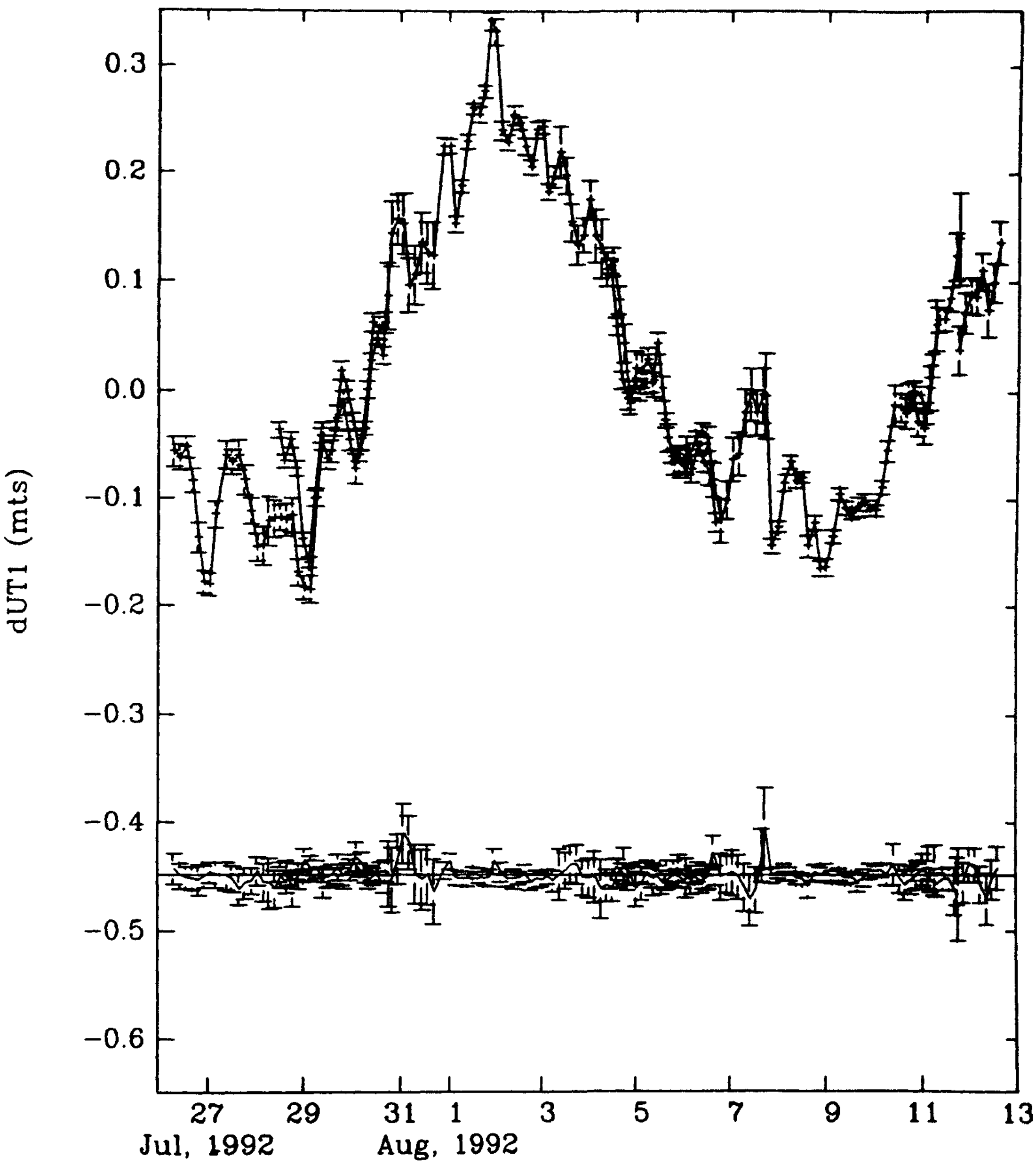

Figure 6. Same as Figure 4 except UT1-AT differences are shown.

UNIVERSAL TIME DERIVED FROM VLBI, SLR AND GPS

D.Gambis, N. Essaïfi, E.Eisop and M. Feissel

Universal Time solution combined by IERS from individual series is mainly based on VLBI inertial techniques. Although satellite methods like SLR or GPS have reached a remarkable precision, they do not give access to a highly accurate non-rotating reference frame, which restricts the possibility of determining directly UT1 from their data processing. This is mainly due to uncertainties in the even zonal harmonics of the gravity field and in various models (ocean tides). We show here that it is still possible to combine the high-frequency fluctuations contained in GPS "UT1" series with the long-term variations in the VLBI solution to derive a mixed UT1(VLBI+GPS) solution of great interest for its accuracy, time resolution but also for its economic advantage.

INTRODUCTION

By 1988, GPS had shown its ability to monitor polar motion. As a result IERS decided to include this technique as a part of its activities. After IGS'92 campaign extending from June through September 1992, five analysis centers continued their work on a routine basis. IERS has recently begun to incorporate these data in its regular analyses. In addition to the pole components estimation some analysis centers, CODE, JPL, ESOC and EMR [1,2] are also computing an internal "UT1" series or a derived quantity (*e.g* the excess to 86400 s of the length of the day, LOD). Due to the fact that satellite methods are not inertial the celestial reference system they define is not stable over long periods of time; this prevents the satellite technique to accurately determine long-term UT1 variations. We show in the present paper that their high-frequency signal is still valuable when associated to the long-term variations of UT1 VLBI series.

DATA USED IN THE ANALYSES.

Four GPS analysis centers currently derive UT1-UTC (or LOD values). The present sudy is only concerned by UT1 for Earth orientation purposes, consequently, LOD series given by JPL and ESOC have been integrated to give a "UT1" series. Because of missing values or gaps in some series, interpolation was required to derive continuous and homogeneous "UT1" series. Due to large jumps in the data, the analysis was made on a restricted interval for EMR. The characteristics of each series are listed on table 1. Other operational series used in the analyses and/or in the comparisons are also listed.

	int. (d)	sampl. (d)	1992 June	Sept.	1993 Jan.	March
GPS						
EOP(CODE) 92 P 04	1	1	:::::::::	:::::::::	:::::::::	:::::::::
EOP(JPL) 92 P 02	1	1		:::::::::	:::::::::	
EOP(JPL) 92 P 03	1	1			:::::::::	:::::::::
EOP(ESOC) 92 P 02	1	1			:::::::::	:::::::::
EOP(EMR) 92 P 04	1	1			:::::::::	:::::::::
VLBI						
EOP(NOAA) 93 R 01	3	1	:::::::::	:::::::::	:::::::::	:::::::::
EOP(NOAA) 93 R 03	1	0.1	:::::::::	:::::::::	:::::::::	:::::::::
SLR						
EOP(CSR) 91 L 01	3	3	:::::::::	:::::::::	:::::::::	:::::::::

Table 1 - GPS, VLBI and SLR Universal Time available at IERS/CB as of 15 March 1993

Differences between the "UT1" series for each GPS center and an external reference like the IERS combined solution (EOP (IERS) C 04) show a wide range of errors (Fig. 1) mainly linked to inaccuracy in the celestial frame defined in orbit computation. Fig.2 shows the geometrical configuration of the satellite orbit relatively to the various reference frames implied. Due to mismodeling in the even zonal harmonics of the gravity field, to ocean tides and also to atmospheric gravitational effects linked to pressure variations, the node longitude and consequently UT1 (hour angle, reckoned from the prime meridian, of a point on the celestial equator)[3] are affected by long-term errors. This prevents the satellite technique to accurately determine long-term UT1 variation. Some analysis centers like CSR have solved this problem by using external a-priori VLBI values in their computations[4].

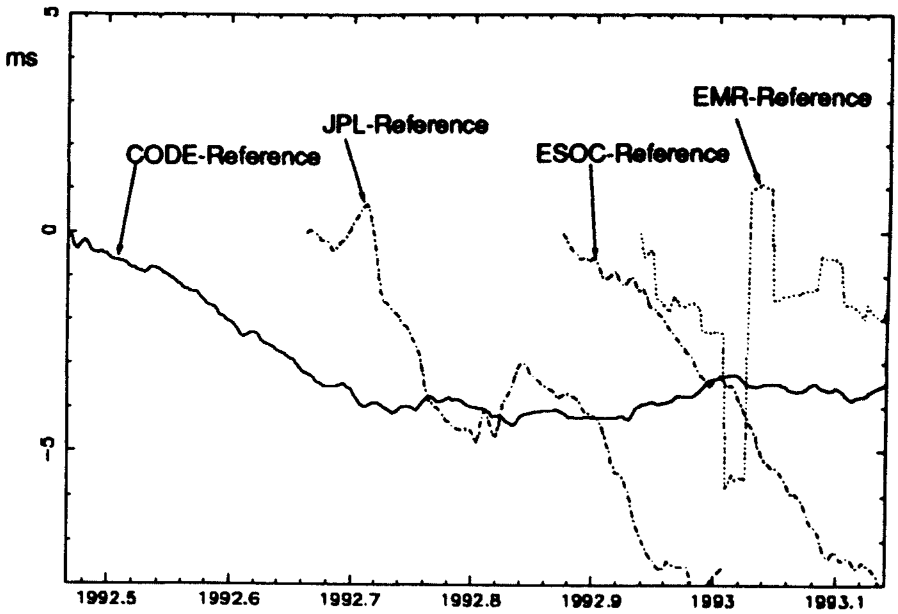

Fig. 1 - Raw "UT1" (or integrated values of LOD for JPL and ESOC) derived from GPS analysis present large systematic low-frequency errors relatively to external series (IERS combined solution) which prevents their direct use in current analyses. The plotted differences are arbitrarily set to zero at the start of the time series.

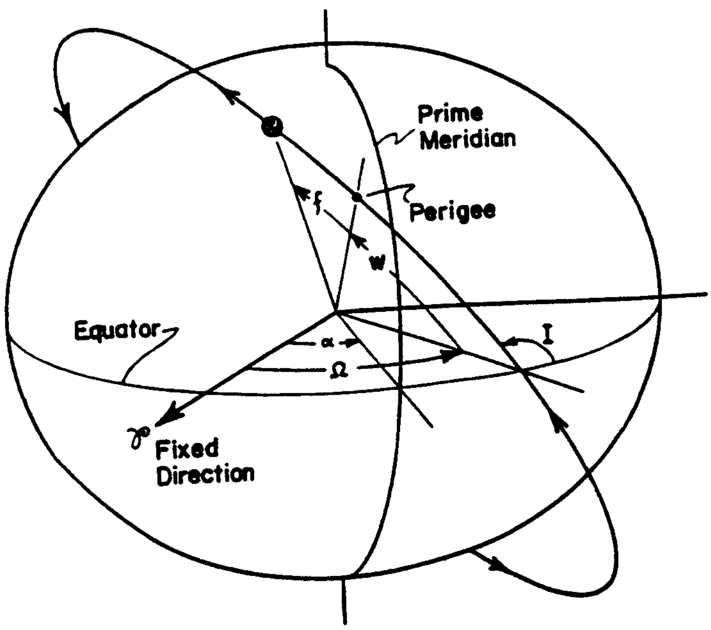

Fig. 2 - Representation of the orbit configuration relative to various reference frames. α : angle proportional to UT1 is obviously correlated to Ω, longitude of the ascending node of the satellite orbit; its determination suffers from mismodeling of Ω .

CONSTRUCTION OF A UT1 SERIES BASED ON GPS AND VLBI SOLUTIONS

We want to set up a procedure of constructing a mixed UT1 series involving long-term VLBI variations of EOP(NOAA) 93 R 01 associated to high-frequency variations given by GPS analysis *e.g.*UT1(VLBI+GPS) the most simple possible for clarity of the process. High frequency terms are removed in VLBI series while they are kept for internal GPS "UT1" series. The critical point concerns the threshold determination within which the high-frequency information contained in the GPS series is valuable. The criteria we have chosen is the following:

Parallel periodograms are made for CODE, JPL and the VLBI solutions. Depending on the analysis center (CODE or JPL) the agreement is fair until a specific period (respectively about 80 and 30 days) which is the threshold corresponding to the optimal filtering (Fig.3). This analysis could not be done for ESOC and EMR because of the relatively short data interval available.

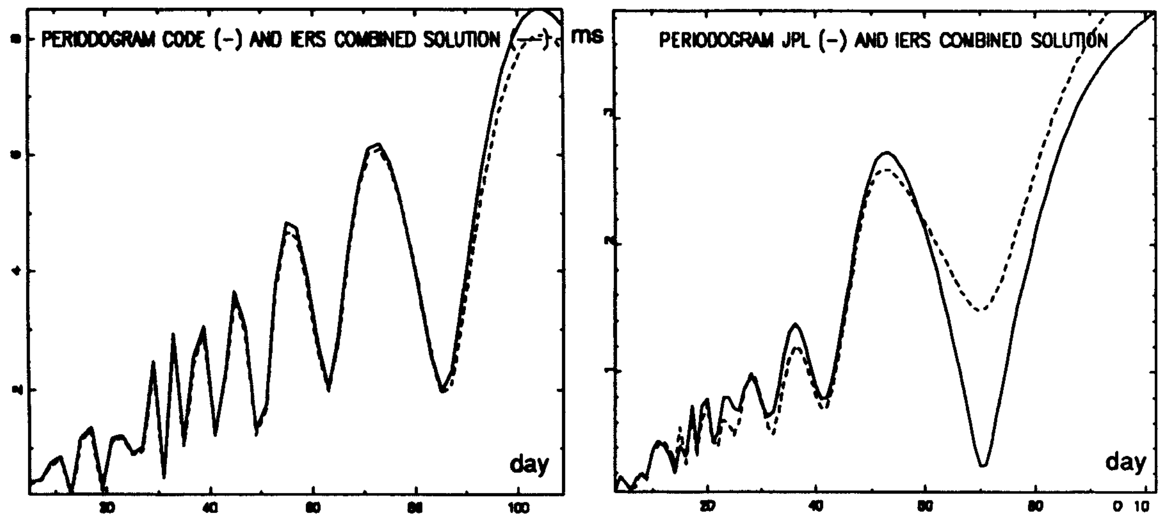

Fig. 3 - Periodograms of raw "UT1" GPS series compared to those of EOP(NOAA) 93 R 01. This analysis gives the threshold for smoothing characteristics determination

COMPARISONS OF UT1(VLBI+GPS) WITH VLBI AND SLR SERIES

In order to estimate the precision of the obtained mixed UT1(VLBI+GPS) solution comparisons with various series have been made. Fig. 4 shows its difference with NOAA and CSR solution; the rms differences of the three series are of the same order. Fig. 5 shows the differences between the mixed UT1(VLBI+GPS) solution and VLBI (EOP(NOAA) 93 R 01) and SLR (EOP(CSR) 91 L 01).

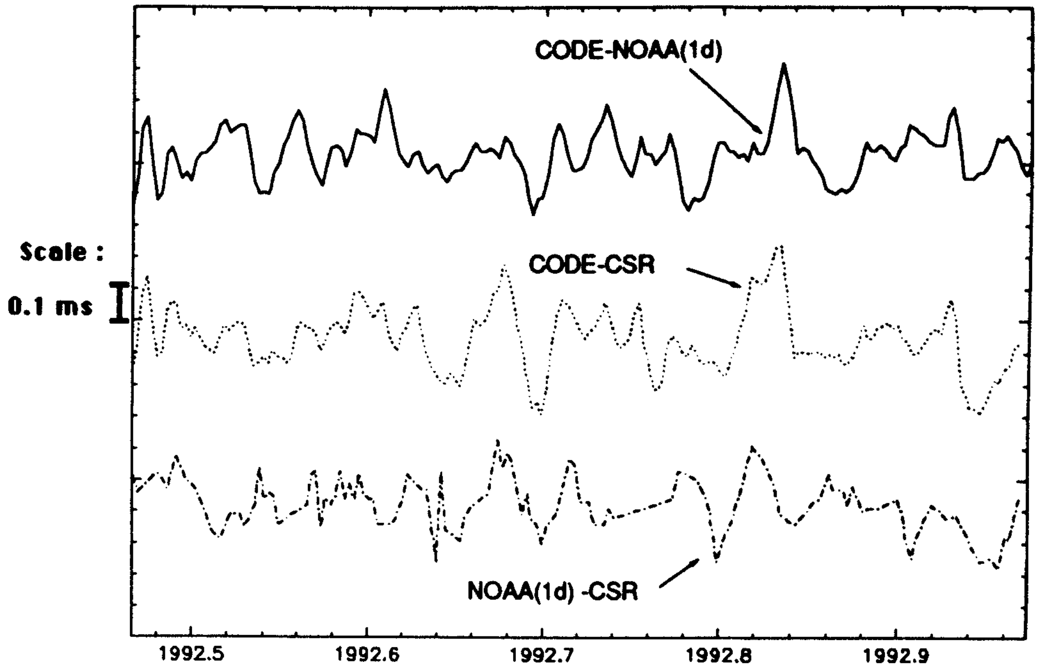

Fig. 4 - Differences between UT1(NOAA+CODE) solution with respectively EOP(NOAA) 93 R 01 and EOP(CSR) 91 L 01. RMS of the three series give estimation of the precisions.

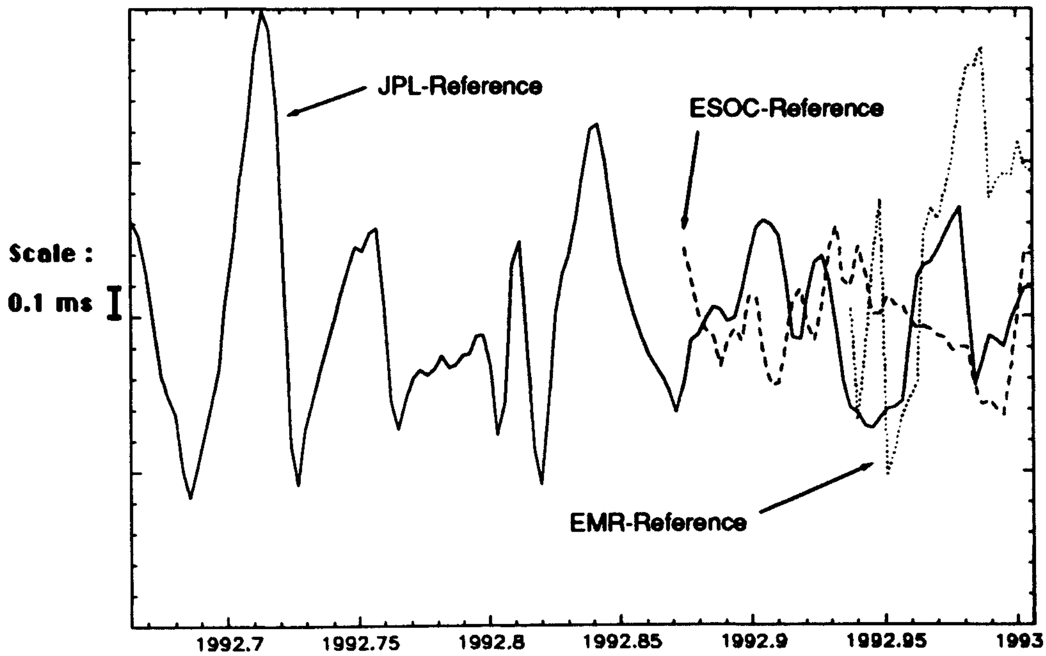

Fig. 5 - Differences between UT1(GPS+NOAA) solutions with an external reference (here EOP(IERS) 90 C 04).

Table 2 gives an estimation of the precision of each series by comparison to EOP(IERS) 90 C 04. These values are only indicative, the combined IERS solution being dependant on VLBI and SLR series.

Series		UT1 (0,0001s)
GPS		
	UT1(NOAA+CODE)	0.81
	UT1(NOAA+JPL)	2.80
	UT1(NOAA+ESOC)	1.47
	UT1(NOAA+EMR)	3.87
VLBI		
	EOP(NOAA) 93 R 02	0.41
	EOP(NOAA) 93 R 03	0.64
SLR		
	EOP(CSR) 91 L 01	0.73

Table 2 - RMS differences of various series with EOP(IERS) 90 C 04.

CONCLUSIONS

Although the internal UT1 series derived from GPS determinations are not directly usable for Earth Orientation monitoring, its high-frequency information can be used together with an external long-term calibration to derive a combined UT1(VLBI+GPS) solution which may be used both for scientific and operational purposes. Outside its high accuracy comparable to other series (NOAA, CSR) the advantage is its high sampling contribution (sub-diurnal) and also, what is not negligible its low production price due only to an additional effort in analyses. Moreover, monthly VLBI contribution seems sufficient to ensure long-term stability of the solution. Refinements of the data analyses are assumed to improve the results in a near future.

REFERENCES

[1]- Annual Report for 1991.

[2]- IGS'92 campaign, IERS Reports.

[3]- IERS Technical note 8

[4]- Aoki S.,Guinot B., Kaplan K.H.,Kinoshita H.,McCarthy D.D. and P.K. Seidelman, 1982, *Astron. Astrophys.*,105,359-361.

SUB-DAILY EARTH ROTATION DURING EPOCH '92

A. P. FREEDMAN, R. IBANEZ-MEIER, J. O. DICKEY, S. M. LICHTEN
Jet Propulsion Laboratory
California Institute of Technology
Pasadena, California 91109

T. A. HERRING
Department of Earth, Atmospheric, and Planetary Sciences
Massachusetts Institute of Technology
Cambridge, Massachusetts 02139

ABSTRACT. Earth rotation data were obtained with GPS during the Epoch '92 campaign in the summer of 1992. About 10 days of data were acquired from 25 globally distributed stations and a constellation of 17 GPS satellites. These data were processed to estimate UT1 corrections every 30-minutes, then smoothed to form a UT1 series with 3-hour spacing. Earth orientation data during Epoch '92 were also obtained by several VLBI groups, and were processed together to yield VLBI estimates of UT1 with 3-hour time resolution. The high frequency behavior of both GPS and VLBI data sets is similar, although drifts between the two series of ~0.1 ms over 2-5 days are evident. Tidally induced UT1 variations from both theoretical ocean models and empirical determinations were compared with the GPS and VLBI series. Estimates of atmospheric angular momentum (AAM) at 6-hour intervals generated by several meteorological centers were also compared with the geodetic data. These comparisons indicate that most of the GPS signal in the diurnal and semidiurnal bands can be attributed to tidal processes, and that UT1 variations over a few days are mostly atmospheric in origin.

1. Introduction

Variations in the rate of rotation of the solid Earth result both from torques applied to the Earth from the exterior or interior and from mass redistributions within the Earth. For high-frequency Earth rotation variations, defined here as rotation rate changes occurring over time scales of a week or less, the principal forces on the solid Earth are thought to come from the atmosphere and oceans. In particular, tidal forcing of the oceans is expected to dominate the rotational variations at periods of one day and less.

A variety of techniques have historically been used to monitor the rotation of the Earth, but only over the past few years has the capability for daily and even sub-daily monitoring of Earth rotation with the requisite precision become available. Current high-precision techniques include very long baseline interferometry (VLBI), satellite laser ranging (SLR), lunar laser ranging (LLR), and, most recently, the Global Positioning System (GPS). VLBI estimates of Earth's rotation angle (UT1 – UTC) at daily intervals and SLR estimates at roughly 3-day intervals have been made for several years. Over the past four years, measurements of UT1 variations with hourly or so time resolution have been made sporadically by both VLBI and GPS techniques [1, 2].

In association with the International GPS Geodynamics Service's (IGS) proof of concept campaign for the summer of 1992, an additional campaign known as SEARCH '92 (Study of Earth-Atmosphere Rapid Changes) was held to monitor high-frequency Earth orientation variations utilizing all space geodetic techniques and to advocate for and facilitate the collection of the best available related geophysical data [3]. Data from a variety of complementary techniques providing a good level of redundancy were acquired, in particular, during the intensive two-week period known as Epoch '92. In this paper, we present GPS estimates of sub-daily variations in UT1 during Epoch '92 and compare these results with a number of these other related data sets. This intercomparison should provide a robust estimate of Earth's true rotational variations at time scales as short as a few hours, and should help as well to improve strategies for processing GPS data.

2. Data sets

2.1. GPS

The GPS data processing strategy is a version of that discussed elsewhere using the JPL GIPSY/OASIS II software [4, 5] and is summarized in Table 1 [see also Zumberge et al., this volume]. Data from a network of 25 stations using a GPS constellation of 17 satellites were acquired over more than 10 days during the last week of July and first week of August, 1992. Owing to the use of anti-spoofing (AS) signal encryption over the weekend, these data are not continuous but are divided into two groups from which two multi-day GPS orbit arcs were created. Corrections to a nominal UTPM series (derived from the IERS Bulletin B) were obtained from the data, with UT1 estimated every 30 minutes and polar motion every two hours. UT1 was modeled as a Gauss-Markov (AR1) process with a steady-state sigma of 0.06 ms and a time constant of 4 hours. Thus, over 30 minutes, 0.028 ms of process noise was added.

Table 1. GPS ESTIMATION STRATEGY

Estimated parameters	
Station locations (8 fiducial sites)	Wet zenith troposphere (random walk)
Satellite states	Clock biases (white-noise)
Solar radiation pressure	Carrier phase biases
UT1 (AR1)	Polar motion (white noise)
Standard models	
Solid Earth tides and equilibrium ocean tides from Yoder et al.[6]	
Gravity field coefficients: GEMT3, 8x8 truncation	
Nutation model: 1980 IAU model	
A priori and fiducial site locations ITRF 91	
Nominal UTPM from IERS Bulletin B	
Rogue receivers: Pseudorange (1-meter), Carrier Phase (1 cm)	
6-minute data interval (obtained by decimation)	

We generated UT1 time series using a variety of orbit modeling strategies [Zumberge et al., this volume]. Our preferred strategy employed multi-day orbit arcs wherein one set of satellite states (positions and velocities) was estimated for each satellite. Three stochastic solar radiation parameters for each satellite were modeled as AR1 processes and estimated every hour. Alternative estimation strategies yield UT1 series that differ, but the results and conclusions described below do not significantly change if these other UT1 series are used.

For comparison with the VLBI data, we constructed a smoothed GPS UT1 data set by applying a Gaussian filter with a half-width of about one-half hour to smooth the 30-minute data and interpolate them to the epochs of the VLBI data. Although it contains GPS-derived UT1 measurements every 3 hours, this smoothed data set is not identical to a 3-hour GPS solution, since the latter contains UT1 values averaged over a 3-hour window whereas the former is effectively smoothed over a 1- to 2-hour window.

2.2. VLBI

VLBI data were acquired from the three networks described in Table 2. Note that on certain days, UT1 was measured by more than one VLBI network, enabling an estimate of the quality of the VLBI data. The correlated VLBI data were combined using the MIT Kalman filter programs CALC/SOLVK. UT1, polar motion, nutation corrections, and station troposphere parameters were estimated over 24 hour time spans, with UT1, polar motion, and the troposphere parameters modeled as random walks [see Herring, this volume].

Several solutions were generated in which UT1 was estimated either every 30 minutes or every 3 hours. The 30-minute solutions were rather noisy, so a 3-hour series, in which UT1 was estimated every 3 hours with 0.04 ms sigma resets after a diurnal and semidiurnal a priori tide model had been applied, was used in this study. A final smoothed VLBI solution was generated in which the 24-hour data sets from all the networks were combined using a mild Gaussian filter.

Table 2. VLBI DATA

NASA's Goddard Space Flight Center (GSFC) – NASA R&D
8 experiments, 5-6 sites in N. America, Hawaii, and Europe
National Oceanic and Atmospheric Administration's (NOAA) Laboratory for Geosciences – IRIS
4 experiments (one mobile, three IRISA), 5 sites in N. America and Europe
Unites States Naval Observatory (USNO) – NAVNET
6 experiments, 4-6 sites, located around globe

Data run from July 26 through August 11. Four days have measurements by both NAVNET and NASA R&D. Each experiment can have significantly different formal errors.

2.3. TIDE MODELS

A variety of additional data sets were used in evaluating the GPS and VLBI time series. Two models for tidally-induced diurnal and semidiurnal UT1 variations were compared, one based on theoretical ocean models [7] and one empirically derived from many years of measured UT variations [8]. The theoretical series, referred to as the Gross tide model, is based on the oceanic angular momentum model of Seiler [9]. This formulation also contains corrections to the standard tide model [6] for non-equilibrium ocean tides at fortnightly and monthly periods. The empirical model, referred to as the Herring tide model, is based on 8 years of VLBI data. It contains estimates of the diurnal and semidiurnal tidal terms only. Note that this empirical tide series may contain additional diurnal signals other than those due to the non-equilibrium ocean tides, such as the effects of atmospheric tides. Both tidal UT1 series may be compared directly to geodetic UT1 estimates.

2.4. AAM 6-HOURLY DATA

If angular momentum were exchanged solely between the atmosphere and the solid Earth, atmospheric angular momentum (AAM) variations would result in corresponding changes in the length of the day (LOD), the time derivative of UT1. Several sets of AAM were computed every 6 hours as part of the SEARCH/IGS effort by three meteorological centers: the U. S. National

Meteorological Center (NMC), the European Centre for Medium-Range Weather Forecasts (ECMWF), and the Japanese Meteorological Agency (JMA). For each center, the AAM quantity that we use consists of the χ_3 AAM wind term integrated to the top of the model atmosphere (either 50 mbar or 10 mbar, depending on center) plus the full pressure (not inverted-barometer) term. Gaps in the AAM series were filled by linear interpolation.

We used these data sets to estimate atmospherically induced variations in UT1. Since AAM is a substitute LOD, the AAM series must be integrated to be compared to a UT1 series. However, two arbitrary constants, effectively a bias in LOD and a bias in UT1, enter into this integration. For the comparisons shown below, linear models are removed from the AAM and geodetic UT1 series to account for these constants.

2.5. SMOOTHED REFERENCE SERIES

A reference series, based on the IERS Bulletin B nominal values used for the GPS analysis, was used to remove long-period UT1 variations. Note that all the geodetic series shown have the shorter-period (<35 day) tides explicitly removed according to the standard Yoder et al. [6] model, while subtracting the nominal UT1R series effectively removes the longer period terms of [6].

3. Results

3.1. GPS VS. VLBI

We have compared the GPS-derived UT1 with VLBI estimates of UT1 – TAI for each network-day of data. UT1 was estimated every 30 minutes in both sets of data. Typical formal errors of the various time series are summarized in Table 3. We present below only results for the smoothed and interpolated sets of VLBI and GPS data. These two data sets are shown in Figure 1. For display purposes, the UT1 values have been differenced with the IERS Bulletin B reference series. The bias between GPS and VLBI is arbitrary. Note the gap in GPS data due to the use of AS during the weekend of August 1-2 which precludes the construction of a continuous two-week long GPS time series. The 6-day time span at the end of July where data exist from both techniques is referred to below as period A, while the 4.5-day time span in August is referred to as period B.

Although there appears to be a drift between the two series over several days, their diurnal variability is similar. If the two series are differenced, linear trends can be fit separately to periods A and B to quantify both the drift and residual scatter in GPS minus VLBI. These values are given in Table 3. Over 4 to 6 day time spans, the GPS shows a fairly linear drift with respect to VLBI, with drift rates of ±20-40 μsec/day. After removing these drifts, the total RMS scatter of GPS minus VLBI UT1 is 0.023 ms. These drifts are probably a result of drift in the GPS time series caused by systematic effects such as orbit mismodeling.

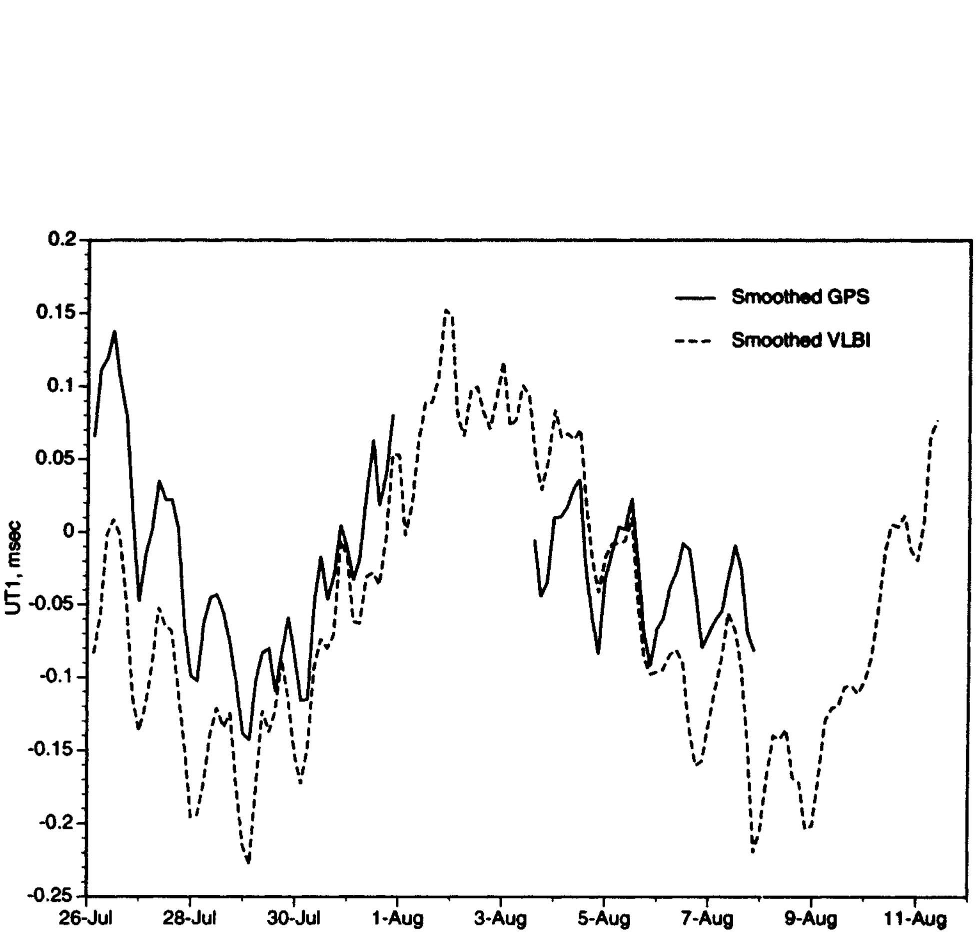

Fig. 1. UT1 from GPS and VLBI evaluated every 3 hours.

Table 3. STATISTICS

	Typical 30-Minute UT1 Formal Errors		
GPS	**IRIS VLBI**	**NAVNET**	**NASA R&D**
0.02-0.03 ms	0.02-0.04 ms	0.015-0.04 ms	0.01-0.025 ms
	GPS Minus VLBI		
	Period A	**Period B**	**Entire time span**
Slope	-0.018 ms/day	0.041 ms/day	--
RMS scatter	0.022 ms	0.026 ms	0.023 ms
	GPS Minus Tides		
	GPS UT1 only	**GPS minus Herring**	**GPS minus Gross**
RMS Scatter	0.032 ms	0.018 ms	0.035 ms
	UT1 Minus (AAM+Tides)		
RMS of difference	**NMC AAM**	**ECMWF AAM**	**JMA AAM**
GPS UT1	0.021 ms	0.022 ms	0.019 ms
VLBI UT1	0.027 ms	0.022 ms	0.022 ms

The relationship between GPS and VLBI may be further explored by computing power spectra of the GPS and VLBI UT1 and their difference (Fig. 2). Power spectra were obtained separately for the two periods A and B (after padding with zeros to the same length) and averaged together. A 3-point spectral smoothing was used (corresponding to a bin width of 0.375 cycles per day). Both the VLBI and GPS series show similar power in the diurnal and semidiurnal bands. Differencing the two removes the peaks in power at both frequencies, suggesting that there is a true geodetic signal in these bands that is accurately sensed by both techniques. This signal is for the most part tidal in origin, as shown below.

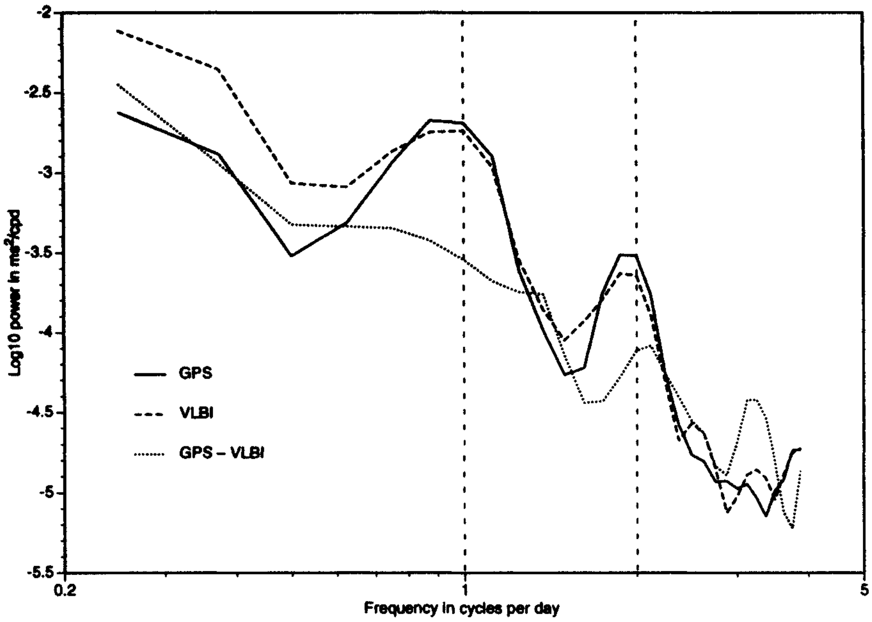

Fig. 2. Power spectra of the GPS and VLBI UT1 series and their difference.

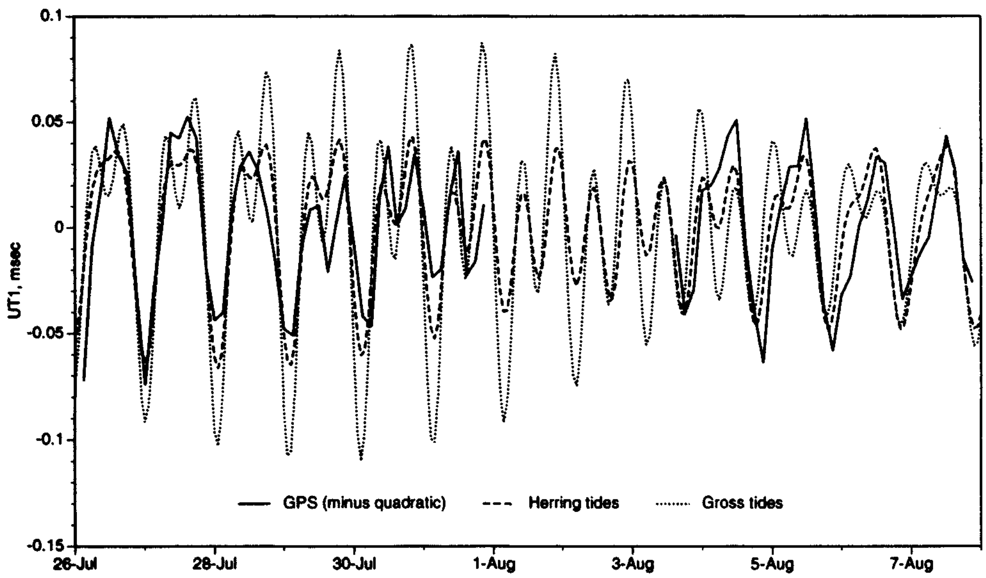

Fig. 3. GPS UT1 compared to two models of tidally induced UT1 variations.

3.2. GPS VS. TIDES

In Figure 3, we compare the smoothed GPS UT1 to the two models of tidally-induced UT1 variations. The GPS series for each period (A and B) has had a best-fitting quadratic subtracted to remove longer-period fluctuations, thus making the residual series easy to compare with the tides. Note that the Herring, empirical model more accurately reflects the observed UT1 variability than does the Gross, theoretical model.

These differences can again be described through the use of power spectra. Power spectra (computed as before) of the GPS UT1 series and the GPS series minus the two tide models are shown in Fig. 4. The Herring model removes most of the excess power in the diurnal and semidiurnal bands, with a hint of signal remaining at 2 cycles per day (cpd). The Gross model removes some power at diurnal frequencies, but adds substantial power at semidiurnal frequencies (consistent with the large amplitudes seen in Fig. 3). These differences are quantified in Table 3, which shows the RMS scatter of the three time series whose power spectra are plotted in Fig. 4. The Herring model appears to more accurately reflect the actual UT1 variations at diurnal and semidiurnal frequencies. Reasons for this may include inaccuracies in the theoretical ocean models and additional non-oceanic signal at these frequencies.

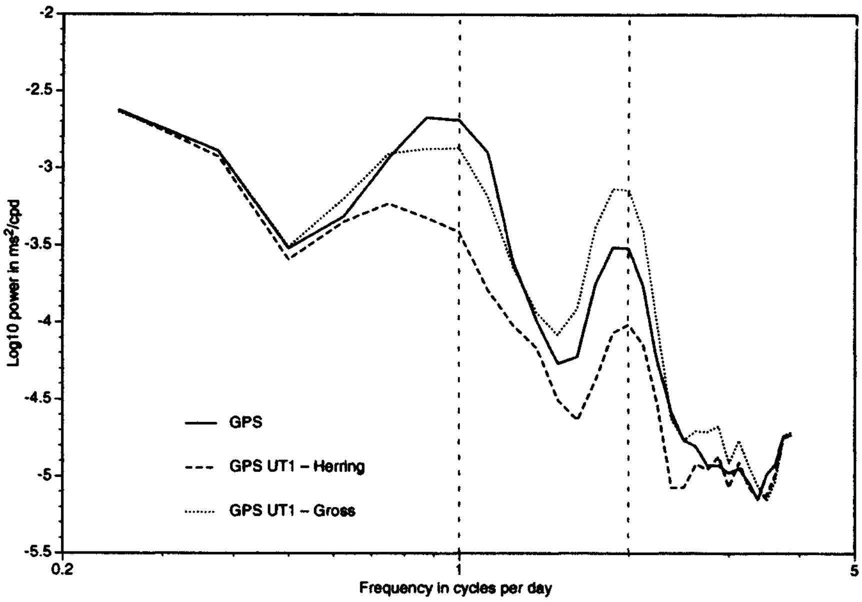

Fig. 4. Power spectra of the GPS UT1 series and the GPS series differenced with each of the two tide models.

3.3. GPS VS. AAM

The three series of atmospheric angular momentum (AAM) values evaluated every 6 hours provided by the NMC, the ECMWF, and the JMA are shown in Fig. 5. The variations in each series over periods greater than 1 to 2 days are similar, but the higher frequency fluctuations do not appear to be common among the three. The biases between the series are real, and come from differences in the meteorological models of the centers.

Since AAM represents a form of LOD, the curves in Fig. 5 must be numerically integrated to generate UT1 series whose variations are implied by the AAM. These series are shown in Figure 6. Also shown are a GPS UT1 series and the UT1 variations expected from the longer-period (14 and 30-day) non-equilibrium ocean tides emerging from the numerical ocean model [7]. Each series for each of periods A and B has had a best-fitting linear bias and trend removed. Since the ECMWF series for period A starts on July 27 and thus is one day shorter, it has had a trend removed which minimizes the differences between the ECMWF curve and the other two AAM curves. The three integrated AAM curves show similar behavior for period A, with more contrasting forms for period B. All the AAM curves appear consistent with the overall shape of the GPS UT1 curve. The longer-period tide corrections do not add substantial signal at these few-day periods.

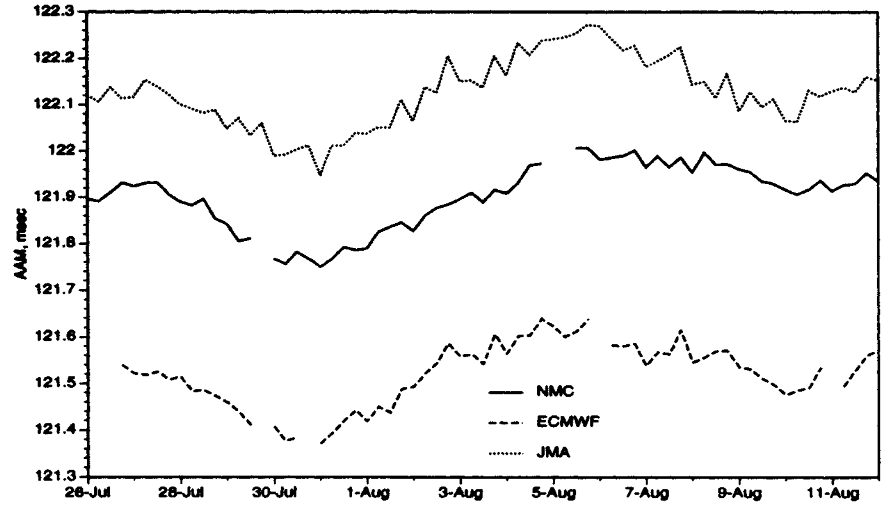

Fig. 5. Three series of atmospheric angular momentum (AAM) values.

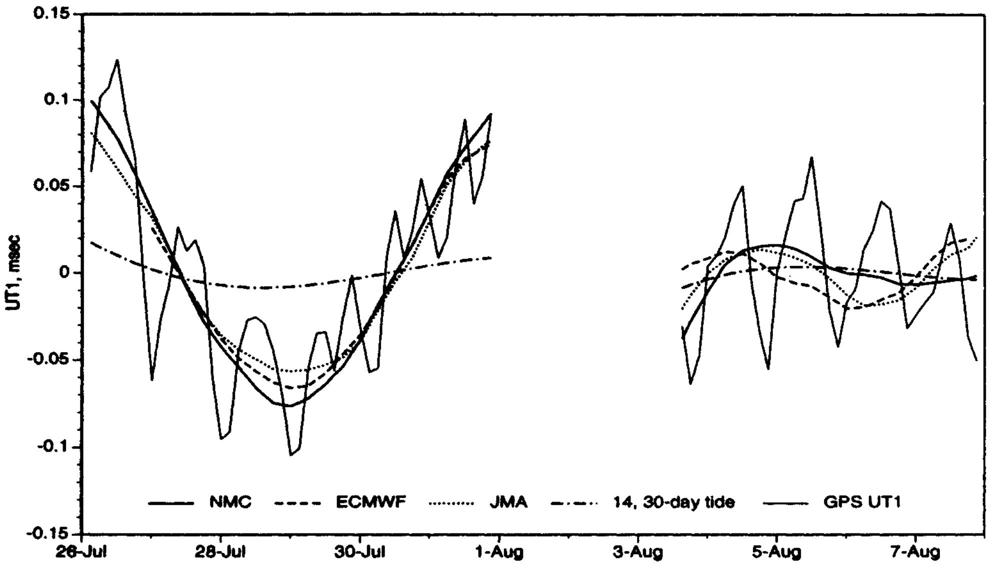

Fig. 6. Comparison of integrated AAM with geodetic UT1 variations.

The sum total of the integrated AAM, diurnal and semidiurnal tides (from [8]) and longer-period tides (from [7]) are shown in Figure 7, together with the observed UT1 variations from GPS and VLBI. Linear trends were removed from each series for each period. Most of the geodetic signal can be described by the sum of AAM variations and tidally induced UT1, with the tides acting at periods of one day and less and AAM acting at periods greater than a day. The differences between GPS and VLBI are at least as large as those between the AAM series themselves and the AAM and geodetic series. Thus, no center or technique stands out as superior. The RMS of the differences between the geodetic and AAM+tides series are shown in Table 3; all are consistent with the typical GPS and VLBI formal errors of 0.02-0.03 ms.

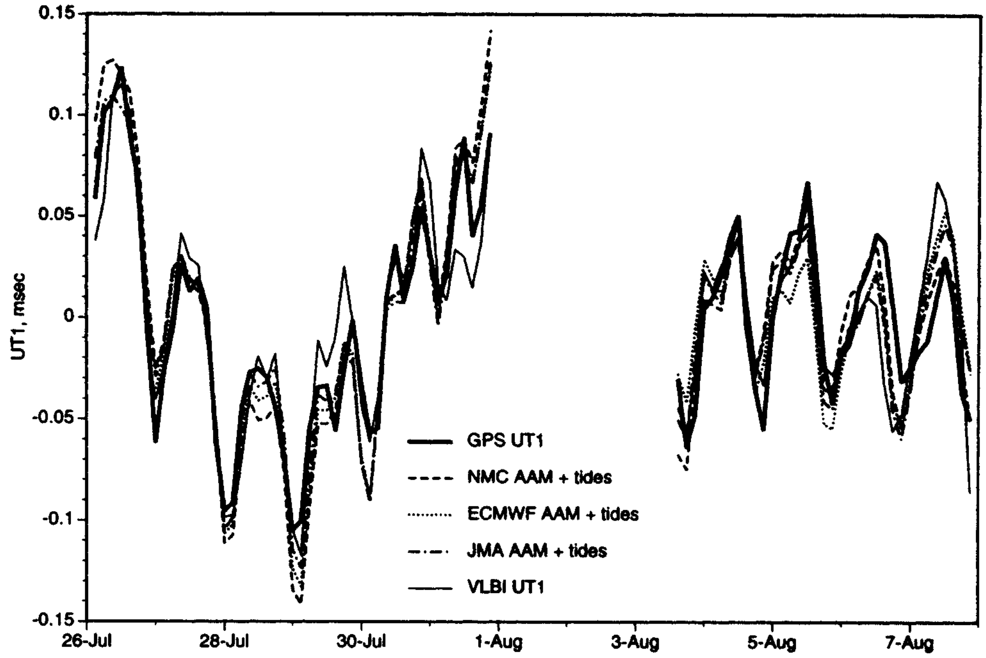

Fig. 7. The sum of the integrated AAM and diurnal, semidiurnal, and longer-period tides compared with the observed UT1 variations from GPS and VLBI.

4. Conclusions

Differences between the various series considered here tend to be at the level of 0.02 to 0.03 ms. These RMS differences are consistent with the formal uncertainties of the data themselves. The main exception is the theoretical tide model, which simply does not yield the signal seen geodetically. There is also a drift in the GPS data relative to VLBI which, over time spans of 6 days or so, appears to be linear but with a non-unique drift rate.

Both GPS and VLBI exhibit nearly identical variability in the diurnal and semidiurnal bands, attributable to tidal variations whose values are well derived from many years of geodetic VLBI data. There is no residual signal in these frequency bands that exceeds the level of formal error of the data, although residual signals with amplitudes smaller than 0.02 ms could certainly be present. Although the theoretical tide model does not agree with observations in either band, the disagreement is largest in the semidiurnal frequency band.

The multi-day variability of AAM from all the meteorological centers is similar, and yields AAM-derived UT1 curves that are consistent with the variability of the geodetic UT1 at periods longer than one day. At diurnal and shorter periods, however, the AAM centers generate inconsistent estimates. Moreover, the sub-daily variability of the AAM is quite small and cannot, at this point, be disentangled from oceanic tidal effects and noise in the geodetic data. However, limits can be placed on the size of any residual AAM signal.

Thus the signal seen in the GPS time series can be represented by the sum of four effects: tides at diurnal and semi-diurnal periods, AAM fluctuations at periods of one to at least several days, a linear drift in UT1 due possibly to orbit mismodeling, and a high-frequency noise component. To accurately solve for UT1 with GPS at these frequencies, the tidal variations in UT1 must certainly be modeled, either by explicit use of the Herring tide model, or by allowing adequate variability in the estimated UT1. AAM-induced variations are slow enough that if UT1 (or LOD) is estimated at least daily, this variability need not be explicitly modeled. Further research is necessary to investigate and reduce both the drift in UT1 of ~0.1 ms over 2-5 days, and the level of high-frequency noise present in the data.

ACKNOWLEDGMENTS. The authors thank and acknowledge the cast of literally thousands who were involved in collecting and processing the vast quantities of data from both GPS and VLBI, as well as the people and institutions involved in generating the AAM data sets. The work described in this paper was carried out by the Jet Propulsion Laboratory, California Institute of Technology, under contract with the National Aeronautics and Space Administration.

References

[1] Herring, T. A., and D. Dong, "Current and Future Accuracy of Earth Rotation Measurements," in *Proceedings of the AGU Chapman Conference on Geodetic VLBI: Monitoring Global Change (Washington DC, April 22-26, 1991)* pp. 306-324, NOAA Technical Report NOS 137 NGS 49, NOS/NOAA, Rockville, MD, 1991.

[2] Lichten, S. M., S. L. Marcus, and J. O. Dickey, "Sub-Daily Resolution of Earth Rotation Variations With Global Positioning System Measurements," *Geophys. Res. Lett.*, **19**, 537-540, 1992.

[3] Dickey, J. O., "High Time Resolution Measurements of Earth Rotation," in *Advances in Space Research*, Pergamon, in press, 1994.

[4] Lichten, S. M., and J. S. Border, "Strategies for High-Precision Global Positioning System Orbit Determination," *J. Geophys. Res.*, **92**, 12751-12762, 1987.

[5] Lichten, S. M., "Estimation and Filtering for High-Precision GPS Positioning Applications," *Man. Geod.*, **15**, 159-176, 1990.

[6] Yoder, C. F., J. G. Williams, and M. E. Parke, "Tidal Variations of Earth Rotation," *J. Geophys. Res.*, **86**, 881-891, 1981.

[7] Gross, R. S., "The Effect of Ocean Tides on the Earth's Rotation as Predicted by the Results of an Ocean Tide Model," *Geophys. Res. Lett.*, **20**, 293-296, 1993.

[8] Herring, T. A., and D. Dong, "Measurement of Diurnal and Semidiurnal Rotation Variations and Tidal Parameters of the Earth," *J. Geophys. Res.*, submitted, 1993.

[9] Seiler, U., "Periodic Changes of the Angular Momentum Budget Due to the Tides of the World Ocean," *J. Geophys. Res.*, **96**, 10,287-10,300, 1991.

SUB-DAILY POLAR MOTION DURING EPOCH '92 WITH GPS

R. IBANEZ-MEIER, A. P. FREEDMAN, S. M. LICHTEN, U. J. LINDQWISTER, R. S. GROSS
Jet Propulsion Laboratory,
California Institute of Technology
Pasadena, California 91109

T. A. HERRING
Department of Earth, Atmospheric, and Planetary Sciences,
Massachusetts Institute of Technology
Cambridge, Massachusetts 02139

ABSTRACT. Data from a worldwide Global Positioning System (GPS) tracking network spanning six days during the EPOCH '92 campaign are used to estimate variations of the Earth's pole position every 30 minutes. The resulting polar motion time series is compared with estimates derived from very long baseline interferometry (VLBI) observations. A time domain comparison of the semidiurnal and prograde diurnal bands yields better than 0.3 milliarcsecond rms differences between the series. Additional comparison with an ocean tidally-induced polar motion model suggests that most of the periodic subdaily variations in the GPS polar motion signal can be attributed to ocean tides.

1. Introduction

Observations of the motion of the pole have a long history [See Lambeck, 1980; Eubanks, 1993, and references therein]. Polar motion, which is the movement of the Earth's rotation axis with respect to its crust, is a dynamic response of the Earth forced by its interactions with other celestial bodies and its own internal dynamics. The location of the rotation axis is given with respect to a crust-fixed, reference point (e.g., the International Earth Rotation Service (IERS) reference pole [McCarthy, 1992]) by using two coordinates, polar motion x (PMX) and polar motion y (PMY), where the x-axis lies along the Greenwich meridian, orthogonal to the reference pole z-axis, and the y-axis lies 90 degrees to the west.

Angular momentum changes in the oceans at daily and sub-daily periods of tidal origin, a product of the response of the world's oceans to the tidal potential at high frequencies, lead to associated diurnal and semidiurnal changes in polar motion [Seiler, 1991; Gross, 1993; Wunsch and Seiler, 1992]. Since the tendency in the polar motion is towards decreasing amplitudes at shorter periods, increasing sensitivity has been necessary to detect these high-frequency pole position changes. Herring et al. [1991] and Lindqwister et al. [1992] obtained GPS daily polar motion estimates in agreement with VLBI at the 0.5 mas (1.5 cm) level or better, and subsequently several GPS processing centers have been routinely reporting daily estimates of pole position as part of the International GPS and Geodynamics Service (IGS). We report here on sub-daily time-domain GPS-based polar motion measurements and their comparison with VLBI. The data were collected during the intensive observing period known as EPOCH '92 (part of the SEARCH '92 Campaign organized by the IERS), during which time continuous and high time resolution data were obtained by both VLBI and GPS.

2. Data Sets and Estimation Strategies

Data from 25 globally distributed GPS Rogue receivers tracking 17 GPS satellites from July 26 through July 31, 1992 were processed with the Jet Propulsion Laboratory's (JPL) GIPSY-OASIS II software. The data arc could not span more contiguous days due to anti-spoofing (AS) signal encryption on August 1-2. The JPL software and standard JPL GPS estimation strategies, incorporating Kalman filtering, are described in detail by Lichten [1990a, 1990b] and Blewitt [1993]. The estimation strategy for this study is described by Zumberge et al. [this volume]. GPS orbit states and three solar radiation parameters corresponding to three orthogonal flux components were estimated for each satellite. Earth orientation parameters were estimated by using the IERS Bulletin B time series as the source for nominal values. Earth rotation (UT1 – UTC) variations were estimated every 30 minutes starting from an initial fixed value by using first-order Markov process updates with a correlation time of 6 hours and a steady-state process noise 1-sigma constraint of 0.06 ms [Freedman et al., 1993, and this volume]. Station geocentric coordinates, except those for up to 8 fiducial (fixed) sites, were estimated as constants over the entire six day period, with ITRF 1991 coordinates [Boucher et al., 1992] used as a priori station locations. As observed by Lindqwister et al. [1992], changing fiducial sites in our estimation strategies induced only bias changes in our polar motion series, consistent with small rigid-body rotations of the reference frame. The pole position variability remained nearly invariant even in the absence of fiducial sites.

Two different estimation strategies for the satellite orbits were employed [see Zumberge et al., this volume]. The strategy which proved superior for polar motion estimation consisted of re-estimating each satellite state (position, velocity and solar radiation pressure coefficients) every 24 hours. The white noise restarts for each GPS satellite were staggered over a 5 hour interval around noon to maintain continuity in the UT1 series. We then tried a variety of estimation strategies for polar motion and found that unconstrained white noise estimates, every 30 minutes or less, gave consistent results in the prograde diurnal and semidiurnal bands discussed below. Typical postfit rms residuals were close to 6 mm for carrier phase and 35 cm for pseudo-range data.

The VLBI series used for comparison in this study was generated from data acquired by three different VLBI networks: "NASA R&D", "IRIS" and "NAVNET" (see Freedman et al. [1993], and Herring [this volume] for more details). UT1, polar motion, nutation corrections, and station troposphere parameters were estimated over 24 hour time spans, with UT1, polar motion and troposphere parameters modeled as random walks. Polar motion was estimated every 2 hours with 1.2 mas 1-sigma resets.

We have also compared our series to a model of tidally-induced polar motion variations. This model, referred to as the Herring tide model [Herring and Dong, 1993], is an empirically determined model based on eight years of VLBI observations. Because it is empirical rather than theoretical, this model may contain contributions from sources other than ocean tides, such as the atmosphere.

3. Results and Discussion

As is well known, the retrograde diurnal motion of the pole is degenerate with long period nutation, and estimates of sub-daily polar motion can be contaminated by nutation model errors (see Eubanks [1993] for a lucid discussion). This is a result of retrograde diurnal polar motion being nearly fixed in Earth-centered inertial coordinates. Similarly, in our estimation strategies, mismodeled orbital variations in the GPS constellation that appear slow in an inertial frame can be readily absorbed by the retrograde diurnal component of polar motion. To avoid ambiguities from these error sources, we removed the retrograde diurnal band in our comparisons with VLBI data sets. (The VLBI polar motion data already have very little power at retrograde diurnal periods, owing to the explicit estimation of nutation corrections in the VLBI estimation strategy.) Furthermore, since we found that non-periodic signatures in our GPS polar motion series varied significantly with estimation strategy (and observed similar behavior among preliminary VLBI solutions), we restricted comparisons in this study to the semidiurnal (both prograde and retrograde) and diurnal prograde bands.

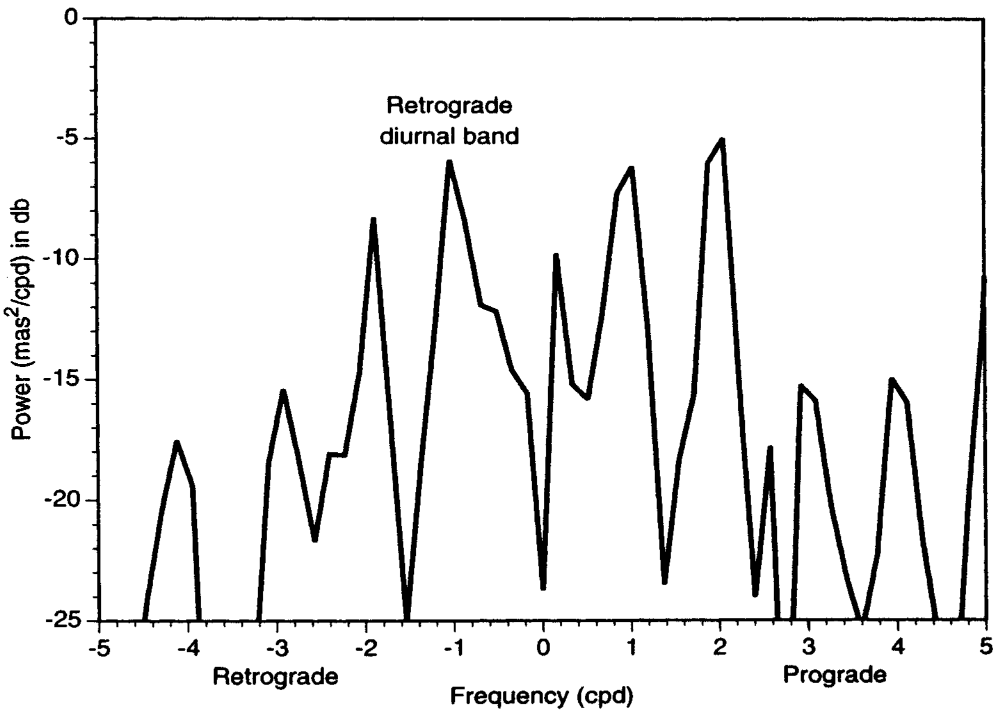

Fig. 1. GPS polar motion power spectral density.

In Figure 1, we show the power spectrum of the GPS polar motion series estimated every 30 minutes with loose (120 mas) constraints. As already mentioned, the GPS retrograde diurnal peak at –1 cycle/day (cpd) is contaminated by nutation and orbit mismodeling. The spectrum clearly shows peaks in the semidiurnal (±2 cpd) and prograde diurnal (+1 cpd) bands, with relatively little power elsewhere. The estimates are passed through a band reject filter so that only the +1 cpd and ±2 cpd bands, with bandwidths of 0.4 cpd, are retained. Identical filtering is applied to the VLBI series prior to comparison with the GPS data.

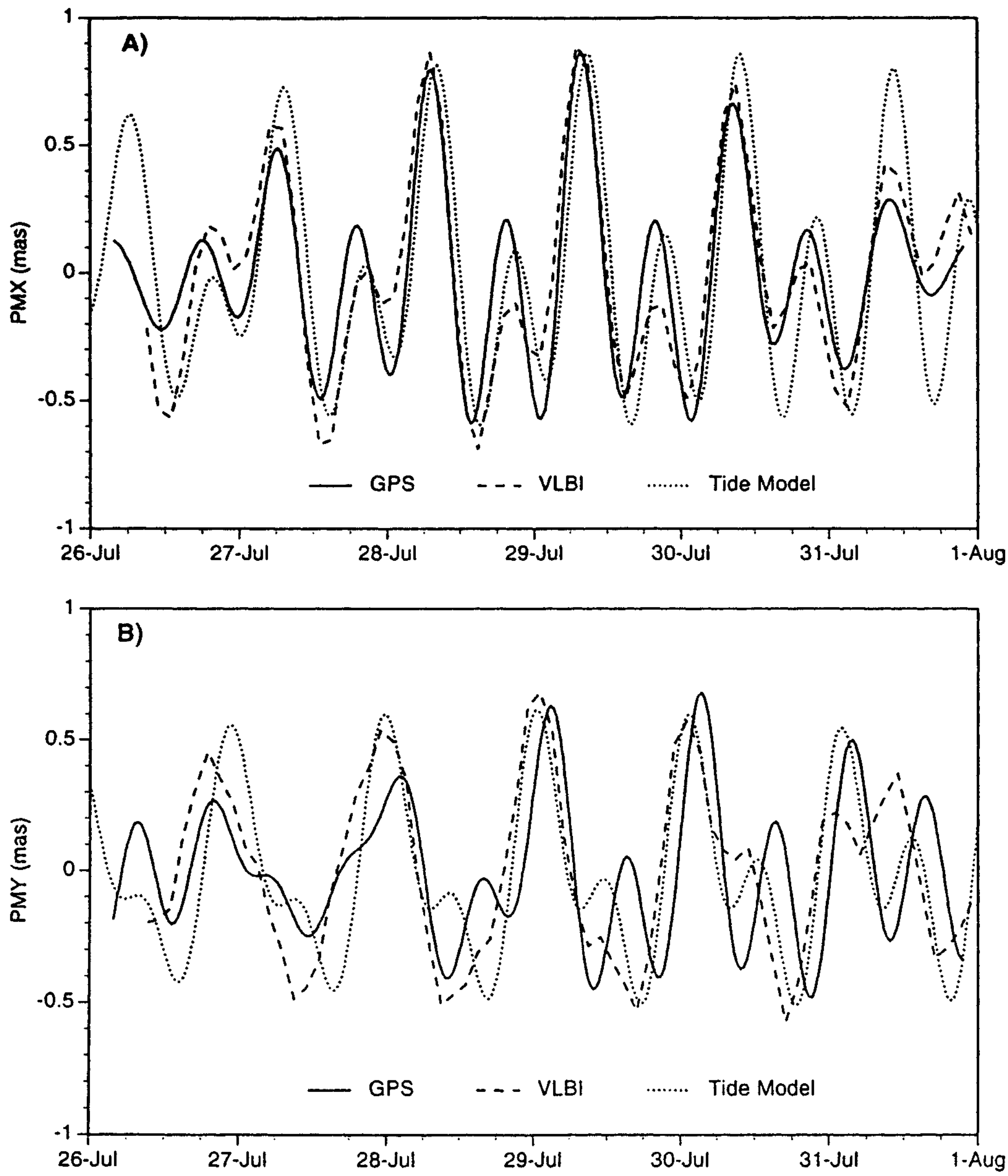

Fig. 2. (a) PMX semidiurnal and prograde diurnal bands for the GPS, VLBI, and Herring tide model time series. (b) Same as (a), but for PMY.

Figure 2 shows time-domain PMX and PMY plots of the diurnal (prograde) and semidiurnal (prograde and retrograde) bands of both the GPS and VLBI series, together with the Herring tide model. The rms difference between the VLBI and GPS series is 0.17 and 0.29 mas in PMX and PMY respectively. The overall level of agreement in both amplitude and phase is noteworthy, particularly in the x-component, and especially in light of the fact that the approximately 12-hour orbits of the GPS satellites might lead one to expect poor results at semidiurnal frequencies. Comparison statistics on rms differences and series cross-correlations are given in Table 1. The results in the table suggest that most of the GPS signal in Figure 2 can be attributed to ocean tides. The polar motion results presented here are very encouraging, and are consistent with similar good agreement between GPS and VLBI estimates of sub-daily UT1 variability [Freedman et al., 1993, and this volume]. We hope that this study will help in part to motivate future intensive VLBI campaigns to provide high-quality data for intercomparison with GPS.

Table 1. RMS Differences and Correlations

	x rms (mas)	y rms (mas)	x corr.	y corr.
VLBI - GPS	0.17	0.29	0.90	0.55
Tide Model - GPS	0.26	0.26	0.78	0.60
Tide Model - VLBI	0.25	0.26	0.80	0.77

ACKNOWLEDGMENTS. We are grateful to B. Haines, G. Hajj, L. Romans, J. Dickey, and R.. Muellerschoen for enlightening discussions. The work described in this paper was carried out in part by the Jet Propulsion Laboratory, California Institute of Technology, under contract with the National Aeronautics and Space Administration.

4. References

Boucher, C., Z. Altamimi, and L. Duhem, ITRF 91 and Its Associated Velocity Field, *IERS Technical Note 12*, Central Bureau of IERS, Observatoire de Paris, October 1992.

Blewitt, G., Advances in Global Positioning System Technology for Geodynamics Investigations: 1978-1992, in *Contributions of Space Geodesy to Geodynamics: Technology*, edited by D. E. Smith and D. L. Turcotte, pp. 195-213, Am. Geophys. Un., Washington, D.C., 1993.

Eubanks, T. M., Variations in the Orientation of the Earth, in *Contributions of Space Geodesy to Geodynamics: Earth Dynamics*, edited by D. E. Smith and D. L. Turcotte, pp. 1-54, Am. Geophys. Un., Washington, D.C., 1993.

Freedman, A. P., R. Ibanez-Meier, S. M. Lichten, J. O. Dickey, and T. A. Herring, Sub-Daily Earth Rotation During the EPOCH '92 Campaign, *Geophys. Res. Lett.*, submitted, 1993.

Gross, R. S., The Effect of Ocean Tides on the Earth's Rotation as Predicted by the Results of an Ocean Tide Model, *Geophys. Res. Lett.*, *20*, 293-296, 1993.

Herring, T. A., D. Dong, and R. W. King, Submilliarcsecond Determination of Pole Position using Global Positioning System Data, *Geophys. Res. Lett.*, *18*, 1893-1897, 1991.

Herring, T. A., and D. Dong, Measurement of Diurnal and Semidiurnal Rotation Variations and Tidal Parameters of the Earth, *J. Geophys. Res.*, submitted, 1993.

Lambeck, K. , *The Earth's Variable Rotation: Geophysical Causes and Consequences*, 449 pp., Cambridge University Press, New York, 1980.

Lichten, S. M., Toward GPS Orbit Accuracy of Tens of Centimeters, *Geophys. Res. Lett.*, *17*, 215-218, 1990a.

Lichten, S. M., Estimation and Filtering for High Precision GPS Positioning Applications, *Man. Geod.*, *15*, 159-176, 1990b.

Lindqwister, U. J., A. P. Freedman, and G. Blewitt, Daily Estimates of the Pole Position With the Global Positioning System, *Geophys. Res. Lett.*, *19*, 845-848, 1992.

McCarthy, D. D. (ed.), IERS Standards, *IERS Technical Note 3*, Central Bureau of IERS, Observatoire de Paris, 1992.

Seiler, U., Periodic Changes of the Angular Momentum Budget Due to the Tides of the World Ocean, *J. Geophys. Res.* , *96*, 10287-10300, 1991.

Wunsch, J., and U. Seiler, Theoretical Amplitudes and Phases of the Periodic Polar Motion Terms Caused by Ocean Tides, *Astron. Astrophys.*, *266*, 581-587, 1992.

DIURNAL AND SEMIDIURNAL VARIATIONS IN EARTH ORIENTATION DETERMINED FROM LAGEOS LASER RANGING AND GPS

MICHAEL M. WATKINS, RICHARD J. EANES,
AND JOHN G. SONNTAG
The University of Texas at Austin
Center for Space Research 60605
Austin, TX 78712 U.S.A.

ABSTRACT. Two analyses of high frequency Earth orientation were performed. In the first study, variations in universal time and polar motion due to ocean tides at nearly diurnal and nearly semidiurnal frequencies were determined from analysis of laser ranging to the Lageos satellite over the period from 1987 to 1992. The adjusted diurnal tides were K_1, S_1, P_1, O_1 and Q_1, while the semidiurnal tides were K_2, S_2, M_2, and N_2. In the second study, daily estimates of diurnal and semidiurnal UT1 variations were determined for a 49-day interval during the summer 1992 IGS campaign using doubly differenced GPS phase data. The results were then compared to the tidal variations observed from Lageos. For both studies, formulations were used that explicitly separated prograde and retrograde terms in the polar motion in order to eliminate aliasing from the singularity of retrograde wobble with long period orbit error and nutation. The results of the EOP variations at tidal frequencies obtained in this study agree well with those from the VLBI studies, typically at the 2–3 µs level in universal time and 30–50 µas level in polar motion. The results from the GPS analysis indicated independent daily determination of diurnal and semidiurnal variations of UT1 with accuracies at the 20–30 µs level.

1. Procedure

The solution for the tidal variations, described in detail in Watkins and Eanes [1993], was performed using the exact alias frequency of the tides in question as shown below, and adjusting a single amplitude and phase for each tidal frequency.

$$m = \sum_{s=1}^{N} [m_p^{s+} \exp(i\,\theta_s) + m_p^{s-} \exp(-i\,\theta_s)] = x - iy$$

where θ_s is the instantaneous phase of the particular tide in question, and m_p^{s+} and m_p^{s-} are complex prograde and retrograde subdiurnal polar motions modulated by the tidal frequency. We define the real and imaginary parts of m_p^{s+} and m_p^{s-} in terms of the usual x_p and y_p components as:

$$m_p^{s+} = x_p^{s+} - iy_p^{s+}$$

$$m_p^{s-} = x_p^{s-} - iy_p^{s-}$$

where x_p^{s+}, x_p^{s-}, y_p^{s+}, and y_p^{s-} were the real variables estimated using the SLR data. The singularity between retrograde nearly diurnal polar motion and the satellite orbit is avoided by removal (nonestimation) of the retrograde quantities for diurnal tides.

High frequency variations in UT were modeled as.

$$\delta \mathrm{UT1} = \sum_{s=1}^{N} [u^{sc} \cos(\theta_s) + u^{ss} \sin(\theta_s)]$$

where u^{sc} and u^{ss} were the real parameters estimated. For both wobble and UT1, the index s varied over 9 total ocean tide frequencies listed above. The preliminary solution described above was performed using 6 years of Lageos data spanning the period 1987–1992, the period of highest quality Lageos data. Approximately 400,000 two-minute normal points from 70 tracking sites formed this data set. The models used in the data analysis adhered generally to the IERS standards with several notable exceptions. The static geopotential model was JGM-1, and changes in the geopotential due to ocean tides were modelled using an enhanced model which included all terms, chosen from a degree and order 20 spherical harmonic expansion, with perturbations that exceeded 1 mm in either the radial, normal, or transverse components of the orbit, respectively. The nominal coefficients were from the model of Schwiderski [1980], with a subset of terms adjusted at the UTCSR from a multisatellite solution. The perturbations were determined from an analytic approach due to Casotto [1989]. The tidal amplitudes at frequencies not included in the original Schwiderski model were extrapolated using an assumption of admittances which vary linearly with frequency.

The solid tide model was expanded to include geopotential variations due to third degree terms, assuming the Love number, k_3 of 0.093 [Wahr, 1981]. Finally, the free core nutation period was changed from 460 to 430 days.

The reference frame was fixed to the CSR93L01 system of Eanes and Watkins [1993] which was determined from analyses of the entire Lageos mission, adjusting positions for over 110 sites and horizontal velocities for 47 sites. Sites with unadjusted velocities were assumed to have the velocities predicted by the NUVEL-1NNR model of Argus and Gordon [1991]. Site-dependent nuisance parameters such as range or clock biases were adjusted where necessary.

In the estimation process, mean orbital elements (excluding the nodal longitude), x_p, y_p, and UT1 were adjusted every 3 days, along with the diurnal and semidiurnal prograde and retrograde wobbles and UT1 variations. Using the above modelling and parametrization, the postfit range residual rms was 22 millimeters. The results of the adjustment are presented in the following table, along with conservative estimates of the uncertainties. The uncertainties included in the table are scaled formal uncertainties. The scale factor has been derived through comparison of Earth orientation and site positions with external solutions, such as those derived from VLBI, in order to make the formal uncertainties consistent with the inferred accuracy. Error analyses described in Watkins and Eanes [1993] support these uncertainties.

For the second study, the analysis of 49 days of GPS data, variations in universal time at exactly once and twice per sidereal day were adjusted for each day, along with initial conditions for each

Observed Tidal Variations in UT1 and Polar Motion

Tide	X_p^+, µas	Y_p^+, µas	X_p^-, µas	Y_p^-, µas	$UT1_c$, µs	$UT1_s$, µs
K_1	158±30	5±30	–	–	4.8±3	14.7±3
K_1^*	–	–	–	–	5.7±3	13.1±3
S_1	–51±30	–38±30	–	–	1.3±3	4.4±3
P_1	–25±30	19±30	–	–	–2.0±3	–1.1±3
Q_1	–41±20	–5±20	–	–	–4.0±2	–7.9±2
O_1	–131±20	9±20	–	–	–20.8±2	–17.3±2
O_1^*	–	–	–	–	–17.0±2	17.2±2
K_2	0±20	–23±20	20±30	–5±30	1.4±3	0.6±3
S_2	7±20	–81±20	–56±30	127±30	3.0±3	7.8±3
M_2	51±20	–114±20	25±20	195±20	–7.6±2	15.1±2
N_2	2±20	–21±20	2±20	18±20	–2.8±2	3.8±2

* corrected for 18.6-year sideband effects

GPS satellite, site dependent zenith delays every 2.5 hours, and phase ambiguities where necessary. The model for EOP variations was:

$$\delta \mathrm{UT1} = \sum_{n=1}^{N} [u^{nc} \cos(n\,\theta_g) + u^{ns} \sin(n\,\theta_g)]$$

where θ_g is the Greenwich sidereal time, and u^{nc} and u^{ns} are the real parameters estimated with the GPS data. The models used in the analysis generally adhered to the IERS Standards or appropriate International GPS Service recommendations, as above, with the exception of the use of the University of Texas TEG-2 gravity field.

In order to compare these results to the EOP variations at the tidal frequencies derived above, we reconstructed the equivalent variations at exactly once and twice per sidereal day from the sum of the 5 diurnal and 4 semidiurnal tides, respectively. These variations were then compared with the variations observed with GPS. The results, discussed in Sonntag and Watkins [1993], indicated 20 to 30 microsecond agreement between the two series, with slightly better agreement for the semidiurnal terms. The formal uncertainties on the daily GPS estimates were on the order of 15 to 20 microseconds.

2. References

Argus, D.F. and Gordon R.G. (1991) No-net-rotation model of current plate velocities incorporating plate motion model NUVEL-1, *Geophys. Res. Lett., 18*, 2039–2042.

Casotto, S. (1989) Ocean tide models for TOPEX precise orbit determination, Ph.D. dissertation, Univ. of Tex. at Austin.

Eanes, R.J. and Watkins, M.M. (1993) The Center for Space Research Solution CSR93L01, submitted to the International Earth Rotation Service.

Schwiderski, E.W. (1980) Ocean tides. Part I: Global ocean tidal equations, *Marine Geod.*, *3*, 161–216.

Sonntag, J.G. and Watkins, M.M. (1993) Measurement of subdiurnal variations in UT1 using the Global Positioning System, submitted to *Geophys. Res. Lett.*

Wahr, J.M. (1981) Body tides on an elliptical, rotating, and oceanless Earth, *Geophys. J. R. Astron. Soc.*, *64*, 677.

Watkins, M.M. and Eanes, R.J. (1993) Diurnal and semidiurnal variations in Earth orientation determined from Lageos laser ranging, submitted to *J. Geophys. Res.*

HIGH FREQUENCY FLUCTUATIONS OF POLAR MOTION DURING IGS'92 CAMPAIGN

Huang Chengli[1], Jing Wenjin[1], Liao Dechun[1], Zhu Wenyao[1], Wang Jiexian[2]
[1] *Shanghai Observatory, Chinese Academy of Sciences, 80 Nandan Road, Shanghai 200030, P.R.China*
[2] *Tongji University, Shanghai 200092, P.R.China*

ABSTRACT. During IGS'92 Campaign seven PM(Polar Motion) series provided by GPS Processing Centers are analysed in this paper. Some similar high frequency fluctuations in these PM series are detected by using spectral analyses, least square adjustment and F-test as follows: there are short periodic fluctuations of 27.0, 16.5, 13.4, 10.4 day in X direction; and of 10.0, 20.5, 15.8 day in Y direction. And there are similar systematic deviations derived from the comparison of each series with EOP(IERS) 92 C 04. The main cause of these systematic deviations is that the rotation between the reference frames of these series and ITRF91 exists. As for the reason, the coordinates of stations are not fixed (or partly fixed only) when solving X and Y with GPS data. The high frequency fluctuations of polar motion are explained to some extent by the excitation of atmospheric angular momentum.

1. Introduction

With the improvement of GPS observational precision and the increase of the observations, especially due to its convenience and cheapness, GPS has become an important technique for geodesy and geodynamics. GPS Coordinating Centre was set up by IERS at 1989. Some scientific results have been attained from the GIG'91 Campaign (Jan.22- Feb.13,1991) which is the first attempt at coordinating on an international basis and is the efforts of a number of participants in deploying a globally distributed network of GPS tracking stations[1]. IGS'92 Campaign completed its scientific task during Jun.21-Sep.22,1992. More than six hundred stations took part in EPOCH'92 (Jul.26-Aug.8) in which VLBI, SLR and LLR were also adopted in order to campare various techniques. Shanghai Observatory(China) attended this Campaign, and has processed global GPS data. There is now a total of eight GPS analysis centers contributing on a regular basis their EOP(Earth Orientation Parameters) and TRF(Terrestrial Reference Frame)results to the IERS Central Bureau and sub-Bureau for rapid service and predictions. During IGS'92 Campaign, some polar motion series accumulated by these centers are analysed and compared in this paper.

2. Materials and data used

Six polar motion series[2] discussed in this paper are obtained from IGS'92 Earth Orientation Bulletin (Table 1).

Table 1. Materials and data used

No.	Series	Interval
1	EOP(CSR) 92 P 01	27 Jun. - 5 Sep. 1992
2	EOP(CODE) 92 P 04	27 Jun. - 5 Sep. 1992
3	EOP(JPL) 92 P 02	27 Jun. - 5 Sep. 1992
4	EOP(SIO) 92 P 03	27 Jun. - 5 Sep. 1992
5	EOP(ESOC) 92 P 01	27 Jun. - 5 Sep. 1992
6*	EOP(GFZ) 92 P 01,02	27 Jun. - 5 Sep. 1992
7	EOP(SHA) 92 P 01	24 Jul. - 10 Aug. 1992
8**	EOP(COM.) 92 P 01	27 Jun. - 5 Sep. 1992

* Because EOP(GFZ) 92 P 01,02 is not in the same series, we do not use this series for the following analyses.

A new combined EOP(COM.) 92 P 01 series marked on " * *" at above table is obtained from series No.1,2,3,4,5 in order to compare with AAM instead of each series in section 5 this paper. For this series the weight is considered as follow:

$$p_{ij} = (e_i^{-2} / \sum_{i=1}^{5} e_i^{-2}) \cdot (u_{ij}^{-2} / \sum_{j=1}^{n_i} u_{ij}^{-2})$$

So

$$r_{cj} = \sum_{i=1}^{5} r_{ij} \cdot p_{ij} / \sum_{i=1}^{5} p_{ij}$$

where for ith series

- e_i estimated uncertainty (from Tab.4 cited in [3])
- r_{ij} value of X,Y at epoch j
- u_{ij} observational error
- r_{cj} combined value of X,Y at epoch j
- n_i number of observational data of the ith series

In 1992, a software SHAGAP was developed in Shanghai Observatory. Using this program, the global GPS observational data during EPOCH'92 were processed and many scientific results were obtained. The series of polar motion EOP(SHA) 92 P 01[4] is one result.

3. High frequency fluctuations and systematic deviations of polar motion

3.1. METHODS

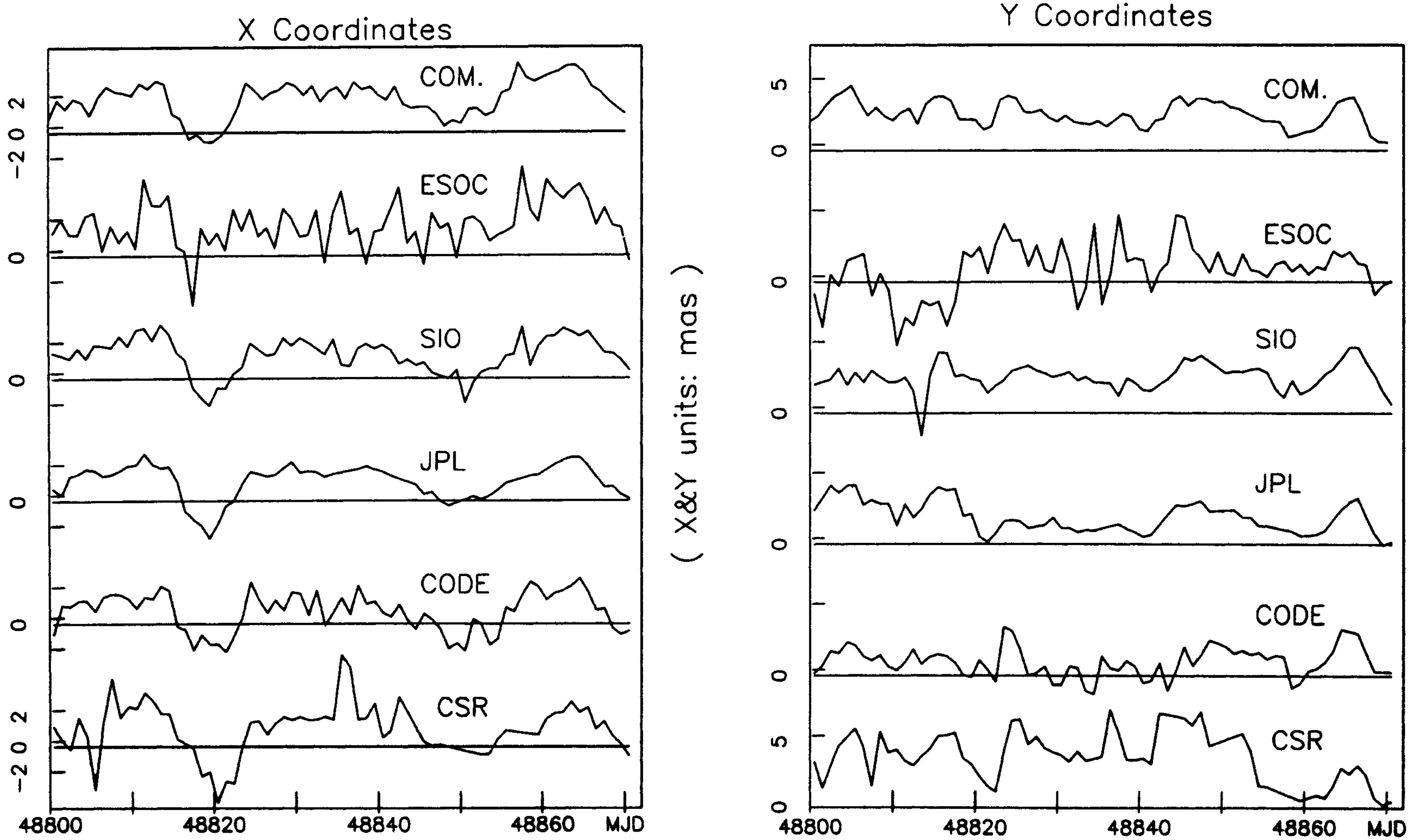

Fig.1 High-pass-filtered Polar Motion

Fig.2 Spectra of Polar Motion

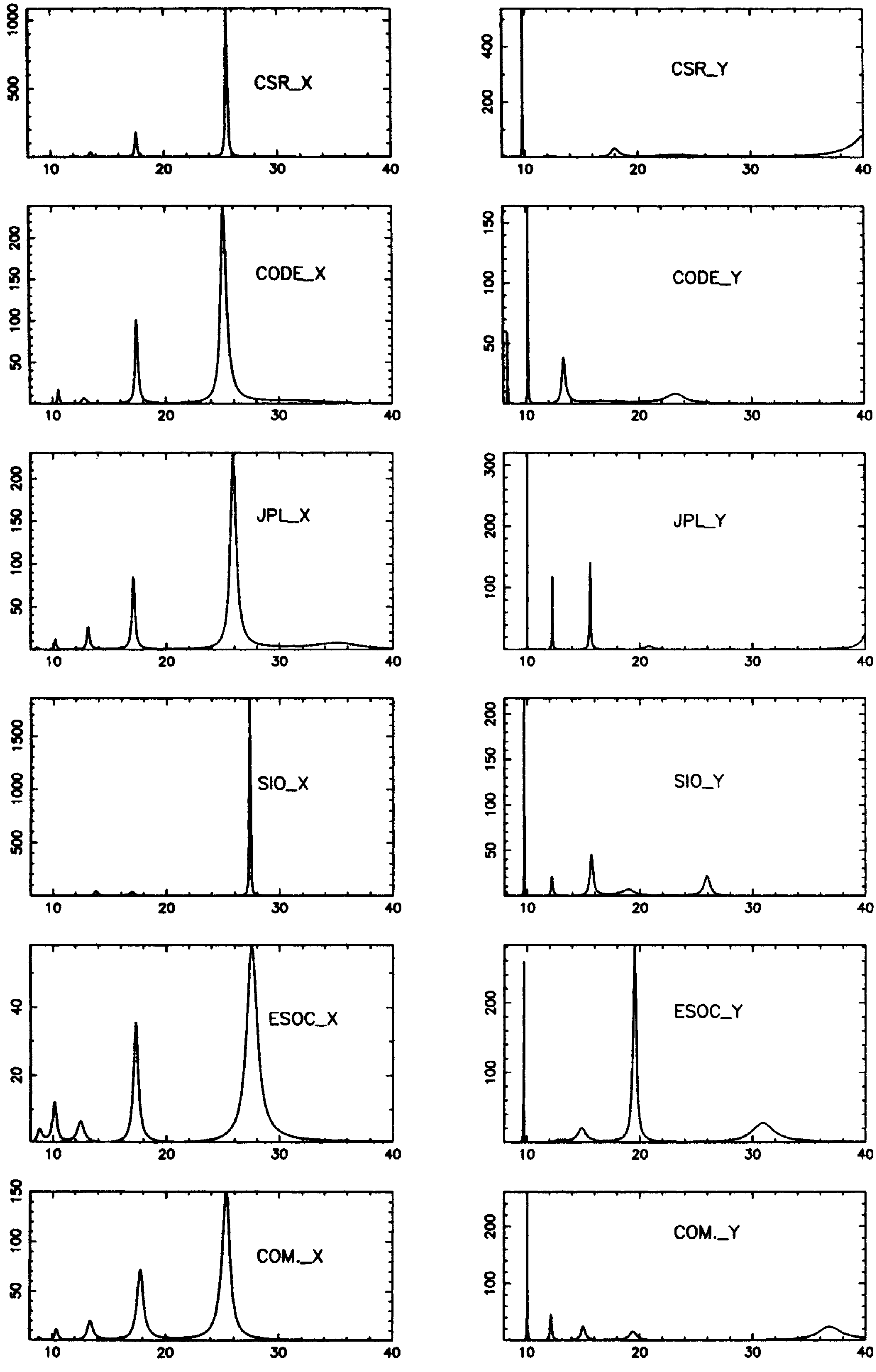

In order to analyse the high frequency variations of X and Y, it is necessary that the part of low frequency of above series should be removed and the parts of high frequency were reserved. Firstly, the part of low frequency (longer than 35 day) for EOP(IERS) 90 C 04 is obtained by using Vondrak low-pass-filter (filter factor ϵ =3.d-5). Secondly, the parts of high frequency (sub-35 day) of above series are derived after reduction of the part of low frequency of EOP(IERS) 90 C 04 from each series (Fig.1). Finally, the spectra of each series (Fig.2) were processed by maximum entropy method, and simultaneously, some periodic fluctuations P_i(day), amplitude Am_i(mas) and bias a(mas) of each series (Table 2) are fitted by least square adjustment and tested by F-test, where the bias a is the systematic deviation between each series and IERS. Because the interval of EOP(SHA) 92 P 01 is too short (18 day only) to make spectral analyses, the systematic deviation a is obtained only.

Table 2 : High frequency fluctuations and systematic deviations

	Series	a^* (mas)	P_1 (day)	Am_1 (mas)	P_2 (day)	Am_2 (mas)	P_3 (day)	Am_3 (mas)	P_4 (day)	Am_4 (mas)
X	CSR	1.2	27.5	1.3 ± 0.3	16.4	0.9 ± 0.3	13.0	0.8 ± 0.3	9.4	0.4 ± 0.2
	CODE	0.8	27.4	1.3 ± 0.2	16.8	0.7 ± 0.2	12.3	0.4 ± 0.2	10.2	0.3 ± 0.2
	JPL	1.3	28.7	1.2 ± 0.1	17.3	0.5 ± 0.1	12.5	0.5 ± 0.1	/	/
	SIO	1.5	27.2	1.3 ± 0.1	16.0	0.6 ± 0.1	12.8	0.5 ± 0.1	/	/
	ESOC	2.0	27.2	0.8 ± 0.2	16.5	0.8 ± 0.2	/	/	10.4	0.4 ± 0.2
	COM.	2.1	26.9	1.2 ± 0.2	16.2	0.7 ± 0.1	13.4	0.4 ± 0.1	10.4	0.3 ± 0.2
	SHA	5.7								
Y	CSR	3.8	10.0	1.1 ± 0.3	20.6	0.6 ± 0.3	22.8	0.6 ± 0.3		
	CODE	1.0	10.0	0.8 ± 0.2	20.5	0.5 ± 0.2	13.8	0.7 ± 0.2		
	JPL	2.1	9.9	0.9 ± 0.2	/	/	15.9	0.5 ± 0.2		
	SIO	2.7	9.7	0.9 ± 0.2	19.2	0.4 ± 0.2	15.8	0.5 ± 0.2		
	ESOC	0.9	9.9	0.6 ± 0.3	20.0	0.9 ± 0.3	/	/		
	COM.	2.7	10.0	0.7 ± 0.2	20.5	0.5 ± 0.2	15.3	0.4 ± 0.2		
	SHA	3.5								

* a is systematic deviation

3.2. RESULTS

As shown in Fig.2 and Table 2, similar fluctuations exist in the above series. In X direction, there are fluctuations with periods of 27.0, 16.5, 13.4 and 10.4 day and its maximum amplitude is 1.2mas (27.0day). In Y direction, there are of 10.0, 20.5, 15.8 day, the maximum amplitude is 0.9mas (10.0day). And there are also systematic deviations for combined series. They are about 2.1mas(X) and 2.7 mas(Y).

4. Systematic deviation and reference frame

In processing GPS data, in order to set up a reference frame, it is usual to fix the coordinates of some stations (theoretically more than three) with high precision as fiducial stations which are not considered in the adjustment. But there are two problems. One is that there are no or few stations satisfying the demand of precision of fiducial station[5] (i.e. better than 2 cm). For example, when GPS data observed during EPOCH'92 Campaign are processed in Shanghai Observatory, the criterion of fiducial station is the priori error of station coordinates smaller than 2 cm. As a result, there are about twenty coordinates (no height) fixed, and they are mostly coordinates of American sites. The other problem is that the selected fiducial stations may altogether locate at one region (i.e. American or European). That is to say, they may not be well-distributed globally. And even if there are a few fiducial stations meeting the need, from the point of view of the effect to fix reference frame, these stations are of little use. The direct result of these two problems is that the reference frame is not perfectly fixed as need (i.e. fixed at ITRF91), it has a rotation relative to ITRF, so the solved station coordinates and polar coordinates have a rotation too. As a result, the rotation induces the systematic deviations between various series and IERS as mentioned above.

For example, EOP(SHA) 92 P 01 is taken to study the relation between its reference frame (named TRF(SHA)) and ITRF91.

Among the twenty-four stations of TRF(SHA), just seven station coordinates are given directly in Table T-3 cited in [1] in which station coordinates in the ITRF91 are listed, and similarly, there are twenty-one stations are listed in ITRF92 Table T-3 cited in [6]. And noted that there is not rotation between ITRF91 and ITRF92[6], so ITRF92 are used to compare with TRF(SHA) instead of ITRF91. These twenty-one stations are well-distributed globally, they are: ALBH, ALGO, DRAO, DS10, DS60, FAIR, GRAZ, HART, JPL1, KOSG, MASP, METS, ONSA, PAMA, PIN1, SANT, STJO, TAIW, USUD, YAR1 and YELL.

$\vec{r}_{SHA}$ is the average position during EPOCH'92 at epoch MJD48835.5, so the coordinates of the twenty-one stations of ITRF92 should be transferred from epoch 1988.0 (MJD47160) to MJD48835.5. Here the plate motion is considered only and the equation for this transfer will be as follows:

$$\vec{r}_{IERS} = \vec{r'}_{IERS} + \vec{V} \cdot (t - t_0)$$

so observational equation is

$$\vec{r}_{SHA} = \vec{r}_{IERS} + \vec{t} + \Theta \vec{r}_{IERS} + \vec{e}$$

where

$$\vec{t} = (t_1, t_2, t_3)^T$$

$$\Theta = \begin{pmatrix} D & -R_3 & R_2 \\ R_3 & D & -R_1 \\ -R_2 & R_1 & D \end{pmatrix}$$

$$\vec{e} = \text{accidental error}$$

equation can also written as

$$\vec{L}_{63\times1} = \Theta_{63\times7} \vec{X}_{7\times1} + \vec{e}_{63\times1}$$

the least square solution will be

$$\vec{X} = (\Theta^T \vec{P} \Theta)^{-1} \Theta^T \vec{P} \vec{L}$$

where weight $\vec{P}$ are calculated from the precision of $\vec{r}_{SHA}$

$$p_i = \sigma_i^{-2} / \sum_{i=1}^{n} \sigma_i^{-2}$$

thus, the transfer parameters from TRF(SHA) to ITRF92 are solved:

$$t_1 = -18.4 \pm 1.7cm$$
$$t_2 = -13.3 \pm 1.8cm$$
$$t_3 = 2.7 \pm 1.5cm$$
$$D = (-1.08 \pm 0.22) * 10^{-8}$$
$$R_1 = 2.67 \pm 0.75mas$$
$$R_2 = 5.14 \pm 0.63mas$$
$$R_3 = 8.87 \pm 0.52mas$$

Using these transfer parameters, polar coordinates of EOP(SHA) 92 P 01 are transfered from TRF(SHA) to ITRF92, then, the average difference between them and the polar coordinates of IERS in eighteen days are obtained, they are about 4.92mas (X) and 3.46mas (Y). And they correspond to the solution derived in section 2 ($\Delta X_p = 5.7mas, \Delta Y_p = 3.5mas$).

These results have shown that the systematic deviations of series are mainly induced by the rotation of terrestrial reference frames of series which are not completely fixed on ITRF91(or ITRF92) during the processing of GPS data.

So, it is recommended that it should have more and globally well-distributed stations possibly fixed at ITRF91 or ITRF92 when X and Y are solved, or the rotation parameters be given and the influence of them be considered.

5. High frequency fluctuation in X and Y and the excitation of Atmospheric Angular Momentum(AAM)

The correlation between the variation of earth rotation and the atmospheric excitation has been studied by many authors[7], who explained well that the variations of Length Of Day(LOD) from irregular short periodic (40-50 day) to years are caused by the exchange of angular momentum between the Earth and atmosphere, and the sub-daily variation of LOD is due to ocean and tide[8][9]. But the explanation of variation of polar motion caused by atmosphere is not as good as that in LOD.

Taking EOP(COM.) 92 P 01 as an example, the correlation between the polar motion during IGS'92 Campaign and the AAM-induced polar motion is studied in this section.

The atmospheric data are from NMC(USA) and JMA(Japan). In NMC, the data of effective excitation functions $\vec{\chi}(\chi_1, \chi_2, \chi_3)$ cover whole year of 1992 and are given at two points each day. There are wind component in southern and northern hemisphere χ^{sw}, χ^{nw} (limit to 50 mb and to 100mb) and pressure component χ^{sp}, χ^{np} (No Inverter-Barometer(N.I.B.) and With I.B.(W.I.B.)). In JMA $\vec{\chi}$ data have four points each day during Jun.21-Sep.30,1992 and there are wind component χ^{w} and pressure component χ^{p}(N.I.B. and W.I.B.). Then effective excitation functions are expressed as the following formulum:

$$\vec{\chi} = \chi^{sw} + \chi^{nw} + \chi^{sp} + \chi^{np}$$

In this paper, wind component is limited to 50 mb, and pressure component(W.I.B.) is used. PM reduced by $\vec{\chi}$ is[10]:

$$\vec{m}(t) = e^{i\sigma t}[\vec{m}(0) - i\sigma(1 + \sigma/\Omega) \int_0^t \vec{\chi}(\tau)e^{-i\sigma\tau}d\tau] - (\sigma/\Omega)[\vec{\chi}(t) - e^{-i\sigma t}\vec{\chi}(0)]$$

where,$\sigma = 2\pi/435day^{-1}$, the mean rotation rate of the solid earth $\Omega = 7.29 \times 10^{-5}s^{-1}$

$\vec{m}(t)$ depends on initial value $\vec{m}(0)$, but $\vec{m}(t)$ will rapidly tend to be stable after calculation several times repeatedly. In this paper, $\vec{m}(0)$ is adopted from EOP(IERS) 90 C 04. And using one-degree integration approach:

$$\int_0^t f d\tau = \frac{1}{2}(f + f')t$$

In order to compare with the high frequency fluctuation of PM of EOP(COM.) 92 P 01, it is necessary to filter $\vec{m}$ induced from atmospheric data of NMC and JMA as done in section 3.1 for keeping the fluctuation of sub-35 day (ϵ = 3.d-5, Fig.3). In plot, the X and Y coordinates of EOP(COM.) 92 P 01 move downwards with a constant i.e. their systematic deviations:

$$X = x - 2.1mas$$

$$Y = y - 2.7mas$$

As shown in Fig.3, there are some similar trends between X and m1, but it does not happen between Y and m2.

In Table 3 the correlation coefficients between PM of EOP(COM.) 92 P 01 and AAM-induced PM of two meterological centers, JMA and NMC are given.

Table 3 Correlation between GPS-observed and AAM-induced Polar Motion

	NMC	JMA
X	0.70	0.81
Y	0.10	0.21

From Fig.3 and Table 3, some results can be obtained:
(1) The amplitudes of X and Y are larger than those of m1,m2, and the high frequency variation in X can be explained partly as the results of excitation of AAM;
(2) Due to the growth in number of observations and the improvement of the observational precision during EPOCH'92 (MJD48828-48840), X and Y are well consistent with m1,m2;
(3) The systematic deviations of X and Y are confirmed again.

6. Summary

Fig.3 Polar Motion of high frequency

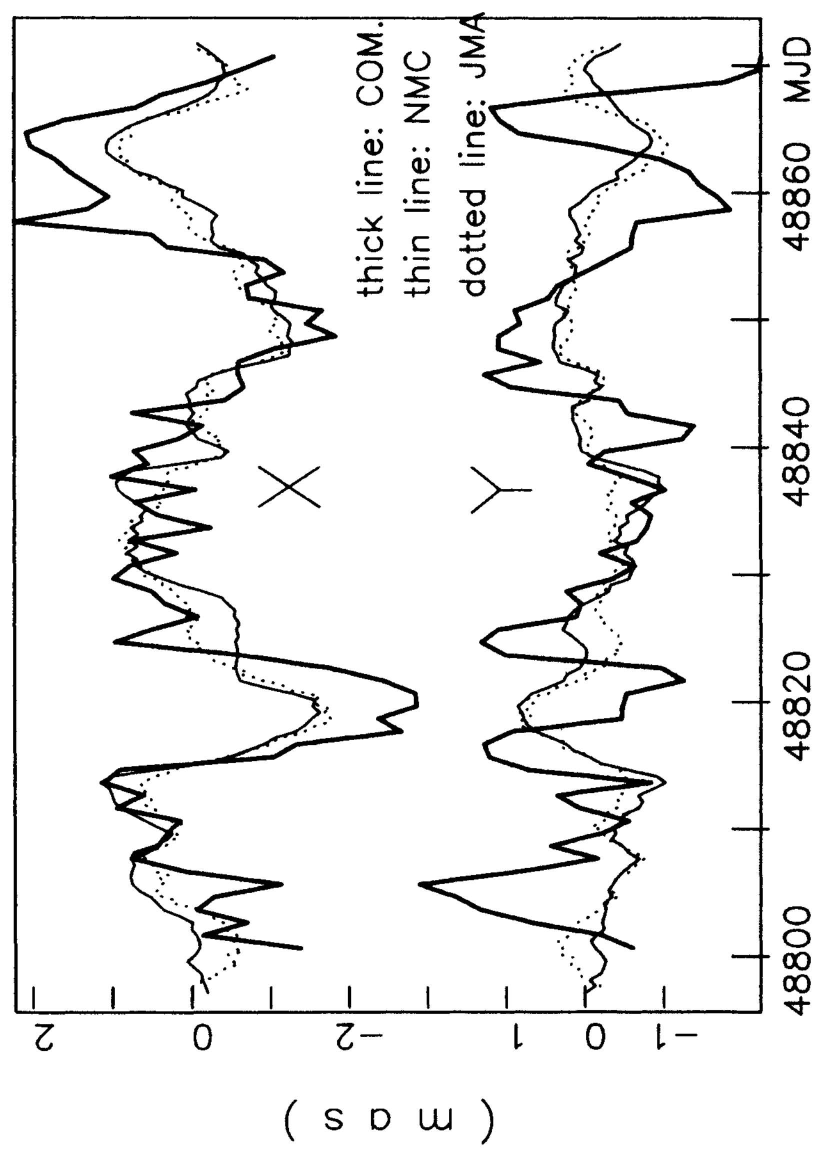

(1) There are similar high frequency fluctuations among the series of Polar Motion during IGS'92 Campaign. In X direction, the fluctuations have periods of 27.0, 16.5, 13.4, 10.4 day, of which the maximum amplitude is 1.2 mas(27.0day), and in Y direction, the fluctuations are of 10.0, 20.5, 15.8 day, of which maximum amplitude is 0.9 mas(10.0day).

(2) There are also systematic deviations with the same sign between above series and EOP(IERS)92 C 04. which values are about 2.1 mas in X and about 2.7 mas in Y while they are 5.7 mas in X and 3.5 mas in Y reduced in Shanghai Observatory. The main reason of these systematic deviations is that there is rotation between the reference frame of these series and ITRF91 (or ITRF92). The station coordinats are not fixed (or are partly fixed only) when solving X and Y with GPS data so the rotation exists.

(3) The high frequency fluctuations of polar motion can be explained partly as the result of excitation of atmospheric angular momentum. And the systematic deviations are confirmed again.

Acknowledgement We thank IERS for disturbuting the EOP series from six analysis centers, thanks to Dr. Richard S. Gross and David A. Salstein for their kindness to offer us the atmosphere data of JMA and NMC, and special thanks are due to Professor Dawei Zheng for his help on many details.

Reference

[1] 1991 IERS Annual Report, pp.IV-15, pp.II-38

[2] Huang,C.L., et al., 1993, High frequency fluctuations of X and Y polar coordinates derived from various GPS analysis centers, IAG General Meeting, Beijing, 1993

[3] IGS'92 Campaign: Comparisons of GPS, SLR and VLBI, Earth Orientation Determinations (Final Report), 1992

[4] Wang,J.X., 1993, The application of GPS to Geodesy and Geodynamics (in Chinese, Dr. thesis)

[5] IGS'92 Campaign: Comparisons of GPS, SLR and VLBI, Earth Orientation Determinations (First Report), 1992

[6] 1992 IERS Annual Report, pp.II-46, pp.II-38

[7] Lambeck,K., 1980, The Earth's variable rotation: geophysics causes and consequences, Cambridge University Press, pp.449

[8] Hide,I.N., et al. 1980, Nature, Lond., 286, pp.114-117

[9] Langley,R.B., et al. 1981, Nature, Lond., 294, pp.730-732

[10] Barnes,R.T.H., et al. 1983, Proc. R. Soc. Lond., A387, pp.57

SHORT - TERM POLAR MOTION AND UT1 VARIATIONS OBSERVED BY IGS

Jan Hefty*

The GPS polar motion and UT1 series available from the IGS'92 Campaign and its continuation are compared with the geodetic IERS combined series and the modelled atmospheric series based on effective atmospheric angular momentum functions. The short-term oscillations are obtained by removing the long periodical variations of the individual series. Polar motion variations in range from days to months are observed by GPS and significant correlation with both IERS combined and atmospheric series is found. The correlation of GPS UT1R with geodetic combined and atmospheric series reaches maximum for weekly variations. The monthly GPS UT1 oscillations exhibit discrepancies with other series.

ANALYZED DATA

The daily GPS series from 3 processing centers CODE, JPL and SIO are available for almost whole period 1992.5-1993.0. They give polar motion and the CODE series also UT1. The daily IERS series based on combination of VLBI, SLR and LLR observations [1] gives x, y, UT1 and covers the whole IGS Campaign. For the UT comparisons we use also the daily VLBI series from Westford - Wettzell baseline. The complete Yoder et. al [2] model for periodic variations due to zonal tides is removed from all UT1 series. In Table 1 we summarize the data used in further comparison studies.

The EOP variations caused by meteorological excitations have been obtained from time series of atmospheric angular momentum χ-functions at 12-hour intervals computed from pressure and wind fields generated at the Japan Meteorological Agency [3]. The motions of Celestial Ephemeris Pole $\mathbf{p}(t)=p_1+ip_2$ induced by atmospheric fluctuations $\chi=\chi_1+i\chi_2$ are computed from linearized Liouville equation [4]

* Observatory of the Slovak Technical University, Department of Theoretical Geodesy, Radlinskeho 11, 81368 Bratislava, Slovak Republic

$$\mathbf{p}(t)+\frac{i}{\sigma_0}\frac{d\mathbf{p}(t)}{dt}=\boldsymbol{\chi}(t) \ , \tag{1}$$

where σ_0 is frequency of Chandler wobble. Let $\mathbf{P}(\omega)$ denote the Fourier transform of $\mathbf{p}(t)$ and $\mathbf{X}(\omega)$ the Fourier transform of $\boldsymbol{\chi}(t)$. Then eq.(1) transformed into frequency domain becomes

$$\mathbf{P}(\omega)=\frac{\sigma}{\sigma-\omega}\mathbf{X}(\omega) \ . \tag{2}$$

The procedure used to compute the AAM induced polar motion consist in Fast Fourier Transform (FFT) of $\boldsymbol{\chi}(t)$, multiplication with transfer function (2) and recovering $\mathbf{p}(t)$ by inverse FFT. Two alternatives of $\mathbf{p}(t)$ from χ-functions have been obtained according to the pressure term used - with and without the inverted barometer (IB) approximation.

The atmosphere induced UT is inferred from χ_3 component (wind term and pressure term with IB) by numerical integration.

Table 1
Analyzed series

Technique	Series	Period	EOP
GPS	EOP(CODE) 92 P 04	1992 Jun. 19 - 1993 Jan. 26	x,y,UT1
GPS	EOP(JPL) 92 P 02 EOP(JPL) 92 P 03	1992 Jul. 17 - 1992 Nov. 14 1992 Nov. 15 - 1993 Jan. 16	x,y
GPS	EOP(SIO) 92 P 03	1992 Jun. 7 - 1993 Nov. 12	x,y
Combined	EOP(IERS) 90 C 04	1992 Jan. 1 - 1993 Jan. 31	x,y,UT1
VLBI	EOP(NOAA) 92 R 02	1992 Jan. 1 - 1992 Dec. 31	UT1
AAM	AAM(JMA) 92 * 01	1992 Jan. 1 - 1992 Dec. 31	χ_1,χ_2,χ_3 -> x,y,UT

HIGH FREQUENCY VARIATIONS OF EARTH ROTATION PARAMETERS

The short-term oscillations of x, y and UT1R as well as of the AAM induced series are obtained by removing the long periodical variations of the individual series. Three types of residuals according to degree of Vondrak [5] smoothing are analysed. Fig.1 shows transfer functions of the used filters. The cut-off periods 9 days (filter I), 30 days (filter II) and 90 days (filter III) correspond roughly to daily, weekly and monthly variations of residuals.

Fig.2 and Fig.3 show the high pass filtered monthly and daily oscillations of the three GPS polar motion solutions and the AAM induced polar motion based on JMA pressure term without IB approximation for the period 1992.5-1993.0. Mean formal uncertainties of GPS series are 0.11 mas for CODE, 0.18 mas for JPL and 0.20 mas for SIO. The upper graphs show that the individual GPS series follow the same pattern which is sporadically identical with AAM variations. The daily variations in lower graphs have significantly larger scatter for CODE and SIO series when compared with JPL polar motion and significantly exceed the formal uncertainties.

Fig.4 shows the UT1R residuals of GPS CODE series, combined IERS series as well as the UT AAM series. The monthly GPS variations differ from IERS and AAM in the beginning of IGS campaign, the daily variations of the three series have similar behaviour.

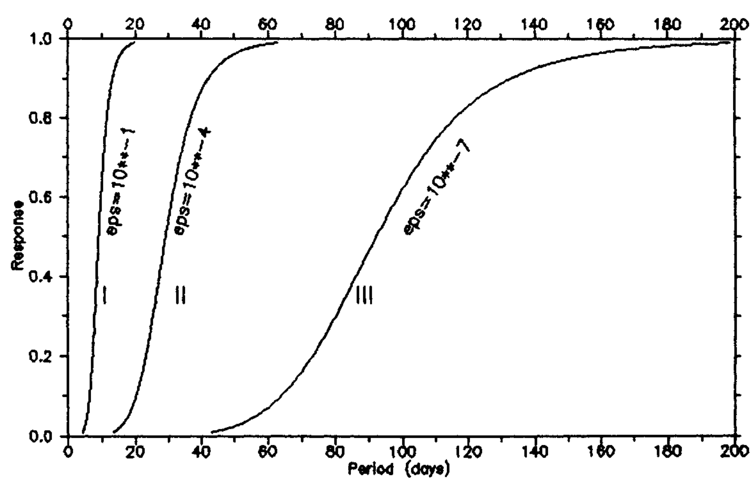

Fig.1 Transfer functions of Vondrak smoothing

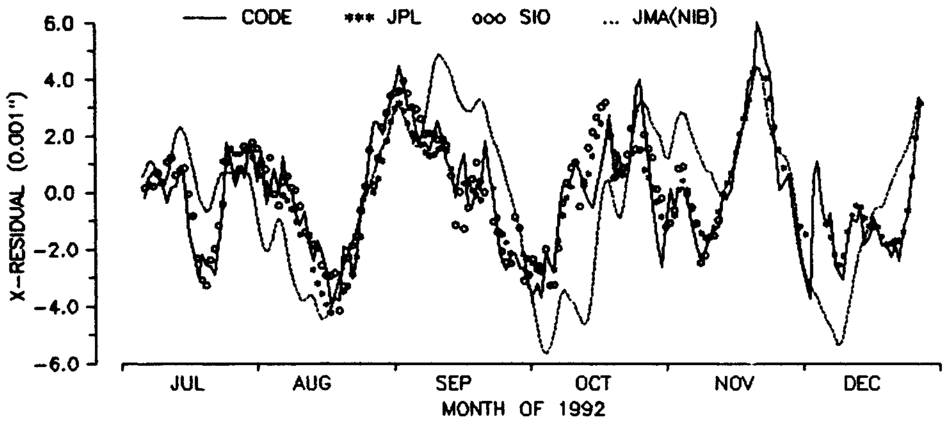

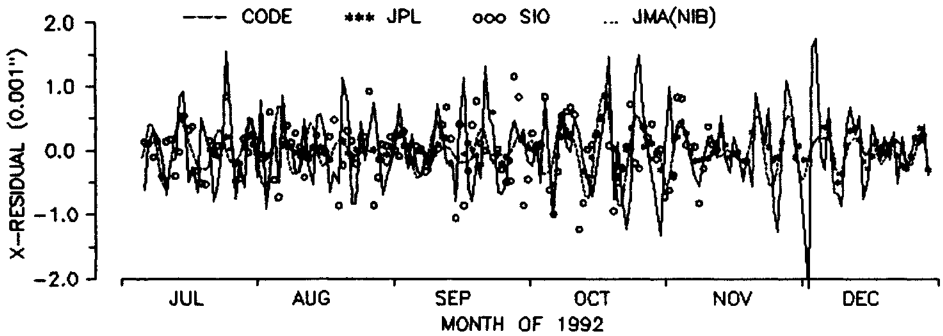

Fig.2 x-coordinate residuals from smoothing III (upper graph) and from smoothing I (lower graph)

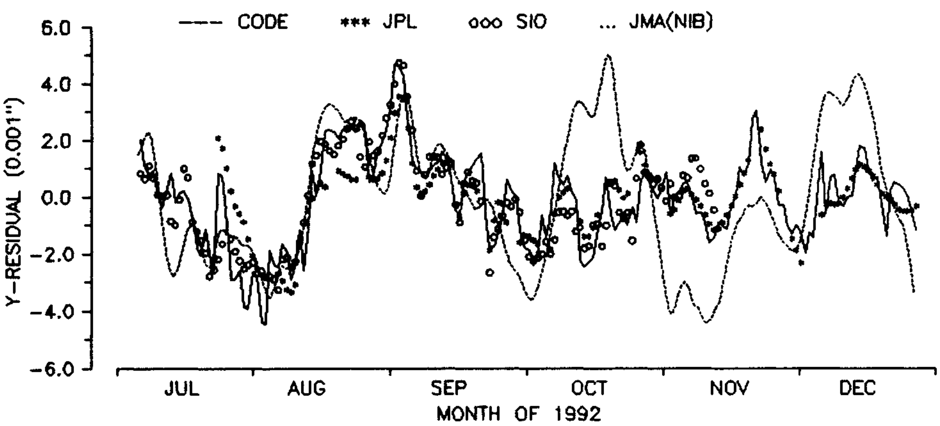

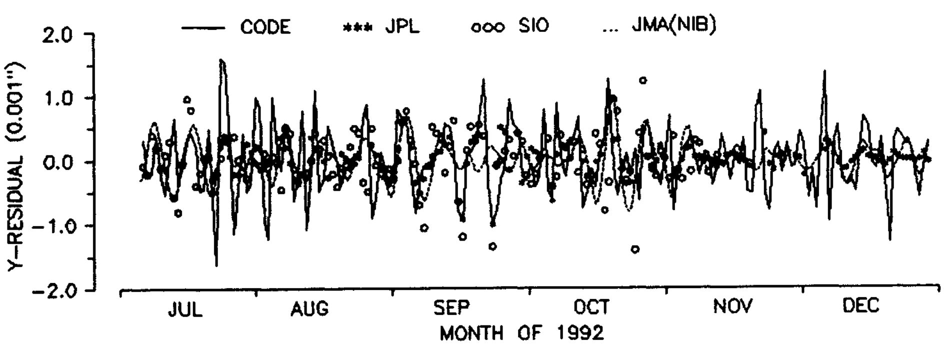

Fig.3 y-coordinate residuals from smoothing III (upper graph) and from smoothing I (lower graph)

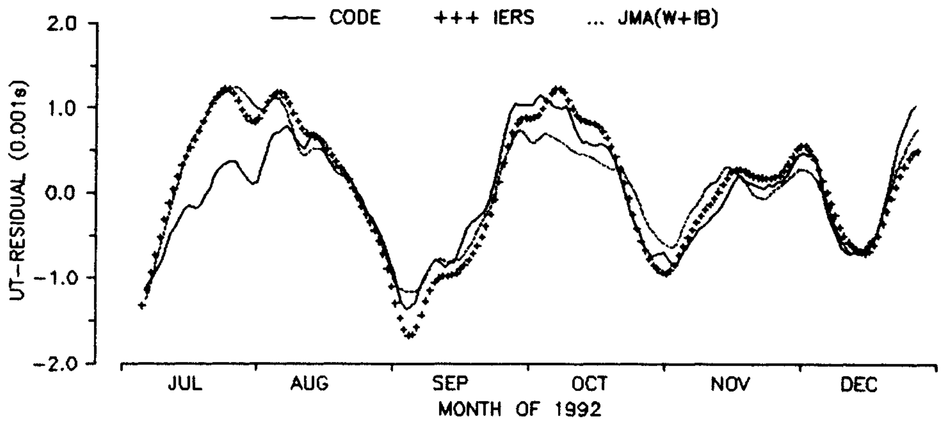

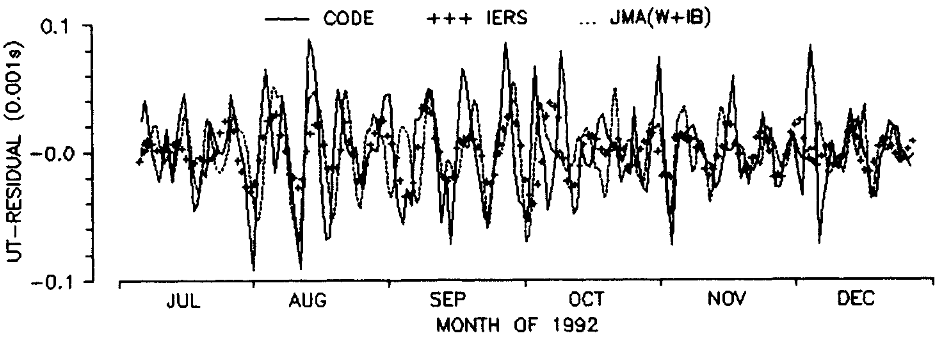

Fig.4 UT1R residuals from smoothing III (upper graph) and from smoothing I (lower graph)

DIFFERENCES OF EOP SERIES - UNCERTAINTIES AND CORRELATIONS

The residuals of GPS solutions, combined series and AAM series (with IB and without IB) representing the monthly, weekly and daily variations are compared pair by pair. Table 2 gives the estimates of rms differences after removing bias. As we are analyzing the residuals, bias of their differences is close to zero. For pairs of GPS series also the corresponding formal uncertainties based on information from processing centers are shown. Fig.5 is a plot of rms differences between GPS solutions. Displayed are also rms differences between JPL GPS series and IRES combined solution - two series with the best mutual agreement.

Table 3 summarizes correlation coefficients for pairs considered in Table 2. Correlation exceeding critical values at 0.01 significance level is found for each pair of geodetic series except the difference between SIO and CODE daily variations (0.05 level). Correlation coefficients between GPS series and between JPL and combined series are shown in Fig.6.

Table 2
Rms differences of various pole coordinates series (units 0.001"). Unc. means the formal uncertainty of GPS series differences.

Series	Filter	JPL	IERS	SIO	AAM (NIB)	AAM (IB)
CODE	III x	0.89	0.95	1.09	2.23	1.75
	y	1.00	0.85	0.98	2.14	1.53
	II x	0.70	0.80	0.95	1.03	1.11
	y	0.71	0.79	0.91	1.07	0.95
	I x	0.48	0.59	0.70	0.57	0.58
	y	0.51	0.56	0.66	0.61	0.58
	Unc.	0.20	-	0.23	-	-
AAM(IB)	III x	1.40	1.42	1.48		
	y	1.07	1.23	1.48		
	II x	0.67	0.80	0.75		
	y	0.63	0.53	0.74		
	I x	0.17	0.14	0.39		
	y	0.23	0.13	0.42		
	Unc.	-	-	-		
AAM(NIB)	III x	2.04	1.98	2.26		
	y	2.18	1.98	2.07		
	II x	0.71	0.75	0.82		
	y	0.74	0.72	0.89		
	I x	0.25	0.21	0.46		
	y	0.31	0.23	0.42		
	Unc.	-	-	-		
SIO	III x	0.89	0.77			
	y	0.87	0.71			
	II x	0.58	0.64			
	y	0.43	0.53			
	I x	0.35	0.42			
	y	0.31	0.38			
	Unc.	0.26	-			
IERS	III x	0.82				
	y	0.69				
	II x	0.48				
	y	0.39				
	I x	0.18				
	y	0.23				
	Unc.	-				

Table 3
Correlation coefficients for x and y pole coordinates
Crit. means the critical value for α=0.01.

Series	Filter	JPL	IERS	SIO	AAM (NIB)	AAM (IB)
CODE	III x	0.97	0.89	0.82	0.57	0.54
	y	0.81	0.86	0.84	0.48	0.37
	II x	0.78	0.74	0.55	0.54	0.38
	y	0.68	0.73	0.53	0.40	0.40
	I x	0.44	0.36	0.15	0.42	0.48
	y	0.37	0.30	0.20	0.16	0.18
	Crit.	0.22	0.18	0.21	0.22	0.22
AAM(IB)	III x	0.65	0.65	0.60		
	y	0.51	0.45	0.44		
	II x	0.43	0.51	0.60		
	y	0.45	0.60	0.22		
	I x	0.34	0.61	0.35		
	y	0.33	0.49	0.34		
	Crit.	0.22	0.18	0.21		
AAM(NIB)	III x	0.65	0.66	0.50		
	y	0.51	0.55	0.49		
	II x	0.57	0.65	0.55		
	y	0.61	0.63	0.47		
	I x	0.49	0.68	0.28		
	y	0.34	0.61	0.34		
	Crit.	0.22	0.18	0.21		
SIO	III x	0.91	0.91			
	y	0.89	0.91			
	II x	0.71	0.73			
	y	0.84	0.72			
	I x	0.49	0.31			
	y	0.64	0.39			
	Crit.	0.26	0.21			
IERS	III x	0.91				
	y	0.88				
	II x	0.85				
	y	0.83				
	I x	0.50				
	y	0.43				
	Crit.	0.18				

Standard deviations and correlations for pairs of UT1R series - GPS, combined, daily VLBI and AAM are given in Table 4 and Table 5. The statistics obtained for weekly variations and daily variations have similar value for all compared series. This proves that GPS observed variations are reliable for periods shorter than one month.

Table 4
Rms differences between GPS, daily VLBI, IERS combined and atmospheric UT series (units 0.001 ms)

Series	Filter	IERS	VLBI	AAM
CODE	III	0.507	0.527	0.522
	II	0.103	0.096	0.093
	I	0.034	0.048	0.037
AAM	III	0.229	0.298	
	II	0.108	0.093	
	I	0.021	0.041	
VLBI	III	0.261		
	II	0.093		
	I	0.036		

Table 5
Correlation coefficients between GPS, daily VLBI, IERS combined and atmospheric UT series.
Crit. means the critical value at significance level α=0.01.

Series	Filter	IERS	VLBI	AAM
CODE	III	0.77	0.71	0.71
	II	0.80	0.80	0.79
	I	0.39	0.17	0.37
	Crit.	0.18	0.24	0.18
AAM	III	0.96	0.91	
	II	0.78	0.80	
	I	0.50	0.14	
	Crit.	0.18	0.24	
VLBI	III	0.94		
	II	0.84		
	I	0.23		
	Crit.	0.24		

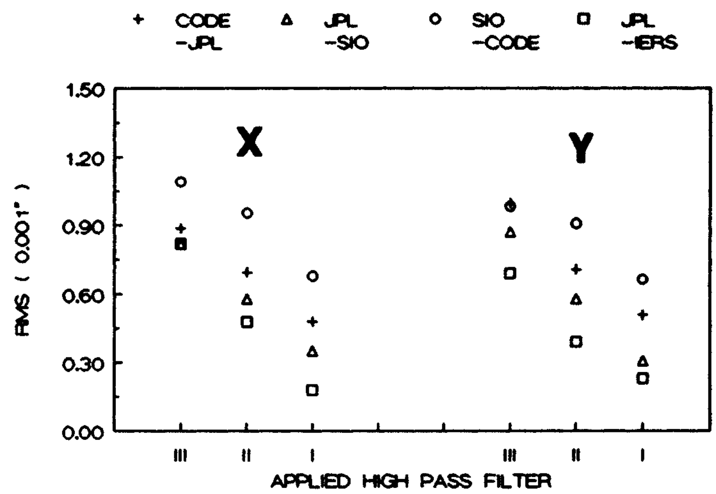

Fig.5 Rms differences of polar motion series

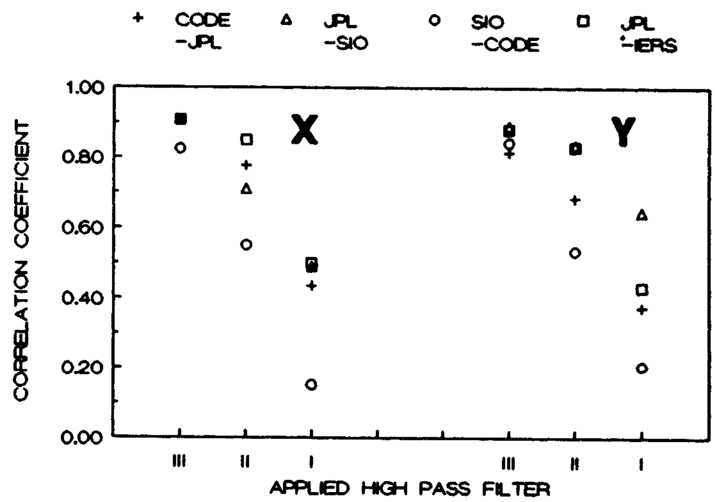

Fig.6 Correlation coefficients between polar motion series

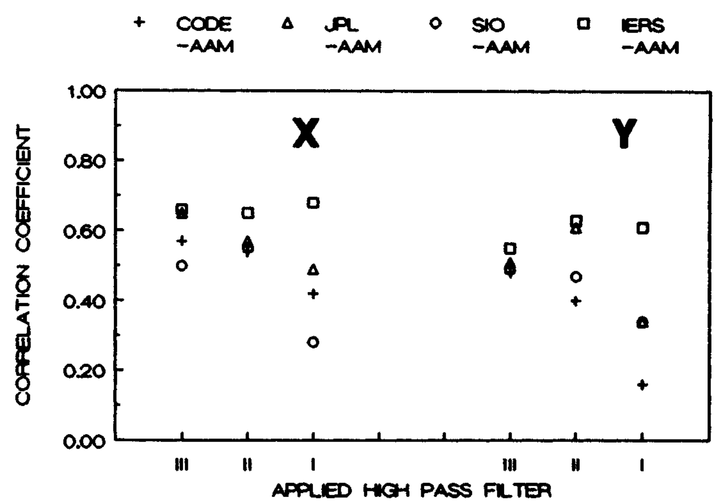

Fig.7 Correlation coefficients between geodetic and AAM polar motion

CONCLUSIONS

The short-term polar motion variations in range from days to months observed by GPS are at 0.5 - 5 mas level according to used high pass filtering and significantly exceed the formal uncertainties. Rms differences for pairs of geodetic series (GPS and combined) are bellow 1 mas and gradually decrease towards high frequencies. Correlations between geodetic series is also decreasing but remains significant for daily variations except the SIO-CODE pair. Significant correlation 0.4 - 0.6 results from comparison of GPS polar motion series with both IB and without IB approximation atmospheric models.

Monthly, weekly and daily non-tidal UT variations are well observed by GPS CODE series. The monthly GPS oscillations exhibit the most significant discrepancies with other geodetic series, especially in the beginning of IGS campaign. The atmospheric driving of short-term Earth's rotation is recognized by GPS at the time scales from days to months.

ACKNOWLEDGEMENT

Author thanks N. Essaifi from IERS/CB for providing the GPS EOP series and I. Naito and Y. Tamura from NAO Mizusawa for granting the atmospheric angular momentum data.

REFERENCES

[1] IERS,"1991 IERS Annual Report",Central Bureau of IERS, Observatoire de Paris, 1992

[2] Yoder,C.F.,Williams,J.G.,Parke,M.E.,"Tidal Variations of Earth Rotation", J.Geophys.Res.,86,881-891, 1981.

[3] Ozaki,T., Kuma,K., Kikuchi,N., Naito,I., "Effective Atmospheric Angular Momentum Functions Computed from the Japan Meteorological Agency Data", Priv. Comm., 1993.

[4] Gross R.S., Lindqwister U.,"Comparison of GIG'92 Polar Motion Results with Atmospheric Angular Momentum CHI Functions", JPL Geodesy and Geophysics Preprint No.222, 1992.

[5] Vondrak,J.,"A Contribution to the Problem of Smoothing Observational Data", Bull. Astron. Inst. Czechosl. 20, 349-355, 1969.

SHORT PERIODIC OSCILLATIONS IN GPS POLE COORDINATES DATA

W. KOSEK
Space Research Centre, PAS
ul. Bartycka 18a, 00–716 Warsaw
Poland

ABSTRACT. The 3.5 day oscillation has been found in GPS x, y pole coordinates data determined by different processing centers in July 1992 - March 1993 using the Band Pass Filter Spectral Analysis and the Ormsby band pass filter.

1. Introduction

Earth rotation parameters have recently been obtained from networks observing Global Positioning System (GPS) satellites (Herring et al., 1991; Lichten et al., 1992). Analyses of GPS data of pole positions indicate about 0.5 mas agreement with the VLBI estimates (Lindqwister et al., 1992). The GPS results are obtained usually from one day observations of 16-18 satellites in a network of different number of stations ranging from 10 to about 30. The analysis of 17-60 days common time intervals between the pairs of series of x, y pole coordinates during the SEARCH 92' Campaign found no significant correlation between them (IGS'92 Campaign third report, 1992).

2. Analysis of GPS pole coordinates data

The pole coordinates series from the following centers and data intervals have been used in order to analyze the short periodic oscillations from 2 to about 15 days in pole coordinates data:

BERNE (University of Berne (AIUB)) 48792.5-49042.5
EMR (Energy Mines and Resources, Canada) 48838.5-49038.5
ESOC (European Space Operations Center) 48794.5-49038.5
GFZ (GeoForschungsZentrum, Potsdam) 48795.0-48925.5
JPL (Jet Propulsion Laboratory, Pasadena) 48794.5-49024.5
SCRIPPS (Scripps Institute (UCSD)) 48780.5-49038.5
UTX (University of Texas at Austin) 48794.5-48870.5
COMBIN (U.S. Naval Observatory, Washington D.C.) 48781.0-49042.0

The sampling interval of all these data is equal to 1 day except the GFZ solution in which there is a 1.5 day gap in the middle of data and some gaps noticed in the UTX, EMR and ESOC solutions. All the data were interpolated at 1 day time intervals using the first order linear interpolation.

Next, long periodic and the Chandler and annual oscillations were removed by computation of the second difference by the following formula:

$$\Delta^2 x_{j,k} = x_{j+2,k} - 2x_{j+1,k} + x_{j,k}, \tag{1}$$

where $x_{j,k}$ are data points of kth solution interpolated at the moments of $t_m = 48792.5 + \Delta t(m-1)$, Δt is the sampling interval.

This second difference is the high pass filter enlarges amplitudes of high frequency oscillations ranging from $\frac{1}{2\pi\Delta t}$ to $\frac{1}{2\Delta t}$. The band pass filter spectral analysis (BPFSA) (Kosek, 1991) has been applied in order to compute spectrum estimations by the following formula:

$$\hat{S}(\lambda_o) = \frac{1}{N(k) - 2L + 1} \sum_{j=1}^{N(k)-2L+1} [\sum_{l=-L}^{L} \Delta^2 x_{j+l,k} h_l(\lambda_o)]^2 \tag{2}$$

where $\frac{\Delta t}{15days} < \lambda_o < \frac{\Delta t}{2days}$, $N(k)$ is the number of interpolated data of kth solution, L is the length of the Ormsby band pass filter with the impulse response given by the following formula:

$$h_l(\lambda_o) = \frac{2sin(\pi l \lambda)cos(2\pi\lambda_o)sin(2\pi\beta)}{\lambda(\pi l)^2} \tag{3}$$

where λ is the transition band, β is the half of the sum of the pass band and the transition band, $\lambda_o = \frac{\Delta t}{T_o}$ is the normalized frequency, for which the oscillation with period T_o is computed.

The spectra $\hat{S}(\lambda_o)$ have been computed assuming $\lambda = 0.03$, $\beta = 0.03$ and $L = 50$. In these spectra (Fig. 1) two main peaks correspond to about 2.4 and 3.5 days oscillations except the spectrum of the COMBIN solution where the power corresponds to the lower frequency oscillations. The COMBIN solution does not represent the solutions determined by different processing centers in the case of short periodic oscillations. The weighted mean which enables to transfer all frequency information to the output has been computed by the following formula:

$$\hat{x}_m = \frac{\sum_{k=1}^{M} x_{j,k} p_{j,k}}{\sum_{k=1}^{M} p_{j,k}} \quad for \quad j = 1, 2, ..., N(k) \tag{4}$$

where $M = 7$ is the number of solutions and the weight of such interpolated point is assumed:

$$p_{j,k} = \frac{t_{i+1,k} - t_{i,k}}{\hat{\sigma}^2_{x_{i,k}}(t_{i+1,k} - t_m) + \hat{\sigma}^2_{x_{i+1,k}}(t_m - t_{i,k})} \tag{5}$$

where $t_{i,k}$ is the MJD of data $x_{i,k}$.

Usually all these data are equidistant, so $t_m = t_{i,k}$ and the weight of the point is expressed by $p_{j,k} = 1/\hat{\sigma}^2_{x_{i,k}}$ where $\hat{\sigma}^2_{x_{i,k}}$ is the RMS of the ith point in the kth solution.

The spectrum of the second difference of such weighted data has the peaks corresponding to around 2.5 and 3.5-4.0 day oscillations and looks very similar to the spectra of solutions from different processing centers (Fig. 1).

3. Model data analysis

The spectra of x, y pole coordinate second differences computed by the BPFSA do not have the confidence intervals for their values and its difficult to say whether detected peaks are real or not. In order to check the reality of detected peaks in x, y pole coordinates the BPFSA spectra have been also computed for the model data of 260 data points sampled at 1 day intervals. This model consists of the Chandler oscillation with the amplitude of 200 mas, the annual oscillation with the amplitude of 100 mas and the white noise with standard deviation of 1 mas. The spectra computed for the second difference of such 4 different model data increase their power almost monotonically toward higher frequencies and show no significant power around 3.5 day oscillation (Fig. 2).

4. The 3.5 days oscillation determined by the Ormsby filter

Next, the Ormsby band pass filter has been applied in order to compute the 3.5 day oscillation in the second difference of pole coordinates. The parameters of the Ormsby band pass filter are the same as for the spectrum computation except the filter length, which was reduced to $L = 30$. The amplitude of the output was multiplied by the factor of $-(\frac{3.5 days}{2\pi\Delta t})^2$ in order to convert it to the amplitude of data. In the case of x, y pole coordinates of BERNE. SCRIPPS, and JPL there is some agreement in phase and in some sense in the amplitude of 3.5 day oscillations (Fig. 3). This amplitude is variable and of the order of 0.3 mas.

5. Conclusions

The COMBIN solution computed from 7 GPS pole coordinates does not contain information about short periodic oscillations from 2 to about 15 days.

The Ormsby band pass filter spectra of second differences of GPS x, y pole coordinates have the common peaks corresponding to 3.5 and about 2.5 days oscillations. There is some phase and amplitude agreement of the 3.5 days oscillations in the case of BERNE, SCRIPPS and JPL solutions.

Acknowledgements. I thank very much Dr. D.D. McCarthy from the U.S. Naval Observatory for the GPS pole coordinates data and Dr. B.E. Schutz, R. Eanes and M. Watkins for comments that helped me to fulfill this work during my stay in the CSR in 1993.

References

Burg J.P. (1967). Maximum Entropy Spectral Analysis, 37th Ann. Int. Meet. Society of Exploration Geoph., Oklahoma City, October 31, 1967.

IGS'92 Campaign (1992). Comparison of GPS, SLR and VLBI Earth Orientation Determinations (third report). IERS, Bureau Central de L'IERS Observatoire de Paris.

Kosek W. (1991). On high frequency spectral analysis of very noisy stochastic processes and its application to the ERP series determined by VLBI and SLR. U.S. Naval Observatory Circular No 177, Washington D.C. 20392-5100, Feb., 15.

Lichten S.M., Marcus S.L. and Dickey J.O. (1992). Sub-Daily Resolution of Earth Rotation variations with Global Positioning System Measurements, Geoph. Res. Letters, 19, 537-540, 1992.

Lindqwister U.J., Freedman A.P., Blewitt G. (1992). Daily Estimates of Earth's Pole Positions with Global Positioning System., Geoph. Res. Letters., 19, 845-848, 1992.

Ormsby J.F.A. (1961). Design of Numerical Filter with Application of Missile Data Processing., J. Assoc. Comput. Mach. 8, pp 440-466.

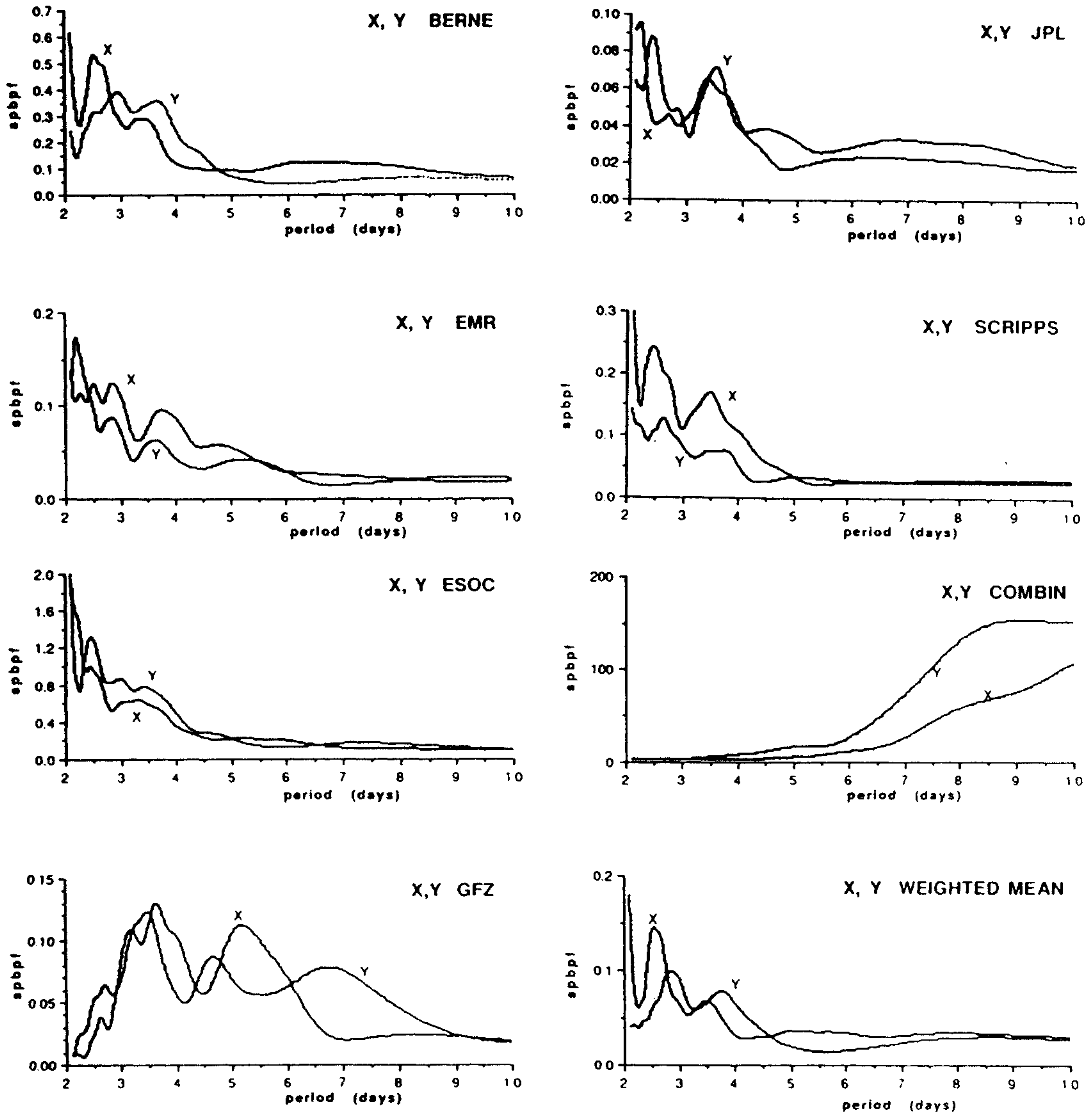

Fig. 1. The BPFSA spectra of the second difference of pole coordinates determined by different processing centers.

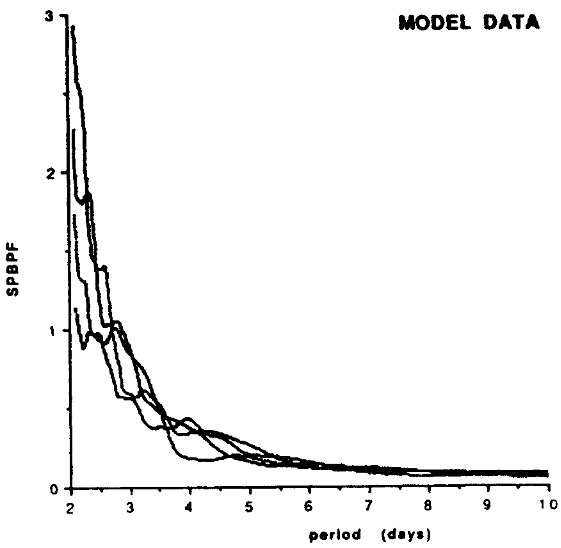

Fig. 2. The BPFSA spectra of the second difference of 4 model data.

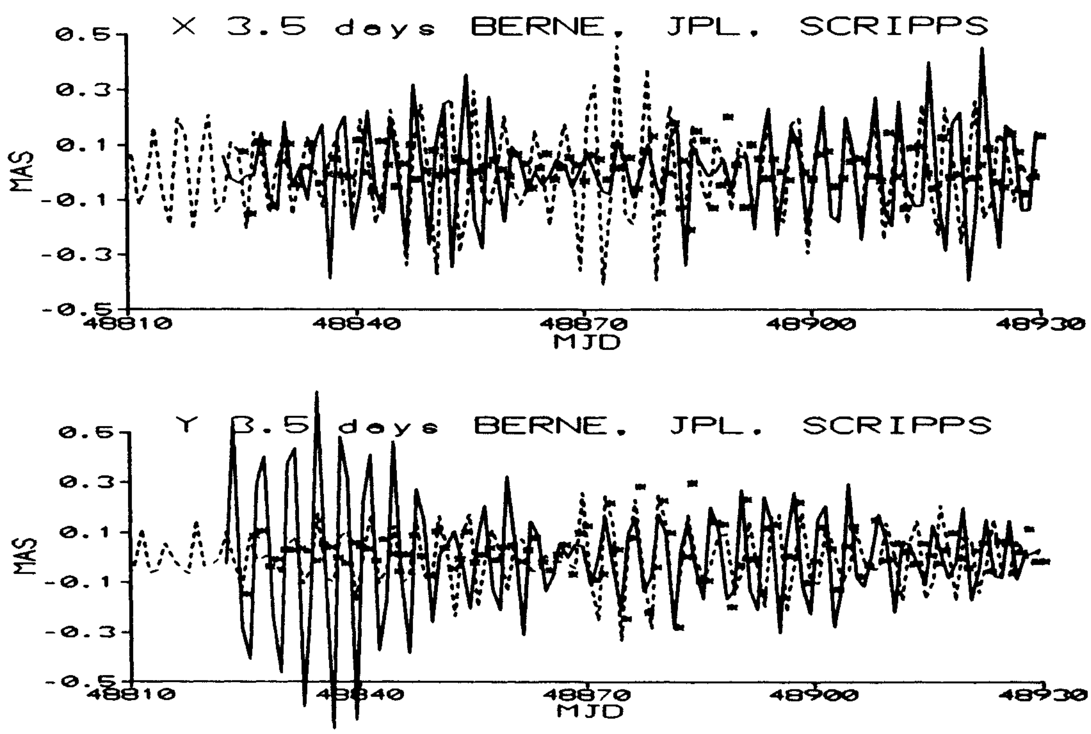

Fig. 3. 3.5 day oscillation computed by the Ormsby band pass filter in x,y pole coordinates determined by BERNE (thin line), JPL (stars), SCRIPPS (dotted line).

COMPARISON OF WET DELAY ESTIMATES USING VLBI, GPS, AND WVR DATA AT THE ONSALA SPACE OBSERVATORY DURING SEARCH'92

G. Elgered, J. M. Johansson
Onsala Space Observatory, Chalmers University of Technology
S-439 92 Onsala
Sweden

J. L. Davis
Harvard-Smithsonian Center for Astrophysics
60 Garden St., CAMBRIDGE, MA 02138
USA

ABSTRACT. Unmodeled variations in the wet propagation delay are a major source of error in space geodetic techniques using radio signals, such as VLBI and GPS. The most common method to deal with this error is to estimate the equivalent zenith wet delay at each site. Wet delays estimated using VLBI and GPS data are compared with microwave radiometer measurements.

1. Introduction

It is well known that the varying amount of atmospheric water vapor affects the propagation time of a radio signal. The common method to deal with this excess propagation time in radio based space geodetic techniques is to estimate an atmospheric correction using the geodetic data themselves. This correction may be modelled as a constant, a piece-wise linear function, or a stochastic process. In this study we compare estimates of the wet propagation delay using two space geodetic techniques, Very-Long-Baseline Interferometry (VLBI) and the Global Positioning System (GPS) with estimates from a ground-based microwave radiometer. The model used in both the VLBI and the GPS analysis is a Markov process or more specifically a random walk process.

The variance between values separated by the time Δt for a random walk process scales linearly with the separation

$$< (x(t + \Delta t) - x(t))^2 >= \sigma^2 \Delta t \qquad (1)$$

In addition to study the influence of the wet delay on the accuracy of VLBI and GPS another goal of this work is to evaluate the use of GPS networks for meteorological measurements (see, *e.g.*, Bevis et al. (1992)).

2. Instrumentation and Estimation Techniques

The maximum distance between the 20 meter radio telescope used for VLBI observations, the GPS antenna and the Water Vapor Radiometer (WVR) is approximately 80 m. The intersection of azimuth and elevation axises of the VLBI antenna is 22 m above the mean sea level whereas both the GPS and WVR antenna heights above sea level are 9 m. This means that for a standard atmosphere with a scale height equal to 2 km the VLBI antenna senses a wet delay which is 0.6% less than the other two methods. This effect is of the order of 1 mm and will be ignored in the following.

Three contiguous 24 hour long VLBI experiments were carried out during July 1992. The two first were dedicated mobile experiments and the third was IRIS-A 751. All of them included the mobile VLBI antenna (MV-2) at Høfn, Iceland. Because of the lower sensitivity of the mobile VLBI antenna typically 180 observations were carried out during one 24 hour experiment. For example, the R&D experiments during 1993, using larger antennas, typically include 300 observations at each site.

The GPS receiver, a Rouge SNR-800 with a Dorne-Margolin antenna operated continuously without any problems during this time period.

The WVR, measuring the atmospheric emission at 21.0 and 31.4 GHz was operated in a "sky mapping mode" with a cycle of approximately 8 minutes rather than pointing at each VLBI source. Approximately 60 observations spread over the sky down to an elevation angle of 23° was acquired during one such cycle.

The VLBI estimates use observations down to elevation angles of approximately 7°. The hydrostatic mapping function is used to calculate the actual hydrostatic delay from the equivalent zenith value based on ground pressure observations (Davis et al. 1985). The wet delay is estimated using a special wet delay mapping function (Chao 1972). The VLBI data analysis is carried out with the SOLVK software (Herring et al. 1990). The value of the random walk variance, σ^2 in (1), is estimated for each site using the delay rate residuals. For the three experiments the estimated values of σ^2 were 0.19, 0.90, and 0.46 ps^2/s, respectively.

The GPS estimates use observations down to an elevation angle of 15°. One mapping function (Lanyi 1984) is used to estimate the total propagation delay in the GIPSY software (Lichten and Border 1987). The standard value used for the data in this study was 0.32 ps^2/s. The wet delay is, thereafter, calculated by subtracting the zenith value of the hydrostatic delay based on the ground pressure observations. In this presentation a mean ground pressure has been used for each day but this will be improved in the near future.

The microwave radiometer data are presented as equivalent zenith values of actual observations at different elevation angles using the simple cosecant law. In this data set the radiometer was scanning the entire sky but always above an elevation angle of 23°. Otherwise the typical observation strategy using the WVR is to observe in the same direction as the VLBI antenna and perform so called tip-curves during the time between the VLBI observations.

3. Results

Below we present the estimated wet delays using the three different methods. Figure 1 shows the results when the GPS data were processed in 24 hour long daily data sets independently. It should be noted that when we processed the first two days of GPS data, the large increase in the wet delay around midnight between July 25–26 is in better agreement with the WVR and the GPS data. The VLBI processing has been made independently for each experiment.

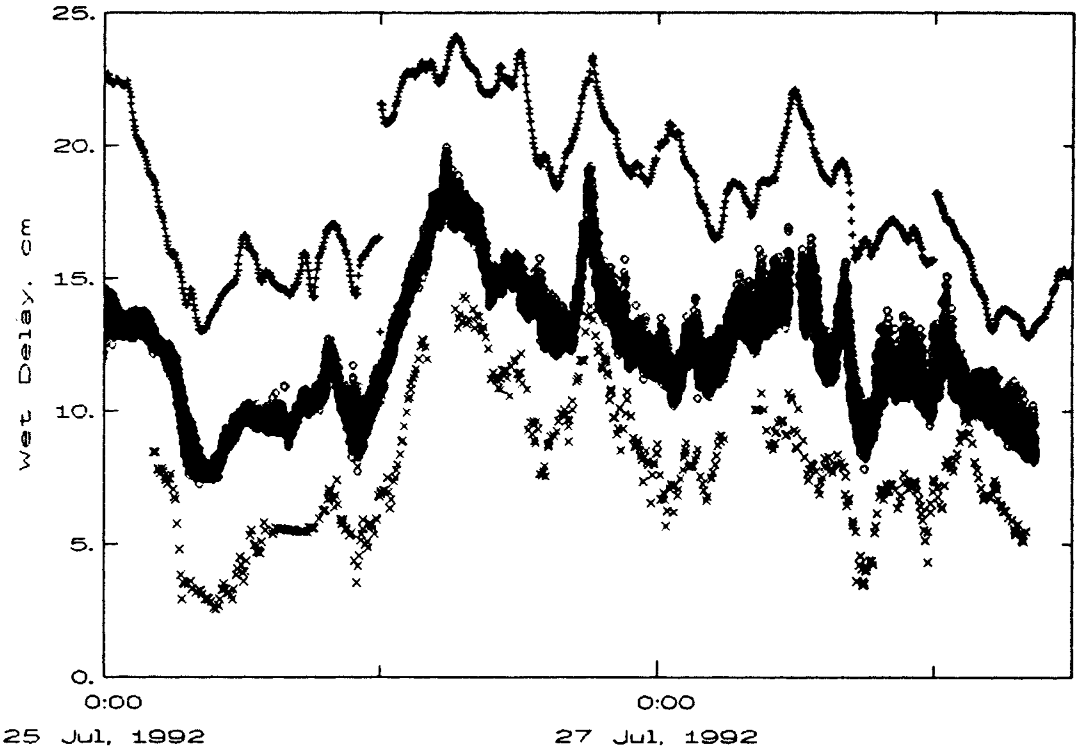

Figure 1. Comparison between estimated equivalent zenith wet delays using GPS, VLBI and microwave radiometer data. In order to make it easier to compare the results biases of +5 cm and -5 cm have been added to the GPS (upper curve) and VLBI (lower curve) estimates, respectively. The microwave radiometer data (middle curve) have been acquired by scanning the instrument in azimuth and elevation in a cycle repeated every 12 minutes.

4. Discussion

Slowly varying differences at the centimeter level exist between all data sets. The typical mean biases calculated for one day is about 1 cm. This is true also when the imperfect correction of the hydrostatic delay in the GPS data sets is taken into account.

The WVR data are less accurate when there are large amounts of liquid water in the atmosphere. An advantage is, however, that the liquid water content can be estimated simultaneously with the wet delay using the WVR data. In this presentation we have discarded all data for which the estimated integrated liquid water content is larger than 0.7 mm. In the evening of July 26 the rapid increase suggested by the WVR data is supported by the VLBI data. (The liquid water content at the peak is 0.7 mm.) On the other hand events with a liquid water content of 0.7 mm have been seen in other data sets where the WVR data seem to overestimate the wet delay.

5. Conclusions and Future Work

Variations in the wet propagation delay are in general "detected" by all three methods.

This type of comparison has proven valuable for detecting errors (such as ignored clock-breaks) in the VLBI and the GPS data analysis.

As more data are being analyzed the goal is to search for systematic differences in the wet delay estimates.

References

Bevis, M., S. Businger, T.A. Herring, C. Rocken, R.A. Anthes, and R.H. Ware (1992), GPS Meteorology: Remote Sensing of Atmospheric Water Vapor Using the Global Positioning System, *J. Geophys. Res.*, **97**, pp. 15787–15801.

Chao, C.C., A model for tropospheric calibration from daily surface and radiosonde balloon measurements (1972), *Tech. Mem. 391-350*, Jet Propulsion Lab., Pasadena, California.

Davis, J.L., T.A. Herring, I.I. Shapiro, A.E.E. Rogers, and G. Elgered, Geodesy by Radio Interferometry: Effects of Atmospheric Modeling Errors on Estimates of Baseline Length (1985), *Radio Sci.*, **20**, pp. 1593–1607.

Herring, T.A., J.L. Davis, and I.I. Shapiro, Geodesy by radio interferometry: The application of Kalman filtering to the analysis of very long baseline interferometry data (1990), *J. Geophys. Res.*, **95**, pp. 12,561–12,581.

Lanyi, G., Tropospheric delay effects in radio interferometry (1984), *TDA progress report 42–78*, Jet Propulsion Laboratory, Pasadena, California.

Lichten, S.M., and J.S. Border, Strategies for high-precision Global Positioning System orbit determination (1987), *J. Geophys. Res.*, **92**, pp. 12751–12762.

Reproduit par INSTAPRINT S.A. – 1-2-3, levée de la Loire – LA RICHE – B.P. 5927 – 37059 TOURS Cedex – Tél. 47 38 16 04

Dépôt légal 3ème trimestre 1994